Distribution Agreement

In presenting this thesis or dissertation as a partial fulfillment of the requirements for an advanced degree from Emory University, I hereby grant to Emory University and its agents the non-exclusive license to archive, make accessible, and display my thesis or dissertation in whole or in part in all forms of media, now or hereafter known, including display on the world wide web. I understand that I may select some access restrictions as part of the online submission of this thesis or dissertation. I retain all ownership rights to the copyright of the thesis or dissertation. I also retain the right to use in future works (such as articles or books) all or part of this thesis or dissertation.

Signature:

_____ _____

Stefka Gyoneva Date

Microglial motility under pro-inflammatory conditions *in situ*:
Relevance to neurodegeneration

By

Stefka Gyoneva
Doctor of Philosophy

Graduate Division of Biological and Biomedical Science
Molecular and Systems Pharmacology

_____
Dr. Stephen F. Traynelis
Advisor

_____
Dr. John Hepler
Committee Member

_____
Dr. Gary W. Miller
Committee Member

_____
Dr. Yoland Smith
Committee Member

_____
Dr. Malu Tansey
Committee Member

Accepted:

_____
Lisa A. Tedesco, Ph.D.
Dean of the James T. Laney School of Graduate Studies

_____ Date

Microglial motility under pro-inflammatory conditions *in situ*:
Relevance to neurodegeneration

By

Stefka Gyoneva
B.S., Georgia Institute of Technology, 2008

Advisor: Stephen F. Traynelis, Ph.D.

An abstract of
A dissertation submitted to the Faculty of the
James T. Laney School of Graduate Studies of Emory University
in partial fulfillment of the requirements for the degree of
Doctor of Philosophy
in Graduate Division of Biological and Biomedical Science
Molecular and Systems Pharmacology

2013

Abstract

Microglial motility under pro-inflammatory conditions *in situ*:
Relevance to neurodegeneration

By Stefka Gyoneva

Microglia are the resident immune cells of the central nervous system. In the healthy brain, microglia continuously survey the parenchyma to maintain homeostasis. When a disturbance is detected, microglial processes migrate toward the site of injury and surround it to help with tissue repair in a process that depends on ATP release and activation of $P2Y_{12}$ receptors on microglia. However, in prolonged injury and in many neurodegenerative conditions microglia assume an amoeboid "activated" phenotype commonly associated with release of pro-inflammatory factors. Microglial activation with lipopolysaccharide (LPS) *in vitro* results in $P2Y_{12}$ receptor downregulation, concurrent adenosine A_{2A} receptor upregulation, and ATP- and adenosine-induced process retraction (rather than extension). The work presented here examines the effects of A_{2A} receptor activation under pro-inflammatory conditions in acute brain slices and *in vivo* with emphasis on the response of microglia to tissue damage. Time-lapse confocal microscopy showed that activated microglia in slices from LPS-treated $CX_3CR1^{GFP/+}$ mice, which have microglia-specific GFP expression, displayed reduced process displacement in the direction of mechanically induced tissue injury. Similar results were seen in slices prepared from the 1-methyl-4-phenyl-1,2,3,6-tetrahydropyridine (MPTP) mouse model of Parkinson's disease. Consistent with the *in situ* observations, microglia in LPS-treated $CX_3CR1^{GFP/+}$ mice imaged with *in vivo* two-photon microscopy showed a delayed response to a laser-induced localized tissue damage. The involvement of A_{2A} receptors in modulating the delayed response to damage was confirmed with the use of the selective adenosine A_{2A} receptor antagonist preladenant. Finally, the effects of norepinephrine receptor activation in microglia were characterized to determine if the purinergic (ATP/adenosine) receptor system is unique among neurotransmitters in modulating microglial motility. Application of norepinephrine to both resting and LPS-activated primary microglia *in vitro* resulted in process retraction. Interestingly, simultaneous activation of adrenergic and purinergic receptors prevented ATP-induced motility responses in microglia *in vitro*, suggesting that norepinephrine might interfere with the ability of microglia to respond to tissue damage *in vivo*. The differential regulation of microglial motility under resting and neuroinflammatory conditions by various G protein-coupled receptors can have implications on microglial ability to effectively respond to tissue disturbances such as the extensive neuronal death in neurodegenerative conditions.

Microglial motility under pro-inflammatory conditions *in situ*: Relevance to neurodegeneration

By

Stefka Gyoneva
B.S., Georgia Institute of Technology, 2008

Advisor: Stephen F. Traynelis, Ph.D.

A dissertation submitted to the Faculty of the
James T. Laney School of Graduate Studies of Emory University
in partial fulfillment of the requirements for the degree of
Doctor of Philosophy
in Graduate Division of Biological and Biomedical Science
Molecular and Systems Pharmacology

2013

Acknowledgements

I would like to acknowledge several people for their support during my graduate school training. First, I am especially thankful to my advisor, Dr. Stephen F. Traynelis, for his support and outstanding guidance with my research project and professional development. It was a great pleasure working in Dr. Traynelis's lab, and interacting with him and past and current lab members. I would also like to thank the members of my dissertation committee (Drs. John Hepler, Gary W. Miller, Yoland Smith and Malu Tansey) for their advice and input with my project and other scientific matters. Next, I greatly appreciate the personal support that I received from my parents, Elisaveta Gyoneva and Ivan Gyonev, my sister, Lazarina Gyoneva, and many of my friends. Finally, I would like to thank the Molecular and Systems Pharmacology faculty and staff for providing an excellent academic and work environment during my stay in graduate school.

Table of Contents

Figures and Tables

List of Abbreviations

6-OHDA	6-hydroxydopamine
ABC	Avidin-biotin complex
aCSF	Artificial cerebrospinal fluid
AD	Alzheimer's disease
ADAM	A disintegrin and metalloproteinase-containing protein
ALS	Amyotrophic lateral sclerosis
ANOVA	Analysis of variance
APP	Amyloid precursor protein
BBB	Blood-brain barrier
BSA	Bovine serum albumin
CCL2/CCR2	CC-type chemokine ligand/receptor-2
CD	Cluster of differentiation
cDNA	Complementary DNA
CNS	Central nervous system
COX-2	Cyclooxygenase-2
CR	Complement receptor
CSF	Cerebrospinal fluid
CSF-1(R)	Colony stimulating factor-1 (receptor)
CX_3CL1/CX_3CR1	CX_3C-type chemokine ligand/receptor-1
CXCR3	CXC-type chemokine receptor-3
DAB	3,3'-diaminobenzidine
DAMP	Danger-associated molecular pattern
DMEM	Dulbecco's Modified Eagle Medium
DMSO	Dimethylsulfoxide
DSU	Disk spinning unit
E	Embryonic day
EGF	Epidermal growth factor
ERK1/2	Extracellular signal-regulated kinases-1/2
FAM	6-hydroxyfluorescein
Fbn	Forebrain
FPR	Formylpeptide receptor
GAPDH	Glyceraldehyde phosphate dehydrogenase
GEF	Guanine nucleotide exchange factor
GFP	Enhanced green fluorescent protein
GPCR	G protein-coupled receptor
HBSS	Hank's Balanced Salt Solution
HEK	Human embryonic kidney
HLA	Human leukocyte antigen
HMGB1	High-mobility group protein B1
HRP	Horseradish peroxidase
IB_4	Isolectin B_4
IFN	Interferon

IL	Interleukin
i.p.	Intraperitoneal
IR	Infrared
JNK	c-Jun N-terminal kinase
LC	Locus coeruleus
LPS	Lipopolysaccharide
Ly-6C	Lymphocyte antigen 6 complex
LXR	Liver X receptor
M-CSF	Macrophage colony stimulating factor
MGB	dihydrocyclopyrroloindole tripeptide/minor groove binder
MHC	Major histocompatibility complex
MPTP	1-methyl-4-phenyl-1,2,3,6-tetradydropyridine
MS	Multiple sclerosis
NADPH	Nicotinamide adenine dinucleotide phosphate, reduced
NE	Norepinephrine
NLRP3	Nod-like receptor family, pyrin domain-containing protein-3
NMR	Nuclear magnetic resonance
NSAID	Non-steroidal anti-inflammatory drug
P	Postnatal day
PAMP	Pathogen-associated molecular pattern
PBS	Phosphate-buffered saline
PD	Parkinson's disease
PET	Positron emission tomography
PFA	Paraformaldehyde
PPARγ	Peroxisome proliferator-activated receptor-γ
qPCR	Real-time quantitative PCR
RAGE	Receptor for advanced glycation end-products
ROS	Reactive oxygen species
RT-PCR	Reverse transcriptase-PCR
Runx1	Runt-related transcription factor-1
SA/V	Surface area-to-volume ratio
s.c.	Subcutaneous
s.e.m.	Standard error of the mean
SN(c/r)	Substantia nigra (pars compacta/reticulata)
TGF-β	Transforming growth factor-β
TH	Tyrosine hydroxylase
TLR	Toll-like receptor
TNF(R)	Tumor necrosis factor (receptor)
TTx	Tetrodotoxin

CHAPTER 1: Background

1.1. Abstract

Microglia are considered to be resident immune cells in the central nervous system (CNS). They share many functional properties with monocytes and tissue macrophages, but also display unique characteristics that are not seen in other cell types. In this chapter, I will review the basic properties of microglia that showcase their immune function. Then, I will discuss the current understanding of the origin of the cells, and how their origin relates to some of their functional properties. Later, I will critically discuss how microglial phenotypes are regulated in the brain and how they determine microglial function. In order to highlight the importance of microglia in neurological diseases, I will discuss the involvement of microglia in Parkinson's disease (PD) and Alzheimer's disease (AD) onset and progression. Finally, I will provide an overview of the regulation of microglial motility and why it needs to be studied in the context of neuroinflammation.

1.2. Introduction to microglia

1.2.a. Basic properties

Microglia are a unique cell type in the central nervous system that has intrigued scientists for over a century. They were first described in the 1880s by Franz Nissl using his newly developed cell staining technique as brain cells with small rod-shaped bodies. Much of the early characterization of microglia was performed by Pio del Rio Hortega. He coined the term "microglia" to refer to the small cells that Nissl had identified. Del Rio Hortega recognized that microglia represent the "third element" of the CNS, a population distinct from neurons ("first element') or the supporting astrocytes and oligodendrocytes ("second element"). By 1939, when del Rio Hortega delivered a lecture in London, he was aware of what we recognize today as the major properties of microglia: they had mesenchymal origin, were similar to tissue macrophages, invaded sites of injury, and performed phagocytosis when activated (del Rio-Hortega, 1939).

If microglia are a type of tissue macrophage in the CNS parenchyma, then they must show similarities with other immune cells. Indeed, microglia can be stained using antibodies directed against macrophage-specific markers such as F4/80, the phagocytic receptor for immunoglobulins FcR, and complement receptor 3 (CR3), and the leukocyte markers major histocompatibility complex (MHC) and human leukocyte antigen (HLA) *in situ* and in primary cultures (Buttini et al., 1996; Gehrmann et al., 1993; Giulian and Baker, 1986; Hoek et al., 2000; Perry et al., 1985; Streit et al., 1989; Ulvestad et al., 1994a; Ulvestad et al., 1994b; Ulvestad et al., 1994c; Vedeler et al., 1994; Williams Jr et al., 1993; Williams et al., 1992; Woodroofe et al., 1989). Moreover, when primary microglia are challenged with pro-inflammatory mediators such as lipopolysaccharide (LPS), interferon-γ (IFN-γ) or others, they secrete a variety of cytokines, including interleukin (IL)-1β, IL-6, IL-8, IL-18, tumor necrosis factor α (TNF-α), macrophage colony-stimulating factor/colony stimulating factor-1 (M-CSF/CSF-1) (Ehrlich et al., 1998; Giulian et al., 1986; Giulian et al., 1991; Hanisch, 2002; Hayashi et al., 1995; Kiefer et al., 1993; Lee et al., 1993; Perry and Gordon, 1988; Prinz and Hanisch, 1999; Sawada et al., 1989), reactive oxygen species (ROS), and others (Banati et al., 1993; Chao et al., 1992; Colton and Gilbert, 1987; Colton et al., 1992; Giulian et al., 1993; Gottschall et al., 1995; Vaca and Wendt, 1992; Woodroofe et al., 1989). Furthermore, microglia express certain chemokines and chemokine receptors [CSF-1 receptor, CX_3C-type chemokine receptor 1 (CX_3CR1), others] (Biber et al., 2002; Calvo et al., 1998; Cross and Woodroofe, 1999; Flynn et al., 2003; Hanisch, 2002; Harrison et al., 1998; Hughes et al., 2002). In addition, microglia can participate in the support of brain function and tissue repair by secreting neurotrophins and growth factors (Elkades et al., 1996; Hanisch, 2002). Finally, activated microglia (for example, with LPS- or IFN-γ) have the capacity to present antigens to T cells, albeit to a lower capacity than peripheral antigen presenting cells (Askew and Walker, 1996; Cash and Rott, 1994; Cash et al., 1993; De Simone et al., 1995; Williams Jr et al., 1993). Overall, these findings confirm that microglia are immunocompetent cells resident to the CNS.

1.2.b. Origin and turnover

The origin of microglia had long remained a mystery. Using immunohistochemistry to detect macrophage markers in the brain, the presence of monocyte-derived macrophages was first detected early in the developing brain (Perry et al., 1985). Amoeboid microglia could be seen in the brain as early as embryonic day 11 (E11), and spread to different brain regions with the appearance of blood vessels (Ashwell, 1991). The exact progenitors of microglia were not identified until later, when they were detected in the yolk sac. These primitive yolk sac macrophages remain there until the development of blood vessels and circulation, which allows them to colonize the brain parenchyma (Alliot et al., 1999). The same sequence of events occurs during the development of microglia in the zebrafish, as well (Herbomel et al., 2001). Recent studies using careful lineage tracing experiments and *in vivo* two-photon microscopy confirmed these initial observations. Now we know that microglia arise from Ly-6C^{hi}CCR2^{+} monocytes (Ly-6C: lymphocyte antigen 6 complex; CCR2: CC-type chemokine receptor 2) (Mildner et al., 2007). They first appear in the yolk sac before E7.5. Unlike peripheral macrophages, these yolk sac progenitors require the hematopoietic Runt-related transcription factor-1 (Runx1) for development. They later migrate into the brain parenchyma between E8.5 and E9.5 through the blood circulation in a Pu.1-, CCR2-, CSF-1R-dependent manner (Mildner et al., 2007). Despite the requirement for CSF-1R receptor, microglia do not require CSF-1/M-CSF, which is essential for monocyte differentiation. Instead, IL-34 appears to be the ligand for CSF-1R (Ginhoux et al., 2010; Ginhoux et al., 2013).

These fate mapping experiments indicate that microglia and monocytes derive from distinct progenitor populations: microglia arise from yolk sac macrophage progenitors, while monocytes differentiate from bone marrow progenitors. The differential origin of microglia raises questions about the replacement of microglia in the healthy and diseased brain. Are microglia maintained locally, or are they replenished from the periphery? Does the situation change under

pathological conditions? Do peripheral monocytes contribute to the pathology of neurological disorders? Brain-resident microglia are capable of DNA replication (Lawson et al., 1992), thus they appear to be capable of self-renewal. However, studies using whole body irradiation and bone marrow transplantation have challenged this idea. If mice are irradiated to kill their hematopoietic cells and then receive bone marrow from donors that express enhanced green fluorescent protein (GFP) in their cells, the donor cells can be detected in the brain parenchyma in a CCR2-dependent process (Priller et al., 2001; Simard and Rivest, 2004). These peripherally-derived monocytes appeared specifically targeted to sites of damage, suggesting that monocytes, rather than resident microglia, might play important roles in pathological processes (Priller et al., 2001). However, the radiation used for whole body irradiation causes a disruption of the blood-brain barrier (BBB) that is not seen in most brain pathologies, so care must be taken in drawing conclusions from these studies (Greter and Merad, 2013; Ransohoff and Perry, 2009). If the BBB breakdown is prevented, for example by shielding the head during irradiation, peripheral monocytes do not populate the brain to an appreciable extent, even after local (facial nerve axotomy) or degenerative (cuprizone-induced demyelination) injury (Mildner et al., 2007). Similar results were obtained with parabiosis experiments in which the circulatory systems of two animals are combined. If the cells of one of the mice are GFP-positive, they can be detected in the circulation of the recipient animal, but not in the brain parenchyma (Ajami et al., 2007). These GFP-positive cells do not enter the parenchyma even after facial nerve axotomy or in a mouse model of amyotrophic lateral sclerosis (ALS) (Ajami et al., 2007). Indeed, pre-conditioning and ablation of the resident microglial population appear essential for the efficient long-term engraftment of hematopoietic stem cells in the brain (Capotondo et al., 2012; Varvel et al., 2012). In conclusion, it appears that the brain microglial population is self-renewing. Blood monocytes are generally excluded from the brain parenchyma, unless a disruption of the BBB occurs, as in stroke or chronic inflammatory disorders like MS (Ginhoux et al., 2013; Yenari et al., 2010). Thus, resident microglia are likely the cells that will respond to most brain pathologies.

1.2.c. Microglial phenotypes

In addition to microglial origin, the fate mapping experiments described above revealed another property of microglia – they can change their morphology. The migrating microglia during development have an amoeboid morphology, which later turn into the ramified microglia seen in adulthood. In the adult healthy brain, microglia have small cell bodies [5-15 μm diameter; Vela et al. (1995)] and long branching processes. Microglial cells are regularly spaced throughout the brain parenchyma, with the processes of neighboring cells occupying non-overlapping areas (Lawson et al., 1990). Yet, there are differences in the proportion of cells that are microglia between brain regions. The substantia nigra (SN) appears to have one of the densest microglial populations, comprising ~12% of all Cressyl Violet-positive cells, while the average proportion in the cortex is 5% (Lawson et al., 1990). There is also some heterogeneity in microglial morphology in the adult brain. Cells with longitudinal branching patterns are seen in fiber tracts, with branches likely following axonal projections. In contrast, microglia in brain regions with more pearmeable BBB, such as the circumventricular organs, have a more amoeboid morphology (Lawson et al., 1990). Microglia in disease states ranging from acute injury to chronic neurodegenerative conditions also assume an amoeboid morphology (Kreutzberg, 1996). The rounded morphology is generally associated with an activated or reactive microglial phenotype, and seems to represent a switch in microglia's functional state. Conversion to this activated state can be induced by pathogens, pro-inflammatory cytokines and constituents from damaged cells following binding to pathogen- or danger-associated molecular pattern (PAMPs and DAMPs, respectively) receptors on microglia such as Toll-like receptors (TLRs) or scavenger receptors (Wyss-Coray and Mucke, 2002).

Because of the similar morphology seen throughout the brain, microglia were thought to be a uniform population, with no obvious functional differences. However, now we know that microglia possess a certain phenotypic plasticity that allows them to perform diverse responses to a variety of stimuli. In the healthy brain, microglia in different brain regions express variable

levels of surface markers such as cluster of differentiation-11b (CD11b), F4/80, CXC-type chemokine receptor-3 (CXCR3) and others (de Haas et al., 2008). Microglial activation with LPS, TNF-α or INF-γ induces the expression of divergent sets of gene, depending on the exact stimulus or combination thereof (Colton and Wilcock, 2010; Flynn et al., 2003). Individual microglia differ in their responsiveness to TLR activation and antigen presenting abilities *in situ* and *in vitro*, suggesting the existence of subsets of microglia (Askew and Walker, 1996; Scheffel et al., 2012). Lastly, IL-1β and TNF-α are induced in distinct microglial populations after ischemic stroke, and cells that co-express both cytokines are rarely observed (Clausen et al., 2008). Thus, like neurons, it is highly likely that microglia belong to distinct subpopulations that possibly display specific receptor expression patterns in different brain regions.

Another feature associated with the uniform ramified morphology of microglia in the healthy adult brain is the so called "resting" phenotype. In the absence of a pathology, microglia are thought to exist in a largely immunosuppressed, resting, state in which microglia do not perform immune functions to an appreciable degree (Kreutzberg, 1996). This suppressed state is likely the result of active inhibition of microglial reactivity by components of the brain parenchyma. Two of the best characterized "calming" signals acting on microglia are the cell-cell interactions mediated by the CX_3CL1-CX_3CR1 and CD200-CD200 receptor ligand-receptor pairs.

CX_3CL1, a chemokine also known as fractalkine, signals through the CX_3CR1 receptor (Bazan et al., 1997; Imai et al., 1997). Fractalkine appears to be expressed by neurons in the brain, while CX_3CR1 is found on microglia (Harrison et al., 1998; Maciejewski-Lenoir et al., 1999; Zujovic et al., 2000), but primary astrocytes in culture also contain mRNA for fractalkine and/or its receptor (Hatori et al., 2002; Maciejewski-Lenoir et al., 1999). Peripheral monocytes can also express CX_3CR1, but at much lower levels than microglia (Harrison et al., 1998; Jung et al., 2000). CX_3CL1 can exist in either a cell membrane-associated form, or undergo constitutive cleavage by A disintegrin and metalloproteinase-containing protein-10 (ADAM10) or inducible

cleavage by ADAM17 to produce soluble CX_3CL1 (Garton et al., 2001). Fractalkine-CX_3CR1 signaling reduces microglial reactivity, for example by reducing pro-inflammatory cytokine secretion by microglia *in vitro* (Zujovic et al., 2000). Inhibiting fractalkine signaling by its neutralization with antibodies or deletion of CX_3CL1 or CX_3CR1 generally results in increased microglial activation and enhanced pathology (Rogers et al., 2011; Zujovic et al., 2001), but protective effects have also been observed (Denes et al., 2008; Lee et al., 2010). Even though direct neuronal-microglial interactions through membrane-bound CX_3CL1 might be important for cell adhesion (Haskell et al., 1998; Imai et al., 1997; Kim et al., 2011), the soluble form of fractalkine seems to be the neuroprotective isoform *in vitro* and in models of Parkinson's disease (Zujovic et al., 2000).

Similar to the CX_3CL1-CX_3CR1 pair, the CD200-CD200R pair of ligand-receptor also modulates microglial functions to reduce microglial reactivity *in vivo*. CD200 (also known as OX2) is expressed on a wide range of cells in the periphery (Wright et al., 2001; Wright et al., 2000), but appears restricted to neurons in the brain (Koning et al., 2009). CD200R is restricted to cells of the myeloid lineage, including microglia (Hoek et al., 2000; Koning et al., 2009; Wright et al., 2000). Disruption of CD200-CD200R signaling results in exacerbated inflammatory responses both in the periphery and the CNS. Specifically, deficiency in CD200 leads to accelerated onset of experimental autoimmune encephalomyelitis, a mouse model of multiple sclerosis (MS) and increased microgliosis following facial nerve axotomy (Hoek et al., 2000; Meuth et al., 2008; Wright et al., 2000). Preventing CD200-CD200R interaction with a blocking antibody sensitizes dopaminergic neurons to rotenone toxicity (Wang et al., 2011). Finally, brain samples from AD patients show reduced CD200 and CD200R expression compared to non-demented controls (Walker et al., 2009), confirming that CD200 signaling is also dysregulated in human disease states.

In conclusion, the presence of fractalkine and CD200 on healthy neurons maintains microglia in a non-reactive state, allowing microglia to participate in normal brain functions (see

Section 1.3). If these immunosuppressive signals are removed, or activating signals appear, microglia assume the activated, cytokine-secreting and phagocytic phenotype seen in different disease states.

1.3. Microglia in the healthy brain

Microglia do perform many functions as part of an immune response when needed. However, they are not quiescent in the unperturbed brain. Instead, they participate in numerous processes that likely help maintain CNS homeostasis. To highlight the contribution of microglia to normal brain function, I will focus on the involvement of microglia in tissue surveillance, synapse surveillance and regulation of synaptic function, and the role of microglia in instructing and facilitating brain development.

1.3.a. Tissue surveillance

Their ramified morphology in the healthy brain has been one of the main defining characteristics of resting microglia. The term "resting" was used to mean "stationary" and "unmoving," which contrasted the locomotory amoeboid microglia that migrated to damaged neurons, for instance, following facial nerve axotomy (Kreutzberg, 1996). Early imaging studies of microglia in acute brain slices seemed to confirm this view of microglia as static in the brain (Stence et al., 2001). The situation dramatically changed following the development of two-photon microscopy to allow the imaging of microglia in the brain of live, anesthetized mice. Using transgenic animals that express GFP under the control of the CX_3CR1 promoter (Jung et al., 2000), two studies showed that microglia are exceptionally active in the healthy brain. While the cell bodies indeed remain stationary over long periods of time, microglia move the tips of their fine processes, displaying short extensions and retractions on the order of seconds (Davalos et al., 2005; Nimmerjahn et al., 2005). The stochastic nature of the movement suggests that microglial processes might be engaging in tissue surveillance, contacting unknown structures

briefly, and then retracting to their original position.

The extensive branching of microglial processes allows the cells to sample the whole brain parenchyma, and in this way to immediately detect any disturbances in normal homeostasis. For example, natural cell death and rupture of brain capillaries that might occur as part of normal aging (Hanisch and Kettenman, 2007) may stimulate a microglial response, converting the stochastic movement of microglial processes to directional extension to the site of damage. Experimentally, the response can be mimicked by mechanical damage, laser-induced damage to the brain or rupturing a blood vessel (Davalos et al., 2005; Nimmerjahn et al., 2005). The mechanism underlying this response involves ATP release at the site of damage, likely as a spillout from the cytoplasm of damaged cells, activation of ATP receptors on astrocytes, and additional release of astrocytic ATP through connexin hemichannels to amplify the original signal (Davalos et al., 2005). The ATP in the brain parenchyma can be very quickly broken down to ADP by CD39 [also known as apyrase; Zimmermann (2000)]. Both nucleotides can bind to and activate purinergic $P2Y_{12}$ receptors, which are selectively expressed in brain microglia (Haynes et al., 2006). $P2Y_{12}$ receptor signaling induces the directional process extension of microglia, allowing the processes to completely surround the damage and prevent the spread of debris. The rapid process outgrowth also requires activation of volume-sensing chloride channels, and blocking the channels delays the response and allows the damaged area to grow in size (Hines et al., 2009). Even though it has not been demonstrated in real time *in vivo*, microglia likely clear the debris by phagocytosis to restore the parenchyma to an unperturbed state.

1.3.b. Synapse surveillance

The apparently random motion of microglial processes in the healthy brain (see Section 1.3.a above) might, in reality, be directed to specific targets, namely synapses. *In vivo* two-photon imaging of mice in which both the microglia and neurons express fluorescent proteins indicates that microglial processes extend, make a brief contact with synaptic spines (~5 min long), and

then retract (Wake et al., 2009). The interactions occur on a regular basis, with a frequency of approximately one contact per hour (Wake et al., 2009). The frequency and duration of contacts can be regulated by neuronal activity and pathological processes. The interactions are reduced in frequency if synaptic transmission is suppressed with tetrodotoxin (TTx), and increased in frequency following glutamate release or visual stimulation (Li et al., 2012; Wake et al., 2009). The duration of the contact is significantly prolonged after transient cerebral ischemia (~1 hr), often leading to the elimination of the synaptic spine (Wake et al., 2009).

As the ischemia experiments suggest, microglial contact of synapses might affect synaptic signaling by causing the removal of spines. Indeed, microglia in zebrafish preferentially contact synapses with high spontaneous or visually evoked activity (Li et al., 2012). A few minutes after the contact, neuronal activity is downregulated both in terms of frequency and magnitude of intracellular calcium transients (Li et al., 2012). In the mouse visual system, light deprivation induces contact of microglial processes with synapses and elimination of the contacted spines (Tremblay et al., 2010). Thus, the constant movement of microglial processes might play a role in regulating synaptic signaling and preventing overactivation of synapses. Interestingly, ATP signaling through P2Y receptors regulates the baseline process dynamics of microglia in addition to the process extension to injury (Davalos et al., 2005; Li et al., 2012). Microglia also express metabotropic glutamate receptors, norepinephrine (NE) receptors, serotonin receptors, and others (Pocock and Kettenmann, 2007), all of which could facilitate the ability of microglia to monitor synaptic activity and maintain normal signaling, if needed.

1.3.c. Microglia promote neurogenesis

Another important microglial function aimed to ensure normal brain function appears to be regulation of neurogenesis. Primary microglia can promote the proliferation and differentiation of neural precursor cells in culture (Aarum et al., 2003; Morgan et al., 2004; Walton et al., 2006). In tissues, microglia are found in zones of neurogenesis, and deactivating microglia *in utero*

results in abnormal cortical development (Cunningham et al., 2013). The involvement of microglia continues after birth, when microglia are required for the survival of layer V cortical neurons at the early postnatal days [P3-P5; Ueno et al. (2013)]. At this stage, synaptic connections undergo profound reorganization to achieve appropriate circuit connectivity. Microglia appear to be involved in this process by removing inappropriate synapses through synaptic pruning (Paolicelli et al., 2011; Schafer et al., 2012; Stevens et al., 2007). Interfering with the synaptic pruning results in the persistence of immature synapses (Paolicelli et al., 2011) or inappropriate targeting of axons (Schafer et al., 2012; Stevens et al., 2007). Finally, microglia might also help remove extranumerary Purkinje cells in the cerebellum in order to achieve the correct connectivity (Marin-Teva et al., 2004).

It is clear from the sections above that microglia are tightly involved in normal brain function, both during development and in adulthood. Thus, it is not surprising that dysregulation of microglial functions is a feature of many neurological diseases, which is the focus of the next section.

1.4. Microglia in disease states

Microglia have been implicated in the etiology of various neurological disorders, ranging from neurodegenerative diseases to psychological disorders (Blank and Prinz, 2013). For instance, microglia respond to acute injury in the CNS, including stroke and traumatic brain injury, spinal cord injury, and peripheral nerve transection [for reviews, see Yenari et al. (2010); Loane and Byrnes (2010); Moore and Thanos (1996); Kreutzberg (1996)]. Surprisingly, microglia seem to contribute to the pathology of the neurodevelopmental disease Rett syndrome (Derecki et al., 2012), and the obsessive-compulsive-like pathological grooming in mice (Chen et al., 2010). However, the focus of this section will be the role of microglia in neurodegenerative diseases, in particular Parkinson's disease and Alzheimer's disease. These diseases were selected because they are the two most common neurodegenerative conditions in the United States, and because of

the relevance of these diseases to the results presented later.

1.4.a. Inflammation in Parkinson's disease

Parkinson's disease, the second most common neurodegenerative disorder in the United States, is clinically characterized by tremor, bradykinesia, rigidity, and postural instability. At the cellular level, a hallmark of the disease is loss of dopaminergic neurons originating in the substantia nigra and projecting to the striatum, and adrenergic neurons originating in the locus coeruleus (LC) and projecting to many cortical and subcortical structures (Pakkenberg et al., 1991). Another prominent feature of the disease is the presence of neuroinflammation, especially in the SN and striatum. Interestingly, certain influenza epidemics have been associated with development of parkinsonian symptoms later. Some of the manifestations of the inflammation in PD are the presence of activated microglia and increased levels of pro-inflammatory cytokines. The neuroprotective properties of anti-inflammatory treatments further showcase the involvement of inflammation in PD. The evidence supporting these findings is discussed below.

The first hints for the possible involvement of inflammation in PD onset came from the correlation between the 1918 flu pandemic and the subsequent appearance of parkinsonian symptoms. The flu epidemic was closely associated in space and time with encephalitis lethargica (Dickman, 2001; Reid et al., 2001), but a direct causation has not been established yet (McCall et al., 2008). Many patients who suffered from encephalitis lethargica soon developed post-encephalitic parkinsonism, the clinical features of which were almost indistinguishable from those of idiopathic PD (Jang et al., 2009b; Ravenholt and Foege, 1982; Reid et al., 2001). Similar correlations have been observed with other viruses causing encephalitis, such as the Japanese encephalitis B virus (Jang et al., 2009b). Even though viral RNA has not been detected in the brains of patients suffering from post-encephalitic parkinsonism or PD, viral antigens are present at the protein level (Gamboa et al., 1974; McCall et al., 2001; Rohn and Catlin, 2011). More recently, studies with the neurotropic H5N1 flu strain have revealed that the virus can enter the

brain, induce persistent microglial activation and cytokine secretion, and transient loss of dopaminergic neurons in the SN, and even affect cognition (Jang et al., 2012; Jang et al., 2009a; Jurgens et al., 2012; Mori et al., 2000). Overall, it appears that viral infections, which activate the immune system, can contribute to the cellular pathology and motor symptoms of PD.

Additional evidence for the role of inflammation in the etiology of PD comes from the presence of activated microglia in the brains of PD patients and animal models of the disease. Microglia with activated morphology and expressing MHC class II molecules can be found in the SN in postmortem samples from PD patients (McGeer et al., 1988a). MHC II-positive microglia are also a prominent feature of the neurodegeneration caused by the dopaminergic toxins 6-hydroxydopamine (6-OHDA) and 1-methyl-4-phenyl-1,2,3,6-tetrahydropyridine (MPTP) and the inflammogen LPS (Akiyama and McGeer, 1989; Barcia et al., 2004; Czlonkowska et al., 1996; Herrera et al., 2000; Kanaan et al., 2008; Kohutnicka et al., 1998; Qin et al., 2007), and remain positive for HLA-DR even years after the MPTP administration in both monkeys and humans (Barcia et al., 2004; Langston et al., 1999; McGeer et al., 2003). Furthermore, the development of [^{11}C](*R*)-PK11195, a ligand for the peripheral benzodiazepine receptor that is upregulated in activated microglia (Venneti et al., 2013), for positron emission tomography (PET) imaging has allowed the identification of activated microglia in the brain of living PD patients, as well (Gerhard et al., 2006).

The use of primary dopaminergic neuron-microglia co-cultures has allowed the elucidation of the mechanisms by which microglia might affect PD progression. Neurotoxins such as 6-OHDA, MPTP, and rotenone, induce greater neuronal cell death in neuron-microglia co-cultures than in neuron-enriched cultures (Gao et al., 2002; Gao et al., 2003b; Gao et al., 2003c; Gao et al., 2003d; Kim et al., 2000; Liu et al., 2000; Tran et al., 2008), but neuroprotection by microglia has also been reported (Bronstein et al., 1995; Polazzi et al., 2009; Zietlow et al., 1999). One possible signal from the damaged neurons that might initiate this signaling cascade is the release of high-mobility group protein B1 (HMGB1), which binds to Mac-1/CR3 to promote

nicotinamide adenine dinucleotide phosphate, reduced (NADPH) oxidase activation and pro-inflammatory cytokine secretion (Gao et al., 2011a).

The main mechanisms by which microglia appear to contribute to neuronal death involve NADPH oxidase activation and release of extracellular ROS by microglia, and increased TNF-α signaling. Support for the importance of these microglia-derived factors comes from several lines of research. First, NADPH oxidase-derived ROS can directly damage neurons, impairing their function. Inhibition of NADPH oxidase or genetic deletion of $p91^{phox}$, an enzymatically active subunit of NADPH oxidase, in microglia attenuates their neurotoxic potential in culture (Gao et al., 2003a; Gao et al., 2003b; Gao et al., 2003c; Gao et al., 2003d; Zhang et al., 2005). Similarly, blocking microglial activation *in vivo* and genetic deletion of $p91^{phox}$ result in reduced dopaminergic neuron toxicity induced by treatment of mice or rats with 6-OHDA, MPTP or LPS (He et al., 2001; Qin et al., 2004; Sriram et al., 2006b; Tomas-Camardiel et al., 2004; Wu et al., 2002). Second, TNF-α could contribute to dopaminergic neurotoxicity by cytokine production or release of glutamate from microglia, which then act on nearby neurons (Harms et al., 2012; Takeuchi et al., 2006). Consistent with this, genetic deletion of the TNF-α receptors TNFR1 and TNFR2 protects against MPTP toxicity in the mouse (Sriram et al., 2006a), and expression of a dominant-negative inhibitor of soluble TNF in the brain reduces LPS and 6-OHDA toxicity in the rat (McCoy et al., 2006; McCoy et al., 2008). It is noteworthy that dominant-negative TNF is able to halt degeneration even if it is administered after 6-OHDA (Harms et al., 2011).

The detection of elevated levels of proinflammatory factors in PD patients also suggests a role for inflammation in disease progression. IL-1β, IL-2, IL-4, IL-6, TNF-α and epidermal growth factor (EGF) have been reported to be elevated in the cerebrospinal fluid (CSF) of patients with PD compared to age-matched controls (Mogi et al., 1994). The association with cytokine levels in the periphery is not as strong, but there is some evidence that serum TNF-α and IL-6 might be increased in the blood of PD patients compared to controls (Dobbs et al., 1999; Scalzo et al., 2010). Consistent with the involvement of cytokines in PD, both systemic and

central IL-1β administration exacerbate the neurotoxic effects of 6-OHDA in the rat (Godoy et al., 2008).

Because of the molecular evidence linking inflammation and neurodegeneration in PD, numerous studies have examined the association between blocking inflammation with non-steroidal anti-inflammatory drugs (NSAIDs) and risk for PD. Most studies, especially those following large cohorts and meta-analyses, report an inverse relationship between NSAIDs use and PD risk (Chen et al., 2005; Chen et al., 2003; Gagne and Power, 2010; Powers et al., 2008; Samii et al., 2009), but not for aspirin (Chen et al., 2005; Chen et al., 2003; Gagne and Power, 2010; Gao et al., 2011b; Samii et al., 2009). Interestingly, some of the studies detected a significantly reduced risk for PD with the NSAID ibuprofen, but not other NSAIDs (Chen et al., 2005; Gao et al., 2011b; Samii et al., 2009). Yet, at this time, it remains unknown why ibuprofen appears to be more protective than other NSAIDs. While some reports show no association between NSAID use and PD risk (Hernan et al., 2006; Ton et al., 2006), the general consensus is that NSAIDs use reduces the risk for developing PD.

Finally, mutations in genes related to immune system function appear to be associated with Parkinson's disease risk. A genetic variation in the *HLA-DRA* locus associated with late-onset PD was identified in a genome-wide association study in people with European ancestry (Hamza et al., 2010), and confirmed in a Dutch population (Simon-Sanchez et al., 2011). Associations with the *HLA-DRB1* locus were identified by genotyping British and Han Chinese populations (Saiki et al., 2010; Sun et al., 2012), but not in additional Asian or European populations (Chiang et al., 2012; Pihlstrom et al., 2013; Puschmann et al., 2011). One meta-analysis failed to detect associations between HLA polymorphisms and PD risk, as well (Mata et al., 2011). Yet, meta-analyses of genome-wide association studies identified additional HLA variants, in the *HLA-DRB1* and *HLA-BRB5* loci, that also increase the risk for PD (Ahmed et al., 2012; Nalls et al., 2011). Thus, the identification of several variants in different *HLA* loci indicates that HLA must play an important role in PD pathogenesis, but more work is needed to

confirm some of the associations and to establish a mechanism by which HLA might affect PD risk.

As discussed above, a wealth of data exist on the involvement of inflammation and microglia in PD pathogenesis. Yet, there are currently no studies that have examined microglial motility in the context of PD. I will examine this in Chapter 4 by using acute brain slices prepared from MPTP-treated mice.

1.4.b. Inflammation in Alzheimer's disease

Alzheimer's disease, the most common neurodegenerative disease in the United States, is characterized by a gradual loss of memory and cognitive decline. At the molecular levels, AD pathology includes the accumulation of the Aβ peptide, cleaved from amyloid precursor protein (APP), into extracellular amyloid plaques, and accumulation of hyperphosphorylated tau protein inside neurons into neurofibrillary tangles. Either the Aβ plaques, or the tau tangles, or both together, cause neuronal dysfunction and progressive neurodegeneration that is most prominent in the hippocampus and cortex (Hardy and Allsop, 1991; Hardy and Selkoe, 2002). Similar to Parkinson's disease, the evidence for inflammation comes from multiple lines of research: activated microglia and inflammatory markers are found in patients suffering from AD, the Aβ in plaques can activate microglia, microglia and/or peripheral monocytes might be involved in plaque clearance, epidemiological data suggests that NSAIDs are protective in AD and immune-related genes modify the risk for AD. Each of these is reviewed below.

Even though wide areas of the brain are affected by AD (cortex and hippocampus), the hallmark extracellular Aβ plaques represent a very localized pathology. Corresponding to this, activated microglia expressing HLA and MHC molecules are specifically found around plaques in postmortem tissue from AD patients (Dickson et al., 1988; Haga et al., 1989; Itagaki et al., 1994; McGeer et al., 1988a; McGeer et al., 1987; Perlmutter et al., 1992; Rogers et al., 1988; Sasaki et al., 1997; Styren et al., 1990; Tooyama et al., 1990). Microglia also surround amyloid

plaques in mouse models engineered to develop AD-like pathology by expression of mutant APP or APP with tau, or APP and the enzymes that process it to generate Aβ (Frautschy et al., 1992). Other immune-related molecules, such as complement proteins and receptors and cytokines, have also been found in the vicinity of plaques and tau-containing tangles (Akiyama et al., 1994; Itagaki et al., 1994; McGeer et al., 1989). Furthermore, activated microglia can be identified in the brains of living AD patients using PET imaging with [^{11}C](*R*)-PK11195 (Cagnin et al., 2001; Edison et al., 2008), indicating that inflammation is present throughout the course of the disease. Most, but not all, studies suggest that NSAIDs might lead to a reduced risk for AD (Etminan et al., 2003; in't Veld et al., 2001; McGeer et al., 1996; Stewart et al., 1997; Vlad et al., 2008; Yip et al., 2005; Zandi et al., 2000). However, an NSAID prevention study for AD, which had to be stopped early because of fear of vascular side effects, failed to show efficacy in preventing AD onset (Breitner et al., 2011; ADAPT Research Group, 2006; ADAPT Research Group et al., 2007). Even if general inhibition of inflammation with NSAIDs does not contribute to AD progression, the presence of activated microglia around Aβ plaques suggests that microglia are involved in the pathogenic processes.

Interestingly, plaque evolution from diffuse Aβ deposits as seen in early AD to compact insoluble plaques in late AD is accompanied by an increase in the number of microglia surrounding the plaques from 2-3 microglia around diffuse plaques to dozens in compact plaques (Mackenzie et al., 1995; Ohgami et al., 1991; Sasaki et al., 1997). For this reason, and because Aβ peptides could be found inside microglia, it was initially proposed that microglia participate in Aβ deposition and plaque compaction (Frackowiak et al., 1992; Huell et al., 1995; Wegiel and Wisniewski, 1990; Wisniewski et al., 1990). However, *in vitro* cultures show that microglia phagocytose Aβ rather than secrete it, thus attempting to clear the plaques (Ard et al., 1996; Shaffer et al., 1995). Yet, microglia are not very efficient at digesting Aβ (Hickman et al., 2008), which leads to plaque accumulation. According to one of the main hypotheses for AD development, Aβ is constantly generated by neurons and cleared by microglia. However, if there

is increased generation or reduced elimination, the steady-state balance of Aβ levels is upset, and the increased free Aβ accumulates in plaques (Hardy and Selkoe, 2002). Thus, microglia have been proposed to play a central role in the pathogenesis of AD by failing to remove Aβ.

Once the Aβ has accumulated, it can directly activate microglia through its interaction with three main receptors on microglia. Aβ binding to the receptor for advanced glycation end-products (RAGE), scavenger receptors, formylpeptide receptor 2 (FPR2), and various co-receptors induces ROS generation and cytokine secretion (Reed-Geaghan et al., 2009), both of which can be detrimental to neuronal health. RAGE and FRP2 can also mediate microglial migration (El Khoury et al., 1996). Aβ-induced microglial activation can then contribute to the demise of neurons through the secretion of neurotoxic compounds (Della Bianca et al., 1999), perpetuating a cycle of neurodegeneration (Cotman et al., 1996).

However, experimental manipulation of inflammation has given conflicting results on the role of inflammation in AD progression. Enhancing inflammation through overexpression of IL-1β or CCL2 or depletion of norepinephrine in mouse models of AD leads to accelerated Aβ pathology (total Aβ levels and plaque load) and functional deficits, such as impaired memory and cognition (El Khoury et al., 2007; Kiyota et al., 2009). Consistent with this, blocking pro-inflammatory signaling mediated by TNF-α, INF-γ, CCL2, and the Nod-like receptor family, pyrin domain-containing protein-3 (NLRP3) inflammasome (a complex that leads to IL-1β processing and secretion) has been shown to reduce Aβ pathology (Yamamoto et al., 2007). Paradoxically, activation of TLR2 or TLR4 (with LPS) can enhance Aβ clearance and improve cognition (Chen et al., 2006), at the expense of increased tau phosphorylation (Kitazawa et al., 2005). The dual role of inflammation in AD progression might be best exemplified with studies using $CX_3CR1^{-/-}$ mice, which exhibit enhanced microglial activation (see Section 1.2.c). CX_3CR1 knock-out in the context of AD mouse models have exacerbated tau pathology (Bhaskar et al., 2010), but reduced neuronal loss (Fuhrmann et al., 2010). In addition, both enhanced and reduced Aβ pathology have been observed in mice lacking CX_3CR1 in different transgenic models of AD

(Cho et al., 2011; Lee et al., 2010).

Despite these contradictory findings, promoting Aβ removal from the brain has been one important therapeutic approach in AD research. One strategy to accomplish this is by active or passive immunization with Aβ peptides and anti-Aβ antibodies, respectively. Both approaches appear successful in reducing Aβ load (Schenk et al., 1999; Sudduth et al., 2013), but fail to stop AD progression in humans (Robinson et al., 2004). More recently, activation of Aβ phagocytosis by alternative pathways has been investigated. Stimulation of the nuclear receptors peroxisome proliferator-activated receptor-γ (PPARγ) and liver X receptor (LXR), and enhanced norpeinephrine signaling increase microglial uptake of Aβ in culture and in animal models, and improve mouse cognition (Mandrekar-Colucci et al., 2012). However, these approaches await safety and efficacy trials in humans. Finally, recent genetic studies have highlighted the role of phagocytosis in AD. Polymorphism in the genes for *CD33*, *CLU*, *CR1* and *TREM2*, all of which have been implicated in phagocytosis of Aβ and cellular debris are associated with increased (*CLU*, *CR1*, *TREM2*) or decreased (*CD33*) risk for AD [see Section 7.3; (Griciuc et al., 2013; Guerreiro et al., 2013; Jonsson et al., 2013; Lambert et al., 2009)].

Another controversial area of research in AD is whether peripheral monocytes are involved in the progression of the disease. In order to answer this question, investigators first turned to total body irradiation and bone marrow transplantation experiments. Transplanted donor cells can enter the brain of mouse models of AD in a CCR2-dependent manner and reduce Aβ load (Malm et al., 2005; Mildner et al., 2011; Simard et al., 2006). Protecting the head during irradiation results in enhanced Aβ pathology, suggesting that irradiation-induced changes contribute to Aβ homeostasis (Mildner et al., 2011). Even though some blood vessels appear abnormal in AD tissues and Aβ might affect the integrity of tight junctions (Kalaria and Hedera, 1995; Kook et al., 2012; Winkler et al., 2001), the breakdown of the BBB that occurs with irradiation (see Section 1.2.b) likely does not occur in AD, questioning the extent to which bone marrow-derived cells are involved in AD. Simply blocking the ability of bone marrow-derived

monocytes to enter the brain by deletion of CCR2 does not affect Aβ load (Mildner et al., 2011), which indicates that bone marrow-derived cells are dispensable for Aβ plaque development or maintenance. Even if donor cells are allowed to enter the brain, they represent only ~20% of the total microglial population. Moreover, they can be found around only ~20% of all compact plaques with an average density of 1-2 cells per plaque (Jucker and Heppner, 2008; Stalder et al., 2005), questioning whether they might exert wide effects in AD progression. Alternatively, the turnover of brain hematopoietic cells (resident microglia or blood marrow-derived monocytes) can be manipulated in the brains of AD transgenic mice that express thymidine kinase from the Iba1 promoter: treatment with low doses of ganciclovir preferentially inhibits brain infiltration of proliferative peripheral monocytes while high doses of the drug eliminate resident microglia via unknown mechanisms. Preventing monocyte infiltration with a 28-day treatment of low-dose ganciclovir results in increased Aβ pathology in 6 month-old mice, but not younger animals (Simard et al., 2006), arguing for the beneficial role of blood-derive monocytes in plaque removal. In contrast, microglial elimination by a 2-4-week treatment with high doses of ganciclovir does not affect plaque load in either young mice (before plaque deposition has started) or old mice (Grathwohl et al., 2009). However, the short time period used in this study (2-4 weeks) might not be sufficient to detect changes in amyloid pathology. Yet, more work is needed before a consensus is reached about the relative contribution of microglia and blood-derived monocytes in regulating AD pathology.

1.5. Expression of G protein-coupled receptors (GPCRs) on microglia

GPCRs, as a receptor class, are targets for ~50% of small molecule therapeutic agents clinically approved for the use in humans. They modulate a great variety of cellular processes ranging from changes in gene expression to cell motility. At the organismal level, they are involved in regulation of glucose homeostasis, cell adhesion and tissue organization, response to hormones, and many others. In the nervous system, GPCRs are widely expressed on neurons

where they serve as receptors for neurotransmitters and neuromodulators. The importance of GPCRs on non-neuronal cell types has also been recognized. For example, astrocytes express many GPCRs for neurotransmitters (Hansson and Ronnback, 2004). In addition to the traditional role of astrocytes in supporting brain function, these neurotransmitter GPCRs allow astrocytes to sense and respond to synaptic activity. The close apposition between astrocytic processes and synapses has given rise to the concept of a "tripartite synapse." According to this concept, astrocytes not only sense synaptic transmission and integrate synaptic information through their neurotransmitter receptors, but also play an instructive role by releasing neuromodulatory compounds such as ATP and glutamate that can affect synaptic signaling (Perea et al., 2009).

GPCRs are also widely expressed on microglia. Consistent with their monocytic origin, microglia express several chemokine receptors, which are GPCRs (Ransohoff, 2009). Chemokines and their receptors can regulate microglial responses to damage, but also downregulate microglial reactivity as in the case of CX_3CL1-CX_3CR1 ligand-receptor pair (see Section 1.2.c). Similar to astrocytes, microglia also express receptors for many of the known neurotransmitters that are involved in the regulation of several microglial functions [reviewed in Pocock and Kettenmann (2007)]. For example, metabotropic glutamate receptors regulate microglial activation in response to certain stimuli; purinergic receptors control microglial motility (see also Section 1.6.a), cytokine secretion, and phagocytosis; adrenergic receptors also mediate cytokine secretion and microglial responses to Aβ (see Section 1.6.b); serotonin receptors increase microglial migration, but reduce phagocytosis (Krabbe et al., 2012); and others. The ability of microglia to sense neurotransmitter levels suggests that synaptic transmission might affect microglial function. As a result, our perception of what constitutes a synapse might evolve to include microglia, giving rise to a "quad-partite synapse" (Schafer et al., 2013). In this work, I focus on how purinergic and adrenergic receptors modulate microglial motility. In general, the presence of various GPCRs on microglia and the hypothetical role of microglia in neurodegenerative diseases provides an opportunity to develop novel therapeutics

that regulate the harmful actions of microglia through cell surface receptors.

1.6. Modulation of microglial motility

The motile behavior of microglia was first deduced from their origin and observations of microglial colonization of different brain regions during development. Moreover, the increase in microglial numbers in response to injury such as facial nerve axotomy was thought to involve both cell proliferation and migration (Kreutzberg, 1996; Schiefer et al., 1999). Because of the similarities between microglia and macrophages, Yao et al. (1990) were the first to examine the ability of microglia to migrate *in vitro* using primary rat microglia. Using a transwell migration assay, they showed that microglia migrate in response to the known macrophage chemoattractants C5a complement, zymosan-activated serum and transforming growth factor-β (TGF-β), and thus establishing the chemotactic potential of microglia. Growth factors (such as EGF or M-CSF) and Aβ were later added to the list of microglial chemoattractants (Nolte et al., 1997; Yan et al., 1996), showing that a wide range of molecules can induce migration of microglia. A common feature of many of the chemoattractants is that they signal though PTx-sensitive G_i protein-coupled receptors (Nolte et al., 1996; Tiffany et al., 2001).

The importance of microglial motility was already introduced in Sections 1.3.a and 1.3.b above. To summarize, microglia in the healthy brain constantly move their processes to sample the brain parenchyma and possibly contact synapses based on level of synaptic activity. Following injury to the brain, such as laser-induced tissue damage, microglial processes extend to the site of damage and surround it. In this section, I will focus on additional aspects of microglial motility, especially its regulation by purinergic and adrenergic signaling.

1.6.a. Regulation of microglial motility by purinergic signaling

The initial recognition that ATP, which is released as a cotransmitter at many CNS synapses (Zimmermann, 1994), affects microglial functions came from the finding that ATP

induced an inward potassium current and intracellular calcium transients in microglia (Walz et al., 1993). Later, while studying the control of the ramified morphology of resting microglia in astrocyte co-cultures, Wollmer et al. (2001) identified ATP and adenosine as factors in astrocyte conditioned medium that promote process outgrowth. They also found that the presence of adenosine was required for efficient process extension and maximum ramification of resting microglia. If ATP and ADP are applied locally to generate a gradient, for example by adding it to only one chamber in a migration assay, the microglia migrate in the direction of ATP/ADP (Honda et al., 2001). The chemotaxis could be blocked by P2Y receptor agonists and pre-treatment with PTx, suggesting the involvement of a G_i-coupled P2Y receptor. At the intracellular level, ATP and ADP induce Rac activation to mediate changes in the actin cytoskeleton (Honda et al., 2001), possibly through $G_{\beta\gamma}$ (Dong et al., 2005; Yan et al., 2012). Moreover, β-arrestin-mediated activation of Erk1/2 and phosphorylation of paxillin also has been shown to regulate cytoskeleton dynamics and ADP-induced migration of microglia (Lee et al., 2012). Thus, multiple pathways mediate ATP/ADP-induced migration of microglia (Fig. 1.1).

As discussed in Section 1.3.a, ATP is involved in the regulation of baseline process motility and mediates process extension in response to tissue damage *in vivo* (Davalos et al., 2005). Haynes et al. (2006) eventually identified the receptor responsible for the effects of ATP as the $P2Y_{12}$ subtype of purinergic receptors. Genetic deletion of $P2Y_{12}$ prevents microglial chemotaxis to ATP and ADP *in vitro*, and significantly reduces the approach to the site of a laser ablation *in vivo* (Haynes et al., 2006). Similarly, neurons damaged in the process of preparation of acute brain slices release ATP to attract microglia. Disrupting the gradients created by the damaged cells by exogenous addition of ATP or ADP, or breakdown of ATP/ADP with apyrase prevent the directional microglial approach (aka, homing) to the damaged cells in slices (Kurpius et al., 2007). Despite the many similarities between macrophages and microglia, ATP does not induce migration of macrophages (Lambert et al., 2010), suggesting that peripheral cells are not recruited by ATP released from damaged cells. However, this does not preclude the

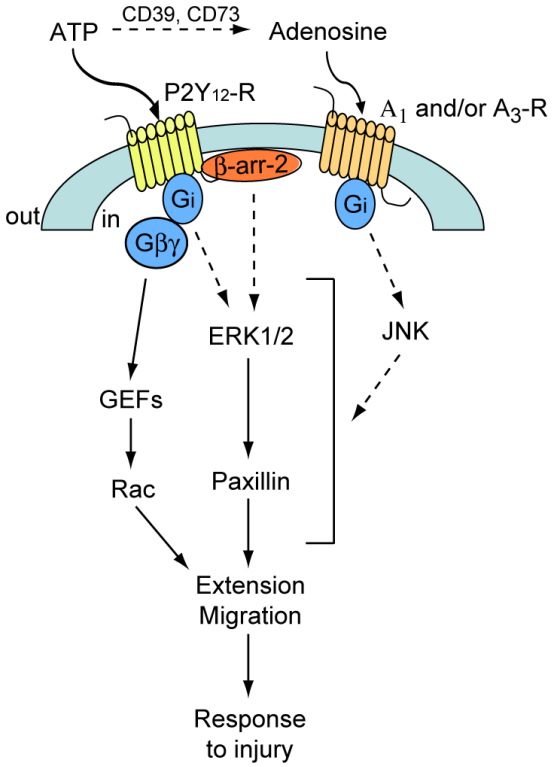

Figure 1.1. Intracellular pathways mediating ATP-induced microglial migration. Resting microglia express $P2Y_{12}$ receptors, which are activated by ATP, and A_1 and/or A_3 receptors, which are activated by adenosine. Activation of $P2Y_{12}$ receptors has been shown to induce Rac activation through Gβγ and guanine nucleotide exchange factors (GEFs), and paxillin activation by extracellular signal-regulated kinases-1/2 (ERK1/2). Both of these can lead to actin cytoskeleton rearrangements to promote process extension and migration in response to injury. Adenosine enhances ATP-induced migration and activation, likely through activation of c-Jun N-terminal kinase (JNK), but it is not known where adenosine signaling intersects with $P2Y_{12}$ receptor signaling.

chemoattraction of monocytes by other factors released by the damage.

An interesting characteristic of ATP/ADP-induced microglial migration and process extension is the potentiation of the response by adenosine. Addition of adenosine promotes process extension by resting microglia (Ohsawa et al., 2012; Wollmer et al., 2001), which is mimicked by an adenosine A_3 receptor agonist (Ohsawa et al., 2012). Adenosine, acting on either A_1 or A_3 receptors, also enhances ATP/ADP-induced microglial migration (Färber et al., 2005; Ohsawa et al., 2012). Preventing ATP breakdown to adenosine by deletion of apyrase/CD39 (see Fig. 1.2) reduces not only ATP-induced migration *in vitro*, but also accumulation of microglia to sites of damage after ischemia, entorhinal cortex lesion or facial nerve axotomy (Färber et al., 2005). This represents a fascinating phenomenon in which both a compound and its metabolites, acting through different receptors, are essential for a maximum response.

Finally, like many other microglial function, microglial motility is a plastic response that changes under different conditions. For example, LPS-induced microglial activation decreases the cells' responsiveness to P2Y ligands in terms of calcium transients (Möller et al., 2000), likely through downregulation of $P2Y_{12}$ receptors at the mRNA and protein levels (Haynes et al., 2006). In contrast, $P2Y_{12}$ expression is increased in status epilepticus induced by a kainate injection, and microglia in slices prepared from those animals extend processes faster to a point application of ATP from a micropipette compared to untreated animals (Avignone et al., 2008). Adenosine receptor expression is also modified by microglial activation. Treatment of microglia with LPS causes downregulation of A_3 receptors (van der Putten et al., 2009) and upregulation of A_{2A} receptors (Orr et al., 2009). In contrast to the chemoattraction and process extension induced by ATP in resting microglia, ATP causes process retraction and migration away from the ATP source in an A_{2A} receptor-dependent manner in LPS-activated microglia (Orr et al., 2009; van der Putten et al., 2009). Thus, microglia under pro-inflammatory conditions might exhibit different patterns of motility compared to microglia in the healthy brain, which could affect their response to tissue damage and cell death. This possibility is examined in Chapters 4 and 5.

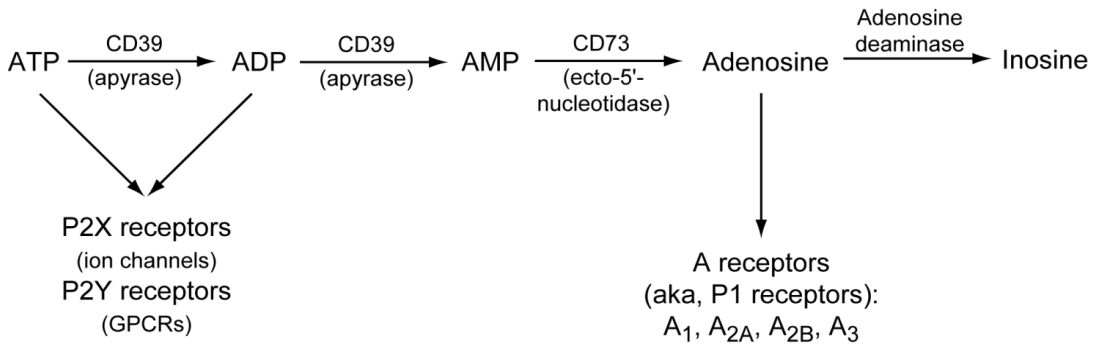

Figure 1.2. Purinergic signaling pathways in the brain. ATP is sequentially broken down to ADP and then AMP by CD39/apyrase. Both ATP and ADP serve as ligands for P2X receptors, which are ion channels, and P2Y receptors, which couple to G-proteins. CD73 (also known as ecto-5'-nucleotidase) converts AMP to adenosine. Adenosine activates the family of A receptors (also known as P1 receptors). The degradation of ATP is completed by adenosine deaminase to generate inosine.

1.6.b. Regulation of microglial motility by adrenergic signaling

The neurotransmitter norepinephrine is well known to modulate microglial cytokine secretion and phagocytosis, and is able to ameliorate AD pathology (discussed in greater detail in Section 6.2). However, not much is known about the effects of NE on microglial motility. NE enhances Aβ-induced migration of resting microglia in a Boyden chamber migration assay, and promotes migration *in vivo* to Aβ injected in the cortex of mice (Heneka et al., 2010). Consistent with this, depletion of NE by toxin-induced degeneration of NE-releasing neurons in the locus coeruleus reduces microglial migration to Aβ plaques *in vivo* (Heneka et al., 2010). Yet, there is no detailed characterization on the effects of NE on microglial process dynamics. Hence, this was carried out here, and the results are presented in Chapter 6.

1.7. Dissertation outline

As the sections above highlight, microglia with an activated morphology are present in neurodegenerative diseases. Moreover, the continuous microglial process motility likely serves important functions in maintaining brain homeostasis. Yet, little is known about the dynamics of activated microglia in neurodegenerative conditions. Thus, the goal of my dissertation was to examine microglial motility under pro-inflammatory conditions, including in native tissues, and to determine how activated microglia respond to disturbances in tissue integrity. In Chapter 2, I describe the methods I employed in answering this question. In Chapter 3, I use pharmacological approaches to elucidate the signaling pathways that regulate microglial motility *in vitro*. The use of isolated primary microglia in this chapter will confirm that all pharmacological tools can directly affect microglia. In Chapters 4 and 5, I use two models of *in vivo* microglial activation to study the ability of microglia to respond to cell death in tissues. First, the inflammogen LPS is used as a model of peripherally induced neuroinflammation (Chapter 4), and I examine microglial responses to a laser ablation in live mice with two-photon microscopy. Next, microglia are

activated indirectly, from the undergoing degeneration induced by dopaminergic neuron death in the substantia nigra of MPTP-treated mice (Chapter 5). To study microglial motility in the substantia nigra, I employ confocal imaging of acute brain slices and mechanical tissue damage. The emphasis of Chapters 3-5 is the involvement of purinergic signaling, especially adenosine A_{2A} receptors, in modulating microglial motility. In order to determine whether other neurotransmitter receptor families can influence microglial process dynamics, I chose to characterize the effects of adrenergic receptors on microglial motility in Chapter 6. Finally, in Chapter 7, I summarize my findings and discuss how they might relate to microglial functions in AD and PD. Studying microglial motility, especially in the context of neurodegeneration, might result in novel insights in the pathology of neurodegenerative diseases and ultimately lead to the development of new therapeutic approaches.

CHAPTER 2: Methods

2.1. Reagents and animals

Chemicals that inhibit or activate various targets were purchased from Sigma (adenosine, ADPβS, ATP, CGS-21680, caffeine, norepinephrine, IBMX, isoproterenol, phentolamine, propranolol), Tocris (2-Cl-IB-MECA, 2'-MeCCPA, clopidogrel, UK-14,304) or Calbiochem (forskolin, NF449, PTx). Stock solutions were prepared in de-ionized water (ATP, adenosine, ADPβS, caffeine, isoproterenol, NF449, phentolamine, propranolol, Pertussis toxin, UK-14,304) or dimethylsulfoxide (DMSO; CGS-21680, 2'-MeCCPA, 2-Cl-IB-MECA, clopidogrel, preladenant; ≤0.1% v/v final DMSO concentration). Working solutions were prepared in the appropriate buffer immediately before use. Preladenant was synthesized by Ethel Garnier-Amblard (Department of Chemistry, Emory University) as described (Neustadt et al., 2007). Chemical analysis with ^{1}H and ^{13}C nuclear magnetic resonance (NMR) and infrared (IR) spectroscopy confirmed the recovery of the intended product at >99% purity. Preladenant used for animal injections was prepared in 50% polyethylene glycol 400 as described (Hodgson et al., 2009).

Different *E. coli* strains were used as sources of LPS for the *in vitro* and *in vivo* activation of microglia. *In vitro* activation was achieved with LPS from strain O26:B6 (Sigma, cat. # L2654), while LPS from *E. coli* strain K-235 (Sigma, cat. # L2143) was used for mouse injections. MPTP for mouse treatments was purchased from Sigma (cat. #M0896).

Microglia for confocal imaging experiments were prepared from *actin-GFP* mice (provided by M. Okabe, Osaka University, Japan) that express GFP in all cells under the control of the actin promoter. $CX_3CR1^{GFP/GFP}$ mice that exhibit microglia-specific enhanced GFP expression (Jung et al., 2000) were purchased from Jackson Labs and bred in-house with C57Bl/6 mice (purchased from Charles River) to generate $CX_3CR1^{GFP/+}$ mice used for *in vivo* imaging and slice preparations. The mice were housed in groups of up to 5 mice per cage and exposed to a normal dark/light cycle. Both males and females were used for experiments. All procedures

involving the use of animals were reviewed and approved by the Emory University or the University of California, San Francisco Institutional Animal Care and Use Committees.

2.2. Primary microglia culture

Primary cortical microglia were obtained from P0-P5 postnatal *actin-GFP* pups using procedures described before (Orr et al., 2009). After decapitation, the brain was taken out of the skull, halved along the midline, and the meninges removed. To obtain cortical cultures, the midbrain and hippocampus were also removed. Then, the tissue was triturated to dissociate cells. The resulting cell cultures were maintained in Dulbecco's Modified Eagle Medium (DMEM) with high glucose (4500 mg/mL) containing 10% heat-inactivated fetal bovine serum, 10% heat-inactivated horse serum, 1% sodium pyruvate, 2 mM L-glutamine, 100 U/mL penicillin and 100 µg/mL streptomycin (all purchased from Invitrogen) to obtain astrocytes-microglia co-cultures. The cultures were then maintained at 37^{o}C, 5% CO_2. Microglia that were 98.0 ± 1.2% pure [assessed by isolectin-B_4 (IB_4) staining; Fig. 2.1] were obtained by aspirating the media containing free-floating microglia from the adherent astrocytes after at least 10 days of incubation. Microglia could be aspirated repeatedly until the cultures reached ~30 days *in vitro* (Floden and Combs, 2007).

2.3. Reverse transcriptase PCR (RT-PCR)

Total cellular RNA was isolated from primary microglia or tissue lysates using the PureLink RNA Mini Kit (Invitrogen). If tissues were the source material, they were added to lysis buffer containing 1% 2-mercaptoethanol (Sigma) and passed ten times through 18-gauge needle to dissociate the cells. The cell suspensions (both from tissues and primary cells) were passed through homogenization tubes (Invitrogen) to lyse the cells. The total RNA, collected on silica membranes, was treated with 2 U/reaction DNase I (Invitrogen) to remove any contaminating DNA. Semi-quantitative reverse transcriptase PCR was carried out with 50 ng RNA as template

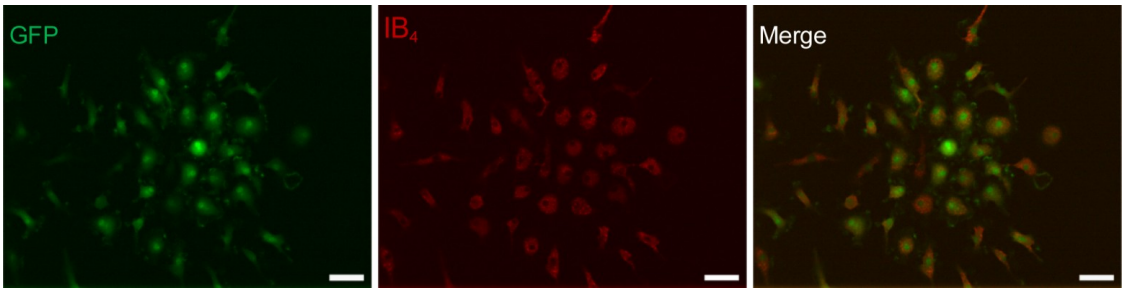

Figure 2.1. Assessing microglial purity by IB_4 staining. Primary *actin-GFP* microglia were plated on coverslips coated with 50 ng/mL poly-D-lysine and stained with Alexa 594-conjugated IB_4 (1:1000 dilution, Invitrogen) for 30 min, which is a marker specific to myeloid cells. Representative image from one out of nine coverslips is shown. Out of 249 GFP-positive cells, 246 were also positive for IB_4. Scale bar: 20 μm.

using the SuperScript III One-Step RT-PCR System with Platinum *Taq* DNA Polymerase (Invitrogen). The protocol included incubation at 60°C for 30 min for complementary DNA (cDNA) synthesis before amplification, which consisted of heating to 94°C for 2 min and 40 cycles of 94°C for 15 s, 60°C for 30 s, and 70°C for 1 min with a final extension at 68°C for 5 min. Increasing or decreasing the number of amplification cycles resulted in an altered level of product, suggesting that this protocol could detect changes in starting template levels. Amplification for TNF-α required 35 cycles in order to clearly see differences in product. Primer sequences are provided in Table 2.1.

2.4. Real-time quantitative PCR (qPCR)

Total cellular RNA was isolated from primary microglia as described in Section 2.3 above. cDNA was synthesized from 1 μg of RNA using random primers and the High Capacity cDNA Reverse Transcription system (Applied Biosystems) by amplification at 25°C for 10 min, 37°C for 2 hr, and 85°C for 5 min. The resulting cDNA (250 ng) was used as starting material for real time PCR using TaqMan Fast Universal PCR Master Mix (Applied Biosystems). Primers for the different adrenergic receptors and glyceraldehyde phosphate dehydrogenase (GAPDH) are available from the Applied Bioscience TaqMan Gene Expression Assays (Table 2.2). Amplification was carried out with the Applied Biosystems 7500 Fast Real-Time PCR System. Running conditions for all probes consisted of incubation at 50°C for 2 min and 95°C for 10 min followed by 40 cycles of 95°C for 15 s and 60°C for 1 min. Data were analyzed using 7500 Software Suite (v2.0). RNA isolated from cortical lysates was used as a positive control for receptor expression. The relative expression of each receptor, normalized to its expression in the cortex of PBS-injected mice, was calculated using the $2^{-\Delta\Delta Ct}$ method that compares the amplification cycle numbers at which a threshold fluorescence is reached between a sample of interest and a control sample (Livak and Schmittgen, 2001). To activate primary microglia *in vitro*, the cells were treated with 100 ng/ml LPS for 24 h. *In vivo* activation was achieved by

Table 2.1. Primers used for reverse transcriptase PCR

Primer		Sequence (5' → 3')	Amplicon size (bp)
IL-1β[a]	Fwd	AATCTCACAGCAGCACATCAA	671
	Rev	AGCCCATACTTTAGGAAGACA	
TNF-α[b]	Fwd	GCGGAGTCCGGGCAGGTCTA	458
	Rev	GGGGGCTGGCTCTGTGAGGA	
$P2Y_{12}$[c]	Fwd	CCTCAGCCAATACCACCTTCTCCCC	1004
	Rev	CGCTTGGTTCGCCACCTTCTTGTCCCTT	
A_1[d]	Fwd	GTGATTTGGGCTGTGAAGGT	322
	Rev	CAAGGGAGAGAATCCAGCAG	
A_{2A}[d]	Fwd	CACGCAGAGTTCCATCTTCA	497
	Rev	AGCAGTTGATGATGTGCAGG	
A_{2B}[d]	Fwd	GCGAATAAAAGCTGCTGTCC	245
	Rev	AAAATGCCCACGATCATAGC	
A_3[d]	Fwd	GACTGGCTTCAGAGAGACGC	202
	Rev	AGGGTTCATCATGGAGTTCG	
β-actin[e]	Fwd	TGACGGGGTCACCCACACTGTGCCCATCTA	660
	Rev	CTAGAAGCATTGCGGTGGACGATGGAGGG	

Sequences for the forward (Fwd) and reverse (Rev) primers used to amplify the indicated targets with RT-PCR. All primers have melting temperature of 60ºC. bp, base pairs. Sources: [a]Tha et al. (2000); [b]This study; [c]Haynes et al. (2006); [d]Hoskin et al. (2002); [e]Bianco et al. (2005).

Table 2.2. Primers used for quantitative real time PCR

Target	TaqMan Gene Expression Assays probe ID	Amplicon size (bp)
α_{1A}	Mm00442668_m1	95
α_{1B}	Mm00431685_m1	97
α_{1D}	Mm01328600_m1	66
α_{2A}	Mm00845383_s1	86
α_{2B}	Mm00477390_s1	59
α_{2C}	Mm00431686_s1	72
β_1	Mm00431701_s1	76
β_2	Mm02524224_s1	75
β_3	Mm00442669_m1	57
GAPDH	Mm99999915_g1	107

All target assays were purchased from Applied Biosystems TaqMan Gene Expression Assays with the provided probe IDs. Each assay consists of unlabeled amplification primers and a fluorescent probe. All probes contained 6-hydroxyfluorescein (FAM^{TM}) as a fluorescent label at the 5' end and dihydrocyclopyrroloindole tripeptide/minor groove binder (MGB) as a non-fluorescent quencher at the 3'end.

injecting mice with 2 mg/kg LPS in the intraperitoneal cavity (i.p.) or vehicle (phosphate-buffered saline, PBS) 2 days prior to tissue isolation.

2.5. cAMP assay

Human embryonic kidney (HEK) 293 cells were plated in 96-well plates at 5,000 cells/well and cultured for 2 days using previously published culture conditions (Ogden and Traynelis, 2013). The cells in each well were transfected with 0.1 μg cDNA for mouse adenosine receptors (A_1, A_{2A}, A_3) using the FuGene6 transfection method at 1:3 ratio of cDNA-to-FuGene (Roche). On the next day, cells were pre-treated with the phosphodiesterase inhibitor IBMX (0.75 mM) for 10 min, followed by treatment with selective receptor agonists alone or in combination with the adenylate cyclase activator forskolin (30 μM) for 30 min. cAMP levels were detected with the CatchPoint cAMP kit (Molecular Devices): cells were lysed and anti-cAMP antibody and cAMP-horseradish peroxidase (HRP) conjugate were added to the lysates in a competition-based mode. After 2 hr of incubation and washing the plate, StopLight Red substrate for HRP was added for 10 min, and fluorescence was read at 530 nm excitation, 590 nm emission wavelengths. cAMP concentrations were calculated from a standard curve.

2.6. Preparation of acute brain slices

Acute brain slices were prepared from 1-4-month old $CX_3CR1^{GFP/+}$ transgenic mice using methods described before (Lee et al., 2007). Mice were deeply anesthetized with isoflurane before decapitation with sharp scissors. The brain was removed from the skull, the cerebellum was discarded, and part of the frontal cortex was cut off to provide a surface for mounting the brain for slicing. The brain was secured to the stage of a Leica VT1000S vibratome, cortex down, ventral side facing the metal razor blade, with SuperGlue (Fig. 2.2A). Coronal slices were cut at a thickness of 200 μm in ice-cold oxygenated cutting solution that contained (in mM) 130 NaCl,

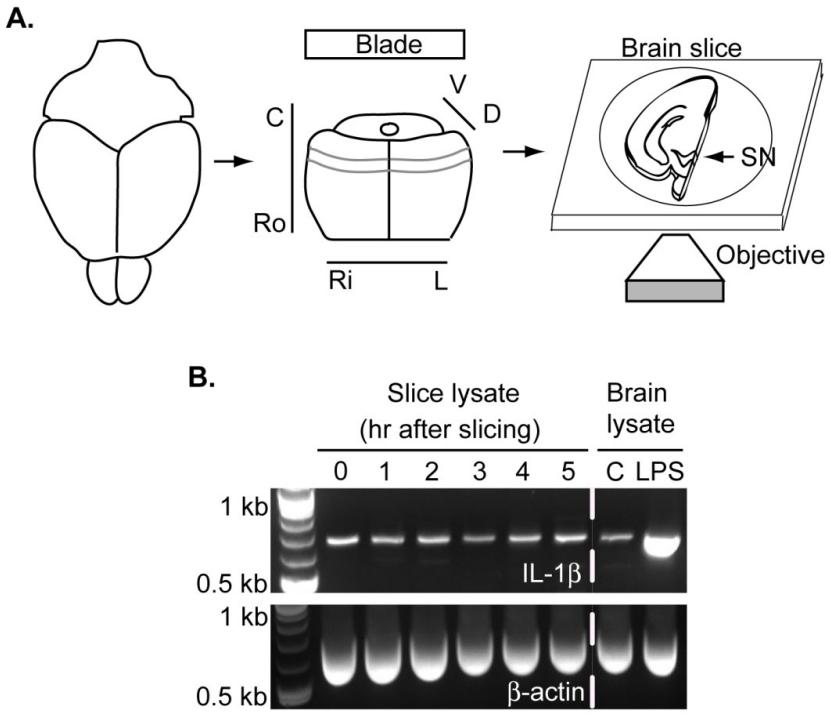

Figure 2.2. Preparation of acute brain slices for imaging. A. Mouse brains were isolated from the skull, the cerebellum, olfactory bulb and part of prefrontal cortex were removed, and the brain was positioned on a vibratome stage for slicing. The orientation of the brain was such that the ventral part of the brain was facing the vibratome blade. Letters refer to coordinate axes: C, caudal; Ro, rostral; Ri, right; L, left; V, ventral; D, dorsal. Once slices were cut, the two hemispheres were separated. Only one hemisphere was imaged at a time. SN, substantia nigra. **B.** The slicing procedure does not induce classical microglial activation. The expression of the pro-inflammatory cytokine IL-1β was determined with RT-PCR at different time points after slice preparation. As positive control for microglial activation, IL-1β expression in slices was compared to midbrain lysates from PBS- (C) or LPS-injected mice.

2.5 KCl, 1.25 NaH_2PO_4, 10 glucose, 24 $NaHCO_3$, 3 $MgSO_4$, and 1 $CaCl_2$ equilibrated with 95% O_2 and 5% CO_2 to bring the pH to ~7.4. The slices were then maintained in oxygenated artificial cerebrospinal fluid (aCSF) for at least 1 hr at room temperature (to allow the tissue to recover from slicing) and up to 5 h before imaging. The composition of the aCSF was (in mM) 130 NaCl, 2.5 KCl, 1.25 NaH_2PO_4, 10 glucose, 24 $NaHCO_3$, 1.5 $MgSO_4$, and 1.5 $CaCl_2$. The cutting procedure and maintenance of slices in aCSF do not affect cytokine mRNA synthesis in this time frame as determined by reverse transcriptase PCR (Fig. 2.2B).

Slices were prepared from either LPS- or MPTP-treated mice (Chapter 4) or untreated mice (Chapter 6). The LPS treatment paradigm consisted of a single injection of 2 mg/kg i.p. and preparation of slices or isolation of tissues two days later. MPTP injections, performed by Dr. Carlos Lazo (Dr. Gary Miller's lab), consisted of daily subcutaneous (s.c.) injections of 20 mg/kg/day of the neurotoxin (free base) for 5 consecutive days for a total dose of 100 mg/kg. This dose is lower than the one commonly used in the literature [30 mg/kg/day for 5 days for a cumulative dose of 150 mg/kg; Jackson-Lewis and Przedborski (2007)]. However, the 150 mg/kg dose resulted in high mortality for the $CX_3CR1^{GFP/+}$ mice. A total dose of 100 mg/kg MPTP is known to induce dopaminergic neuronal loss (Seniuk et al., 1990), which was also detected here (see Section 4.3.c). Mice were sacrificed 4-7 days after the conclusion of the MPTP treatment to obtain slices for immunohistochemistry or imaging experiments.

2.7. Immunohistochemistry

Changes in tyrosine hydroxylase (TH), Iba1, and adenosine A_{2A} receptor expression were detected with immunohistochemistry of free-floating brain sections. The brains of MPTP- or saline-treated mice were collected 5 days following the final MPTP injection, drop-fixed in 4% paraformaldehyde (PFA) overnight, and cryoprotected through passages in 15% and 30% sucrose overnight. Brains were embedded in Optimum Freezing Medium (TissueTek), and sliced on a cryostat to prepare 40 μm-thick coronal slices. Unless otherwise indicated, all solutions were

prepared in PBS, and all incubations were performed with stirring. All washes consisted of three 10-min incubations in PBS.

For TH and Iba1 staining, slices containing the SN or striatum were treated with 3% hydrogen peroxide for 10 min, blocked with 10% normal goat serum + 0.15% Triton X-100 for 1 hr, and incubated in rabbit anti-TH antibody (Millipore AB152, 1:1000 dilution) or rabbit anti-Iba1 antibody (Wako 019-19741, 1:1000 dilution) overnight at 4ºC. After washing out the primary antibody, biotinylated goat anti-rabbit secondary antibody (Vector Labs BA-1000, 1:200 dilution) was applied for 1 hr in blocking buffer. Following a wash step, the signal was visualized using the avidin-biotin complex (ABC) system (Vectastain ABC Kit) and 3,3'-diaminibenzidine (DAB) substrate (Vector Labs). Avidin and biotinylated peroxidase were pre-mixed for 30-40 min before applying them to the slices for 45 min. Finally, after washing off unbound peroxidase complexes, the slices were incubated in DAB substrate solution until signal appeared (~1-2 min). The slices were mounted on coverslips, dehydrated in ethanol, cleared with xylene, and coverslipped with Cytoseal (Richard-Allan Scientific).

To detect A_{2A} receptors, slices were blocked in 10% normal donkey serum + 1 % bovine serum albumin (BSA) + 0.3% Triton X-100 for 1 hr and incubated in mouse anti-A_{2A} antibody (Millipore 05-717, 1:1000 dilution) overnight at room temperature. Slices were then washed and incubated with donkey anti-mouse Texas Red-conjugated secondary antibody (Jackson ImmunoResearch 715-295-150, 1:200 dilution) for 2 hr, washed again, mounted on coverslips, allowed to air-dry and coverslipped with Vectashield (Vector Labs). For visualization of A_{2A} receptor-stained sections, slices were imaged with an Olympus IX51 confocal microscope. Slices from saline-treated mice containing the striatum were used to determine imaging conditions because of the constitutive A_{2A} receptor expression there. The Texas Red fluorophore was detected by excitation at 590 nm. Microglia were visualized by detecting the GFP signal with excitation at 480 nm. Because GFP is genetically encoded in the $CX_3CR1^{GFP/+}$ mice, no staining was necessary. Colocalization of the GFP and Texas Red signals was quantified in Imaris v7.6

(Bitplane AG, Switzerland) using the method developed by Costes et al. (2004). The images were thresholded to the background fluorescence of each individual section and for each channel. The colocalization analysis was carried out only for the brain regions of interest (substantia nigra or striatum) by masking the rest of the image. The average probability of detecting significant colocalization for all images was $P = 1.0$. The average Mander's coefficient for each channel of the signal above the threshold for each image was used to compare different treatments.

Some 200 µm-thick slices were prepared as for imaging (Section 2.6), but used for staining (performed by the lab of Dr. Yoland Smith) in order to quantify the extent of induced mechanical tissue damage (Section 2.8.b). After induction of injury, the slices were fixed in 4% PFA overnight. Slices were treated with 1% sodium borohydride for 20 min before washing five times in PBS and blocking for 1 hr in 1% normal horse serum + 0.3% Triton X-100 + 1% BSA. The primary anti-NeuN antibody (Millipore MAB377, 1:2000 dilution) was applied overnight. After washing off unbound antibody, the slices were incubated with secondary horse anti-mouse antibody at 1:200 dilution in 1% normal horse serum + 0.3% Triton X-100 + 1% BSA for 90 min. Then, the signal was visualized by incubation in ABC as described above, but for 90 min. After two washes in PBS and a wash in Tris, the slices were added to DAB (Sigma) for 10 min before mounting and coverslipping.

2.8. Confocal imaging

2.8.a. Confocal imaging of isolated cells

Microglial process dynamics were studied as described previously (Orr et al., 2009). Primary microglia from *actin-GFP* mice (isolated as described in Section 2.2) were plated on top of the three-dimensional substrate Matrigel (BD Biosciences). Microglia were allowed to enter the ~150 µm-thick gel overnight, and typically assume a 3D morphology. When necessary, microglia were activated with 100 ng/mL LPS for 24 hr. The cells were imaged using an Olympus IX51 inverted confocal microscope equipped with a disk spinning unit (DSU)

attachment and a Hamamatsu 1394 ORCA-ERA CCD camera under 60X magnification (NA 1.1). Microglia were perfused for the duration of the experiment with imaging buffer containing (in mM) 150 NaCl, 10 HEPES, 3 KCl, 22 sucrose, 10 glucose, 2 $CaCl_2$, 1 $MgCl_2$. The imaging protocol included a baseline reading for 5 min to establish resting motility, followed by application of specified treatments for 5 min, and washout for 5 min. Stacks of optical section spaced 1 μm apart were acquired every 30 s with the IPlab image acquisition software v4.0 (Becton, Dickinson and Company) for 25-35 sections per cell.

2.8.b. Confocal imaging of acute brain slices

Slices prepared as described in Section 2.6 were placed on the stage of an Olympus IX51 inverted confocal microscope equipped with DSU attachment and constantly perfused with oxygenated aCSF at 32 °C. To prevent slice movement during solution flow, a platinum ring with nylon threads was placed above the slices. Images were captured with a Hamatsu 1394 ORCA-ERA CCD camera and the IPlab software.

Two experimental protocols were used to image the slices. First, to study the process dynamics of individual cells, slices were imaged at 60x magnification (Olympus LUMFI water-immersion objective, NA 1.10). Imaging consisted of a baseline reading for 5 min followed by application of aCSF alone or different treatments in oxygenated aCSF for 25 min. To better represent the complicated microglial morphology, ~30-50 optical sections along the z axis of the slices were collected every 60 s; each section was located 1 μm above the previous one.

Second, slices were used to study the response of microglia to localized tissue damage. For this imaging protocol, imaging was carried out at 20x magnification (Olympus UPlanFL N air objective, NA 0.50) to obtain 31 optical sections through the slices (1 μm step) every 30-60 s. Following recording of baseline motility for 20 min, a blunted 31-gauge needle with ~300 μm diameter (referred to as “rod”; Fig. 2.3) was lowered into the slice to induce localized tissue injury. The rod was carefully positioned over the substantia nigra pars compacta (SNc) and

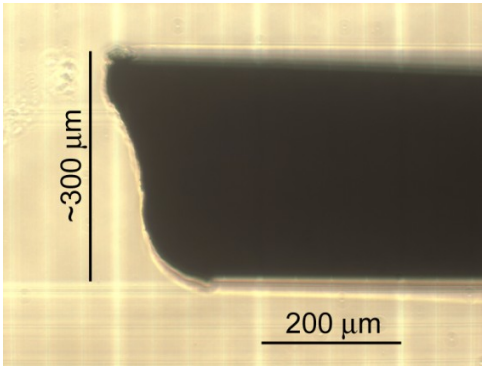

Figure 2.3. Rod used to induce localized injury in acute brain slices. The rod was created by blunting a 31-gauge needle. The final diameter of the rod is ~300 µm.

lowered at a rate of ~100 μm/s for 180 μm into the tissue by a closed-loop micromanipulator (SD Instruments, model MC1000e). A second 20-min recording was set up as soon as the injury was created in order to capture the microglial response. For some experiments, the $P2Y_{12}$ receptor antagonist clopidogrel (2 μM) or the adenosine A_{2A} receptor antagonist preladenant (5 μM) were included in the perfusion solution for the duration of the experiment (baseline recording, induction of injury, response to injury).

2.9. Two-photon imaging

Imaging of the cortex of anesthetized 2-5 month old $CX_3CR1^{GFP/+}$ mice that exhibit microglia-specific GFP expression (Jung et al., 2000) was performed as previously described (Davalos et al., 2005; Haynes et al., 2006). To study microglial motility under pro-inflammatory conditions, mice were injected with 2 mg/kg LPS i.p. two days before imaging. The mice were anesthetized with 200 mg/kg ketamine and 30 mg/kg xylazine in 0.9% NaCl solution. The skin was shaved, incised and retracted, and a small area of the skull (~1 mm in diameter) was thinned to about 50 μm thickness to create an imaging window over the somatosensory cortex of adult mice (Fig. 2.4A). Two multiphoton microscopes, both employing Spectra Physics MaiTai DeepSee Ti-sapphire lasers, were used: a Prairie Technologies Ultima IV and an Olympus Fluoview 1000MPE microscope. Each imaging session consisted of obtaining time-lapse imaging data for baseline microglial behavior, followed by a laser ablation and the recording of microglial responses to it. 3D image stacks were obtained using an Olympus 40x 0.8NA water-immersion objective and 1.5X optical zoom. Stacks spanning 30-40 μm vertical distance of the cortex with 1 μm step between optical planes were acquired every 30 s for 10 min to record baseline process motility. Laser ablations with a diameter of ~20 μm were induced by focusing a high-energy laser beam (800 nm wavelength for 0.5-2 s, depending on bone thickness). Subsequent imaging (60 min total duration, 3 min intervals between stack acquisitions) allowed for the detection of

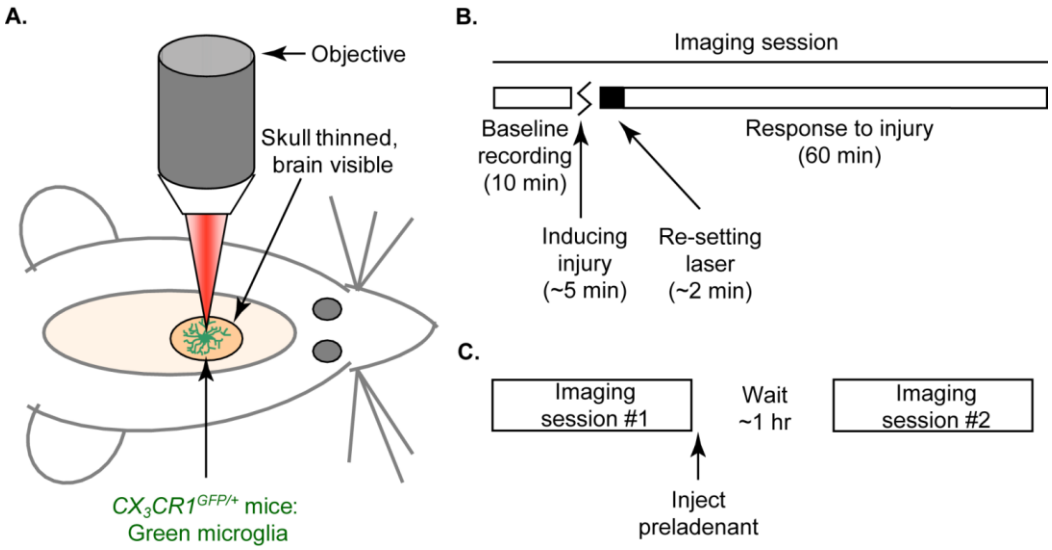

Figure 2.4. ***In vivo*** **two-photon imaging. A.** Preparing the mice for imaging. $CX_3CR1^{GFP/+}$ mice have microglia-specific GFP expression. The mice were anesthetized with ketamine/xylazine, the skin on top of the head was shaved and cut along the midline to expose the skull. The skull was thinned to ~50 µm with a high-speed dental drill to create a "window" with ~1 mm diameter. The mice were then secured on a two-photon microscope for imaging. **B.** General imaging timeline. Each imaging session consisted of four components: baseline recording, induction of injury by increasing the laser power, re-setting the laser to power levels appropriate for imaging, and a recording to capture the response to the laser ablation. **C.** For animals treated with the adenosine A_{2A} antagonist preladenant, the antagonist was administered at the conclusion of the imaging session. A second imaging session was performed ~1 hr later.

microglial responses to injury (Fig. 2.4B). It should be noted that time-lapse imaging of microglial responses to laser injury began ~2-3 min after the induction of injury to allow for the restoration of imaging parameters on the multiphoton laser. To examine the effects of preladenant on process motility *in vivo*, mice were first injected with 2 mg/kg LPS i.p. and imaged with two-photon microscopy two days post injection. After induction of injury and the conclusion of the one-hour imaging session, mice were injected with 3 mg/kg preladenant. A second imaging session, consisting of both a baseline recording and a second laser ablation, was performed ~1 hr following the preladenant injection to allow the antagonist to distribute throughout the body (Neustadt et al., 2007). In this way, we had recordings before and after preladenant treatment in the same animal for a total of seven animals (Fig. 2.4C).

Although thin skull windows were prepared in the same way, the intensity of the detected fluorescence varied between animals depending on depth of imaging field in the cortex, the thickness of the skull, chosen exposure time, and other factors. As a result, poor signal-to-noise ratio in some animals prevented clear representation of microglial processes and data analysis. If the average fluorescence intensity of an image stack was less than ~25 arbitrary units, ImageJ could not threshold the image (see later) as determined by visual examination; time sequences with average fluorescence intensity less than 25 units were eliminated from all analyses. Three control and one LPS-injected mice were excluded, but no preladenant-treated animals were excluded from analysis.

2.10. Image analysis

2.10.a. 3D cell reconstructions

Time sequences recording the dynamics in three dimensions of individual primary microglia in Matrigel (Section 2.8.a) were analyzed with Imaris software (v4.5). The background was subtracted from all recordings using a 10-μm filter. 3D reconstructions of the cells were then generated from the z stacks. To improve the quality of the representations, they were subjected to

a Gaussian smoothing algorithm with a 0.25-μm filter. The software then calculates various parameters of the reconstructed 3D surface such as surface area and volume by breaking the surface into small triangles (for surface area) or voxels (for volume) and summing them up. The surface area-to-volume ratio (SA/V) at each time point was used to determine changes in cell ramification in response to various treatments. Surface area-to-volume ratio values show a strong correlation with measurements of individual process velocity (Orr et al., 2009) and the total process length from maximum intensity projections (Fig. 2.5). The area under the ramification vs. time curves starting at application of treatment (t = 5 min) was used to quantitatively compare different treatments.

2.10.b. Analysis of microglial process length in acute brain slices

Each time point of time sequences of individual cells in acute brain slices was projected onto the xy-plane using the maximum intensity at each pixel position in the stack to obtain a 2D representation of the brain slice. The 2D maximum intensity projections were then used to calculate total process length with the ImageJ software (National Institutes of Health). Each cell process was manually traced and saved as a region of interest. The length of the region of interest was measured at the beginning of imaging, and its length was tracked at 5-min intervals. The sum of all processes was normalized to the total process length (sum of all regions of interest) during the baseline recording to allow comparison between cells with different degrees of starting ramification. It should be noted that changes in process length are likely underestimated because collapsing the stacks to a 2D projection does not allow us to fully capture movement in the vertical direction (Fig. 2.6); errors will be the same for both control and experimental conditions, and only modestly alter the ratio given individual processes do not shift angular displacement with treatment. For illustration of the process traces in Figure 6.2, the 2D projections were imported into Adobe Photoshop, and the processes were manually traced. For better visualization of the thin processes in movies and still images, the brightness and contrast for the whole movie

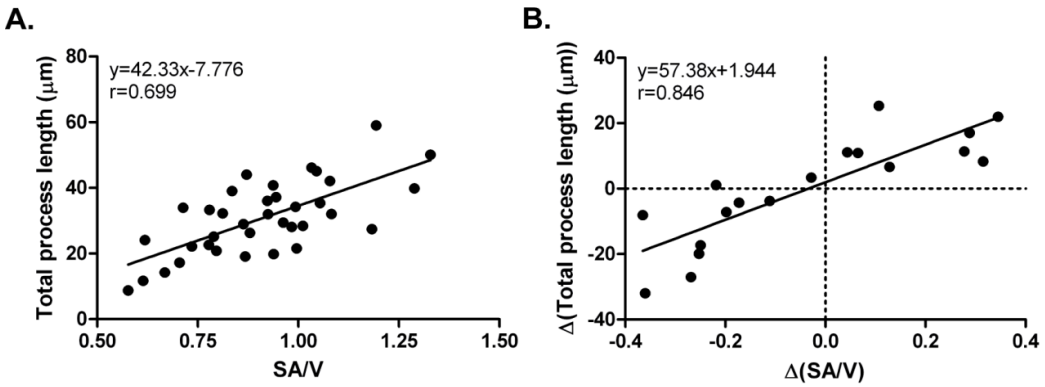

Figure 2.5. Correlation between process length and surface area-to-volume ratios for primary microglia in Matrigel. Optical sections of microglia from *actin-GFP* mice in Matrigel were used for 3D reconstructions of the cells with the Imaris software. Surface area-to-volume ratios were calculated from values of surface area and volume measured by the software. The length of each cell process was determined from maximum intensity projections of the cell in ImageJ. Individual process lengths were summed up to obtain the total length. A. There is a good correlation between SA/V and process length for a wide range of total process lengths. B. The change in SA/V correlates to the change in process length even better. Overall, the data indicate that an increase in SA/V correlate to an increase in process length, and vice versa for decrease. All conclusions about effects of treatments on process length were derived from changes in SA/V.

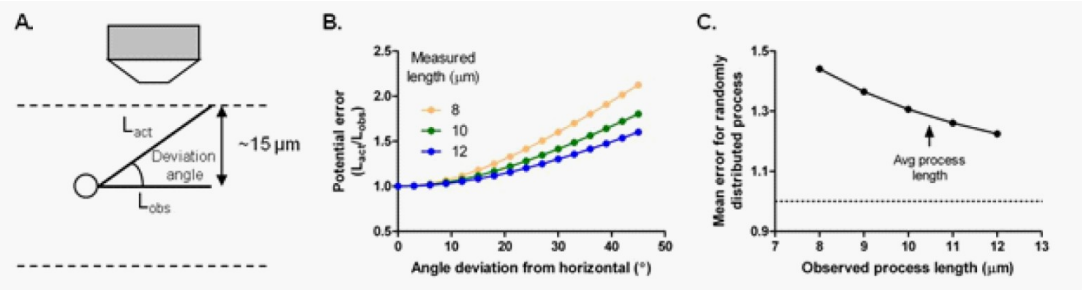

Figure 2.6. Potential error in estimating distances from 2D projections. A. Illustration of the potential problem of underestimating process length in collapsed 2D image of 30 mm z-stack. On average, microglial cell bodies are in the middle of a 30 µm-thick z-stack of optical sections. If a microglial process deviates from the plane of the cell body, the length (L_{act}) will be underestimated in a 2D projection when the whole stack is collapsed onto the xy-plane because the length will only be seen within the xy plane (L_{obs}). **B.** The difference in the actual length and the real length of the process varies as a function of the observed length (measured in 2D projections) and the deviation angle. This difference in actual and observed lengths defines the potential error in estimating process length. **C.** If processes are randomly distributed at different angles in the tissue, we can calculate the mean error for each process length by averaging the errors across all angles; this error decreases as the process length increases. For an average process of 10.5 µm, the observed length in the xy projection plane (L_{obs}) will underestimate the actual length by about 25% (L_{act}). That is, for a measured process length of 10.5 µm, the average actual length will be 13.7 µm. Errors will be the same for both control and experimental conditions, and only modestly alter the ratio given individual processes do not shift angular displacement with treatment.

were adjusted.

2.10.c. Analysis of microglial response to mechanical damage in slices

The optical sections at each time point of the time-lapse recordings (baseline and response to injury) were used to generate maximum intensity projections that were used to quantify microglial movement with the Imaris software (v7.6). The software detected objects with diameter larger than 2 μm, which mostly represents microglial processes. Cell bodies, identified as objects larger than 5 μm-diameter in eleven randomly selected recordings, represented 5.25% ± 0.55% of all objects. All objects were tracked over time with an Autoregressive Motion GapClose algorithm (max distance of 5 μm) to measure the displacement and velocity of each object at each time point in both the x- and y-directions. The net displacement and velocity were calculated with the Pythagorean theorem:

$$Length = \sqrt{(x_{t=20} - x_{t=0})^2 + (y_{t=20} - y_{t=0})^2}$$

The sign of the average displacement and velocity vectors were manually adjusted to reflect movement towards (positive) or away (negative) from the injury based on the signs of the average x- and y-components. While there is no injury in the baseline recording, the damaged site from the corresponding injury recording for each slice was used to adjust the direction of movement. Finally, the fraction of tracks with displacement longer than 5 μm gives an indication of the uniformity of movement – a large fraction of tracks with long displacement would suggest the presence of many processes moving over long distances rather than random motion with frequent changes in direction. There are no significant differences in the fluorescence intensities between paired (control-treatment) recordings, indicating that changes in response reflect changes in motility rather than inability of the software to detect moving objects (Fig. 2.7).

2.10.d. Analysis of in vivo two-photon imaging data

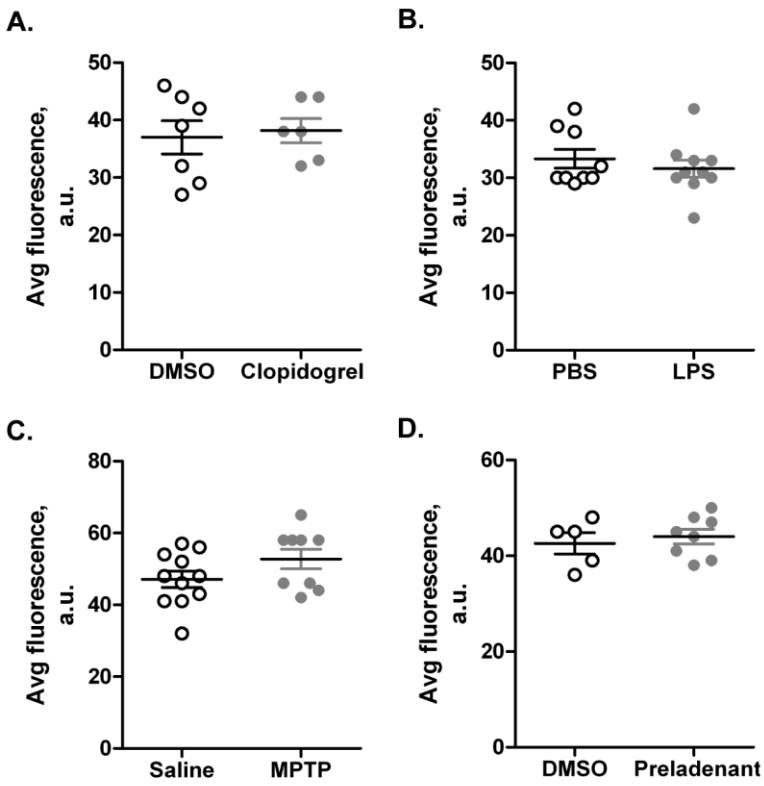

Figure 2.7. Fluorescence intensities of the slice recordings used to evaluate microglial response to injury. The average fluorescence of each file was measured on the first time frame of baseline recordings (in the absence of injury). The same area was imaged after induction of injury. Treatments (explained in detail in Chapter 4) included perfusion of slices with clopidogrel (**A**), preparation of slices from LPS- (**B**) or MPTP- (**C**) injected animals, and perfusion of slices with preladenant (**D**). There are no significant differences between each treatment and its corresponding control in terms of fluorescence intensity. Statistics: Student's *t* test.

The time-lapse two-photon sequences that were acquired *in vivo* were analyzed in two different ways. First, Imaris software (v7.6) was used to quantify the baseline process motility patterns of microglia in the absence of obvious tissue damage. Following 3D recreations of the imaged volumes, the software detected objects with diameter larger than 2 μm and tracked them over time with an Autoregressive Motion GapClose algorithm (max distance of 5 μm) to determine the speed of each object at each time point and the overall distance traveled over the course of imaging. These values were then used to calculate average length and speed of movement (regardless of direction) over the full duration of the recording. The size of microglial cell bodies and number of primary branches were quantified with ImageJ software. To facilitate data analysis, the optical sections over 30 μm were collapsed into a 2D image. The cell bodies that were fully within the imaging field were manually outlined, and the area of the resulting region of interest was measured. Similarly, the primary branches of cell bodies that were fully within the imaging field were manually counted.

Second, the time-lapse recordings of microglial responses to laser ablations were quantified with MGPtracker, a custom-written code implemented in Matlab that was developed by Dipankar Biswas and Dr. Frank Loth at the University of Akron. The code was designed to quantify the radially directed movement of microglial processes in response to tissue damage. Initially, ImageJ software was used to convert image stacks spanning 30 μm of vertical distance over and under the ablation site into maximum intensity projections on the xy plane. The threshold fluorescence that distinguishes fluorescent microglia from background was determined with the MaxEntropy thresholding function. The 2D time sequences were then analyzed with MGPtracker, which converts the recordings to binary (black-and-white) images by applying the previously determined thresholds. It then detects the microglial processes closest to the ablation (circle of autofluorescence close to the middle of the image) at 10° angles; the positions of these processes form the vertices of a polygon that represents a front of microglial processes that will

respond to the damage (Fig. 2.8). The different vertices of the front might move at different rates, but averaging all vertices for a given time point gives the average distance from the ablation of the microglial process at that time point. Repeating the calculations for each time point represents the approach waveform for each animal over time. The automated tracking allowed us to calculate three parameters: (1) the average distance of microglial processes from the ablation; (2) the size of the area surrounding the ablation bound by the polygon; and (3) the instantaneous radial velocity at each time point. Finally, the time when microglial processes reach the ablation site was calculated as the average of the times when individual vertices on the polygon reached the ablation; if a vertex never reached the ablation, its time was considered to be 60 min.

2.11. Iontophoresis

To study microglial chemotaxis, primary microglia from *actin-GFP* mice were plated on Matrigel as previously described (Orr et al., 2009). On the next day, the cells were imaged over time. Only a single optical plane through the middle of the cell was recorded. Chemotactic agents were added to a micropipette with ~3 MΩ resistance prepared by pulling thin-walled capillary tubes with 1.5 mm outer diameter and 1.12 mm inner diameter (World Precision Instruments, Inc). To prevent compound leak, a backing current of 700 nA was applied with a current generator (Dagan, model ION-100T), with the direction of the current depending on the charge of the compound. Negatively charged ATP was retained with positive current, and positively charged adenosine and CGS-21680 were retained with negative current. Ejection was achieved with a current of 1500 nA in the direction opposite to the backing current. Upon ejection, compounds diffuse away from the pipette, generating a gradient. Cells were constantly perfused with imaging buffer with a flow rate of ~1 mL/min; for some experiments, 30 μM NE or 5 μM preladenant were included in the perfusion solution. The time lapse recordings (5-min baseline and 25-min compound ejection) were analyzed with Imaris software (v7.6). Cells were detected using the Spots function and tracked by the software over time using the Autoregressive

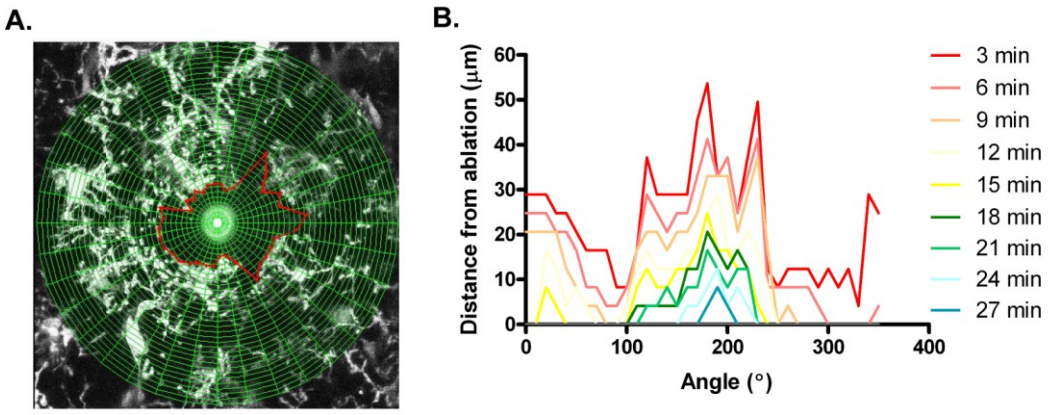

Figure 2.8. Tracking of microglial response to laser ablation *in vivo* with MGPtracker. MGPtracker is a set of algorithms implemented in Matlab that automatically tracks and quantifies the radial response of microglial processes to a laser ablation. **A.** An example of detection of microglial processes; the green radial lines divide the image in 36 sectors. The vertices of the red polygon correspond to the microglial processes closest to the ablation in each sector. **B.** Positions of the vertices of the front-tracking polygon at different time points.

algorithm. The spots had a minimum diameter of 5 μm to restrict tracking only to the cell body rather than processes. The migratory paths of each cell were visualized as tracks, and the magnitude of the vector displacement was calculated for quantification.

2.12. Live-cell calcium imaging

Calcium imaging of primary wild type microglia loaded with 5 μM Fura-2 AM (Invitrogen) was performed in a manner similar to that described for primary astrocytes (Lee et al., 2007). Microglia were treated with Hank's balanced salt solution (HBSS; control) to preserve their resting phenotype or activated with 100 ng/ml LPS for 24 h before imaging. Imaging was performed at room temperature (23 °C) with dual excitation at 340- and 380-nm wavelengths and emission from both at 510 nm. Images were captured with a MicroMax camera (Princeton Scientific Instruments). The emission signals from each excitation wavelength were used for ratio calculations (excitation at 340 nm divided by excitation at 380 nm) using Imaging Workbench software (Axon Instruments). The imaging protocol consisted of baseline reading for 60 s, application of 30 μM NE for 60 s, a wash for 120 s, application of 30 μM ATP for 60 s (positive control), and a final wash for 120 s. To facilitate comparisons between cells with different background levels of free calcium, all calculated ratios were normalized to the baseline reading according to the formula

$$R(t) = \frac{R_x(t)}{R(baseline)}$$

where $R(t)$ is the normalized ratio, $R_x(t)$ is the raw ratio at each time point, and $R(baseline)$ is the average of the raw ratios in the first 60 s before cells were stimulated with NE.

2.13. Statistical analysis

All time lapse recordings for imaging experiments were given non-descriptive names consisting of date and number; the researcher was blind to the particular treatment of each

recording during image analysis. Recordings were performed in random order of control and experimental conditions. Whenever appropriate, the measures under study were quantified and plotted as averages ± standard error of the mean (s.e.m.). Statistical tests were performed in SigmaPlot v11.0 and GraphPad Prism v5. For each experiment, the sample sizes and appropriate tests [analysis of variance (ANOVA), two-tailed Student's *t*-test] and *post hoc* tests, if necessary, are indicated in the text and figure legends. Results were considered to be significantly different if $p < 0.05$.

CHAPTER 3: Modulation of microglial motility by purinergic receptors *in vitro*

3.1. Abstract

Under physiological conditions, microglia are in a "resting" state and constantly sample the brain extracellular environment. In cases of injury and cell death, microglia extend their processes to the site of injury and appear to clear cellular debris by phagocytosis. This extension process is mediated by ATP released by damaged cells that activates $P2Y_{12}$ receptors on microglia. However, ATP causes process retraction and migration away from its source in LPS-activated microglia *in vitro*. The differential effects of ATP can be explained by its breakdown to adenosine and subsequent binding to adenosine A_{2A} receptors in activated microglia. Furthermore, cell activation causes a switch in receptor expression so that $P2Y_{12}$ receptors are expressed on non-activated microglia, while A_{2A} receptors are predominantly expressed on LPS-activated microglia. In order to better elucidate the contribution of the different receptors on microglial process dynamics, I performed *in vitro* time lapse confocal imaging to follow the changes in morphology of primary microglia grown in 3D gels. The non-hydrolysable $P2Y_{12}$ receptor agonists ADPβS and ATPγS caused process extension in resting microglia, but had no effect on process motility in activated cells. On the other hand, the adenosine A_{2A} receptor agonists adenosine and NECA were inactive in resting cells, but caused significant process retraction in activated microglia. The A_1 and A_3 adenosine receptors appear not to contribute to the adenosine-mediated process retraction, as A_1 and A_3 agonists (2'-MeCCPA and 2-Cl-IB-MECA, respectively) had little/no effect on process dynamics. Taken together, these results indicate that activated microglia utilize a different signaling system from non-activated cells that can potentially be targeted to modulate the response of microglia to neuronal injury.

3.2. Introduction

Small-scale damage to the brain parenchyma, such as rupture of small blood vessels and cell death, occurs on a daily basis (Hanisch and Kettenman, 2007). The ability of microglia to

detect and respond to tissue damage is thought to be essential for their role in maintaining normal brain homeostasis (Hanisch and Kettenman, 2007). Microglia extend their processes to surround the damaged area, likely phagocytosing cellular debris to prevent its spread to the surrounding healthy tissue. The response is mediated *in vivo* by ATP released from the dead cells and activation of $P2Y_{12}$ receptors on microglia (Davalos et al., 2005; Haynes et al., 2006; Sasaki et al., 1997). *In vitro*, $P2Y_{12}$ receptor activation induces membrane ruffling, process extension and chemotaxis of primary microglia (Haynes et al., 2006; Honda et al., 2001; Orr et al., 2009). While ATP is the main physiological chemoattractant for microglia released by damaged cells *in vivo* (Davalos et al., 2005; Haynes et al., 2006), the ATP hydrolysis product ADP is the cognate ligand for the $P2Y_{12}$ receptor (Zhang et al., 2001); thus, $P2Y_{12}$ receptors are herein referred to as ATP/ADP receptors. Surprisingly, activation of microglia changes the functional effects of ATP on microglial motility. While ATP serves as a chemoattractant and induces process extension in resting microglia, it induces migration away from its source and process retraction in activated microglia *in vitro* (Orr et al., 2009).

The changes in microglial process dynamics in response to ATP seem to be modulated by $P2Y_{12}$ receptors in resting microglia and adenosine A_{2A} receptors in activated microglia (Gyoneva et al., 2009; Haynes et al., 2006; Orr et al., 2009). The involvement of the A_{2A} receptor comes from several lines of evidence. First, preventing ATP breakdown to adenosine (Fig. 1.2) reduces ATP-induced process retraction in LPS-activated microglia (Orr et al., 2009). Second, accelerating adenosine removal by conversion to AMP or inosine also impairs process retraction (Orr et al., 2009). Although these manipulations can affect signaling through all adenosine receptors, the specific involvement of A_{2A} receptors is suggested by receptor expression data and preliminary pharmacological studies. Concurrent with the $P2Y_{12}$ receptor downregulation following microglial activation with LPS, A_{2A} receptors become upregulated at the mRNA level (Orr et al., 2009). Moreover, the A_{2A} receptor agonist CGS-21680 can induce process retraction in activated microglia, while the A_{2A} receptor antagonist SCH-58261 blocks ATP-induced retraction

(Orr et al., 2009). However, these ligands were used at concentrations (10 μM each) that can affect signaling through some of the other adenosine receptors as well (Table 3.1).

Adenosine, the agonist for A_{2A} receptors, exerts its functions through four different receptors: the G_i-coupled A_1 and A_3 receptors, and the G_s-coupled A_{2A} and A_{2B} receptors (Fredholm et al., 2001; Hasko et al., 2005). In terms of motility, adenosine has been shown to potentiate ATP/ADP-induced migration of primary rat and mouse resting microglia, but it has no effect on its own (Färber et al., 2005; Ohsawa et al., 2012). The effects of adenosine appear to be mediated through A_1 receptors in mice (Färber et al., 2005), while either A_1 or A_3 receptors can potentiate ATP/ADP-induced migration in rat microglia (Ohsawa et al., 2012). Moreover, A_3 receptors potentiate ATP/ADP induced process extension by rat microglia into collagenous gels (Ohsawa et al., 2012). Despite this evidence for involvement of A_1 and A_3 receptors in modulating the motility of resting microglia, their role in activated microglia has not been evaluated directly.

Thus, before studying the physiological roles of A_{2A} receptor-mediated changes in process motility in activated microglia, it was necessary to firmly establish the involvement of the A_{2A} receptor. This was accomplished with a detailed analysis of adenosine receptor expression with RT-PCR and careful pharmacological interventions with subtype-selective ligands, the results of which are presented in this Chapter.

3.3. Results

3.3.a. Changes in purinergic receptor expression in primary microglia

Several activating stimuli, including LPS and Aβ peptides, induce downregulation of the $P2Y_{12}$ receptor for ATP/ADP (Haynes et al., 2006), and upregulation of the adenosine A_{2A} receptor at the mRNA level (Orr et al., 2009). I examined the time course of purinergic receptor expression in microglia by performing semi-quantitative RT-PCR with RNA isolated from primary resting microglia (treated with HBSS), or primary microglia activated with 100 ng/mL

Table 3.1. Potency of commonly-used A_{2A} receptor ligands at the known adenosine receptors

Compound	A_1	A_{2A}	A_{2B}	A_3
			K_i (nM)	
CGS-21680[a]	289	27.1	212,300[c]	67.1
SCH-58261[b]	287	0.6	5,011[c]	>10,000

All values are for human adenosine receptors expressed in a heterologous cell system. [a]K_i values calculated from displacement of radioligands: [^{3}H]DPCPX for A_1 receptors; [^{3}H]NECA for A_{2A} receptors and A_3 receptors. [b]K_i values calculated from displacement of radioligands: [^{3}H]DPCPX for A_1 receptors; [^{3}H]SCH 58261 for A_{2A} receptors; [^{125}I]AB-MECA for A_3 receptors. [c]Potency at A_{2B} receptors was determined by measuring cAMP levels. Sources: Klotz et al. (1998) for CGS-21680; Ongini et al. (1999) for SCH-58261. Concentrations used in Orr et al. (2009) study: 10 μM for both compounds.

LPS for 3, 6, 12 or 24 hr. The expression of both $P2Y_{12}$ and A_{2A} receptors was time-dependent and changed quickly after LPS addition (Fig 3.1A). $P2Y_{12}$ receptor mRNA levels started decreasing after 3 hr, and the mRNA was undetectable after a 24 hr activation with LPS (Fig. 3.1B), consistent with previous observations (Orr et al., 2009). Similarly, A_{2A} receptor mRNA appeared upregulated as early as 3 hr after LPS addition, peaked by 6 hr, and remained significantly upregulated for as long as 24 hr later (Fig. 3.1C).

The A_{2A} receptor mRNA expression seen with RT-PCR was also confirmed at the protein level with immunocytochemistry for the A_{2A} receptor in resting and LPS-treated (100 ng/mL, 24 hr) primary microglia. A_{2A} receptors immunoreactivity was occasionally detected in resting, HBSS-treated, microglia (5/46 cells) as one or several distinct puncta (Fig. 3.2, left). In contrast, all of the LPS-activated microglia examined (32/32 cells) were immunoreactive for the A_{2A} receptor, which seemed to be found throughout the cytoplasm and the cell surface, but not the nucleus (Fig. 3.2, right). However, the subcellular localization of the receptor cannot be established with certainty without colocalization analysis with structure-specific markers.

There are divergent reports about the expression of adenosine receptors in microglia (Hasko et al., 2005). To determine if adenosine might mediate its effects through receptors other than A_{2A}, I examined the expression of all four adenosine receptors (A_1, A_{2A}, A_{2B}, and A_3) in resting and LPS-activated (100 ng/mL, 24 hr) microglia. LPS treatment upregulated the expression of A_{2A} receptors. Occasionally, faint bands could be seen for A_1 and A_3 receptors, but their presence was inconsistent (Fig. 3.3A). Quantifying the expression using densitometry confirmed that only A_{2A} receptors were affected by LPS treatment under the current culture conditions (Fig. 3.3B).

In conclusion, activation of primary microglia with LPS rapidly modifies $P2Y_{12}$ and A_{2A} receptor expression. Moreover, A_{2A} receptors are the only adenosine receptor subtype that becomes upregulated by LPS, suggesting that they might have functional consequences in microglia.

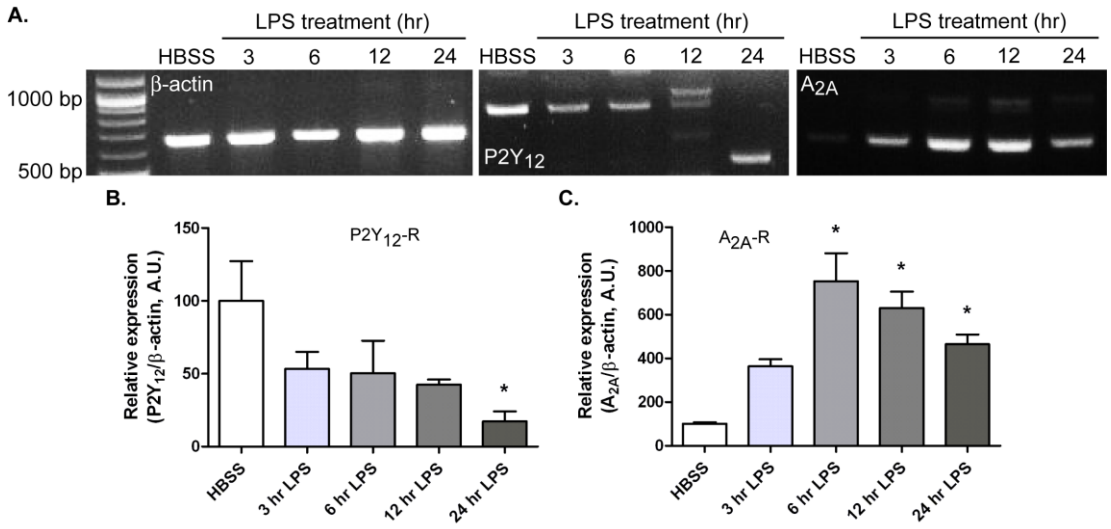

Figure 3.1. Time course of $P2Y_{12}$ and A_{2A} receptor mRNA expression in primary mouse microglia. Primary *actin-GFP* microglia were treated with 100 ng/mL LPS for 3, 6, 12 or 24 hr, or HBSS for 24 hr. mRNA expression was determined with RT-PCR, and amplicons were separated on 2% agarose gels. **A.** $P2Y_{12}$ receptor expression decreases with time. (The band at 24 hr is non-specific.) A_{2A} receptor mRNA increases following LPS treatment in a time-dependent manner. Representative gels from four experiments. **B-C.** Quantification of $P2Y_{12}$ (**B**) and A_{2A} (**C**) receptor expression using densitometry. The relative expression for each receptor at each time point was normalized to the β-actin signal at that time point, and then expressed as percentage of HBSS control. Statistics: one-way ANOVA and Dunnet's *post hoc* test compared to HBSS. *, $p < 0.05$.

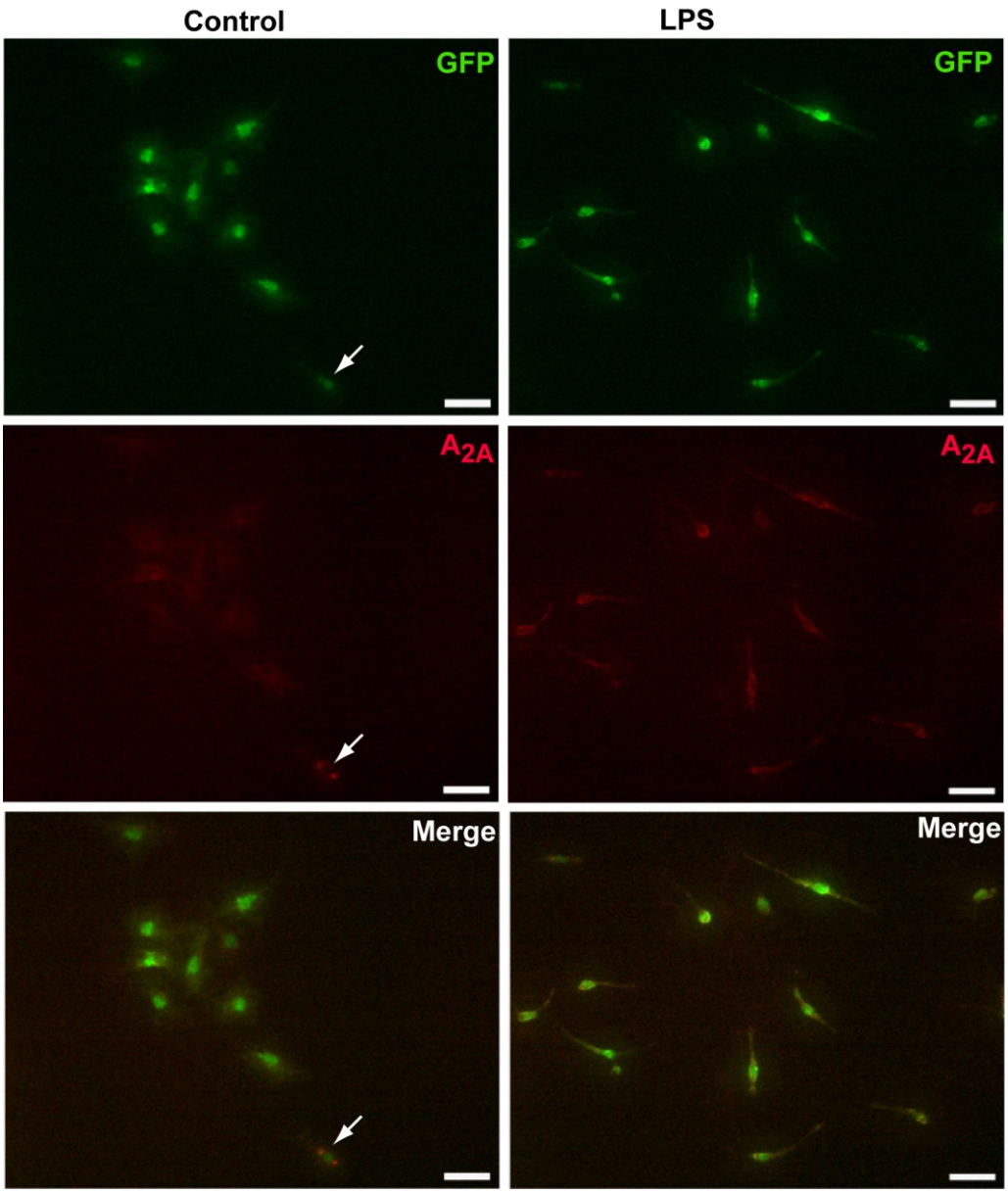

Figure 3.2. Expression of A_{2A} receptor protein in primary mouse microglia. The expression of A_{2A} receptors was examined in primary microglia from *actin-GFP* mice with immunocytochemistry. Microglia were treated with HBSS (control) or 100 ng/mL LPS for 24 hr, fixed for 10 min with 4% PFA, and A_{2A} receptors were detected with an anti-A_{2A} antibody. Control microglia were occasionally immunoreactive for A_{2A} receptors (arrow). All examined LPS-treated microglia seemed to express A_{2A} receptors. Representative images from two experiments, each performed with three wells per condition. Scale bar: 20 μm.

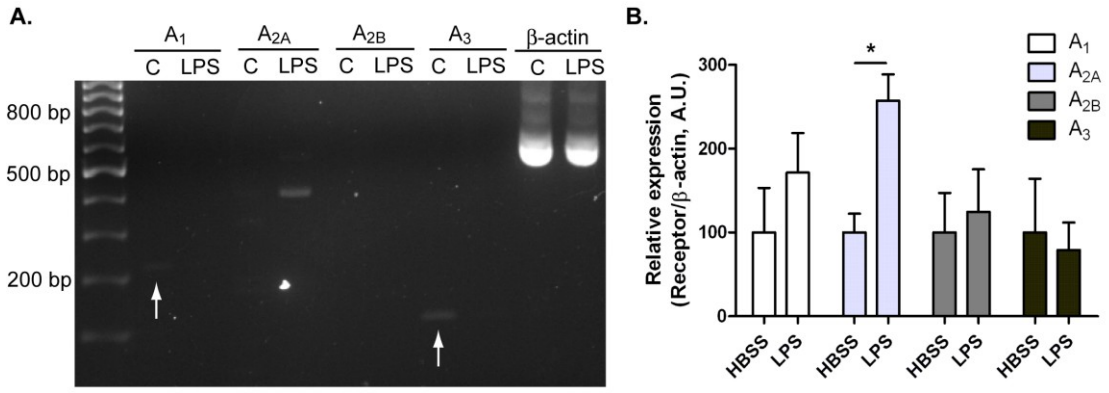

Figure 3.3. Adenosine receptor mRNA expression in primary mouse microglia. Primary *actin-GFP* microglia were treated with HBSS (C) or 100 ng/mL LPS for 24 hr. **A.** mRNA expression for the various adenosine receptors (A_1, A_{2A}, A_{2B}, A_3) was determined with RT-PCR, and amplicons were separated on 2% agarose gels. A_{2A} receptors are upregulated in LPS-activated microglia, while A_3 receptors become downregulated. Representative gel from three experiments. Arrows point to faint bands for A_1 and A_3 receptors that are not always seen. **B.** Quantification of adenosine receptor expression using densitometry. The relative expression for each receptor was normalized to the β-actin signal, and then expressed as percentage of HBSS control. Statistics: two-way ANOVA and Bonferroni's *post hoc* test compared to HBSS. *, $p < 0.05$.

3.3.b. Differential modulation of microglial process motility by ATP and adenosine receptors

ATP exerts opposing effects on the motility of microglia based on the cells' activation status (Orr et al., 2009). The process extension in resting microglia and process retraction in activated microglia are mediated by $P2Y_{12}$ and A_{2A} receptors, respectively (Orr et al., 2009). Both receptor subtypes can be activated by ATP, either directly or by one of its metabolites. To better distinguish between $P2Y_{12}$ and A_{2A} receptor signaling, I employed several selective pharmacological tools. Plating primary cortical microglia inside the gelatinous substrate Matrigel allows the cells to assume a three-dimensional, process-bearing morphology; changes in cell morphology can be studied with time-lapse confocal microscopy followed by 3D reconstructions of individual cells (Fig. 3.4). Changes in cell ramification, measured as the ratio of surface area to volume at each time point, correspond to changes in the velocity (Orr et al., 2009) and length (Fig. 2.5) of microglial processes. An increase in the length of the processes influences surface area more than volume and thus increases the ratio of surface area-to-volume; the opposite occurs for process retraction (Fig. 3.4). Indeed, application of 20 μM ATP caused process extension in control microglia, but process retraction in LPS-activated (100 ng/mL, 24 hr) microglia (Fig. 3.5A, D; two-way ANOVA and Bonferroni's *post hoc* test comparing control to LPS, $p < 0.001$). In contrast, selective activation of $P2Y_{12}$ receptors with 20 μM ATPγS, a non-hydrolysable analogue of ATP (Zhang et al., 2001) which cannot activate adenosine receptors (Table 3.2), was able to induce process extension in resting microglia, but it had no effect on the processes of LPS-activated microglia (Fig. 3.5B, D; two-way ANOVA and Bonferroni's *post hoc* test comparing control to LPS, $p = 0.095$). Similarly, 10 μM ADPβS, a non-hydrolysable derivative of the cognate $P2Y_{12}$ receptor agonist ADP (von Kugelgen and Wetter, 2000), induced significant process extension in resting microglia only (Fig. 3.5 C, D; two-way ANOVA and Bonferroni's *post hoc* test comparing control to LPS, $p = 0.033$). Overall, preventing ATP

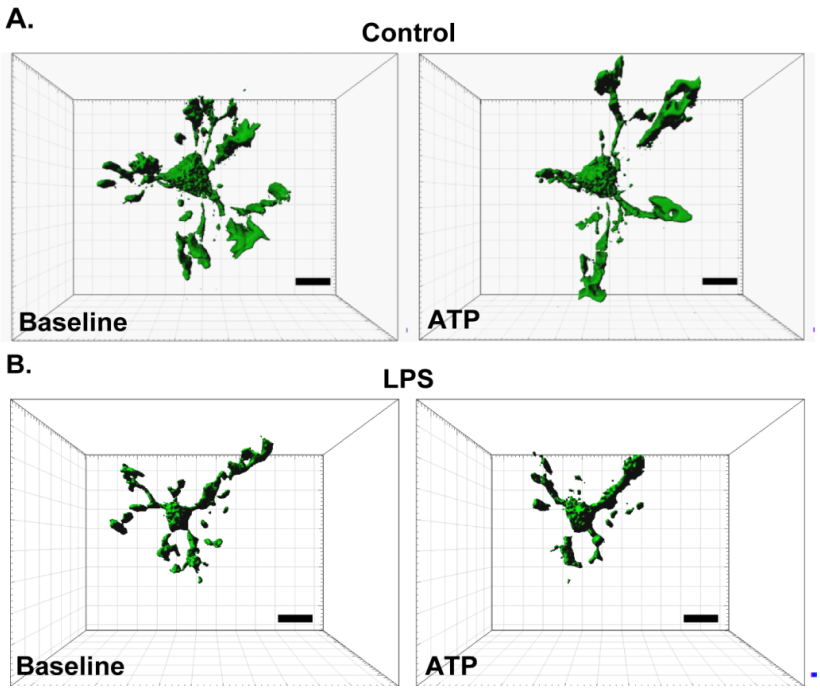

Figure 3.4. Confocal imaging and 3D reconstruction of primary microglia *in vitro*. Primary microglia from *actin-GFP* mice in Matrigel were treated with HBSS (Control) or 100 ng/mL LPS for 24 hr. Confocal imaging over time and 3D reconstructions of the cells at each time point with the Imaris software were used to study cell ramification. The figure shows the effects of ATP treatment on the morphology of a resting (**A**) and LPS-activated (**B**) cell; while ATP induces process extension in the resting cell, it causes retraction of processes in the LPS-activated cell. Scale bar: 10 µm.

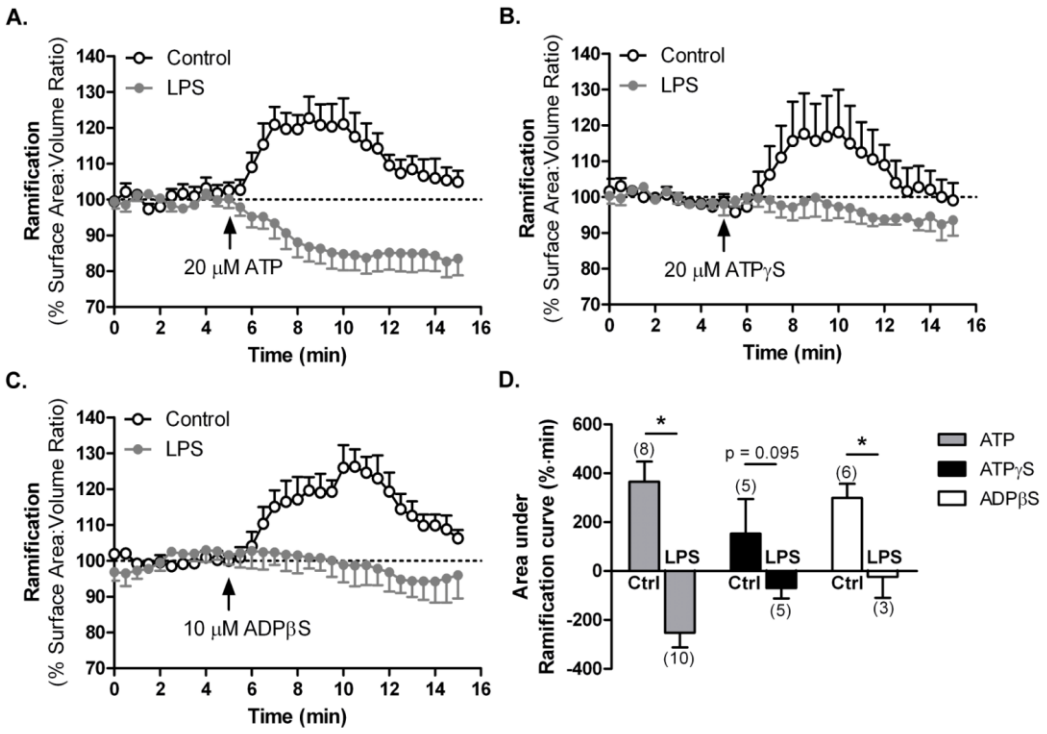

Figure 3.5. Modulation of microglial process dynamics by $P2Y_{12}$ receptors. 3D cell reconstructions from primary *actin-GFP* microglia in Matrigel were used to determine cell ramification (expressed as surface area-to-volume ratios) in response to different treatments. **A.** ATP application (20 μM) exerts divergent effects on the ramification of resting, HBSS-treated (Control) and LPS-activated microglia. **B, C.** The non-hydrolysable $P2Y_{12}$ receptor agonists ATPγS (20 μM, **B**) and ADPβS (10 μM, **C**) increase cell ramification in resting microglia only. **D.** Summary of the effects of purinergic receptor agonists on cell ramification assessed as the area under the ramification curves. Ctrl, control. The number of cells for each treatment is shown in parentheses. Statistics: two-way ANOVA and Bonferroni's *post hoc* test (compared to control cells for each treatment). *, $p < 0.05$.

Table 3.2. Potency of select agonists at purinergic and adenosine receptors

Compound	$P2Y_{12}$	A_1	A_{2A}	A_{2B}	A_3
			EC_{50} (nM)		
ATP	690[a]	n.i.	n.i.	n.i.	n.i.
ATPγS	150[a]	n.i.	n.i.	n.i.	n.i.
ADPβS	191[a]	n.i.	n.i.	n.i.	n.i.
Adenosine[b]	Inactive[c]	310	730	23,500	290
NECA	n.i.	14[d]	20[d]	2,400[e]	6.2[d]

All values are for human adenosine receptors expressed in a heterologous cell system. [a]EC_{50} values calculated from inhibition of forskolin-induced cAMP accumulation. [b]EC_{50} values calculated by measuring agonist-activated cAMP accumulation (A_{2A}, A_{2B} receptors) or inhibition of forskolin-induced cAMP accumulation (A_1, A_3 receptors). [c]Up to 1 mM adenosine failed to stimulate mobilization of intracellular calcium. [d]K_i values calculated from displacement of [^{3}H]DPCPX for A_1 receptors and K_D values for saturation curves at A_{2A} and A_3 receptors. [e]Potency at A_{2B} receptors was determined by measuring cAMP levels. Sources: Zhang et al. (2001) and Takasaki et al. (2001) for $P2Y_{12}$ receptors; Fredholm et al. (2001) for adenosine; Klotz et al. (1998) for NECA. n.i. No information found for the indicated agonist/receptor pairs.

metabolism, as with the use of the non-hydrolysable agonists ATPγS and ADPβS, eliminated the effects of ATP in LPS-activated microglia.

Next, I examined the effects of A_{2A} receptor activation on microglial process motility by using ligands that cannot activate $P2Y_{12}$ receptors. The endogenous A_{2A} receptor agonist adenosine [10 μM; Fredholm et al. (2001)] and the potent synthetic agonist NECA [10 μM; Table 3.2; Klotz (2000)] both induced process retraction in LPS-activated (100 ng/mL, 24 hr) microglia, but had no effect on the process dynamics of resting, HBSS-treated microglia (Fig. 3.6A, B, D; two-way ANOVA and Bonferonni's *post hoc* tests comparing control to LPS, $p = 0.056$ for adenosine and $p = 0.002$ for NECA). The same results were obtained with the A_{2A} receptor agonist CGS-21680 [Fig. 3.6C, D; two-way ANOVA and Bonferroni's *post hoc* test comparing control to LPS, $p = 0.030$; Hutchinson et al. (1989)].

A_{2A} receptor antagonists can block ATP-induced process retraction in activated microglia (Orr et al., 2009), but their effect on adenosine-induced process dynamics has not been described. Co-application of adenosine with either the non-selective competitive adenosine receptor antagonist caffeine [100 μM; Fredholm et al. (2001)] or the selective competitive A_{2A} receptor antagonist preladenant [1 μM; Neustadt et al. (2007)] prevented the adenosine-induced process retraction in LPS-activated microglia (Fig. 3.7A, B; one-way ANOVA and Tukey's *post hoc* test, $p = 0.046$ comparing caffeine to DMSO vehicle control, $p = 0.044$ comparing preladenant to control). Furthermore, there was no significant difference in the magnitude of the effects of preladenant and caffeine (Fig. 3.7B; one-way ANOVA and Tukey's *post hoc* test, $p = 0.988$). Both antagonists were used at concentrations at least 8-times higher than their K_i values at the A_{2A} receptor, but at a concentration that preserved the selectivity of preladenant for the A_{2A} receptor (Table 3.3).

Finally, in contrast to the uniform process extension in resting microglia induced by bath application of ATP (Orr et al., 2009), ATP gradients generated from a localized source induce microglial chemotaxis *in vitro* (Orr et al., 2009) and directional process extension to the ATP

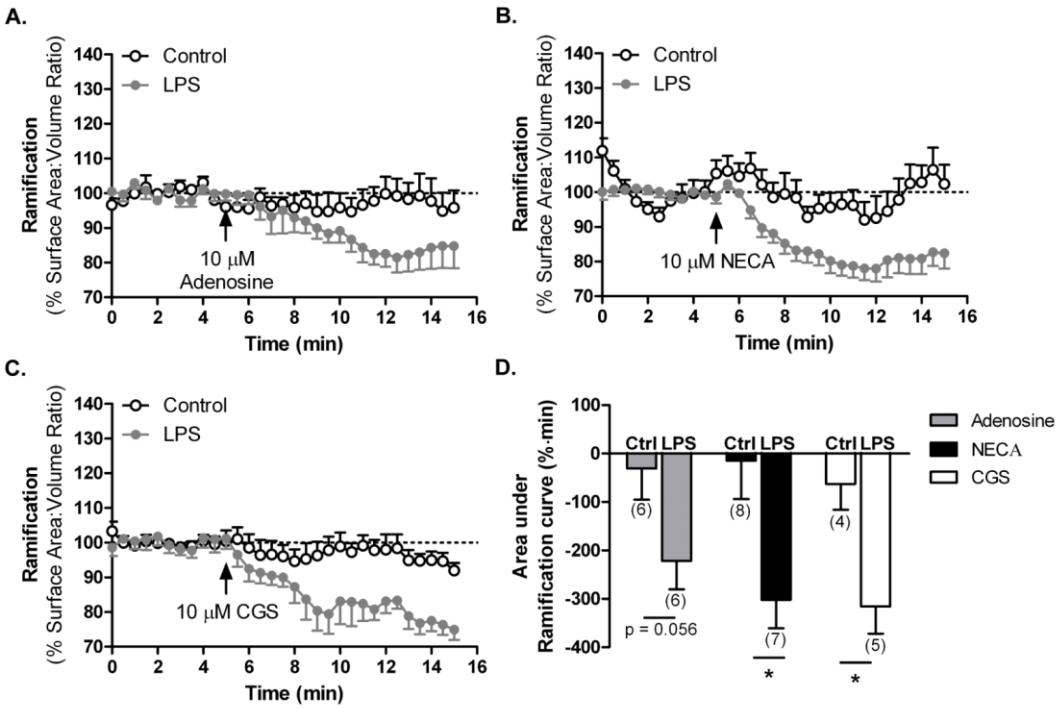

Figure 3.6. Modulation of microglial process dynamics by A_{2A} receptors. 3D cell reconstructions from primary *actin-GFP* microgla in Matrigel were used to determine cell ramification (expressed as surface area-to-volume ratios) in response to different treatments. **A-C.** Application of the physiological ligand adenosine (10 μM, **A**), the synthetic ligand NECA (10 μM, **B**), or the A_{2A} receptor agonist CGS-21680 (CGS, 10 μM, **C**) to resting, HBSS-treated (Control) and LPS-activated microglia. All three agonists induce process retraction only in activated microglia. **D.** Summary of the effects of adenosine receptor agonists on cell ramification assessed as the area under the ramification curves. Ctrl, control. The number of cells for each treatment is shown in parentheses. Statistics: two-way ANOVA and Bonferroni's *post hoc* test (compared to control cells for each treatment). *, $p < 0.05$.

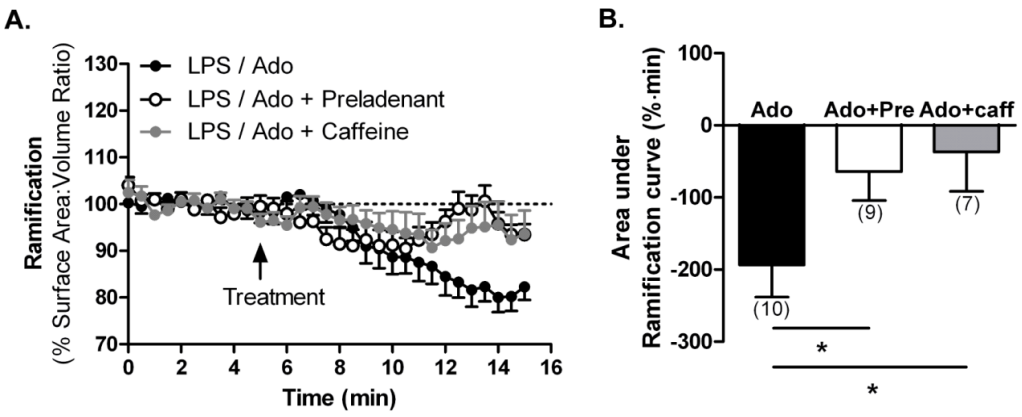

Figure 3.7. Inhibition of adenosine-induced process retraction by A_{2A} receptor antagonists. 3D cell reconstructions from primary *actin-GFP* microglia in Matrigel were used to determine cell ramification (expressed as surface area-to-volume ratios) in response to different treatments. **A.** Microglia were activated with 100 ng/mL LPS for 24 hr and treated with adenosine (Ado) alone or adenosine in combination with the A_{2A} receptor selective agonist preladenant (1 μM) or the non-selective adenosine receptor antagonist caffeine (100 μM). **B.** Summary of the effects of purinergic receptor agonists on cell ramification assessed as the area under the ramification curves. Pre, preladenant; caff, caffeine. The number of cells for each treatment is shown in parentheses. Statistics: one-way ANOVA and Tukey's *post hoc* test. *, $p < 0.05$.

Table 3.3. Potency of A_{2A} receptor antagonists at the various adenosine receptors

Compound	A_1	A_{2A}	A_{2B}	A_3
			K_i (nM)	
Caffeine[a]	33,800	12,300	15,500	>100,000
Preladenant[b]	1474	1.1	>1,700	>1,000

All values are for human adenosine receptors expressed in a heterologous cell system. [a]K_b values calculated from competition experiments with adenosine or NECA. [b]K_i values calculated from displacement of unidentified radioligand. Sources: Fredholm et al. (2001) for caffeine; Neustadt et al. (2007) for preladenant. Concentrations used in this study: 100 μM caffeine and 1 μM preladenant.

source *in vivo* (Davalos et al., 2005). One way to generate chemical gradients *in vitro* is to locally release ATP, or other compounds, from a micropipette; if the compound is charged, its release from the pipette can be controlled by electrical current. Expulsion of the negatively-charged ATP (0.5 mM) from a micropipette by applying negative current to the pipette causes the migration of resting microglia to the pipette and activated microglia away from the pipette (Orr et al., 2009), which can be followed with time-lapse microscopy (Fig. 3.8A, B). In order to determine if the same signaling pathways control process dynamics and whole cell migration in activated microglia, I examined the motility of LPS-activated microglia (100 ng/mL, 24 hr) in an adenosine gradient. Similar to the effect of ATP on activated microglia, release of 0.5 mM adenosine caused mostly migration away from the source micropipette. The movement was quantified by measuring the vector displacement of individual cells for the duration of the recording. Both ATP and adenosine induced significantly different displacement in LPS-activated microglia compared to resting, HBSS-treated, microglia (Fig. 3.8C; one-way ANOVA and Dunnett's *post hoc* test, $p < 0.0001$ for both ATP and adenosine). The A_{2A} receptor agonist CGS-21680 (0.1 mM) also induced significant decrease in migration (Fig. 3.8C; one-way ANOVA and Dunnett's *post hoc* test, $p < 0.0001$ compared to resting microglia), suggesting the involvement of A_{2A} receptors. This was further confirmed with the use of the selective A_{2A} receptor antagonist preladenant (1 μM) during ejection of 0.1 mM adenosine. Even at the highest possible concentration of adenosine before its diffusion from the pipette (0.1 mM), preladenant should efficiently block the receptor as it will be present at levels >100 times higher than the IC_{50}. The inclusion of preladenant in the perfusion solution for the duration of the experiment significantly reduced adenosine-induced migration away from the micropipette (Fig. 3.8D; Student's *t* test, $p = 0.044$).

3.3.c. Involvement of other adenosine receptors in regulating microglial process motility

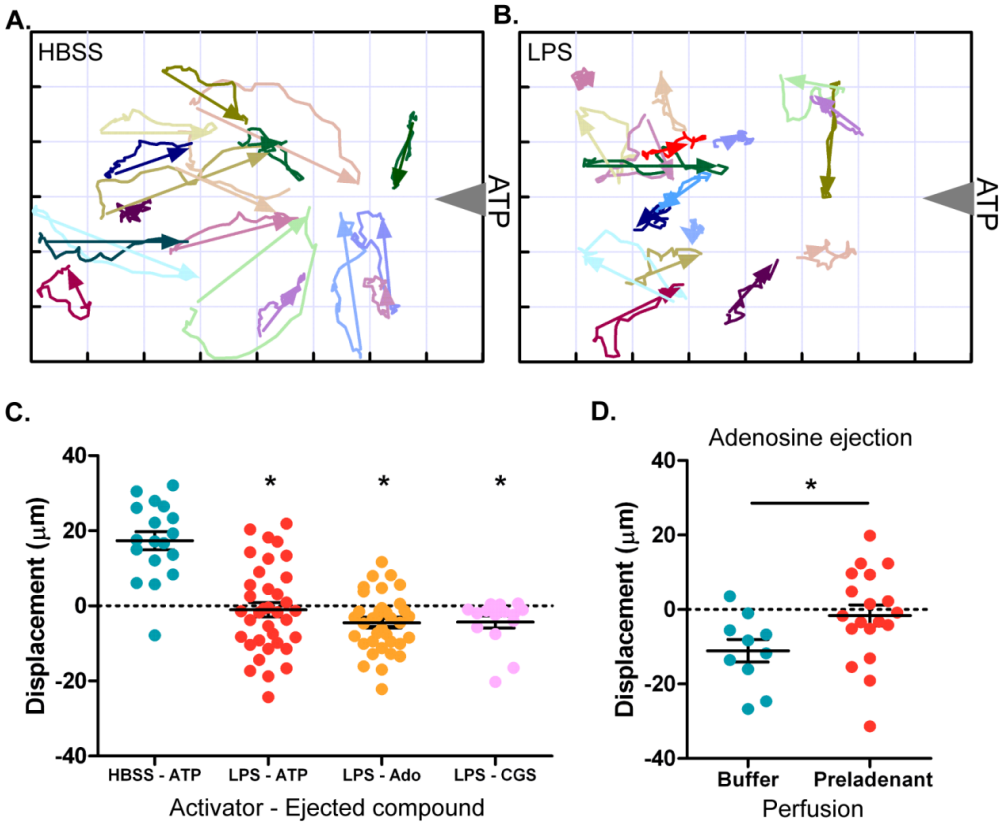

Figure 3.8. Migration of microglia to purinergic agonists released from a micropipette. Primary resting, HBSS-treated, or LPS-activated (100 ng/mL, 24 hr) *actin-GFP* microglia were plated on Matrigel and imaged over time during application of various agonists from a micropipette. Microglial migration of cell bodies was tracked with Imaris v7.6 software. **A, B.** Migration of select HBSS- (**A**) or LPS-treated (**B**) microglia in an ATP gradient. The approximate location of the pipette is indicated with a gray triangle. The paths of individual cells are shown as lines. The overall displacements are represented by arrows. Grid: 10 µm. **C.** Movement in different gradients was quantified by measuring the magnitude of the vector displacement for each cell with positive displacement being movement towards the pipette. In addition to ATP, LPS-activated microglia were exposed to 0.5 mM adenosine and 0.1 mM CGS-21680 (CGS). Statistics: one-way ANOVA and Dunnett's post *hoc test* compared to HBSS – ATP. D. Effect of the A_{2A} receptor antagonist preladenant on the migration of LPS-activated microglia in an adenosine (0.1 mM) gradient. The perfusion solution contained DMSO vehicle (Buffer) or 1 µM preladenant. Statistics: Student's *t* test. *, $p < 0.05$.

Physiological concentrations of adenosine in the brain can activate A_1 and A_{2A} receptors (Fredholm et al., 1999; Fredholm et al., 2001). Using the current culture conditions, activated microglia appear to express only A_{2A} receptors (Fig 3.3), but A_1 and A_3 receptors may also be present on resting and/or activated microglia [Fig. 3.3; Hasko et al. (2005)]. To confirm the lack of A_1 and A_3 receptors in LPS-activated microglia as suggested by RT-PCR (Fig. 3.3), I employed receptor-selective agonists (Table 3.4). Application of the A_{2A} agonist CGS-21680 (3 μM) induced process retraction (Fig. 3.9A, B). In contrast, selective activation of adenosine A_1 or A_3 receptors with 1 μM 2'-MeCCPA and 0.5 μM 2-Cl-IB-MECA, respectively (Franchetti et al., 1998; Gallo-Rodriguez et al., 1994), did not change the process dynamics of LPS-activated microglia (Fig. 3.9A, B; one-way ANOVA and Dunnett's *post hoc* test, $p < 0.05$ for CGS-21680 compared to either 2'-MeCCPA and 2-Cl-IB-MECA). The lack of effect of 2'-MeCCPA and 2-Cl-IB-MECA was not due to their inability to activate their respective G_i-coupled receptors at the concentrations used, as control experiments show that they were able to inhibit forskolin-induced cAMP accumulation in a heterologous expression system (Fig. 3.9C, D). The undetectable expression of A_1 andA_3 receptors in LPS-activated microglia (Fig. 3.3) and the lack of effect of 2'-MeCCPA and 2-Cl-IB-MECA strongly suggest that the effects of CGS-21680 on process dynamics are mediated through the A_{2A} receptor.

3.4. Discussion

The *in vitro* data presented in this Chapter show that ATP mediates microglial process extension and migration to its source via $P2Y_{12}$ receptors in resting microglia (Fig. 3.5, 3.8). The ATP breakdown product adenosine selectively induces process retraction and migration away from its source in LPS-activated microglia (Fig. 3.6, 3.8). The effects of adenosine in activated microglia are mediated through A_{2A} receptors, as confirmed by the use of the selective antagonist preladenant (Fig. 3.7, 3.8). Moreover, the lack of effect of A_1 and A_3 agonists on process motility

Table 3.4. Potency of adenosine receptor agonists at the various adenosine receptors

Compound	A_1	A_{2A}	A_{2B}	A_3
			K_i (nM)	
2'-MeCCPA	0.83	2,270	42,700[a]	42.3
CGS-21680	289	27.1	$212,300_a$	67.1
2-Cl-IB-MECA	3.73	2,520	n.d.	1.20

All values are for human adenosine receptors expressed in a heterologous cell system. K_i values calculated from displacement of [^{3}H]DPCPX for A_1 receptors and K_D values for saturation curves at A_{2A} and A_3 receptors. [a]Potency at A_{2B} receptors was determined by measuring cAMP levels. Source: Klotz et al. (1998). Concentrations used in this study: 1 μM 2'-MeCCPA, 3 μM CGS-21680, 0.5 μM 2-Cl-IB-MECA.

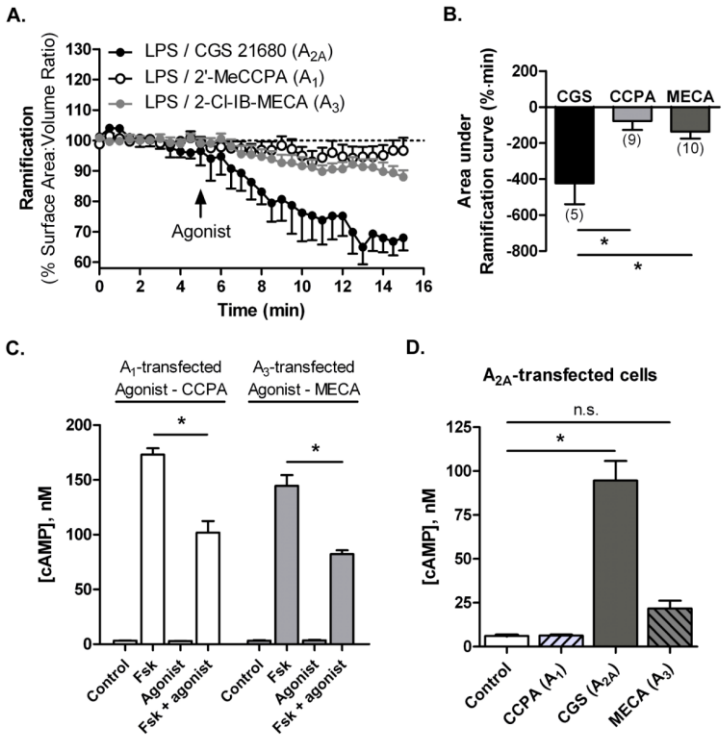

Figure 3.9. Involvement of adenosine A_1 and A_3 receptors in modulating motility of activated microglia *in vitro*. **A.** 3D cell reconstructions from LPS-activated (100 ng/mL, 24 hr) primary *actin-GFP* microglia in Matrigel were used to determine cell ramification (expressed as surface area-to-volume ratios) in response to different treatments. The selective A_1 receptor agonist 2'-MeCCPA (CCPA, 1 μM) or the selective A_3 receptor agonist 2-Cl-IB-MECA (MECA, 0.5 μM) do not affect process dynamics of activated microglia, but the selective A_{2A} agonist CGS-21680 (CGS, 3 μM) induces process retraction. **B.** Summary of the effects of selective adenosine receptor agonists. Statistics: one-way ANOVA and Dunnett's *post hoc* test compared to CGS. **C, D.** cAMP assay in transfected HEK293 cells to confirm activity of CCPA and MECA. HEK293 cells were transfected with cDNA for adenosine A_1, A_{2A}, or A_3 receptors and cAMP levels were measured following the indicated treatments. **C.** CCPA reduces Forskolin- (Fsk) stimulated cAMP accumulation in A_1-expresisng cells, while MECA has the same effect on A_3-expressing cells. Statistics: two-way ANOVA and Tukey's *post hoc* test. **D.** Neither CCPA, nor MECA induce significant cAMP accumulation in A_{2A}-transfected cells. Statistics: one-way ANOVA and Dunnett's *post hoc* test compared to DMSO-treated (control) cells. *, $p < 0.05$.

(Fig. 3.9) suggests that the effects of the non-selective antagonist caffeine (Fig. 3.7) are likely mediated through the A_{2A} subtype of adenosine receptors.

3.4.a. Adenosine A_{2A} receptor expression in the brain

Evidence for adenosine A_{2A} receptor expression in the brain was first obtained with radioligand binding studies. The selective A_{2A} receptor agonist [^{3}H]CGS-21680 prominently labels caudate, putamen, nucleus accumbens, and olfactory tubercle (Jarvis et al., 1989; Jarvis and Williams, 1989; Parkinson and Fredholm, 1990). This pattern of expression largely matches the expression of A_{2A} receptor mRNA determined by *in situ* hybridization (Peterfreund et al., 1996; Schiffmann et al., 1991b) and protein expression assessed by immunohistochemistry (Bogenpohl et al., 2012; Rosin et al., 1998). Detailed localization analysis of the A_{2A} receptor shows that it is exclusively expressed by D_2 dopamine receptor- and enkephalin-containing striatopallidal neurons, but not by D_1 receptor-containing striatonigral neurons (Ferre et al., 1991; Fink et al., 1992; Pollack et al., 1993; Schiffmann et al., 1991a). Recently, non-neuronal cells were also reported to contain A_{2A} receptors. Specifically, a large fraction of glial cells in the external globus pallidus and substantia nigra are immunoreactive for A_{2A} receptors (Bogenpohl et al., 2012). A_{2A} receptor expression appears to be species-specific. For example, the substantia nigra of rhesus monkeys shows stronger expression of A_{2A} receptors than the substantia nigra of rats, and many of these receptors appear to be on glial cells (Bogenpohl et al., 2012).

In addition to species identity, A_{2A} receptor expression may be affected by pathological processes. Neurotoxins such as MPTP may increase A_{2A} receptor expression in the striatum, but the cell localization of these receptors in not known (Singh et al., 2009). On the other hand, binding of [^{3}H]CGS-21680 is reduced the brain of Huntington's disease patients (Martinez-Mir et al., 1991). Cell activation can also change A_{2A} receptor expression in cells of the myeloid lineage. For example, activation of primary mouse microglia with LPS increased A_{2A} receptor mRNA [Fig. 3.1; Orr et al. (2009)] and protein (Fig. 3.2). Upregulation of A_{2A} receptors at the mRNA

level has been reported before for LPS-activated mouse and human macrophages (Murphree et al., 2005) and rhesus monkey microglia (van der Putten et al., 2009). This expression data make the A_{2A} receptor a worthwhile target to regulate microglial motility under neuroinflammatory conditions.

3.4.b. Modulation of microglial motility by adenosine receptors

Bath application of adenosine induced process retraction in LPS-activated primary mouse microglia (Fig. 3.6A, B), and release of adenosine from a point source induced microglial migration away from its source (Fig. 3.8). RT-PCR analysis showed that LPS-activated microglia expressed A_{2A} receptors, but not A_1 or A_3 receptors, using the current culture conditions (Fig. 3.3). Yet, it is possible that activated microglia might express A_1 and A_3 receptors, but at levels undetectable by RT-PCR. Consistent with the mRNA expression, the selective A_{2A} receptor agonist CGS-21680 caused process retraction in LPS-activated microglia, but activation of A_1 receptors with 2'-MeCCPA and A_3 receptors 2-Cl-IB-MECA did not (Fig. 3.9). As a result, it appears that the effects of adenosine on the process dynamics of LPS-activated microglia are mediated selectively via the A_{2A} receptor with little or no involvement of A_1 or A_3 receptors. Thus, there are two types of purinergic receptor switches in microglia as they assume an activated phenotype: (1) a switch from the $P2Y_{12}$ receptor for ATP/ADP to the A_{2A} adenosine receptor, and (2) a switch in the specific subtype of adenosine receptors from A_1 and/or A_3 to A_{2A}. The decreased expression of both $P2Y_{12}$ and A_1/A_3 receptors explains the lack of ATP/ADP-induced migration and process extension in activated microglia (Färber et al., 2005). The receptor switching from $P2Y_{12}$ to A_{2A} and the divergent effects of ATP on microglial motility through activation of these receptors on resting and activated microglia, respectively, could affect the ability of microglia to detect and respond to tissue damage and cell death such as the neuronal death occurring in neurodegenerative diseases. Thus, the following two chapters examine

microglial response to tissue damage using different preparations and types of inflammation (degeneration-induced or systemic).

Additional evidence for the involvement of A_{2A} receptors in mediating motility of LPS-activated microglia comes from the use of adenosine receptor antagonists. Both the non-selective antagonist caffeine and the selective A_{2A} receptor antagonist preladenant reduced adenosine-induced process retraction (Fig. 3.7), and preladenant reduced microglial cell migration away from an adenosine-filled pipette (Fig. 3.8B). Finally, the A_{2A} receptor antagonist SCH-58261 decreases ATP-induced process retraction in LPS-activated microglia (Orr et al., 2009), further supporting the involvement of the A_{2A} receptor. Together with the differential effects of adenosine on the motility of resting and activated microglia, this increases the feasibility of targeting A_{2A} receptors to modulate microglial functions under pro-inflammatory conditions. Indeed, preladenant is currently in clinical trials for the treatment of Parkinson's disease (Barkhoudarian and Schwarzschild, 2011; Hauser et al., 2011). Because of its effects on microglial motility, some of its protective properties might be due to modulation of microglial properties. This is discussed in greater detail in Section 7.3.c.

3.4.c. Modulation of non-motility microglial functions by A_{2A} receptors

A_{2A} receptor signaling has been implicated in various neurological processes and pathological conditions, including release of neurotransmitters (Gomes et al., 2009; Gomes et al., 2006; Higley and Sabatini, 2010; Sebastiao and Ribeiro, 1996), ischemia and excitotoxicity (Pedata et al., 2001; Phillis, 1995), Huntington's disease (Blum et al., 2003; Popoli et al., 2007), cognitive disorders (Takahashi et al., 2008), and Parkinson's disease [see Section 7.4; Schwarzschild et al. (2006); Xu et al. (2005)]. Yet, the majority of these effects are likely mediated by neuronal A_{2A} receptors. There are several studies that show functional consequences of A_{2A} receptor signaling in microglia. Prolonged activation of A_{2A} receptors is reported to increase mRNA expression of cyclooxygenase-2 (COX-2) (Fiebich et al., 1996), the potassium

channels Kv1.3 and ROMK1 (Küst et al., 1999) and nerve growth factor (Heese et al., 1997), and stimulate microglial proliferation [in combination with A_1 receptor activation; Gebicke-Haerter et al. (1996)] in resting rat microglia. However, with the exception of the Fiebich et al. (1996) study in which only low levels of A_{2A} receptor mRNA were detected, the other investigators did not examine A_{2A} receptor expression in their systems. As a result, many of these effects in resting microglia might be due to the unselective nature of the agonists at the concentrations used in the specific studies. In LPS-activated microglia, A_{2A} receptor activation potentiates nitric oxide release in mouse microglia (Saura et al., 2005), but decreases TNF-α and IL-12 secretion from rhesus monkey microglia (van der Putten et al., 2009).

Overall, the majority of studies performed *in vivo* or with isolated microglia suggest that A_{2A} receptor signaling can lead to the generation of a pro-inflammatory or toxic milieu, and antagonizing the receptor will be protective. Nevertheless, modulation of microglial motility by targeting A_{2A} receptors will influence many different processes. Understanding the functional consequences of A_{2A} receptor activation in microglia and other cell types is essential for understanding the potential side effects of A_{2A} receptor modulators as they are being developed for therapeutic purposes, and need to be investigated further.

CHAPTER 4: Microglial response to tissue damage in acute brain slices

4.1. Abstract

Microglia in the healthy brain use $P2Y_{12}$ receptors to detect ATP released by damaged neurons and to respond with directional process extension *in vivo*. However, microglial activation results in $P2Y_{12}$ receptor downregulation and A_{2A} receptor upregulation, and A_{2A} receptor-driven process retraction in response to ATP (Chapter 3). Neuroinflammation and the presence of activated microglia are part of the pathology of many neurodegenerative diseases, such as Parkinson's disease. Yet, the ability of microglia to respond to tissue damage under pro-inflammatory conditions has not been studied in tissues in the context of PD. In an attempt to assess microglial motility in their native environment, I developed an imaging technique that allowed me to study the motion of microglia in acute brain slices in the absence and presence of injury using confocal microscopy. Coronal slices were prepared from $CX_3CR1^{GFP/+}$ mice and imaged over time. Microglia in slices from healthy mice extended processes to the direction of injury in a $P2Y_{12}$ receptor-dependent manner. However, microglia in mice treated with 2 mg/kg LPS i.p. 2 days before slice preparation displayed a diminished process extension. Similarly, microglia in slices from mice treated for 5 days with 20 mg/kg/day MPTP s.c. showed significantly reduced response compared to microglia in control mice in terms of process displacement toward the injury the average velocity of the response. Pre-treatment of slices from MPTP-injected mice with the selective A_{2A} receptor antagonist preladenant restored the ability of activated microglia to respond to tissue damage. These data support the hypothesis that chronic inflammation impedes microglial motility in response to further injury such as cell death.

4.2. Introduction

The ability of microglia to perform immune functions such as cytokine secretion and ROS generation when activated positions them to be potential contributors to the pathology of

neurodegenerative diseases by compromising neuronal survival (Block and Hong, 2005; Block et al., 2007). However, microglia also perform many other functions in the brain that are not directly linked to immune response (Kettenmann et al., 2013). For example, the "resting" microglia in the healthy brain have highly motile processes that can detect disturbances of the brain parenchyma, such as rupture of brain capillaries or cell death that occur throughout life (Davalos et al., 2005; Nimmerjahn et al., 2005). The response to injury *in vivo* is mediated by ATP release by damaged cells, activation of $P2Y_{12}$ receptors on microglia, and directional process extension to surround the damaged area and promote tissue repair (Davalos et al., 2005; Haynes et al., 2006). Interestingly, microglia that are in an activated state downregulate $P2Y_{12}$ receptors and upregulate adenosine A_{2A} receptors (Haynes et al., 2006; Orr et al., 2009), the latter of which are indirectly activated by ATP after its rapid breakdown to adenosine (Zimmermann, 2000). However, unlike the ability of ATP to induce process extension in resting microglia, ATP (and adenosine) induces process retraction in activated microglia [Fig. 3.4, 3.5; Orr et al. (2009)]. This raises a question as to how activated microglia, such as those found in PD, detect and respond to the neuronal death that is characteristic of the disease.

The cellular hallmark of PD is loss of dopaminergic neurons originating in the substantia nigra (SN) and subsequent loss of dopamine in the striatum (Kish et al., 1988; Rinne, 1991). Another prominent feature of PD is the presence of neuroinflammation (see Section 1.4.a). For example, activated microglia, the brain's resident immune cells, are found in the SN in post-mortem samples from PD patients and animal models of the disease (Long-Smith et al., 2009; Tansey and Goldberg, 2010). Moreover, some pro-inflammatory cytokines, such as IL-1β, TNF-α, and others can be found at higher levels in the brains of PD patients compared to age-matched controls (Smith et al., 2012). Further supporting the involvement of inflammation, meta-analyses of several studies show that use of non-steroidal anti-inflammatory drugs (NSAIDs), and specifically ibuprofen, are associated with lower risk for developing PD (Gagne and Power, 2010; Gao et al., 2011b).

To study the ability of activated microglia to respond to tissue damage in their native environment, I developed an assay that allowed me to examine microglial motility in acute brain slices in response to mechanically induced tissue injury. I used this preparation to study microglial response to damage in two different types of inflammation. First, systemic inflammation was induced with a peripheral injection of 2 mg/kg LPS i.p. 2 days before slice preparation. Second, degeneration of dopaminergic neurons induced with MPTP (5 injections, 20 mg/kg/day, s.c.) results in inflammation that also leads to microglial activation. Microglia in slices from LPS- or MPTP-treated mice showed a diminished capacity to extend their processes to the site of damage. Blockade of A_{2A} receptors restored process extension to the damaged area in MPTP-treated mice. These findings suggest that microglia in PD might display a delayed response to the ongoing cell death, which could promote disease progression.

4.3. Results

4.3.a. Microglia in acute brain slices respond to localized mechanical damage

The ability of microglia to detect tissue damage and extend processes to the site of damage is commonly studied *in vivo* with two-photon microscopy. However, the brain regions primarily affected in Parkinson's disease, the substantia nigra and striatum, are beyond the limits of light penetration in the brain, and are thus not amenable to *in vivo* imaging with conventional light microscopy methods. To study microglial motion in a PD-relevant context, I prepared acute brain slices containing the substantia nigra from $CX_3CR1^{GFP/+}$ mice that exhibit microglia-specific GFP expression in the brain [Fig. 4.1A; Jung et al. (2000)]. The substantia nigra was visually easy to locate in the slices because of the high proportion of microglia in this brain region (Lawson et al., 1990) when the slices were examined after GFP excitation (Fig. 4.1B). Despite any microglial activation that might be caused by the slicing procedure itself, microglia in slices extend their processes following localized or bath application of ATP (Avignone et al., 2008;

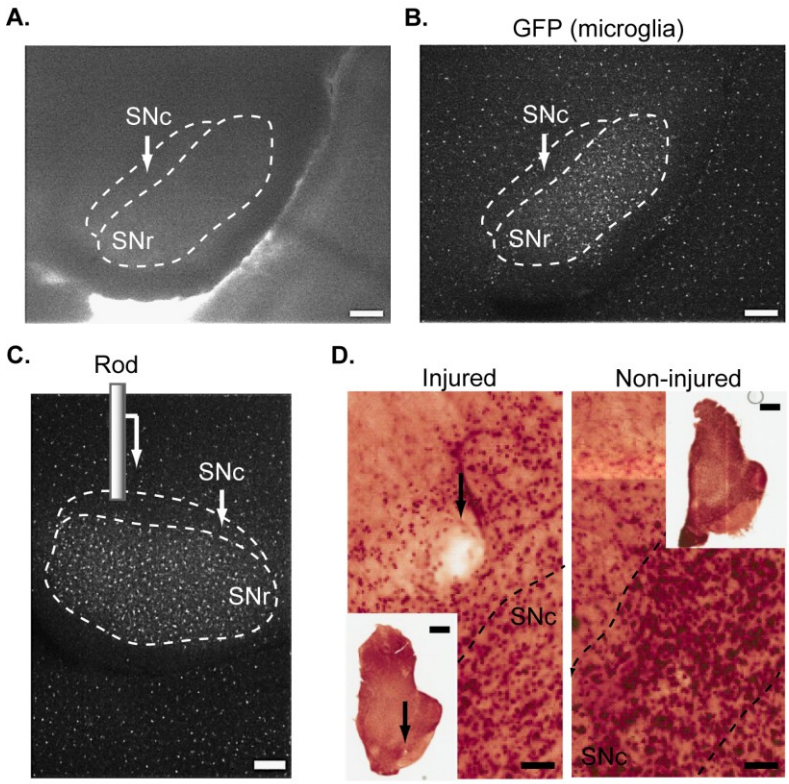

Figure 4.1. Induction of tissue damage in SNc-containing acute brain slices. Coronal slices (200 µm-thick) that contain the substantia nigra were prepared from $CX_3CR1^{GFP/+}$ mice that have microglia-specific GFP expression. **A.** Approximate outlines of the SNc and SNr in a brain slice. **B.** The SNr is easily identified by the high proportion of GFP-positive microglia. **C.** To induce tissue damage, a stainless steel rod is lowered 180 µm into the SNc with a micromanipulator at constant velocity. The rod is drawn approximately to scale. **D.** Quantification of tissue damage. Slices were immunostained for NeuN to determine the approximate number or neurons lost after the injury. Approximate outlines of SNc are shown. Arrow in injured slice points to the location of the injury. Scale bar: **A-C,** 200 µm; **D,** 1 mm for inset and 0.25 mm for magnified image.

Gyoneva and Traynelis, 2013) and surround an ablated area following laser-induced tissue damage in a manner similar to resting microglia *in vivo* (Krabbe et al., 2012).

To model the response of microglia to localized damage, representative of the death of only a few dopaminergic neurons, I lowered a thin rod into the SNc with a micromanipulator (Fig. 4.1C). Staining the slices for the neuronal marker NeuN indicated that the damage had an proximate size of 100 μm (Fig. 4.1D).

Microglial dynamics in the slices was studied with time-lapse confocal imaging to better capture the ramified morphology of microglia. The slices were imaged for 20 min to record the baseline motility of microglia. Similar to microglia in the cortex *in vivo* (Davalos et al., 2005; Nimmerjahn et al., 2005), microglia in the midbrain constantly extend and retract their processes. Next, tissue damage was induced as described above, and followed by a second imaging session to record microglial response to the damage. Unlike the seemingly random motion of microglia before damage induction, microglia in injured slices quickly extended their processes in the direction of damage (Fig. 4.2A, B). Moreover, the cell bodies remained mostly stationary, which is also in agreement to the response of microglia to mechanical or laser damage *in vivo* (Davalos et al., 2005). The response was quantified with an automated object tracking software that detects objects larger than 2 μm, ~95% of which are microglial processes (see Section 2.10.c). Plotting all tracks from the same starting point confirmed that most objects moved in the direction of the injury (Fig. 4.2C).

The extent of the response to the damage was quantified in three different ways: the overall object displacement in the direction of the injury, the average instantaneous velocity for the duration of the imaging, and the fraction of objects that had displacements larger than 5 μm. All three measures were significantly increased in the recordings following injury (Fig. 4.3; two-way repeated measures ANOVA and Tukey's test comparing baseline to injury: displacement: $p = 0.003$; velocity: $p = 0.003$; fraction: $p = 0.001$; 7 DMSO-treated slices). Importantly, the addition of the selective $P2Y_{12}$ receptor antagonist clopidogrel (Savi et al., 2001) for the duration

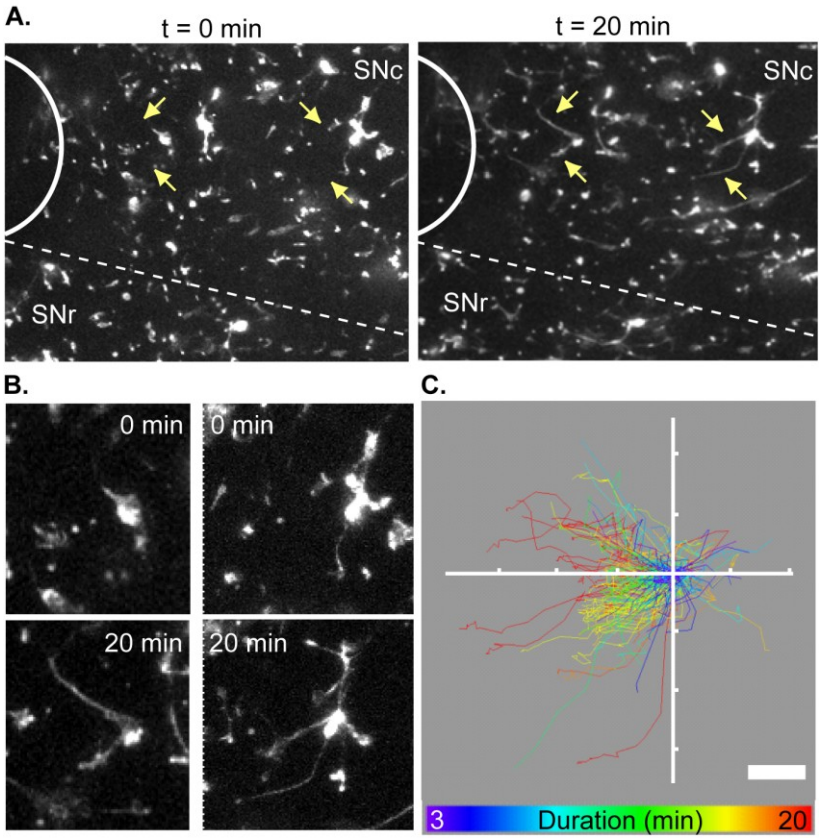

Figure 4.2. Response of microglia to tissue injury in acute brain slices. Acute brain slices from *CX$_3$CR1$^{GFP/+}$* were imaged with confocal microscopy over time before and after induction of tissue injury. For image analysis, the optical stacks at each time point were converted to 2D maximum intensity projections. **A.** A portion from a representative slice showing microglial response to the damage immediately after (t = 0 min) and 20 min after the injury. Location of the injury is indicated with a solid white arc. The approximate border to the SNc and SNr is represented with a dashed line. Arrows point to microglial processes that moved in the direction of the injury. These cells are enlarged in **B. C.** Automated tracking of moving objects with Imaris software was used to quantify different parameters of the response. Objects larger than 2 µm in diameter were tracked over time. The tracks are color-coded according to their duration, and translated to the same starting point; tracks with longer duration move in the direction of the injury. Scale bar and ticks on the coordinate axes: 5 µm.

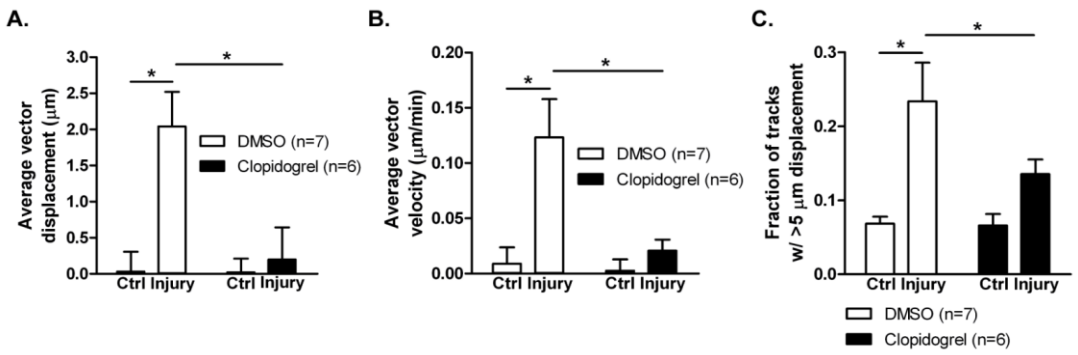

Figure 4.3. Quantification of microglial response to injury in acute brain slices. Slices from *$CX_3CR1^{GFP/+}$* mice were imaged with confocal microscopy for 20 min before induction of injury and 20 min after injury, and 2D projections of the optical stacks at each time point were used for analysis by tracking moving objects larger than 2 μm in diameter. To confirm the involvement of $P2Y_{12}$ receptors in the response to injury, the slices were treated with 2 μM of the selective $P2Y_{12}$ receptor antagonist clopidogrel or DMSO vehicle. The average displacement of all moving objects (**A**), the average velocity of movement (**B**), and the fraction of tracks with longer than 5 μm displacement (**C**) were calculated from baseline recordings of motility (control, Ctrl) before injury and after the induction of the injury in the same slice. Numbers of slices for each condition are shown in parentheses. Statistics: two-way repeated measures ANOVA and Tukey's *post hoc* test. *, $p < 0.05$.

of the experiment (baseline recording, injury, response to injury) prevented microglial process extension to the site of damage (Fig. 4.3; two-way repeated measures ANOVA and Tukey's test comparing injury with and without clopidogrel: displacement: $p = 0.002$; velocity: $p = 0.003$; fraction: $p = 0.036$; 7 DMSO- and 6 clopidogrel-treated slices). These data show that microglia in acute brain slices use the ATP-$P2Y_{12}$ receptor pathway to respond to tissue damage, which is the same pathway that microglia *in vivo* employ (Davalos et al., 2005; Haynes et al., 2006). These data also show that acute brain slices faithfully reproduce the ability of microglia to respond to tissue damage.

4.3.b. Activated microglia have a reduced capacity to respond to tissue damage

As shown in Chapter 3, activated microglia respond to ATP with process retraction *in vitro*, which is in contrast to the process extension displayed by resting microglia (Orr et al., 2009). To determine if this occurs in tissues and affects the ability of microglia to respond to damage, I induced systemic inflammation and microglial activation by injecting $CX_3CR1^{GFP/+}$ mice with LPS (2 mg/kg i.p.), an established activator of microglia (Orr et al., 2009), and prepared slices two days later. To confirm microglial activation in the brain, mRNA isolated from brain slices at different time points after the slicing procedure was used for RT-PCR analysis of cytokine expression. There was no visible change in expression in the pro-inflammatory marker IL-1β in slices prepared from PBS-treated (control) mice, but clear induction in IL-1β transcription following LPS treatment (Fig. 4.4A). Microglia in slices from mice treated with PBS responded to mechanical damage with process extension. Processes showed significantly increased displacement and velocity in the direction of injury, and a significantly increased fraction of tracks with displacement over 5 μm (Fig. 4.4B-D; two-way repeated measures ANOVA and Tukey's test comparing baseline to injury: displacement: $p < 0.001$; velocity: $p < 0.001$; fraction: $p = 0.001$; 9 PBS-treated slices). LPS-induced microglial activation did not seem to affect the baseline motility of microglia (Fig. 4.4B-D; two-way repeated measures ANOVA

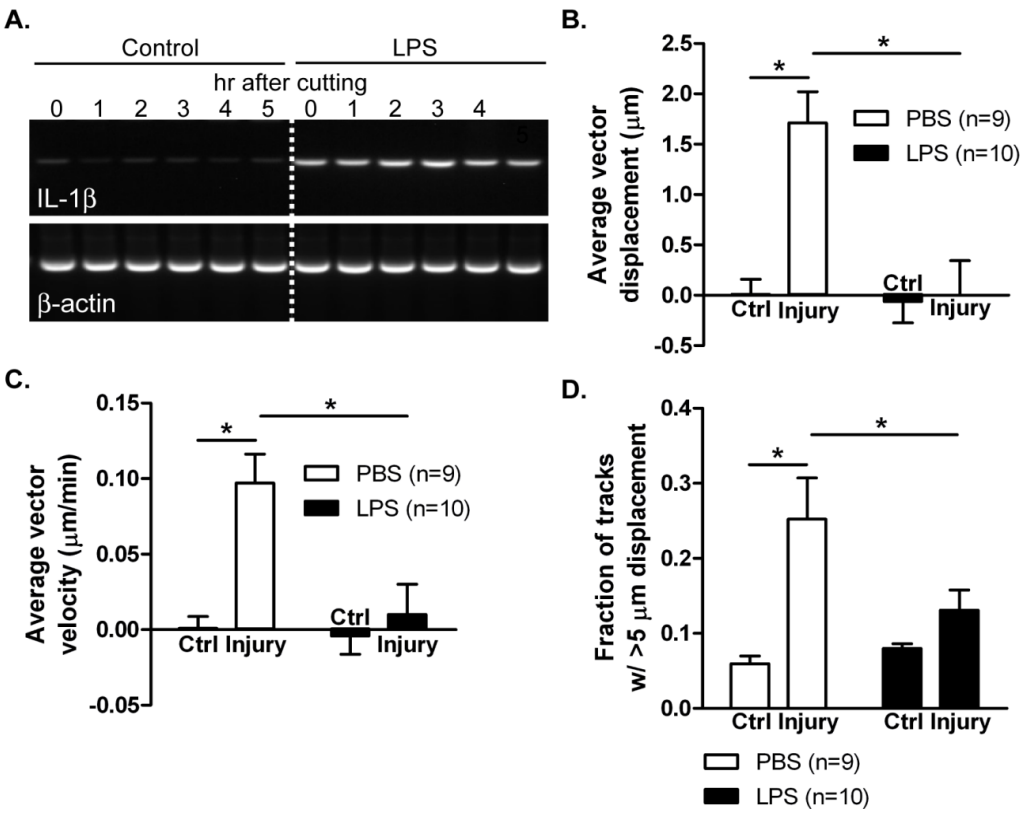

Figure 4.4. Microglial response to tissue damage in slices from LPS-treated animals. *$CX_3CR1^{GFP/+}$* mice were injected with 2 mg/kg i.p. LPS or PBS, and slices were prepared 2 days later. **A.** Microglial activation was assessed by measuring IL-1β mRNA expression with RT-PCR with RNA extracted from slices at different time points after cutting. The cutting procedure does not induce IL-1β expression, but LPS injection 48 hr prior to slice preparation increases IL-1β expression. **B-D.** Quantification of microglial motility in slices from LPS-treated mice by tracking objects in time lapse recordings. The average displacement of all moving objects (**B**), the average velocity of movement (**C**), and the fraction of tracks with longer than 5 μm displacement (**D**) were calculated from baseline recordings of motility (control, Ctrl) before injury and after the induction of the injury in the same slice. Numbers of slices for each condition are shown in parentheses. Statistics: two-way repeated measures ANOVA and Tukey's *post hoc* test. *, $p < 0.05$.

and Tukey's test comparing slices from PBS- and LPS-injected mice: displacement: $p = 0.635$; velocity: $p = 0.823$; fraction: $p = 0.678$; 9 PBS- and 10 LPS-treated slices). However, in slices prepared from LPS-treated mice, microglia had a significantly reduced response to the injury (Fig. 4.4B-D; two-way repeated measures ANOVA and Tukey's test comparing slices from PBS- and LPS-injected mice: displacement: $p < 0.001$; velocity: $p < 0.001$; fraction: $p = 0.008$; 9 PBS- and 10 LPS-treated slices). Thus, activated microglia in tissues appear to have an impaired ability to sense ATP released at the site of damage and/or extend their processes to the damaged area.

4.3.c. MPTP treatment impairs microglial response to tissue damage

The inability of LPS-activated microglia to respond in the normal fashion to tissue damage raised the question of how the activated microglia found in the brains of PD patients will react to the ongoing cell death that is part of the disease. In an attempt to start answering this question, I examined microglial behavior in the substantia nigra of slices from MPTP-treated mice. $CX_3CR1^{GFP/+}$ mice were injected with 20 mg/kg/day s.c. once a day for five days, a treatment regimen that is similar to the one that induces a relatively slow and progressive loss of dopaminergic neurons over at least 25 days (Seniuk et al., 1990; Tatton and Kish, 1997). To examine microglial motility at earlier stages of MPTP-induced toxicity, before all SN neurons are lost, I performed all experiments 4-6 days after the conclusion of the MPTP injection regimen. Even at this stage, there was qualitative loss of TH-positive dopaminergic neurons in the SN and their terminals in the striatum (Fig. 4.5A). Following MPTP injection, microglia started to display an activated morphology; staining for Iba1 revealed cells with larger cell bodies and thicker processes that are easier to see in photomicrographs in both the SN and striatum of MPTP-injected mice (Fig. 4.5B). It should be noted that MPTP-induced microglial activation is likely indirect, from the degenerating dopaminergic neurons, because microglia do not express the dopamine transporter that MPTP uses to enter cells to impair their functions (Storch et al., 2004).

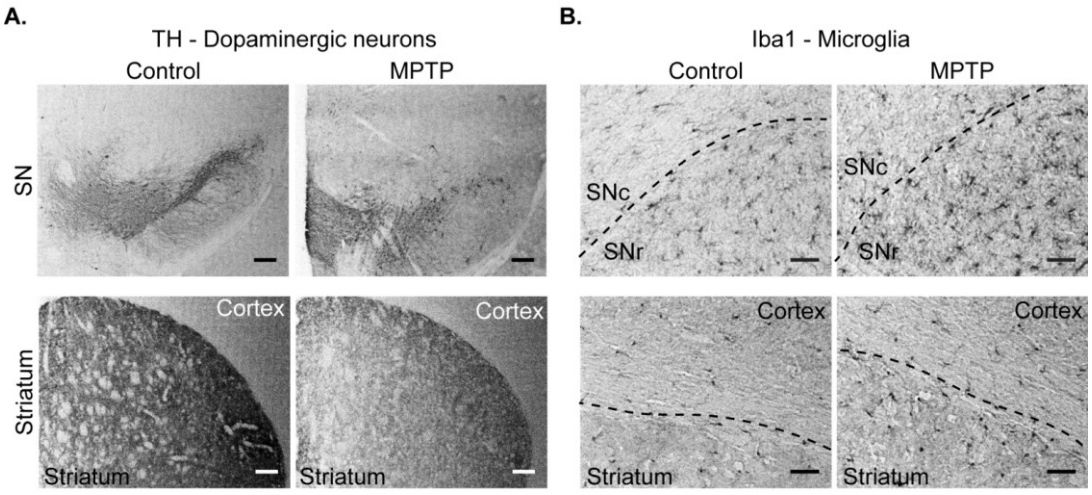

Figure 4.5. Characterization of the effects of MPTP treatment in *$CX_3CR1^{GFP/+}$* mice. *$CX_3CR1^{GFP/+}$* mice were treated with 20 mg/kg/day s.c. MPTP or saline once daily for 5 days, and brains were isolated for immunohistochemistry 5 days after the final MPTP injection. **A.** Staining of dopaminergic neurons with anti-TH antibody shows decreased immunoreactivity in the SN and striatum after MPTP treatment. Scale bar: 200 µm. **B.** Microglia, identified with anti-Iba1 antibody, displayed activated phenotype in the SN and striatum after MPTP treatment. Microglia in the cortex appeared similar to microglia in saline-injected animals. Approximate borders between different brain regions, identified based on microglial distribution and anatomical features, are shown as dashed lines. Scale bar: 50 µm.

After confirming microglial activation in the SN of MPTP-treated mice, I tested their ability to respond to mechanically induced tissue injury designed to damage only a few neurons. I performed time-lapse recordings with slices from saline- or MPTP-treated $CX_3CR1^{GFP/+}$ mice before and after injury, and quantified microglial responses in terms of displacement towards the site of damage, velocity, and fraction of objects with displacements longer than 5 μm. All three measures were significantly increased after damage in saline-treated mice (Fig. 4.6; two-way repeated measures ANOVA and Tukey's test comparing baseline to injury: displacement: p = 0.022; velocity: p = 0.037; fraction: p = 0.029; 11 saline-treated slices). Microglial activation by MPTP did not detectably affect the baseline dynamics (short extensions and retractions) of microglia (Fig. 4.6; two-way repeated measures ANOVA and Tukey's test comparing slices from saline- and MPTP-injected mice: displacement: p = 0.853; velocity: p = 0.897; fraction: p = 0.309; 11 saline- and 9 MPTP-treated slices). However, the displacement and velocity in the direction of injury were significantly reduced in slices from MPTP-treated mice, but not the fraction of tracks with displacement longer than 5 μm (Fig. 4.6; two-way repeated measures ANOVA and Tukey's test comparing slices from saline- and MPTP-injected mice: displacement: p = 0.001; velocity: p = 0.005; fraction: p = 0.197; 11 saline- and 9 MPTP-treated slices). These findings indicate that nigral microglia in MPTP-treated mice did not extend processes toward the region of damage, consistent with activated cortical microglia in LPS-treated animals (Fig. 4.4).

4.3.d. Antagonism of adenosine A_{2A} receptors restores microglial responses to tissue injury

A_{2A} receptors are upregulated in activated microglia and mediate microglial responses to ATP (Chapter 3). Specifically, ATP and adenosine induce process retraction and migration away from the ATP source in primary cultured cortical microglia [Fig. 3.4-6, 3.8; Orr et al. (2009)]. Hence, I examined whether adenosine A_{2A} receptors mediate the inability of nigral microglia in brain slices to respond to tissue damage. I first determined if A_{2A} receptors are expressed in microglia in MPTP-treated mice by performing fluorescent immunohistochemistry. In saline-

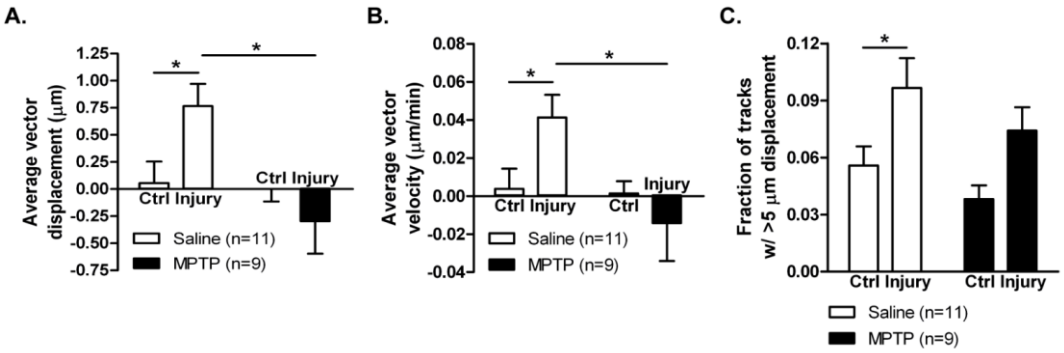

Figure 4.6. Microglial response to tissue damage in slices from MPTP-treated animals. *CX$_3$CR1$^{GFP/+}$* mice were injected with 20 mg/kg/day s.c. MPTP or saline once daily for 5 days, and slices were prepared for imaging 4-7 days later. 2D projections of the optical stacks at each time point were used for analysis by tracking moving objects larger than 2 μm in diameter. The average displacement of all moving objects (**A**), the average velocity of movement (**B**), and the fraction of tracks with longer than 5 μm displacement (**C**) were calculated from baseline recordings of motility (control, Ctrl) before injury and after the induction of the injury in the same slice. Numbers of slices for each condition are shown in parentheses. Statistics: two-way repeated measures ANOVA and Tukey's *post hoc* test. *, $p < 0.05$.

treated mice, most of the A_{2A} receptor immunoreactivity was found in long, thin structures that resembled blood vessels (Fig. 4.7A). Following MPTP treatment, there was a diffuse upregulation of A_{2A} receptors that was more pronounced in the SNr compared to surrounding brain regions (Fig. 4.7A, B, middle). The average Texas Red fluorescence (representing A_{2A} receptor expression) in the SNr was significantly higher in MPTP-treated mice (Fig. 4.7C; Student's *t* test, $p = 0.0208$), indicating that MPTP treatment induced A_{2A} receptor upregulation. To determine whether any of this A_{2A} receptor expression was in microglia, I performed colocalization analysis with the GFP signal that is specific to microglia (Costes et al., 2004). There was an increase in the fraction of microglia (GFP signal) that contained A_{2A} receptors (Texas Red signal) following MPTP treatment (Student's *t* test, $p = 0.0463$; Figure 7D), and the fraction of A_{2A} receptor signal within microglia (Student's *t* test, $p = 0.0251$; Figure 7E). Thus, some of the A_{2A} receptor upregulation is in microglia.

A_{2A} receptor expression in the striatum, where it is constitutively expressed in dopaminergic neurons (Parkinson and Fredholm, 1990) was also characterized. As expected (Bogenpohl et al., 2012), there was a diffuse neuropil staining in the striatum, but not in the neighboring cortex, of saline-treated mice (Fig. 4.8A). Despite the already high expression, there was an increase in A_{2A} receptor immunoreactivity following MPTP treatment (Fig. 4.8B; Student's *t* test, $p = 0.0624$). Quantifying A_{2A} receptor expression in striatal microglia showed that there was no re-distribution of the A_{2A} receptor signal between microglial and non-microglial compartments (Fig. 4.8C, D; Student's *t* test, $p = 0.9704$ for Mander's A coefficient; Student's *t* test, $p = 0.6482$ for Mander's B coefficient). Overall, data from the SN and striatum show that MPTP treatment changed patterns of A_{2A} receptor expression in a region-specific manner.

Finally, I examined the ability of A_{2A} receptor antagonists to modulate microglial response to tissue damage in slices from MPTP-treated mice. In order to do that, I included the selective A_{2A} receptor antagonist preladenant [$K_i = 1.1$ nM in isolated cells; see Neustadt et al. (2007); used at 5 μM here] in the perfusion solution for the duration of the experiment, before

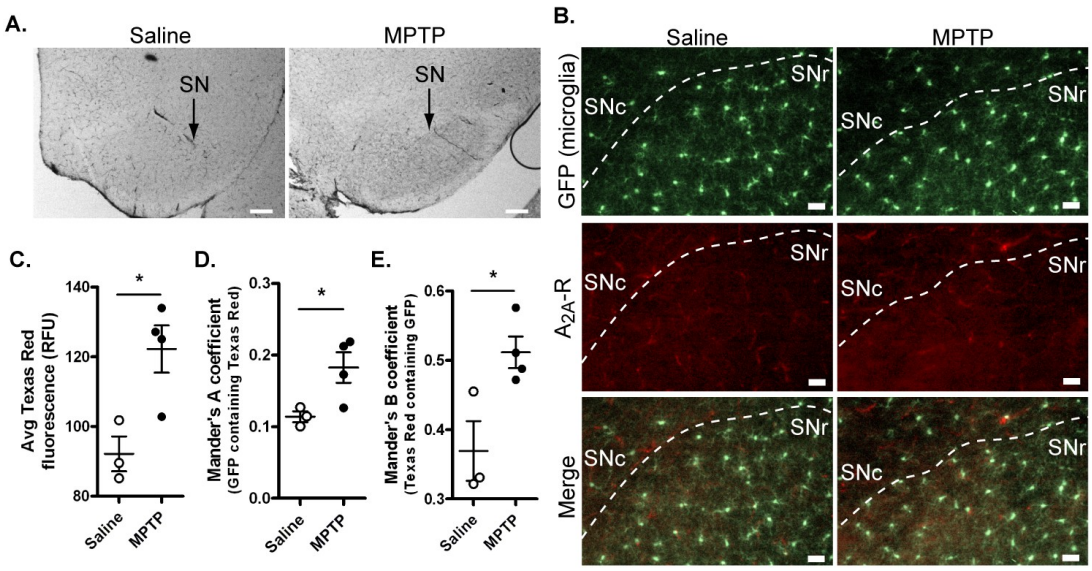

Figure 4.7. Changes in adenosine A_{2A} receptor expression in the substantia nigra of MPTP-treated mice. *$CX_3CR1^{GFP/+}$* mice were treated with 20 mg/kg s.c. MPTP or saline once daily for 5 days, and brains were isolated for analysis 5 days later. **A-B.** Adenosine A_{2A} receptor expression in the substantia nigra was detected with immunohistochemistry using either the DAB method (**A**) or immunofluorescence (**B**). Microglia were identified without staining from the expression of GFP from the CX_3CR1 promoter. Approximate borders between SNc and SNr are given with dashed lines based on microglial cell density. Figure shows representative slices from 3 saline- and 4 MPTP-treated mice. Scale bar: **A**, 200 µm; ***B***, 30 µm. **C,** Upregulation of A_{2A} receptor expression in the SNr following MPTP treatment was determined by measuring the average fluorescence signal. **D-E.** Colocalization analysis of A_{2A} receptor and GFP-labeled microglia in the SN using Mander's coefficients. Mander's A coefficient (**D**) represents the fraction of GFP signal that colocalizes with some Texas Red signal (A_{2A} receptors). Mander's B coefficient (**E**) represents the fraction of A_{2A} receptors that show colocalization with GFP-expressing microglia Statistics: two-tailed Student's *t* test comparing average signals in each animal.

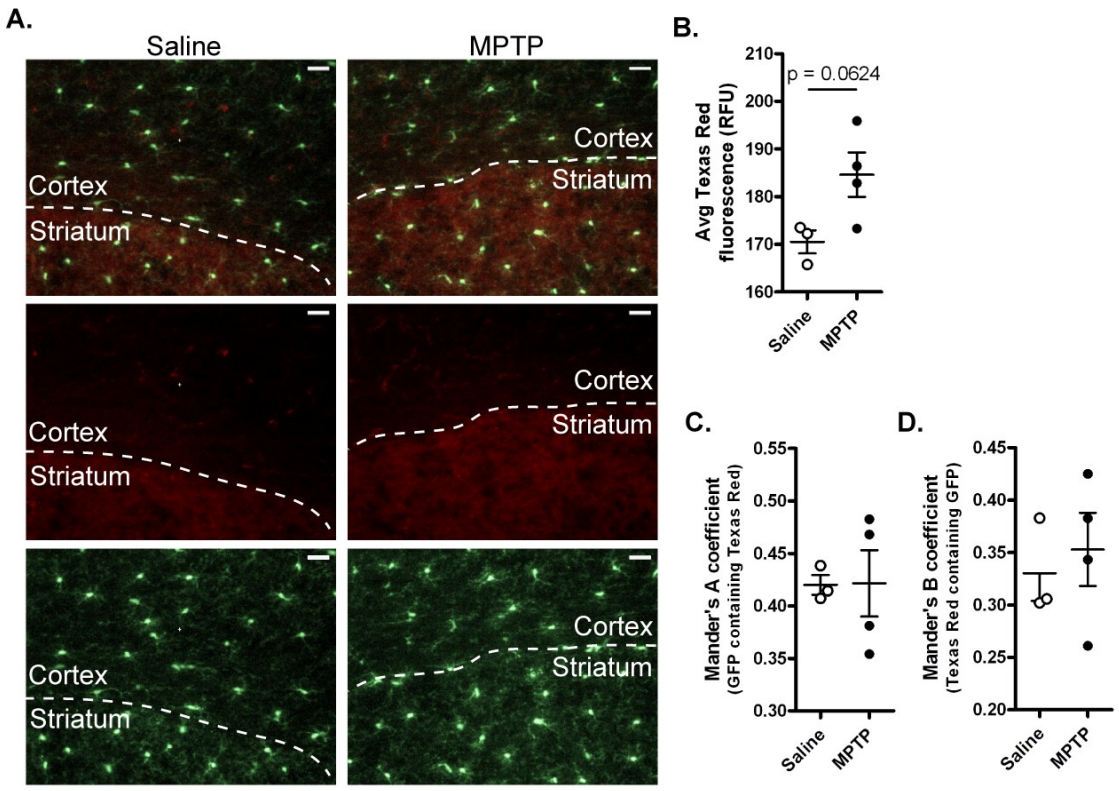

Figure 4.8. Changes in adenosine A_{2A} receptor expression in the striatum of MPTP-treated mice. *$CX_3CR1^{GFP/+}$* mice were treated with 20 mg/kg s.c. MPTP or saline once daily for 5 days, and brains were isolated for analysis 5 days later. **A.** Adenosine A_{2A} receptor expression was detected with immunofluorescence. Microglia were identified without staining from the expression of GFP from the CX_3CR1 promoter. Approximate borders between striatum and cortex, identified based on A_{2A} receptor immunofluorescence, are given with dashed lines. Figure shows representative slices from 3 saline- and 4 MPTP-treated mice. Scale bar: 30 μm. **B.** Upregulation of A_{2A} receptor expression in the striatum following MPTP treatment was determined by measuring the average fluorescence signal. **C-D.** Colocalization analysis of A_{2A} receptor and GFP-labeled microglia in the striatum using Mander's coefficients. Mander's A coefficient (**C**) represents the fraction of GFP signal that colocalizes with some Texas Red signal (A_{2A} receptors). Mander's B coefficient (**D**) represents the fraction of A_{2A} receptors that show colocalization with GFP-expressing microglia Statistics: two-tailed Student's *t* test comparing average signals in each animal.

and after induction of mechanical damage. The inclusion of the antagonist during the baseline recording did not significantly affect the baseline extensions and retractions of microglial processes in the absence of injury (Fig. 4.9; two-way repeated measures ANOVA and Tukey's test comparing slices from MPTP-injected mice before and after preladenant: displacement: p = 0.451; velocity: p = 0.495; fraction: p = 0.009; 5 DMSO- and 8 preladenant-treated slices). This is consistent with the lack of difference in baseline motility of microglia induced by MPTP activation. Yet, microglia in slices from MPTP-treated mice that were pre-treated with preladenant showed significant increases in their displacement towards injury (Fig. 4.9A; two-way repeated measures ANOVA and Tukey's test: displacement: p = 0.014, 8 preladenant-treated slices), velocity (Fig. 4.9B; p =0 .010), and fraction of tracks with displacement longer than 5 μm (Fig. 4.9C; p = 0.009) compared to slices treated with vehicle control (DMSO, 5 slices). That is, preladenant restored process motility in MPTP-treated animals near to the level seen in control animals. These data indicate that the upregulation of adenosine A_{2A} receptors in microglia might mediate the impaired microglial response to tissue damage in the substantia nigra in MPTP-treated mice. In addition, antagonism of A_{2A} receptors with preladenant ameliorate these effects, which may have therapeutic implications.

4.4. Discussion

4.4.a. Microglial motility in acute brain slices

In this chapter, I describe a confocal imaging method to study the motility of GFP-expressing microglia at high spatial and temporal resolution in acute brain slices. Although it is possible to image cortical microglia in the brains of alive, anesthetized animals using two-photon microscopy (Davalos et al., 2005; Haynes et al., 2006; Nimmerjahn et al., 2005), this approach requires specialized expertise and equipment and can only be applied to cells near the pial surface. In contrast, slices can be prepared from any region of interest, including deep brain loci such as nuclei in the midbrain that are affected in some neurodegenerative diseases. While the

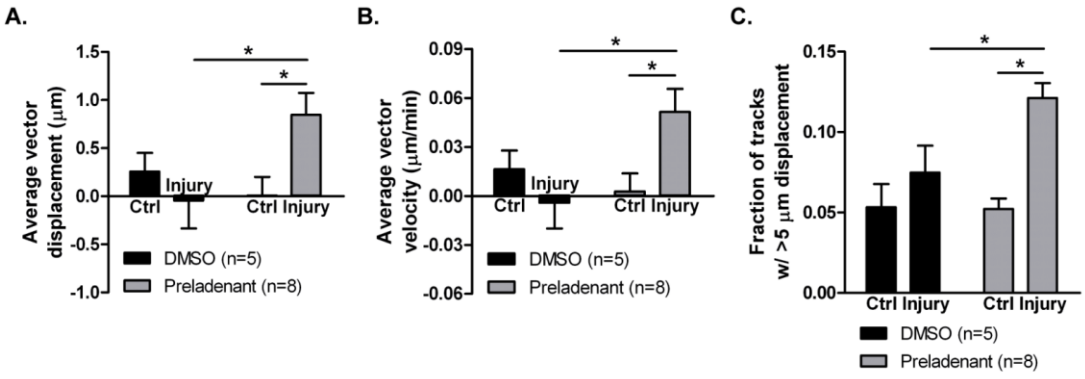

Figure 4.9. Effect of A_{2A} receptor antagonist on microglial response to tissue damage in slices from MPTP-treated animals. *$CX_3CR1^{GFP/+}$* mice were injected with 20 mg/kg/day s.c. MPTP once daily for 5 days, and slices were prepared for imaging 4-7 days later. The perfusion solution contained either the selective A_{2A} receptor antagonist preladenant (5 μM) or DMSO vehicle. 2D projections of the optical stacks at each time point were used for analysis by tracking moving objects larger than 2 μm in diameter. The average displacement of all moving objects (**A**), the average velocity of movement (**B**), and the fraction of tracks with longer than 5 μm displacement (**C**) were calculated from baseline recordings of motility (control, Ctrl) before injury and after the induction of the injury in the same slice. Numbers of slices for each condition are shown in parentheses. Statistics: two-way repeated measures ANOVA and Tukey's *post hoc* test. *, $p < 0.05$.

slicing procedure might transiently affect microglia, the cells still exhibit primarily a "resting" phenotype, which was confirmed by their ability to respond to ATP with process extension to tissue damage in a $P2Y_{12}$-receptor dependent manner [Fig. 4.2, 4.3; Avignone et al. (2008); Haynes et al. (2006)]. Furthermore, the expression of proinflammatory cytokines such as IL-1β was not induced by the process of slicing as opposed to clear induction following a peripheral LPS injection (2 mg/kg i.p.) 2 days before slicing (Fig. 4.4A). I then used this preparation to study microglial response to mechanical damage by lowering a rod with a micromanipulator into the tissue. The use of the micromanipulator ensures that the injury is controlled and reproducible between experiments. Moreover, the injury appeared localized in nature, seemingly sparing the neighboring tissues (Fig. 4.1C, D). Thus, this slice preparation represents a good model system for the study of microglial motion in tissues, and faithfully captures many microglial properties.

Acute slices have been used to study microglial dynamics before. For example, Stence et al. (2001) used slices from wild type mice in which the microglia were fluorescently labeled after slicing to describe the morphological stages microglia go through to transition from a ramified to an amoeboid, locomotory phenotype over 24 hr. Slices can be prepared from animal models of various diseases, as has been the case with status epilepticus and AD (Avignone et al., 2008; Krabbe et al., 2013). This slice preparation could be used to study microglial function in response to tissue damage similar to paradigms available for live animal imaging, including laser or mechanical damage (Krabbe et al., 2013; Krabbe et al., 2012). Most importantly, slices can be prepared from any region of interest, including deep brain loci such as nuclei in the midbrain, allowing examination of region-specific differences in microglial function. Finally, high resolution imaging of microglia in slices could be used to study microglial functions other than motility. For example, slices have been successfully used to examine phagocytosis of dead cells in real time (Brockhaus et al., 1996; Katayama et al., 2012; Kurpius et al., 2007; Petersen and Dailey, 2004).

4.4.b. Activated microglia in Parkinson's disease

Microglia with activated morphology are found in the brains of patients with several neurodegenerative diseases, including PD (Gerhard et al., 2006; McGeer et al., 1988a). Here I show that activated microglia have a reduced capacity to respond to tissue damage in the substantia nigra of acute brain slices using a model of both a direct (LPS) and indirect (MPTP) activation of microglia (Fig. 4.4, 4.6). While the injury paradigm I used is non-physiological, it resulted in the injury of a small, defined, area while recording responses in real time. In this way, I was able to study the immediate microglial response to the death of only a few neurons (Fig. 4.1B, C). The containment of the damaged area by microglial processes is thought to prevent spread of damage and promote tissue healing, and delayed containment is associated with expansion of the injury site (Hines et al., 2009). While these findings were observed in healthy mice, a similar process might be occurring in mice undergoing active cell death in SNc. The delayed response of activated microglia to tissue damage or cell death could prevent efficient clearance of tissue debris, resulting in leakage of debris into the surrounding brain parenchyma and possibly injuring nearby cells and promoting their demise. Therefore, the findings presented here suggest that altered motility of activated microglia in the MPTP model of PD might represent yet another mechanism by which microglia contribute to neurodegeneration in mice and humans. This concept is further discussed in Section 7.3.c.

4.4.c. Possibility for differential motility patterns of microglia in PD

The neuronal population most affected in PD are midbrain neurons, specifically dopaminergic neurons projecting from the substantia nigra to the striatum [Fig. 4.5; Bernheimer et al. (1973); Kish et al. (1988)]. This is closely mirrored by the state of microglial activation: microglia in the midbrain/substantia nigra display higher degree of activation in both patients with PD [in post-mortem samples and assessed with PET imaging; Gerhard et al. (2006); McGeer et al. (1988a)], and in animal models of the disease [see Section 1.4.a; Tansey and Goldberg

(2010)]. In this chapter, I examined the motility of activated microglia in the substantia nigra, showing that they display a delayed response to tissue damage. However, microglia in the striatum might be differentially affected by MPTP treatment. Indeed, the pattern of A_{2A} receptor expression following MPTP treatment was different in the striatum compared to the SN (Fig. 4.7, 4.8). The A_{2A} receptor was upregulated in both brain regions. Yet, there was also an increase in microglial A_{2A} receptors in the SN, but no change in the A_{2A} signal inside microglia in the striatum. Thus, microglia in the striatum might be functionally different than microglia in the SN, particularly in their response to tissue damage and sensitivity to A_{2A} receptor antagonists. Moreover, microglia in the cortex did not display signs of overt activation following MPTP treatment (Fig. 4.5, 4.8). This raises the possibility that there might be a third microglial functional state in MPTP-treated mice. As a result, it is worthwhile examining whether microglia in these two regions might have a different response to tissue damage in MPTP-treated mice compared to microglia in the SN.

4.4.d. Modulation of microglial motility by A_{2A} receptors in tissues

As shown in Chapter 3, A_{2A} receptor antagonists prevent adenosine-induced process retraction in activated microglia (Fig. 3.7). Microglia in the MPTP model of PD also assume an activated morphology (Fig. 4.5), which was associated with a reduced response to tissue damage in slices (Fig. 4.6). Consistent with the properties of A_{2A} receptor antagonists *in vitro*, inhibition of A_{2A} receptors reduced the effects of MPTP treatment on microglial response to damage. Specifically, microglia in slices treated with the selective A_{2A} receptor antagonist preladenant were able to extend their processes in the direction of the injury to an extent similar to the one in healthy mice (Fig. 4.6, 4.9).

Both selective and non-selective A_{2A} receptor antagonists possess neuroprotective properties in animal models of PD (discussed in detail in Section 7.3.c). The ability of preladenant to restore microglial response to tissue injury in slices suggests that at least some of

its neuroprotective properties might be due to modulation of microglial motility. Because of the observed A_{2A} expression in microglia based on colocalization analysis (Fig. 4.7), it is likely that the effects of A_{2A} receptors on microglial dynamics are direct. Yet, I cannot discount the possibility that other mechanisms might be involved in the modulation of microglial response to damage in slices from MPTP-treated mice. For example, A_{2A} receptor inhibition could somehow lead to the release of chemoattractive compounds at the site of damage that result in enhanced microglial process extension. Alternatively, inhibition of neuronal A_{2A} receptors in the striatum could alter the tissue environment of synaptic function of the slice, which could be sensed by microglia in the SN. The altered environment, possibly together with inhibition of microglial A_{2A} receptors in the SN, could be sufficient to restore the ability of microglia to extend their processed to the tissue damage. In reality, it is likely that various mechanisms and cellular populations contribute to the overt neuroprotection of A_{2A} antagonists. Understanding the relative contributions of A_{2A} receptors on different cell types could allow the selective potentiation of certain beneficial effects, for instance, the improved response to damage.

CHAPTER 5: Purinergic control of microglial motility *in vivo*

5.1 Abstract

ATP elicits opposite effects on the motility of resting and activated microglia *in vitro* through the differential activation of $P2Y_{12}$ and adenosine A_{2A} receptors (Chapter 3), leading to reduced ability of activated microglia in acute brain slices to respond to tissue damage (Chapter 4). Inflammation is part of the pathogenesis of most neurodegenerative diseases; however, whether inflammation affects microglial responses to tissue damage *in vivo* remains largely unknown. In this chapter, I employ *in vivo* two-photon imaging of $CX_3CR1^{GFP/+}$ mice injected with LPS to study the motility of microglia under pro-inflammatory conditions in the brain. In the absence of tissue damage, activated microglia display a hypermotile behavior *in vivo*. Yet, they respond to laser-induced ablation injury at a significantly reduced rate compared to microglia in control animals. Administration of the adenosine A_{2A} receptor antagonist preladenant before imaging protected from the inflammation-induced decrease of microglial response to injury. The regulation of rapid microglial responses to sites of injury by A_{2A} receptors could have implications for their ability to respond to the neuronal death occurring under conditions of neuroinflammation in neurodegenerative disorders.

5.2. Introduction

Neurodegenerative diseases such as AD, ALS, MS, and PD are characterized by slow and progressive neuronal death. Despite the differences in neuronal populations affected and subsequent manifestations of the various diseases, one common feature they all share is the presence of neuroinflammation, which likely affects disease progression (Block and Hong, 2005). There are several manifestations of neuroinflammation in neurodegenerative conditions. First, the levels of many pro-inflammatory cytokines are increased in the blood and/or CSF of patients with neurodegenerative conditions (Akiyama et al., 2000; Smith et al., 2012; Tansey and Goldberg,

2010). Furthermore, activated microglia, visualized with PET imaging, are present at much higher levels in the brains of AD, PD and MS patients compared to healthy age-matched controls (Venneti et al., 2013). Microglial activation has been described as one of the earliest pathological alterations that can be detected both in humans and in animal models of MS even in normal appearing white matter and before the onset of clinical pathology (Davalos et al., 2012; Marik et al., 2007). Moreover, systemic inflammation can influence the progression of not only neuroinflammatory or autoimmune diseases like MS (Murta and Ferrari, 2013), but also neurodegenerative diseases (Cunningham, 2013; Perry et al., 2007; Perry et al., 2003). Finally, prolonged use of non-aspirin NSAIDs is associated with reduced risk for developing AD (see Section 1.4.b), while ibuprofen lowers the risk for PD (see Section 1.4.a). On the other hand, mutations in genes related to immune system function can increase the risk for developing AD and PD (see Section 1.4).

In addition to the immune functions that they perform (Hanisch, 2002; Hanisch and Kettenman, 2007; Kreutzberg, 1996), microglia also serve important roles that help to maintain normal activity in the healthy brain [see Section 1.3; Kettenmann et al. (2013)]. Time-lapse imaging studies using two-photon microscopy in living animals show that microglia are highly motile, typically move their processes in a stochastic multidirectional pattern, and appear to monitor the brain parenchyma in the absence of a stimulus (Davalos et al., 2005; Haynes et al., 2006; Nimmerjahn et al., 2005). Another important feature of microglial behavior is the alteration in the movement pattern of their processes when they encounter a stimulus. For example, when challenged by a localized injury, microglial process movements are no longer stochastic, but extend directly toward the location of the injury in an orchestrated manner. This response allows microglial processes to contain localized cortical injuries on a time scale of minutes, and likely facilitate local repair mechanisms by clearing cellular debris (Davalos et al., 2005).

Microglia show a great morphological and functional diversity in the brain, ranging from the ramified, “resting” phenotype associated with tissue surveillance in the healthy brain to

amoeboid, fully activated, cytokine-secreting and phagocytic phenotypes in neurodegenerative diseases [see Section 1.2.c; Colton and Wilcock (2010)]. Interestingly, the purinergic $P2Y_{12}$ receptor that microglia use to sense ATP released at the site of damage is downregulated following microglial activation, for example, by treatment with LPS or amyloid β peptides [Section 3.3.a; Fig. 3.1; Haynes et al. (2006); Orr et al. (2009)]. This is accompanied by upregulation of the adenosine A_{2A} receptor [Section 3.3.a; Fig. 3.1, 3.2; Orr et al. (2009)], which can be activated indirectly by ATP after its rapid breakdown to adenosine (Zimmermann, 2000). In contrast to the ability of ATP to induce process extension and chemoattraction in resting microglia (Davalos et al., 2005; Honda et al., 2001), ATP induces process retraction and migration away from an ATP source in activated microglia *in vitro* in an A_{2A} receptor-dependent manner [Section, 3.3.b; Fig. 3.5, 3.8; Orr et al. (2009)]. Similarly, activated microglia in acute brain slices show reduced process extension to tissue injury (Chapter 4). The lack of $P2Y_{12}$ receptors and the differential effect of ATP in activated microglia make it uncertain how activated microglia will respond acutely to an ATP gradient in the moments after neuronal death *in vivo*.

In this Chapter, I present results from *in vivo* two-photon imaging of LPS-treated mice to study microglial motility in living animals in the presence of LPS-induced neuroinflammation. Microglia in LPS-treated animals showed altered baseline dynamics and displayed a delayed response to laser-induced cell death, which are behaviors that have not been described for microglia *in vivo* before. Importantly, a selective A_{2A} antagonist was able to accelerate the response of microglia to tissue damage in LPS-treated mice. The ability of distinct G protein-coupled receptors to differentially modulate the process motility patterns of resting and activated microglia and their responses to cell death could be explored as a novel strategy for selective therapeutic interventions designed to slow disease progression by attenuating the harmful effects of chronic neuroinflammation.

5.3. Results

5.3.a. Characterization of activated microglia in vivo

The bacterial cell wall component LPS can induce central nervous system inflammation after a single peripheral injection (Qin et al., 2007). $CX_3CR1^{GFP/+}$ mice, which have microglia-specific GFP expression (Jung et al., 2000), were injected with 2 mg/kg i.p. LPS, and two days post-injection there was increased mRNA expression of the pro-inflammatory cytokines IL-1β and TNF-α (Fig. 5.1A) in cortical tissue. Thus, this time point was selected to perform *in vivo* two-photon microscopy using the thinned skull preparation that is commonly used to study microglial behavior in the healthy brain (Davalos et al., 2005; Haynes et al., 2006; Nimmerjahn et al., 2005). Analysis of microglial morphology from the *in vivo* imaging data showed that microglia in LPS-injected mice had an activated phenotype (Fig. 5.1B) characterized by significantly larger cell bodies (Fig. 5.1C; Student's *t* test, $p = 0.003$) and higher number of primary processes (Fig. 5.1D; Student's *t* test, $p < 0.001$). However, there was a decrease in the three-dimensional volume occupied by a microglial cell in LPS-treated animals, likely due to decreased process length (Fig 5.1B).

Next, the baseline process motility patterns of activated microglia in the unperturbed cortex of LPS-injected mice were studied by obtaining optical sections through the cortex every 30 s over a 10-min interval. Time-lapse recordings indicated that 48 hr after LPS injection activated microglia continued to sample the brain parenchyma by process extension and retraction. Quantification of the process motility patterns *in vivo* by automatically tracking moving objects larger than 2 μm with Imaris software (Fig 5.2A) showed that microglia in LPS-treated animals extended and retracted their processes at significantly higher mean instantaneous speeds than control microglia (Fig. 5.2B; Student's *t* test, $p = 0.0052$), which led to longer distances traveled over the 10-min period (Fig. 5.2C; Student's *t* test, $p = 0.0178$).

5.3.b. Response of activated microglia to tissue damage in vivo

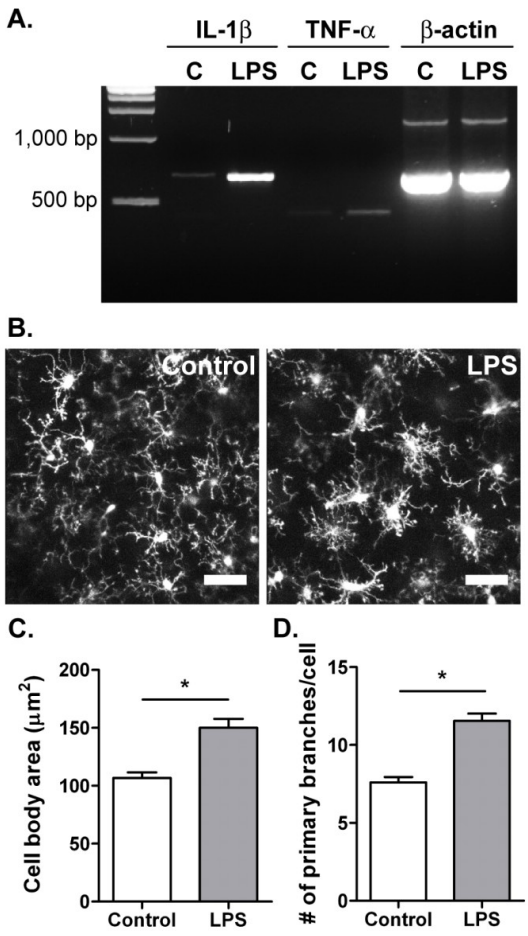

Figure 5.1. Confirmation of microglial activation following LPS treatment *in vivo*. *$CX_3CR1^{GFP/+}$* mice treated with 2 mg/kg LPS i.p. were examined for the presence of neuroinflammation 2 days later. **A.** Expression of the pro-inflammatory cytokines IL-1β and TNF-α, as determined with RT-PCR, increased following LPS treatment. Representative image from one of three PBS- (control, C) or LPS-injected animals for each treatment are shown. **B.** 2D projections of a 30 μm section from the cortex of control (n = 9) and LPS-injected (n = 11) mice showing altered microglial morphology. Scale bar: 50 μm. Increase in the cell body area (**C**) and the number of primary processes (**D**) are morphological changes consistent with microglial activation. Statistics: Student's *t* test. *, $p < 0.05$.

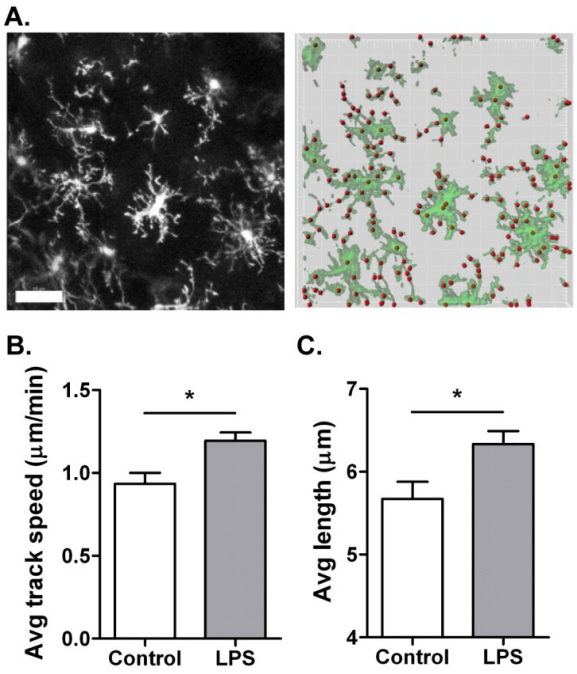

Figure 5.2. Microglial motility under baseline conditions *in vivo*. A. The baseline motility of microglia was assessed with time-lapse two-photon imaging of control (n = 9) or LPS-injected (n = 11) $CX_3CR1^{GFP/+}$ mice. 2D projections of the cortex spanning ~30 μm vertical distance were analyzed with Imaris software to quantify baseline process dynamics. Red dots represent objects identified by the software and tracked over time. Scale bar: 50 μm. The average track speed (**B**) and distance traveled (**C**) increased in magnitude following microglial activation. Statistics: Student's *t* test. *, $p < 0.05$.

In the healthy brain microglia respond to focal damage by extending their processes and surrounding sites of injury within minutes (Davalos et al., 2005; Haynes et al., 2006). Their ability to rapidly respond to localized brain damage is considered essential for maintaining normal brain function in the presence of daily physiological disturbances such as rupture of small blood vessels or death of individual cells (Hanisch and Kettenman, 2007). Considering the divergent effects of ATP on resting vs. activated microglia *in vitro* (Orr et al., 2009) and the impaired motility of activated microglia in slices from LPS- or MPTP-treated mice (Fig. 4.6, 4.9), I wanted to determine whether systemic inflammation affects the ability of microglia to respond to damage *in vivo*. To achieve this, a laser injury was generated in the cortex of control and LPS-injected (2 mg/kg i.p., 2 days before imaging) animals, and microglial response was captured over 60 min with time-lapse two-photon microscopy. In both control and LPS-treated animals microglial cells in the tissue around the laser ablation extended their processes toward the ablation site in the characteristic radial manner that was previously described [Fig. 5.3A, B; Davalos et al. (2005)]. To assess the radial motion quantitatively, our lab initiated a collaboration with Dipankar Biswas and Dr. Frank Loth at the University of Akron to develop a custom algorithm in Matlab (referred to as MGPtracker) that automatically tracks the distance of the closest microglial processes at 10° increments as they converge from every direction around the ablation site. The algorithm then draws a polygon around the laser ablation, the vertices of which form the outline of the microglial processes closest to the ablation. Averaging the distance between each vertex of the polygon and the center of the ablation represents a quantifiable measure of microglial responses toward the ablation, which can be expressed as a function of time (Fig. 2.7). To validate the ability of MGPtracker to capture radial motion, the results obtained with MGPtracker were compared to those obtained by manually measuring the distances of eight microglial processes arranged at 45° increments around the ablation site (Fig. 5.4A-D). Despite the different number of vertices (8 *vs.* 36), the two curves had similar waveforms and

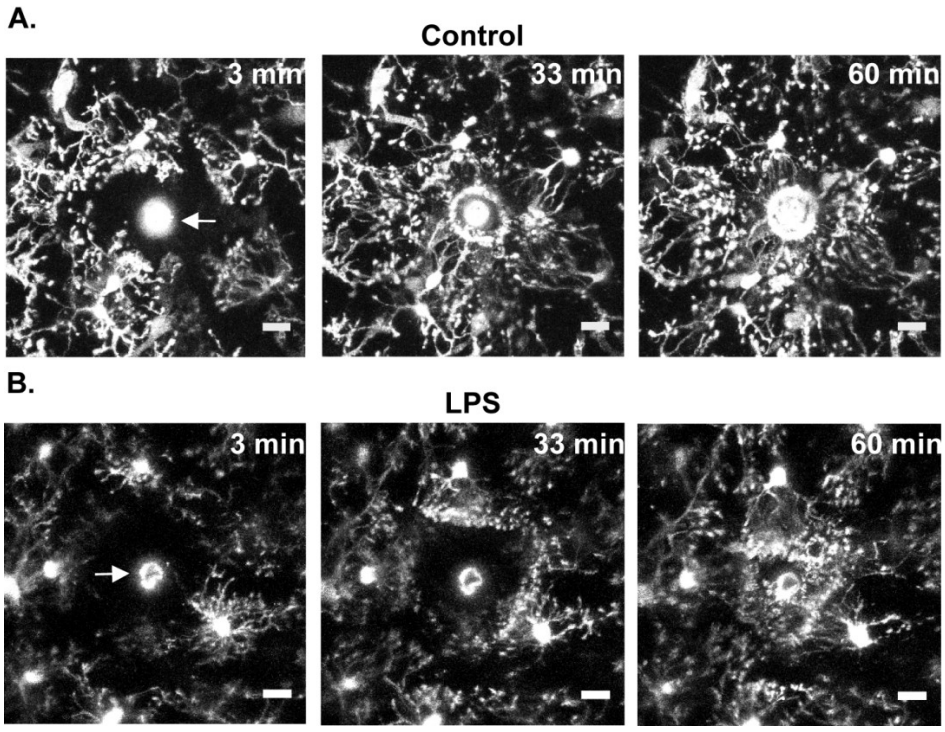

Figure 5.3. Microglial response to laser-induced tissue damage under resting and pro-inflammatory conditions *in vivo*. Select images from time-lapse two-photon recordings from (**A**) control (n = 9) and (**B**) LPS-injected (n = 11) $CX_3CR1^{GFP/+}$ mice show that activated microglia in LPS-treated animals have a delayed response to laser-induced tissue damage. Arrow in first image (t = 3 min) points to the location of the laser ablation. Scale bar: 20 μm.

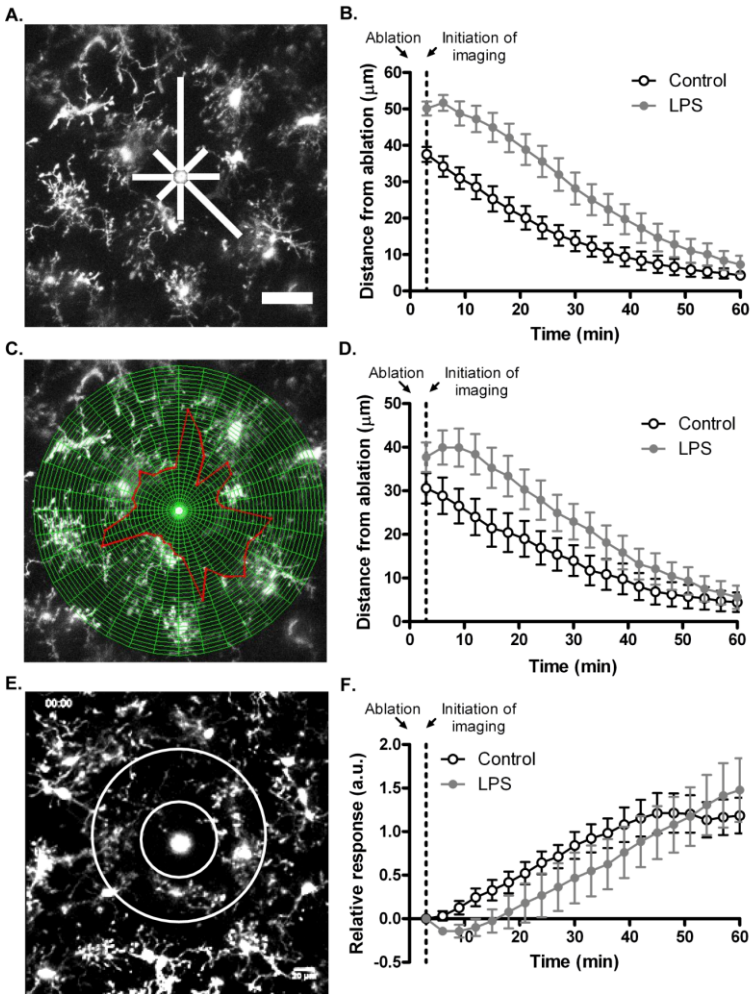

Figure 5.4. Comparison of different methods to quantify microglial response to tissue damage *in vivo*. The same control (n = 9) and LPS-injected (n = 11) animals were used to quantify microglial response to laser-induced tissue damage. **A.** Eight linear ROIs were drawn at 45º angles starting at the ablation and radiating outward until they reach the nearest microglial process. Scale bar: 50 μm. **B.** The average response using manual tracking of distance. **C.** The automated tracking algorithm, MGPtracker, divides the image in 36 sectors. The vertices of the red polygon correspond to the microglial processes closest to the ablation in each sector. **D.** The average response over time using MGPtracker. **E.** Quantification of the response by using the method of Davalos et al. (2005) that measures changes in fluorescence around the ablation. This method normalizes the fluorescence of an inner circular ROI to the fluorescence of a larger ROI. **F.** The average response over time using the Davalos et al. (2005) method. All methods show the same trend of initial microglial retraction away from the ablation.

showed similar trends, confirming that MGPtracker faithfully captured microglial responses toward the site of injury. Moreover, the trends seen by using MGPtracker mirror the trends seen with previously published analysis methods [Fig. 5.4E, F; Davalos et al. (2005)]. An advantage to using MGPtracker is the ability to measure additional parameters of the response, such as the area bound by the polygon and the instantaneous radial velocity at each time point.

Analysis of the average distance between microglial processes and the ablation showed that microglia in LPS-treated animals approached the ablation at a slower rate than microglia in control animals across all time points (Fig. 5.5A; two-way ANOVA, $F_{(1,360)} = 44.74$, $p < 0.0001$). Similarly, the area bound by the polygon, namely the area around the ablation that remains clear of microglial processes, was also significantly larger for LPS-treated animals compared to control throughout the time course of the response (Fig. 5.5B; two-way ANOVA, $F_{(1,360)} = 103.6$, $p < 0.0001$), also implying a slower response to the injury. The instantaneous radial velocity of the response (Fig. 5.5C; two-way ANOVA, $F_{(1,342)} = 3.306$, $p = 0.0699$) and the average time of processes to reach the ablation (45.9 ± 3.4 and 39.2 ± 4.7 min, respectively; Fig. 5.5D; Student's *t* test, $p = 0.2531$) seemed less sensitive to microglial activation. Moreover, all analyzed parameters showed that microglial processes in LPS-treated animals initially retracted from the ablation before eventually approaching the damaged site. Nine out of the eleven LPS-injected mice displayed this type of biphasic response, but only one of nine control animals exhibited any kind of initial retraction ($p < 0.001$, G-test of independence; Fig. 5.5E).

5.3.c. Effects of A_{2A} receptor antagonists on microglial motility in vivo

Because A_{2A} receptor antagonists can reverse the ATP- and adenosine-stimulated microglial process retraction *in vitro* [Section 3.3.b; Fig. 3.5; Orr et al. (2009)] and restore response to damage in tissues (Fig. 3.9), I tested if preladenant, a highly selective and brain permeable A_{2A} antagonist (Neustadt et al., 2007), would be able to ameliorate the delayed response to laser ablation in LPS-injected animals *in vivo*. To control for potential variability

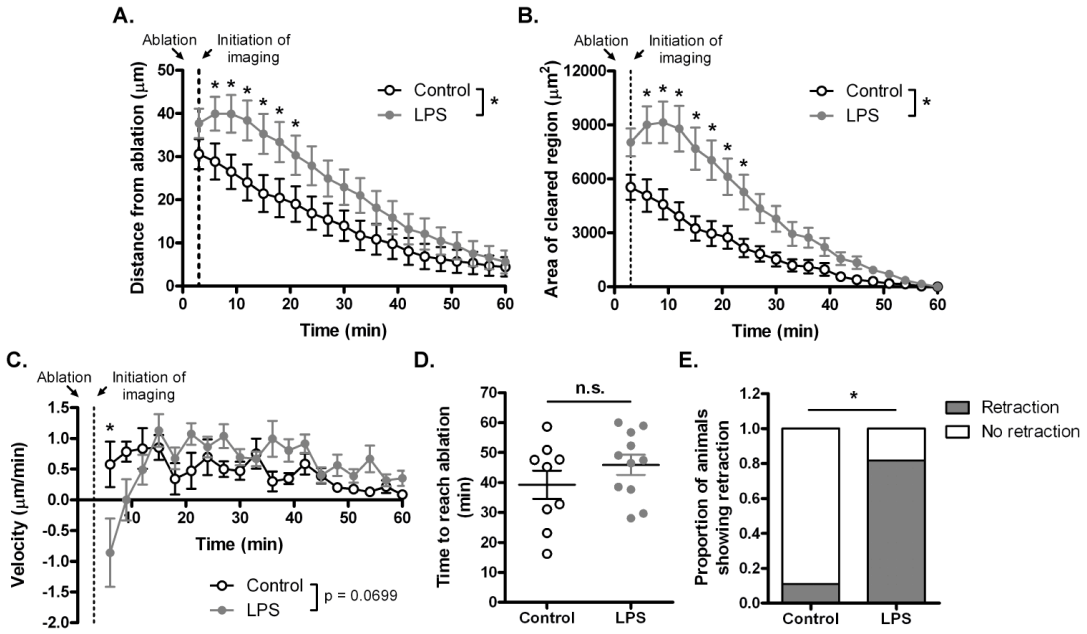

Figure 5.5. Quantification of microglial response to laser-induced tissue damage *in vivo*. Time-lapse two-photon recordings from control (n = 9) and LPS-injected (n = 11) $CX_3CR1^{GFP/+}$ mice were analyzed with MGPtracker to quantify the approach of microglial processes to the site of damage. MGPtracker generates a polygon, the vertices of which are microglial processes closest to the ablation, and tracks its position over time. **A-C.** Shortening of the average distance of the polygon from the ablation site (**A**), the average area bound by the polygon (**B**) and the instantaneous velocity at each time point (**C**) show different rates of approach to the ablation following microglial activation with LPS. Statistics: two-way ANOVA with Bonferroni's *post hoc* test. *, $p < 0.05$ between control and LPS at the indicated time points. **D.** The average time to reach the ablation in control and LPS-injected animals does not change after LPS activation of microglia. Statistics: Student's *t* test, n.s., not significant. **E.** Proportion of control and LPS-treated animals that displayed initial retraction from the ablation site. Statistics: G-test of independence, *, $p<0.05$.

between animals, I performed two imaging sessions in the same LPS-injected animals, and evaluated both baseline motility and responses to laser injury before and after preladenant treatment (3 mg/kg, i.p.; Fig. 2.4C). It previously has been shown that there is no interference between closely spaced ablations (~50 μm apart) even if they are separated in time by as little as 20 min (Davalos et al., 2005). Nevertheless, after the first imaging session was concluded and preladenant was administered, I conducted the second imaging session at a cortical area at least 100 μm away from the first ablation site, and performed the second ablation ~2 hr after the first one. I first examined whether blocking A_{2A} receptors *in vivo* affected the baseline motility of microglia in the unperturbed brain. Preladenant application did not significantly change the baseline microglial process dynamics in terms of speed of movement (Fig. 5.6A; Student's paired *t* test, $p = 0.9857$), and length of total distance traveled (Fig. 5.6B; Student's paired *t* test, $p = 0.8376$), indicating that A_{2A} receptors are not involved in the baseline motility of microglia under pro-inflammatory conditions.

Despite the unaltered baseline motility, microglia in LPS-treated animals appeared to have a faster approach toward the ablation site following preladenant treatment (Fig. 5.7A, B). Indeed, preladenant caused both a significant decrease in the distance from the ablation site (Fig. 5.8A; repeated measures two-way ANOVA, $F_{(1,120)} = 24.14$, $p < 0.0001$), and a significant reduction in the size of the process-cleared area surrounding the ablation (Fig. 5.8B; repeated measures two-way ANOVA, $F_{(1,120)} = 4.200$, $p < 0.0426$) across all time points. Yet, the velocity of the converging processes was not affected by preladenant (Fig. 5.8C; repeated measures two-way ANOVA, $F_{(1,114)} = 0.4151$, $p = 0.5207$). Importantly, preladenant treatment appeared to reduce the time it took for microglial processes to reach the ablation in six out of seven animals resulting in an average time of 35.4 ± 5.9 min before and 26.0 ± 4.1 min after treatment (Fig. 5.8D).

To determine if the presence of a pre-existing ablation might speed up the response to a second ablation, I examined mice injected with PBS rather than preladenant between the two

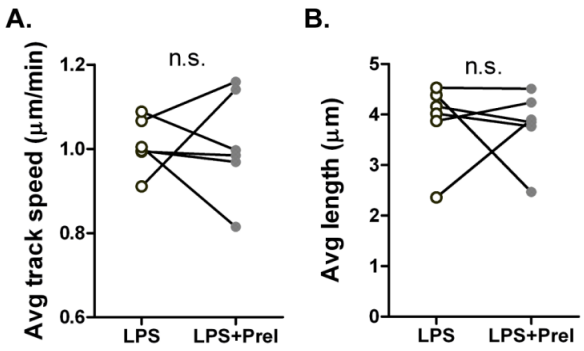

Figure 5.6. Effect of the A_{2A} receptor antagonist preladenant on microglial baseline motility *in vivo*. A. The baseline motility of microglia in LPS-injected $CX_3CR1^{GFP/+}$ mice before and after preladenant (Prel) treatment (3 mg/kg, i.p.) was measured from 2D projections of optical sections through the cortex spanning ~30 μm vertical distance that were analyzed with Imaris. Neither the average track speed (**A**) nor the distance traveled (**B**) change significantly after preladenant treatment. n.s., not significant.

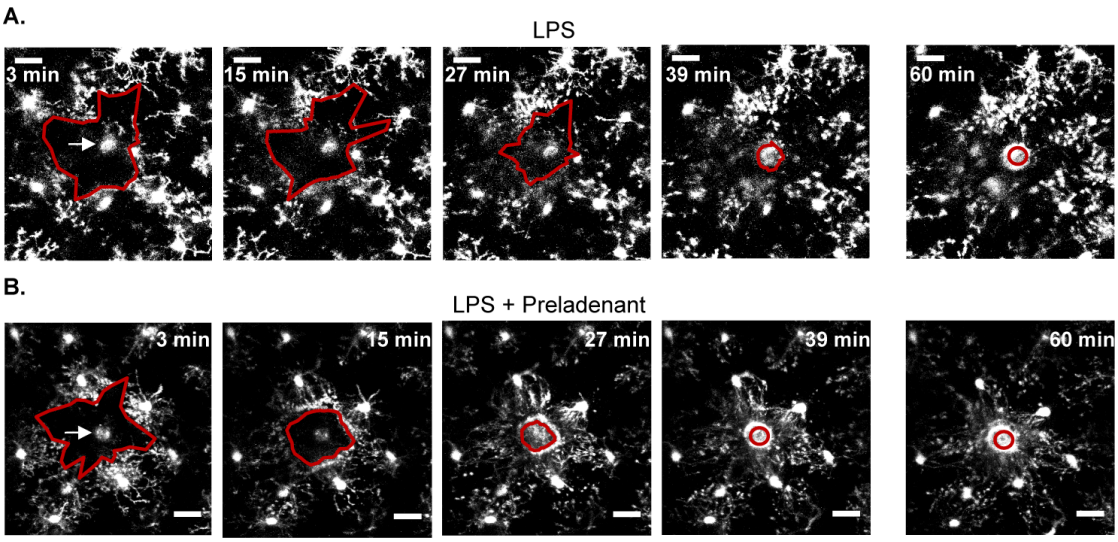

Figure 5.7. Microglial responses to laser-induced tissue damage following treatment with preladenant *in vivo*. Representative maximum intensity projections from time-lapse two-photon recordings from LPS-injected $CX_3CR1^{GFP/+}$ mice before (**A**) and after preladenant (**B**) treatment (3 mg/kg, i.p., 1 hr before imaging) at different time points. Arrow in first image (t = 3 min) points to the location of the laser ablation. Microglia appear to approach the injury site faster following preladenant injection. Red outlines are the vertices of the polygon generated by MGTracker. Scale bar: 20 µm.

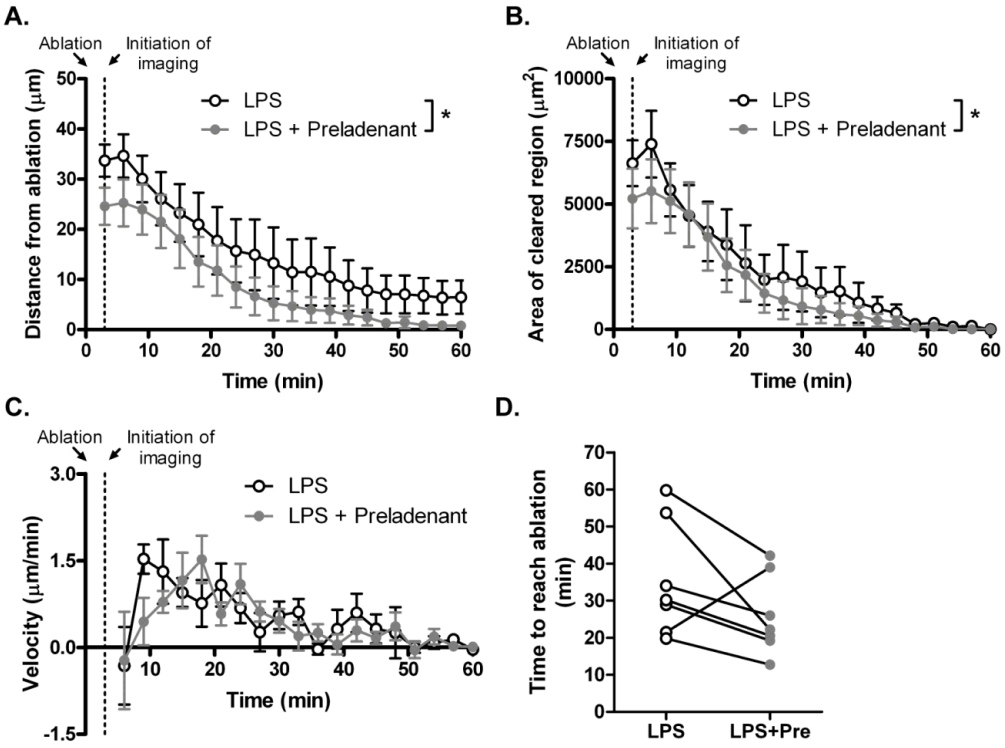

Figure 5.8. Quantification of microglial responses to tissue damage *in vivo* following preladenant treatment. Time sequences from LPS-injected *CX$_3$CR1$^{GFP/+}$* mice before and after preladenant injection (n = 7 mice) were analyzed with MGPtracker to quantify the radial response to injury. **A-C.** Shortening of the average distance of the polygon from the ablation site (**A**) and the average area bound by the polygon (**B**) show different rates of approach to the ablation following preladenant treatment, while the instantaneous velocity at each time point (**C**) is not affected. The faster average time to reach the ablation in six out of seven animals following preladenant treatment (**D**) also suggests differential response. Statistics: two-way repeated measures ANOVA with Bonferroni's *post hoc* test. *, $p < 0.05$ compared to before preladenant treatment at the indicated time points.

imaging sessions. There was no significant difference in the distance from ablation (Fig. 5.9A; repeated measures two-way ANOVA, $F_{(1,30)} = 0.3032$, $p = 0.5839$), area of the cleared region (Fig. 5.9B; repeated measures two-way ANOVA, $F_{(1,60)} = 0.2157$, $p = 0.6440$), and the instantaneous radial velocity (Fig. 5.9C; repeated measures two-way ANOVA, $F_{(1,57)} = 1.021$, $p = 0.3165$) between the two consecutive ablations across all time points. Moreover, there was a measurably faster approach to the second ablation only in one out of four animals that received a PBS injection between laser ablations, compared to six out of seven preladenant-injected animals (Fig. 5.8D, 5.9D; $p = 0.041$, G-test of independence; Fig. 5.9E). Overall, these results suggest that A_{2A} receptors are involved in microglial responses to tissue damage under pro-inflammatory conditions *in vivo*.

5.4. Discussion

5.4.a. Motility of activated microglia in vivo

The motility of resting microglia has been well-studied in the healthy central nervous system (Davalos et al., 2005; Haynes et al., 2006; Nimmerjahn et al., 2005), but to a lesser extent in conditions with an inflammatory component (Bolmont et al., 2008; Davalos et al., 2012; Fuhrmann et al., 2010). Davalos et al. (2012) showed that microglia in the spinal cord of an animal model of MS displayed dysregulated motility to form clusters around sites of blood-brain barrier disruption. Using an animal model of AD, Fuhrmann et al. (2010) observed an increased velocity of microglial cell body migration toward neurons that later die. In contrast, in a different AD model, Bolmont et al. (2008) reported a slightly decreased speed of the baseline process motility in plaque-associated microglia. Here, I performed a comprehensive characterization of the baseline motility of activated microglia in real time *in vivo*, and examined how microglial activation might affect their ability to detect tissue damage. Despite their apparent activation (Fig. 5.1), microglia under LPS-induced pro-inflammatory conditions retain their ability to sample the brain parenchyma by constantly extending and retracting their processes. This is in accord with

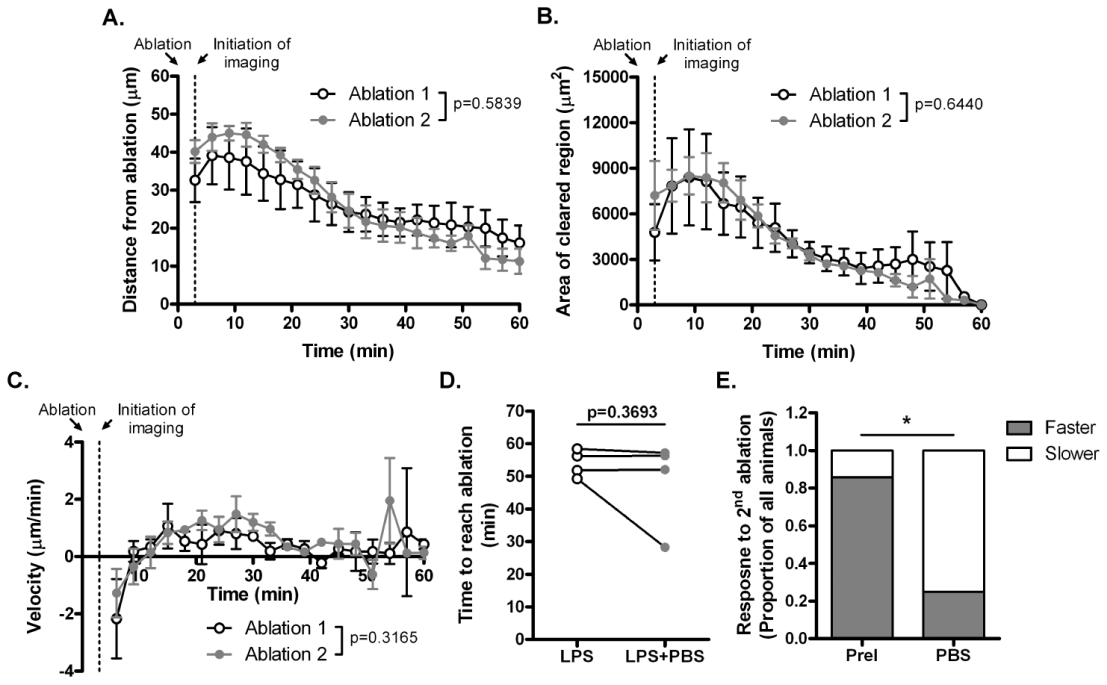

Figure 5.9. Effect of a second ablation on microglial responses to tissue damage *in vivo*. *$CX_3CR1^{GFP/+}$* mice subjected to two ablations with PBS injection in between were used to control for possible interaction between the ablations. Time-lapse sequences from were analyzed with MGPtracker. **A-C.** There was no significant difference between the two ablations in terms of average distance of the polygon from the ablation site (**A**), the average area bound by the polygon (**B**), or the instantaneous velocity at each time point (**C**). **D.** Only one in four animals showed a decrease in the time to reach the ablation. Statistics: two-way repeated measures ANOVA with Bonferroni's *post hoc* test. **E**. Proportion of responses to the second ablation that were accelerated or slowed down by preladenant (see Fig. 5.8) or PBS treatment between the two ablations. Statistics: G-test of independence, *, $p<0.05$.

microglial process extension and retraction dynamics observed in the spinal cord in neuroinflammatory disease and in an AD mouse model (Bolmont et al., 2008; Davalos et al., 2012), confirming that microglial activation *per se* does not inhibit their baseline process motility. The average instantaneous speed of process extension and retraction calculated with an automated object tracking algorithm was ~1 μm/min (Fig. 5.2B), which is comparable to previously reported process speeds in the absence of injury measured *in vivo* by manual tracking of processes (Davalos et al., 2005). Surprisingly, the speed of these movements is higher for microglia in LPS-treated animals than in control animals (Fig. 5.2B). Increased speed of movement for microglial processes has been previously observed in LPS-treated microglia *in vitro* (Orr et al., 2009). This hypermotile behavior of activated microglia is consistent with the idea that the cells have been primed by the presence of inflammation (Perry et al., 2003) and are attempting to respond to the disturbance.

In order to automate the quantification of the microglial response to laser ablation *in vivo*, I coordinated the development of MGPtracker by software engineers at the University of Akron. The code tracks the movement of microglial processes at 10° increments radiating from the point of injury, and in this way captures the complex geometry of the area around the ablation as it is rapidly populated by converging microglial processes after the injury is delivered (Fig. 2.7, 5.4). This automated analysis showed that activated microglia from LPS-treated animals initially retracted their processes away from the ablation site, but later responded by moving toward and surrounding the ablation (Fig. 5.5). This result is consistent with *in vitro* findings that adenosine, generated from ATP breakdown, causes process retraction only in activated microglia (Orr et al., 2009). Importantly, Krabbe et al. (2013) show that microglia in an animal model of Alzheimer's disease also displayed a delayed response to laser ablation *in vivo*. Thus, the impaired microglia response to damage seems to be a general phenomenon induced by both systemic and degeneration-induced damage.

5.4.b. Mechanism underlying delayed response to tissue damage in vivo

There was an initial retraction away from the laser ablation in nine out of eleven LPS-injected animals that were examined. However, microglia did extend their processes to the ablation after the initial retraction (Fig. 5.3, 5.5). These findings suggest the existence of a biphasic response of microglia to tissue damage *in vivo* under pro-inflammatory conditions. Initially, ATP is released by the cells damaged by the laser ablation and amplified by ATP-induced ATP release from surrounding astrocytes (Davalos et al., 2005). It is then rapidly broken down to adenosine, which subsequently activates A_{2A} receptors that are upregulated on activated microglia (Fig. 1.2). In the second phase of the response, other signaling molecules released by the damaged tissue presumably serve as chemoattractants, which eventually surmount the initial delay and ultimately drive microglial process extension toward the site of injury.

An additional component of the delayed response could involve the $P2Y_{12}$ receptor. Haynes et al. (2006) reported that microglia in $P2Y_{12}$ knock-out animals show a delayed response to laser injury, but eventually send processes toward the ablation. LPS treatment downregulates $P2Y_{12}$ expression at both the mRNA and protein level *in vivo* (Haynes et al., 2006). Thus, the data presented here obtained in LPS-treated mice are consistent with results obtained in $P2Y_{12}^{-/-}$ mice, which also show a delay in microglial response to tissue damage (Haynes et al., 2006). It should be noted that the presence of neuroinflammation affects many different processes in addition to purinergic signaling, some of which might be involved in modulating microglial motility.

The results presented in this Chapter show that in the presence of neuroinflammation following peripheral immune system challenge, activated microglia have a different response to laser-induced damage *in vivo* compared to unchallenged microglia of the healthy brain [Fig. 5.3, 5.5; Davalos et al. (2005); Nimmerjahn et al. (2005)]. The initial retraction away from the tissue injury has not been described before. However, the laser-induced lesion model is likely more

destructive in terms of the number of simultaneously injured cells or processes than one might expect from slowly progressing neuronal death in neurodegenerative diseases. Despite the extensive neuronal loss ultimately observed in many such diseases, only a few neurons likely die at each discrete time point (Hanisch and Kettenman, 2007; McGeer et al., 1988b), which makes a direct comparison of the effects not possible. Nevertheless, the laser-induced ablation almost certainly involves the release of a large number of factors, cellular constituents, and debris that could contribute to attracting microglial responses. It therefore seems possible that the delay observed following laser ablation under inflammatory conditions might be even more pronounced in neurodegenerative conditions in which individual neurons die slowly, possibly only few in a given volume of tissue at a time. Hence, in the absence of the broad spectrum of signals generated by the abrupt ablation injury, acute and localized microglial responses to the death of individual neurons may be even more delayed in the context of a neurodegenerative disease. These ideas are discussed in more detail in Section 7.3.b.

5.4.c. Neuroprotective strategies and microglial motility

A large body of evidence from multiple lines of research shows that A_{2A} receptor antagonists have neuroprotective properties. The role of A_{2A} receptor antagonists has been studied most extensively in Parkinson's disease, where both caffeine and selective A_{2A} receptor antagonists can reduce parkinsonian symptoms in combination with L-DOPA [see Section 7.3.c; reviewed in Morelli et al. (2010); Schwarzschild et al. (2006); Xu et al. (2005)]. However, there is ongoing debate whether the neuroprotective properties of A_{2A} antagonists are mediated through neuronal or glial A_{2A} receptors, with divergent results coming from different PD models (Carta et al., 2009; Morelli et al., 2010; Xiao et al., 2006; Yu et al., 2008). Preladenant, a selective A_{2A} receptor antagonist currently in clinical trials for Parkinson's disease (Barkhoudarian and Schwarzschild, 2011; Hauser et al., 2011), partially restored microglial responses to tissue damage in the presence of inflammation *in vivo* (Fig. 5.7, 5.8). Thus, at least some of the

neuroprotective properties of A_{2A} receptor antagonists might be explained by inhibition of microglial A_{2A} receptors.

Finally, NSAIDs also have neuroprotective properties (see Section 1.4). The effects of NSAIDs on microglial function have not been studied extensively, but they might indirectly shift microglia to a phenotype that is closer to their resting state (with reduced A_{2A} receptor expression) by inhibiting COX-2-mediated inflammation in the periphery or the brain. As a result, the neuroprotective properties of NSAIDs and A_{2A} receptor antagonists likely seem to involve different mechanisms at different stages of disease progression, with NSAIDs having potentially useful actions at early stages, and A_{2A} receptor antagonists becoming relevant for later use. If this is the case, A_{2A} antagonists, such as preladenant and caffeine might be more useful after diagnosis, which usually occurs late in the disease, when inflammation is already present. The ability of A_{2A} receptor antagonists to modify other microglial functions warrants further investigation to better understand the roles of microglia and identify novel mechanisms for modulating their functions in a wide range of disease paradigms.

CHAPTER 6: Modulation of microglial motility by adrenergic receptors

6.1. Abstract

To this point, I have characterized the effects of purinergic receptors on microglial motility, focusing on $P2Y_{12}$ and adenosine A_{2A} receptors and activated microglia. In order to determine whether other neurotransmitters modulate microglial motility, I examined the adrenergic receptor system activated by the neurotransmitter norepinephrine in the brain. Analysis of adrenergic receptor expression with quantitative PCR indicated that resting microglia primarily express β_2 receptors but switch expression to α_{2A} receptors under pro-inflammatory conditions modeled by LPS treatment. Bath application of NE to acute brain slices from $CX_3CR1^{GFP/+}$ mice resulted in significant process retraction in microglia. Despite the differential receptor expression, NE caused process retraction in both resting and LPS-activated microglia plated on Matrigel *in vitro*. The use of subtype-selective receptor agonists and antagonists confirmed the involvement of β_2 receptors in mediating microglial process dynamics in resting cells and α_{2A} receptors in activated cells. Co-application of NE with ATP to resting microglia blocked the ATP-induced process extension and migration in isolated microglia, and β_2 receptor antagonists prolonged ATP effects in brain slice tissues, suggesting the presence of cross-talk between adrenergic and purinergic signaling in microglia. These data show that the neurotransmitter NE can modulate microglial motility, which could affect microglial functions in pathogenic situations of either elevated or reduced NE levels.

6.2. Introduction

The ability of microglia to constantly move their processes is thought to be essential for both their role in tissue surveillance and their response to tissue damage (Hanisch and Kettenman, 2007). One of the best characterized signals that modulate microglial process dynamics is ATP, which has divergent effects on microglial motility depending on the cells' activation status (Gyoneva et al., 2009). In order to determine whether ATP is unique in signaling through

different receptors in resting and activated microglia to induce opposing effects on microglial processes, I examined adrenergic receptor signaling in microglia. The adrenergic system was chosen for two main reasons. First, norepinephrine signaling has been implicated in several brain disorders, including neurodegenerative diseases and mood disorders (Chan-Palay and Asan, 1989; Goddard et al., 2010). Second, previous studies show that NE can affect certain microglial functions, including motility.

Both decreased and increased NE levels might lead to dysregulation of NE-dependent functions such as learning and memory, attention, and arousal (Berridge and Waterhouse, 2003; Sara and Bouret, 2012), and could contribute to a pathological state. The loss of LC neurons, which synthesize and release NE, results in a decrease in NE levels in its projection areas (Iversen et al., 1983; Mann et al., 1980), and is an early hallmark of several neurodegenerative diseases including AD, PD, and dementia with Lewy bodies (Chan-Palay and Asan, 1989; German et al., 1992; Iversen et al., 1983; Leverenz et al., 2001; Mann et al., 1980). Moreover, experimental depletion of NE by either toxins or genetic manipulations exacerbates pathological processes in animal models of AD and PD (Fornai et al., 1997; Heneka et al., 2002; Rommelfanger et al., 2007), and elevation of synaptic NE levels by preventing its uptake protects dopaminergic neurons from MPTP toxicity (Rommelfanger et al., 2004). In contrast, NE is released in large amounts during activation of the "fight-or-flight" response by stressful stimuli. Certain types of stress, especially acute stressors, can increase the LC firing rate and NE concentrations throughout the brain (Kvetnansky et al., 2009; Stanford, 1995).

In addition to its role as a neurotransmitter, NE can be released extrasynaptically and can act as a neuromodulator to influence the functions of glial cells and capillaries (Kalaria and Harik, 1989; Paspalas and Papadopolous, 1998). NE seems to possess anti-inflammatory actions as it has been shown to reduce proinflammatory gene expression in microglia (Färber et al., 2005). The beneficial role of NE is especially evident in animal models of AD where it might help resolve pathology in several ways through microglia-dependent actions. First, NE might enhance

microglial chemoattraction to Aβ plaques (Heneka et al., 2010). Second, it promotes the clearance of Aβ plaques by increasing microglial phagocytosis of Aβ and elevating the expression of Aβ-degrading enzymes (Kong et al., 2010). Third, NE treatment prevents the Aβ-induced increase in proinflammatory cytokine expression (Heneka et al., 2002; Heneka et al., 2010), and lack of NE exacerbates microgliosis in a mouse model of AD (Jardanhazi-Kurutz et al., 2011).

Finally, NE is known to increase microglial motility in response to Aβ in Boyden chamber migration assays and *in vivo* (Heneka et al., 2010), but the mechanism by which NE regulates motility has not been well described. Thus, I used acute brain slices to study microglial motility in tissues and isolated microglia plated on Matrigel *in vitro* to determine the receptor involvement and signaling pathways by which NE modulates microglial motility and the dynamics of individual processes. I examined both resting and activated microglia because our previous findings show that different GPCRs control microglial motility in a manner dependent on microglial activation status (Gyoneva et al., 2009; Orr et al., 2009). I found that the expression of the α_{2A}- and β_2-adrenergic receptors markedly changes as a function of microglial activation and that both receptors can regulate microglial process dynamics. These data suggest that both NE and ATP can control how microglia sense and respond to tissue damage, either independently or synergistically, which could hold therapeutic implications for the role of microglia in neurodegeneration.

6.3. Results

6.3.a. Noradrenergic receptor expression in microglia is dependent on their activation status

While several studies have examined the expression of specific adrenergic receptors in microglia, there are no comprehensive studies that determine adrenergic receptor expression in both resting and activated microglia. Thus, I employed qPCR to assess the expression of adrenergic receptors in microglia [Fig. 6.1A; Gyoneva and Traynelis (2013)]. Cortical lysates from control or LPS-injected mice (2 mg/kg i.p. 2 days before slicing) served as a positive control

for receptor expression, confirming that the amplification conditions were able to detect all receptors. Purified resting microglia had detectable mRNA for α_{1A}, β_1, and β_2 receptors, but the signal amplitudes for α_{1A} and β_1 receptors were only about 10% of the signals observed in whole cortical lysates. In contrast, the mRNA for β_2 receptors was 10 times higher in microglia than in the mixed cell types present in cortical lysates. The expression of all three receptors decreased following LPS activation: α_{1A} and β_1 receptors decreased to almost undetectable levels, and β_2 receptors decreased to the background expression levels in the cortex. Interestingly, LPS activation strongly induced the expression of α_{2A} receptors in cultured microglia as well as in the cortex (Fig. 6.1A). Thus, it seems likely that at least part of the increase in cortical expression of α_{2A} induced by LPS can be accounted for by an increase in microglial expression. In summary, resting microglia primarily express the G_s-coupled β_2 receptors, whereas activated microglia primarily express the G_i-coupled α_{2A} receptors.

To determine whether the low levels of α_1 receptor mRNA detected by qPCR lead to expression of functional receptors, I performed live cell calcium imaging of resting and LPS-activated (100 ng/ml for 24 h) primary microglia (Gyoneva and Traynelis, 2013). Activation of G_q-coupled receptors leads to an increase in intracellular calcium that can be detected with calcium-sensitive fluorescent dyes such as Fura-2. Application of 30 μM NE elicited a small Fura-2 response in one (of 12) control and two (of 15) LPS-treated cells (Fig. 6.1B, C). As a positive control, treatment with 30 μM ATP resulted in a strong increase of the Fura-2 response over baseline levels in all cells arising from activation of G_q-coupled purinergic receptors (Fig. 6.1B, C). These results indicate that α_1 receptors are not expressed at an appreciable degree by microglia.

6.3.b. NE modulates microglial process motility in tissues

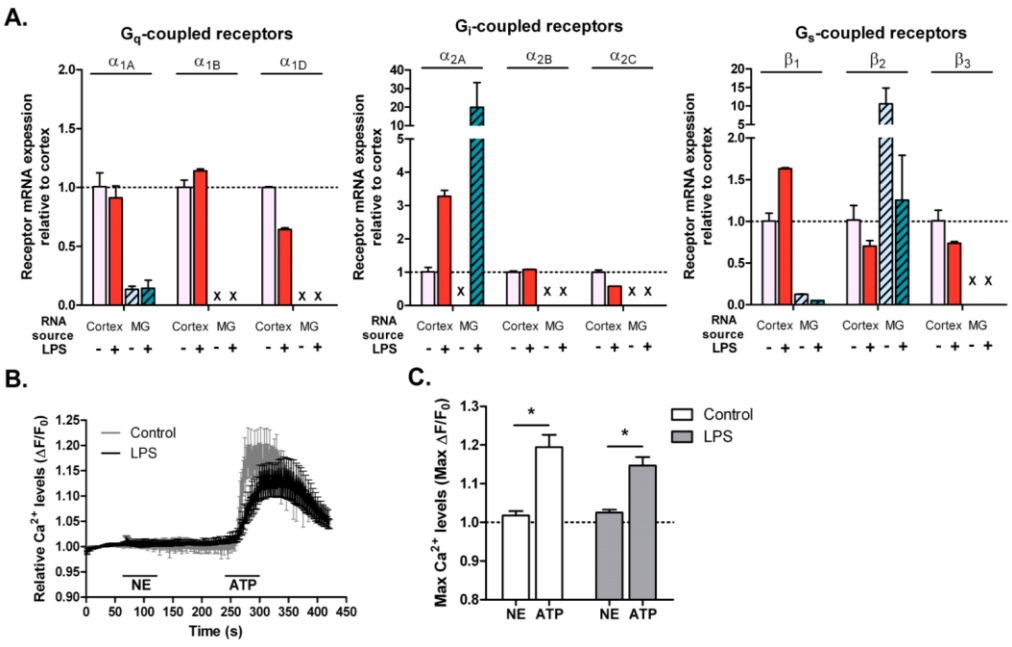

Figure 6.1. Expression of adrenergic receptors in microglia. A. Quantitative real time PCR results for mouse adrenergic receptors in cortical lysates from PBS- (control) or LPS-injected (2 mg/kg) mice or purified primary microglia (MG) treated with 100 ng/mL LPS or HBSS (control) for 24 hr. For each receptor, expression was calculated relative to cortical lysates of PBS-injected animals in three independent experiments, each performed in duplicate. Dotted line: Relative expression = 1 compared to cortex. X = Not detected. **B.** Measurement of Ca^{2+} levels as a readout of G_q-linked receptor activation in primary microglia treated with HBSS (n = 12 cells) or 100 ng/mL LPS for 24 hr (n = 15 cells). NE (30 μM) and ATP (30 μM, positive control) were each applied for 1 min. The average traces from all cells are shown. **C.** Quantification of the maximum Fura-2 response following NE or ATP treatment. Statistics: two-way repeated measures ANOVA and Tukey's *post hoc* test. *, $p < 0.05$. [Figure reproduced with permission from Gyoneva and Traynelis (2013)].

Both *in vitro* and *in vivo* observations suggest that the presence of NE influences microglial motility in response to Aβ (Heneka et al., 2010). To better understand the effects of NE on microglial motility in their native environment in real time, I employed the brain slice imaging system described in Chapter 4. I prepared 200 μm-thick slices (Fig. 2.2A) from $CX_3CR1^{GFP/+}$ mice that exhibit microglia-specific GFP expression (Jung et al., 2000). Microglia in slices likely retain their resting phenotype as evident from the lack of IL-1β mRNA synthesis for several hours after slicing (Fig. 2.2B) and retained ability to respond to tissue damage (Fig. 4.2, 4.3). To confirm that the high resolution process dynamics of microglia are not affected by the slice preparation, I examined the effects of bath-applied ATP on microglial process motility at high magnification (60x). Slices were imaged over a 30-min period, obtaining optical sections of the tissue spaced 1 μm apart every 1 min to capture the complex three-dimensional morphology of microglial processes and their movement over time. Collapsing the 30-50 μm z-stack of optical sections from each time point into a two-dimensional image produced a time series of images with exceptional resolution of individual microglial processes. The morphology was reminiscent of the cells seen in their native environment *in vivo* [Fig. 6.2A, B; Davalos et al. (2005); Nimmerjahn et al. (2005)]. At baseline conditions, cells contained long processes with an average length of 10.5 μm. Bath application of 30 μM ATP to acute brain slices induced process extension in cortical microglia (Fig. 6.2A, B), suggesting that acute slices faithfully reproduce microglial behavior as seen *in vivo* and *in vitro*. Surprisingly, perfusion with 30 μM NE slowly induced process retraction as opposed to the extension seen following ATP treatment [Fig. 6.2C, D; Gyoneva and Traynelis (2013)].

Changes in microglial ramification in slices were quantified by measuring the total process length for each cell over the course of imaging [Fig. 6.3A; Gyoneva and Traynelis (2013)]. Slices perfused with aCSF maintained most of their processes over the course of the

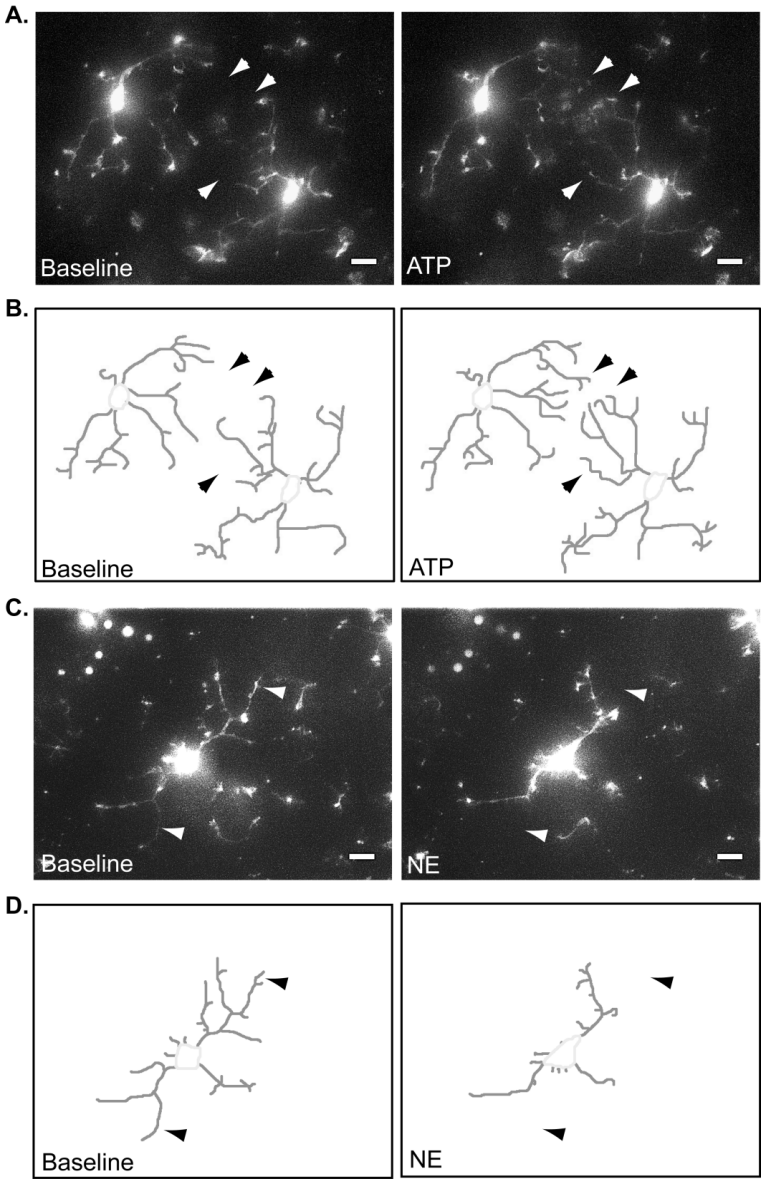

Figure 6.2. Microglial process motility in slices. Coronal slices were prepared from $CX_3CR1^{GFP/+}$ mice and imaged with a confocal microscope over time. **A.** Maximum intensity projections of optical sections spanning 45 μm through representative cells before (left, t = 0 min) and following treatment with 30 μM ATP (right, t = 7 min). **B.** Manually traced out processes for the cell shown in (A). **C.** Maximum intensity projection of a 31 μm section from a slice before (left, t = 0 min) and following application of 30 μM NE (right, t = 25 min). **D.** Manually traced out processes for the cell shown in (C). Arrowheads point to select processes that change over time. Scale bar: 5 μm. [Figure modified from Gyoneva and Traynelis (2013)].

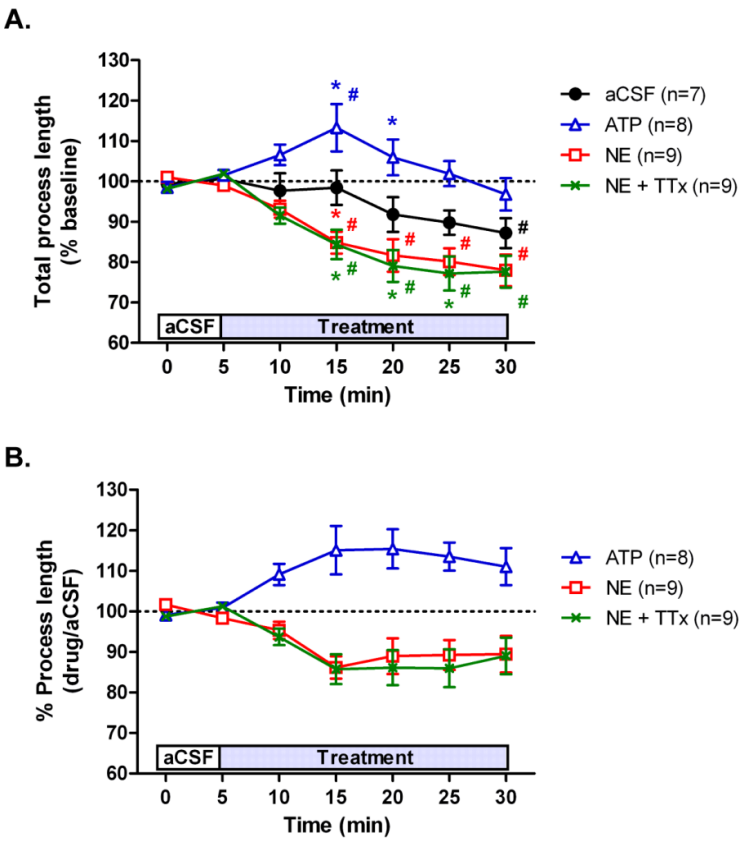

Figure 6.3. Quantification of microglial process dynamics in slices. Coronal slices were prepared from $CX_3CR1^{GFP/+}$ mice and imaged with a confocal microscope over time. **A.** The total process length for each cell was calculated following treatment with 30 µM ATP, 30 µM NE, or 30 µM NE + 0.5 µM TTx and normalized to the total process length during a 5-min baseline recording. **B.** Process length was normalized to the average length of aCSF-treated slices at each time point. The numbers of cells analyzed for each treatment are shown in parentheses. Statistics: two-way repeated measures ANOVA and Tukey's *post hoc* test. #, $p < 0.05$ compared to baseline response, *, $p < 0.05$ compared to aCSF at the corresponding time point. [Figure modified from Gyoneva and Traynelis (2013)].

imaging; the process length often appeared to start decreasing after 15 min of imaging, but did not significantly decrease from baseline until the 30-min time point (Fig. 6.3A). ATP induced an 18% increase in total process length, which was significantly different from aCSF treatment after 15 min of imaging (Fig. 6.3A; two-way repeated measures ANOVA, Tukey's *post hoc* test, $p = 0.001$). In contrast, NE treatment led to a significant decrease in process length by 23% at 30 min of imaging (Fig. 6.3A; two-way repeated measures ANOVA, Tukey's *post hoc* test, $p < 0.001$). To adjust for the observed decrease in total process length over time (Stence et al., 2001) and more clearly compare the effects of NE and ATP, the process length of ATP- and NE-treated slices was normalized to aCSF-treated slices at each time point (Fig. 6.3A, B). Finally, addition of 0.5 μM TTx, a voltage-gated sodium channel blocker, did not prevent the effects of NE (Fig. 6.3A, B; two-way repeated measures ANOVA, Tukey's *post hoc* test comparing NE to NE + TTx, $p = 0.981$). The inability of TTx to block the NE-induced process retraction indicates that NE likely acts directly on microglia rather than through modulation of synaptic transmission and neurotransmitter release.

6.3.c. Norepinephrine modulates microglial process dynamics in vitro

Considering the unexpected finding that NE caused microglial process retraction in native tissues (Fig. 6.2C, D; 6.3), I next examined isolated primary cortical microglia plated on Matrigel *in vitro* [Fig. 6.4; Gyoneva and Traynelis (2013)]. As seen in acute brain slices, bath application of 30 μM NE to resting microglia in Matrigel induced process retraction (Fig. 6.4A). This was quantified by calculating the ramification of the cells as surface area-to-volume ratios from the three-dimensional reconstructions and measuring the area under the time-response curves. The effect of NE was significantly different from the effect of ATP regardless of activation status (Fig. 6.5A, C; two-way ANOVA, Tukey's *post hoc* test, $p < 0.001$), and also in resting microglia (Fig. 6.5A, C; two-way ANOVA, Tukey's *post hoc* test, $p < 0.001$). The ability

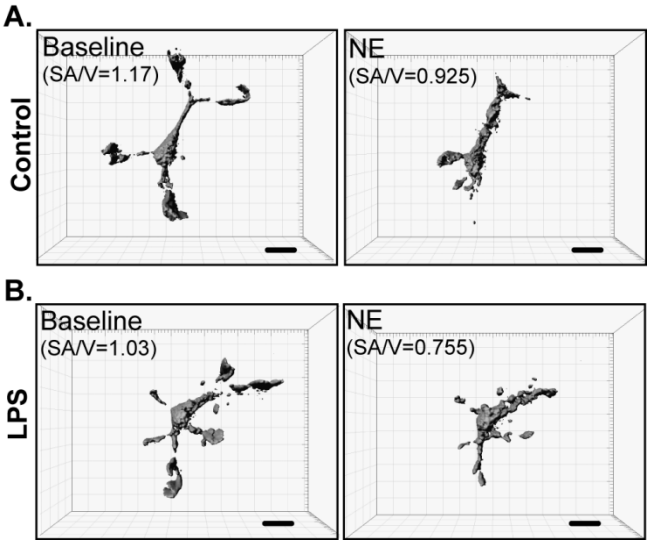

Figure 6.4. Effect of NE on primary microglia plated on Matrigel *in vitro*. 3D reconstructions of primary *actin-GFP* microglia in Matrigel capture the complex, process-bearing morphology of primary microglia. The figure shows an example of a resting, HBSS-treated microglia (control, **A**) or a microglia activated with 100 ng/mL LPS (**B**). Treatment with 30 µM NE induces process retraction in both cases. Changes in the surface area-to-volume ratios (SA/V) correlate to changes in ramification. Scale bar: 10 µm. [Figure reproduced with permission from Gyoneva and Traynelis (2013)].

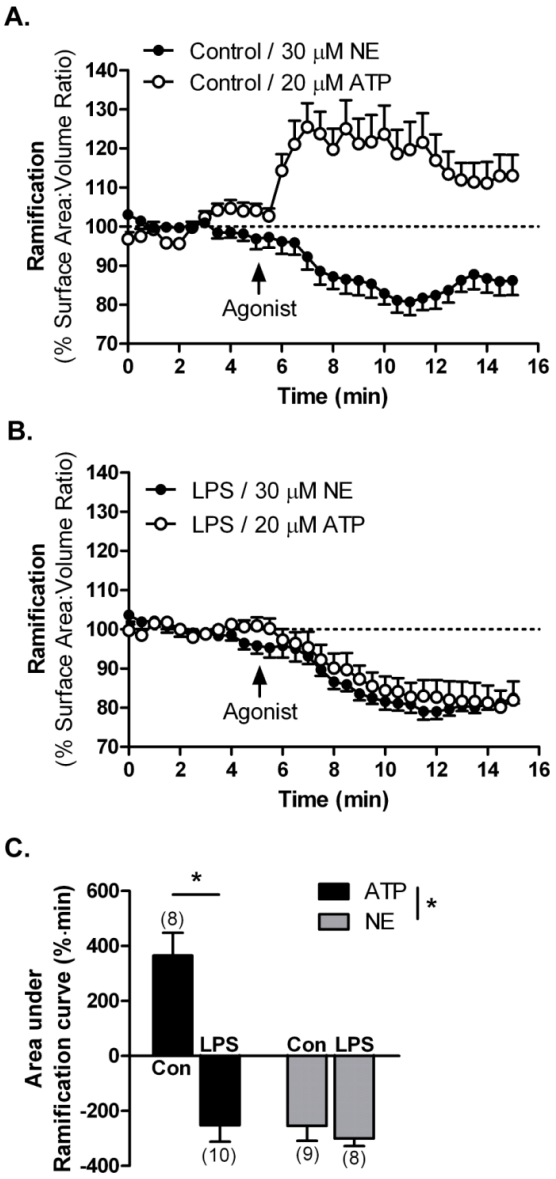

Figure 6.5. Control of microglial process dynamics by adrenergic receptors *in vitro*. 3D representations of primary *actin-GFP* microglia in Matrigel were used to calculate cell ramification as surface area-to-volume ratios at each time point. HBSS- (control, **A**) or LPS-activated microglia (100 ng/mL, 24 hr, **B**) were treated with either 20 μM ATP or 30 μM NE. **C.** A comparison of the effects of NE and ATP by calculating the area under the ramification curves. The number of cells for each treatment is shown in parentheses. Statistics: two-way ANOVA and Tukey's *post hoc* test. *, $p < 0.05$. [Figure modified from Gyoneva and Traynelis (2013)].

of NE to affect process dynamics in isolated microglia further suggests that the effects seen on microglia in slices are through direct modulation of microglia rather than the release of neuroactive substances.

Despite the change in adrenergic receptor expression following LPS activation (Fig. 6.1), NE produced a similar process retraction of ~20% in LPS-activated microglia (Fig. 6.4B; 6.5B, C; two-way ANOVA, Tukey's *post hoc* test comparing control to LPS, $p = 0.597$). Moreover, the extent of retraction was the same for NE and ATP in activated microglia (Fig. 6.5.C; two-way ANOVA, Tukey's *post hoc* test, $p = 0.569$).

6.3.d. Mechanisms underlying NE control of microglial process motility

In order to determine whether NE mediates its effects on process dynamics through different receptors under resting and activating conditions, I employed receptor subtype-selective agonists (Gyoneva and Traynelis, 2013). Bath application of the β receptor agonist isoproterenol (10 μM) induced on average a 16.7% decrease in ramification in resting microglia but had no effect on cell ramification in activated microglia (Fig. 6.6A, C; two-way ANOVA, Bonferroni's *post hoc* test, $p = 0.004$;). This is consistent with the strong expression of β_2 receptors in resting microglia and the down-regulation of β_2 receptors in LPS-activated microglia (Fig. 6.1A). In contrast, the α_2 receptor-selective agonist UK-14,304 (10 μM) had no effect on the ramification of resting microglia, consistent with the minimal expression of α_2 receptors. UK-14,304 decreased ramification on average by 18.7% in activated microglia (Fig. 6.6B, C; two-way ANOVA, Bonferroni's *post hoc* test, $p = 0.012$), a result that is consistent with the increased expression of α_2-adrenergic receptors seen with quantitative PCR (Fig. 6.1A).

Additional support for the involvement of specific adrenergic receptor subtypes in the response to NE for resting and activated microglia was obtained through the use of subtype-selective antagonists (Gyoneva and Traynelis, 2013). Addition of the β receptor antagonist propranolol (10 μM) prevented the NE-induced process retraction in resting microglia (Fig. 6.6D,

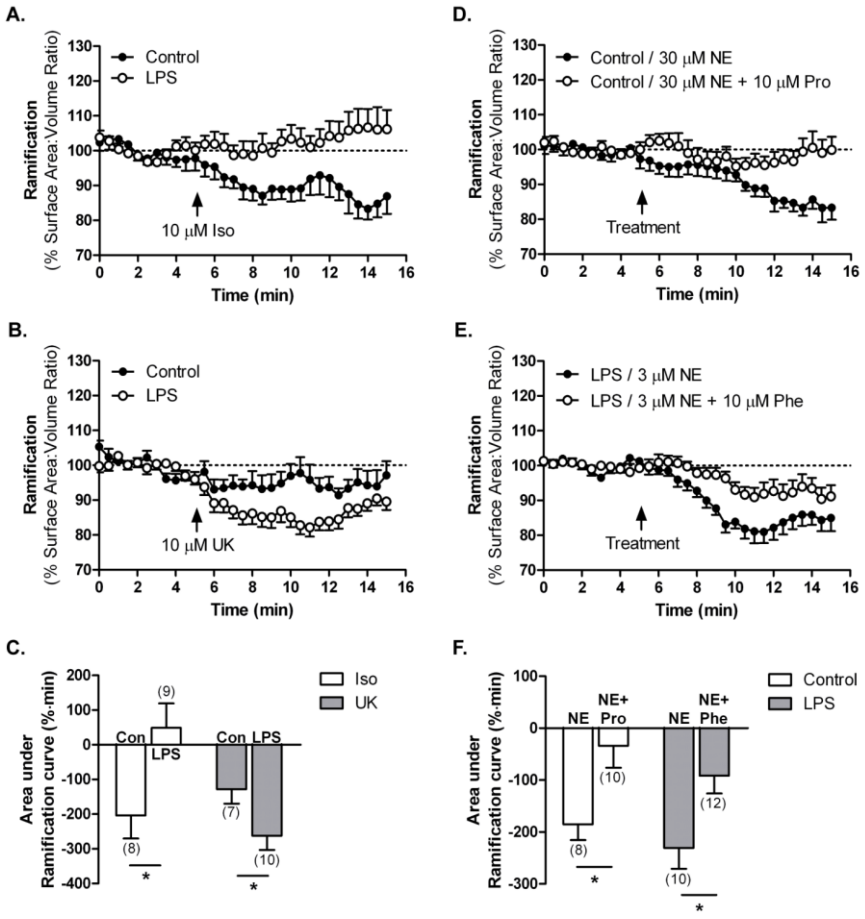

Figure 6.6. Involvement of different adrenergic receptor subtypes in mediating microglial process dynamics. Primary *actin-GFP* microglia were imaged in Matrigel to calculate cell ramification as surface area-to-volume ratios as described. **A-C.** Effects of adrenergic agonists. Treatment of HBSS- (control) or LPS-treated (100 ng/mL, 24 hr) microglia with the β_2 receptor agonist isoprotenerol (Iso, 10 μM, **A**) or the α_{2A} receptor agonist UK-14,304 (UK, 10 μM, **B**). **D-F.** Effects of adrenergic antagonists. **D.** Application of 30 μM NE alone or 30 μM NE and the β receptor antagonist propranolol (Pro, 10 μM) to HBSS-treated (control) microglia. **E.** Treatment of LPS-activated (100 ng/mL, 24 hr) microglia with 3 μM NE alone or 3 μM NE and the α receptor antagonist phentolamine (Phe, 10 μM). The effects of NE receptor agonists (**C**) and antagonists (**F**) were compared by calculating the area under the ramification curves, with the number of cells for each treatment shown in parentheses. Statistics: two-way ANOVA and Bonferroni's *post hoc* test compared to control (**C**) or NE-treated (**F**) cells. *, $p < 0.05$. [Figure modified from Gyoneva and Traynelis (2013)].

F; two-way ANOVA, Bonferroni's *post hoc* test, $p = 0.011$), consistent with mediation by β_2 receptors which are highly expressed in resting microglia. Likewise, the α receptor antagonist phentolamine (10 μM) blocked the actions of 3 μM NE in activated microglia (Fig. 6.6E, F; two-way ANOVA, Bonferroni's *post hoc* test, $p = 0.010$), as predicted given the strong down-regulation of β_2 receptors and up-regulation of α_{2A} receptors by LPS. The lower concentration of NE used with phentolamine (3 vs. 30 μM) was necessary to achieve an efficient blockade of NE signaling by the competitive antagonist phentolamine and was selected based on the relative potencies of both agonist and antagonist at the receptor (Atkinson and Minneman, 1991; Zhang et al., 2004).

Finally, the intracellular effects of β_2 and α_{2A} receptors are mediated through G_s and G_i proteins, respectively. To further elucidate the differential adrenergic receptor modulation of microglial motility, the effects of G_s and G_i inhibitors were examined. Resting or LPS-activated (100 ng/mL, 24 hr) microglia were plated on Matrigel and pre-treated with either the G_s inhibitor NF449 (25 μM) or the G_i inhibitor PTx (100 ng/mL) for at least 8 hr. Surprisingly, pre-treatment of either resting or activated microglia with NF449 did not change the response to 30 μM NE (Fig. 6.7; two-way ANOVA, Bonferroni's *post hoc* test, $p = 0.606$). However, pre-treatment with PTx appeared to partially prevent NE-induced process retraction in both resting and LPS-activated microglia (Fig. 6.7; two-way ANOVA, Bonferroni's *post hoc* test, $p = 0.012$). The unexpected finding that a G_i inhibitor (PTx) can affect the signaling from the G_s-coupled β_2 adrenergic receptor suggests that the modulation of microglial process dynamics by NE might employ non-canonical signaling pathways.

6.3.e. Adrenergic receptor activation interferes with ATP response in resting microglia

Because both NE and ATP can affect microglial process dynamics, I next evaluated whether the two signaling pathways interact by examining resting and LPS-activated (100 ng/ml for 24 h) microglia plated on Matrigel (Gyoneva and Traynelis, 2013). The cells were treated

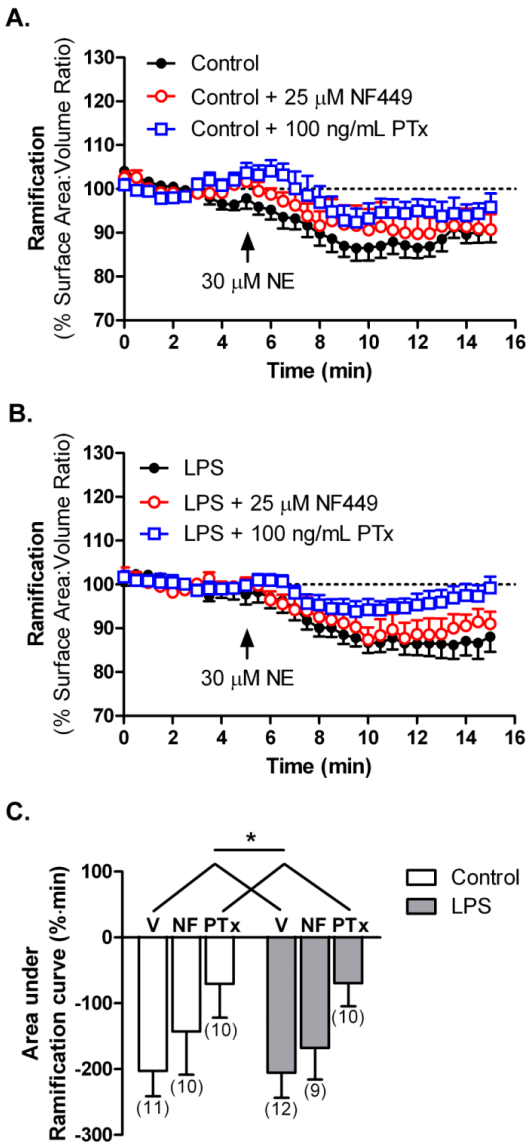

Figure 6.7. Regulation of microglial process dynamics by G proteins. Primary *actin-GFP* microglia were imaged in Matrigel to calculate cell ramification as surface area-to-volume ratios as described. **A.** Pre-treatment of control (HBSS-treated) microglia with the G_s inhibitor NF449 (NF) or the G_i inhibitor Pertussis toxin (PTx). **B.** Pre-treatment of LPS-activated (100 ng/mL, 24 hr) microglia with NF449 or PTx. V, deionized water vehicle. **C.** The effects of the G protein inhibitors were compared by calculating the area under the ramification curves, with the number of cells for each treatment shown in parentheses. Statistics: two-way ANOVA and Bonferroni's *post hoc* test compared to vehicle (V). *, $p < 0.05$.

either with 20 μM ATP or with 20 μM ATP in the presence of 30 μM NE. The inclusion of NE abolished the ATP induced process extension in resting microglia (Fig. 6.8A, C; two-way ANOVA, Bonferroni's *post hoc* test, $p = 0.029$). Both ATP and ATP + NE induced process retraction in activated microglia (Fig. 6.8B, C). Quantitative analysis of the average areas under the ramification curves showed that the degrees of retraction induced by ATP or ATP + NE in LPS-activated microglia were similar, and there are no additive or synergistic effects (Fig. 6.8C; two-way ANOVA, Bonferroni's *post hoc* test, $p = 0.615$).

To further confirm the interaction between NE and ATP in resting microglia, I determined whether NE affects microglial chemotaxis to an ATP gradient in Matrigel (Gyoneva and Traynelis, 2013). To generate the gradient, ATP was locally applied from a micropipette using iontophoresis. ATP was retained in the pipette by applying a positive current and released at a specific time by applying negative current. Resting microglia migrated toward the ATP released from the pipette (Fig. 6.8D). However, if microglia were perfused with 30 μM NE (both during the base-line recording and the ATP application), they displayed reduced or no migration (Fig. 6.8E), which was reflected in significantly reduced cell displacement from an average of 12.9 to 2.57 μm (Fig. 6.8F; Student's *t* test, $p = 0.0041$). Together with the ability of NE to prevent ATP-induced process extension in resting microglia, these findings suggest an interaction between adrenergic and purinergic signaling in microglia.

Finally, the interaction between NE and ATP was also studied for microglia in the native tissues of acute brain slices that have endogenous NE (Gyoneva and Traynelis, 2013); if endogenous NE is interfering with ATP-induced process extension, then blocking NE signaling will enhance the effects of ATP in tissues. Slices were perfused with either aCSF or aCSF containing the β-adrenergic receptor antagonist propranolol (10 μM). After a 5-min baseline recording, the slices were treated with 30 μM ATP in aCSF or aCSF + propranolol. As expected, ATP induced an increase in total process length that reached a peak early at 10 min of imaging and then started decreasing (Fig. 6.9; two-way repeated measures ANOVA, Tukey's's *post hoc*

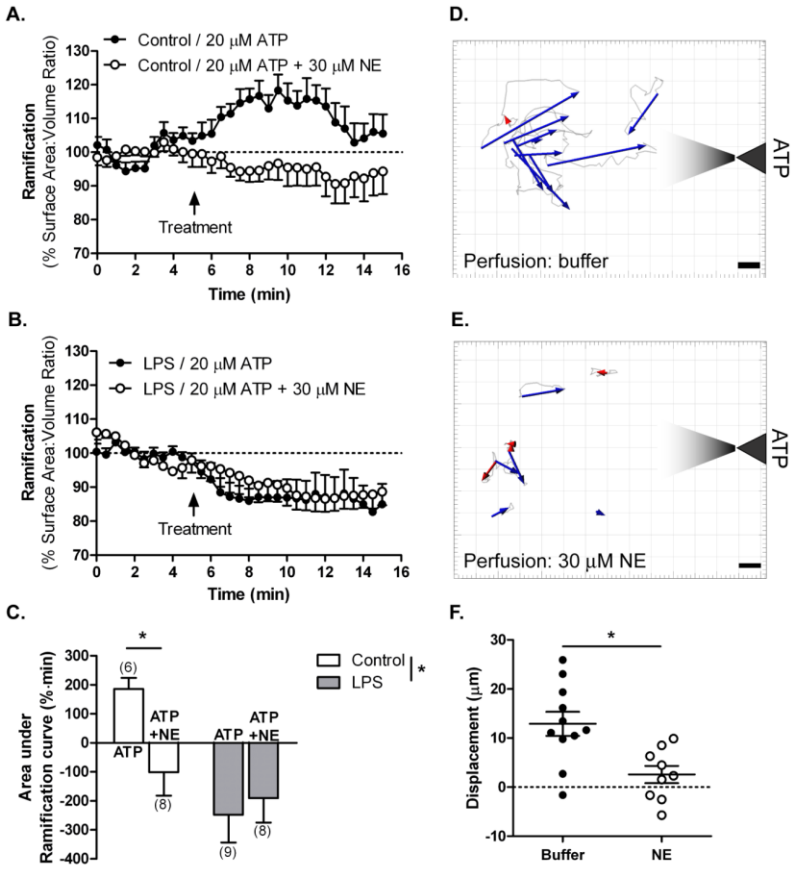

Figure 6.8. Interaction between purinergic and adrenergic signaling in regulating microglial motility *in vitro*. Primary *actin-GFP* microglia were imaged in Matrigel to calculate cell ramification as surface area-to-volume ratios**. A-C.** HBSS- (control, **A**) or LPS-activated microglia (100 ng/mL, 24 hr, **B**) were treated with either 20 μM ATP or 20 μM ATP + 30 μM NE. **C.** Quantification of cell ramification with the number of cells for each treatment is shown in parentheses. Statistics: two-way ANOVA and Bonferroni's *post hoc* test compared to ATP-treated cells. *, $p < 0.05$. **D-F.** Migration of primary *actin-GFP* microglia to ATP released from a micropipette. The cells were perfused with either imaging buffer (**D**) or 30 μM NE (**E**). Paths of cell bodies were tracked with Imaris, and are shown in light gray; overall displacements are represented by blue (movement to pipette) or red (movement away) arrows. Scale bar: 5 μm. **F.** Movement was quantified by measuring the magnitude of the vector displacement for each cell with positive displacement being movement towards the pipette. Statistics: Student's *t* test. *, $p < 0.05$. [Figure modified from Gyoneva and Traynelis (2013)].

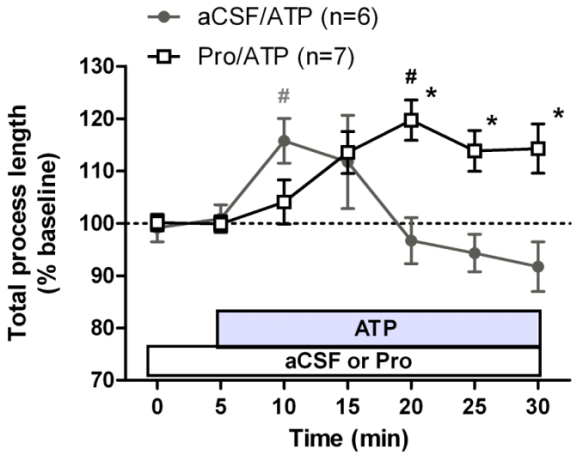

Figure 6.9. Interaction between purinergic and adrenergic signaling in regulating microglial motility in tissues. Coronal slices were prepared from $CX_3CR1^{GFP/+}$ mice and imaged over time. The total process length of microglial processes in 2D projections following ATP treatment was normalized to the total process length during baseline, with the numbers of cells for each treatment shown in parentheses. Statistics: two-way repeated measures ANOVA and Tukey's *post hoc* test. #, $p < 0.05$ compared to baseline response, *, $p < 0.05$ compared to ATP at the corresponding time point. [Figure modified from Gyoneva and Traynelis (2013)].

test, $p = 0.047$ at $t = 10$ min). Inclusion of propranolol in the perfusion solution resulted in a significantly different response across all time points (Fig. 6.9; two-way repeated measures ANOVA, Tukey's's *post hoc* test, $p = 0.044$). Specifically, the response to ATP appeared prolonged, such that there were significant differences between aCSF alone and aCSF with propranolol at 20-30 min of imaging (Fig. 6.9; two-way repeated measures ANOVA, Tukey's's *post hoc* test, $p < 0.001$, $p = 0.002$; $p < 0.001$at $t = 20$, 25, 30 min, respectively). Thus, these results show that NE signaling and ATP signaling interact to modulate microglial motility both *in vitro* and in tissues.

6.4. Discussion

Adrenergic neurons originating in the LC innervate almost all brain regions, and NE released at their terminals regulates both basic (sleep/wake) and higher level (memory/cognition) functions (Berridge and Waterhouse, 2003). In recent years, the ability of NE to act as a neuromodulator in the context of disease has gained attention. NE possesses anti-inflammatory properties (Färber et al., 2005), and thus loss of NE-expressing neurons may influence AD and PD progression (German et al., 1992; Iversen et al., 1983; Mann et al., 1980; Rommelfanger and Weinshenker, 2007).

Here, I described a novel neuromodulatory role of NE in microglial motility both in tissue and *in vitro*. The data leads to three main conclusions. First, NE caused microglial process retraction in the intact tissues of acute brain slices from $CX_3CR1^{GFP/+}$ mice that have microglia-specific GFP expression (Fig.6.2, 6.3). This result was supported by detailed three-dimensional time lapse imaging of isolated microglia obtained in Matrigel (Fig. 6.4, 6.5). Second, the use of receptor subtype-selective agonists and antagonists showed that NE exerted its effects through β_2 receptors in resting microglia and through α_{2A} receptors in LPS-activated microglia (Fig. 6.6). These functional data match the adrenergic receptor expression observed with qPCR (Fig. 6.1). Third, NE co-application to resting microglia blocked ATP-induced process extension and

migration *in vitro* (Fig. 6.8), and the β_2 receptor antagonist propranolol prolonged ATP-induced process extension in tissues (Fig. 6.9). These findings suggest that adrenergic signaling might modulate or control the ability of microglia to respond to tissue damage and subsequent ATP release *in vivo*.

6.4.a. Adrenergic receptor expression in microglia

There are several reports that describe the functional effects of either α- or β-adrenergic receptor activation in cultured primary microglia. Generally, treatment of microglia with NE or selective β receptor agonists such as isoproterenol resulted in decreased cytokine release (Färber et al., 2005), nitric oxide (Färber et al., 2005) and superoxide production (Colton and Chernyshev, 1996), p38 phosphorylation (Morioka et al., 2009), and cell proliferation (Fujita et al., 1998). Some functions of α receptors include reduction of cytokine secretion and upregulation of the anti-apoptotic factor Bcl-xL (Mori et al., 2002). Both α and β receptors appear to modulate inward and outward K^+ currents in microglia (Färber et al., 2005). However, most of these studies were conducted with rat microglia or did not provide data regarding adrenergic receptor expression. Thus, I conducted the first comprehensive evaluation of adrenergic receptor expression in primary mouse cortical microglia, examining both resting and LPS-activated microglia. Analysis of receptor mRNA levels with qPCR showed that mouse cortical microglia primarily express β_2 receptors in the resting state and α_{2A} receptors in the activated state (Fig. 6.1). These findings are consistent with most previous reports of expression of β_1 and β_2 adrenergic receptors in rat microglia (Mori et al., 2002; Morioka et al., 2009). The differences in β_1 receptor expression and the α_1 and α_2 receptors detected by Mori et al. (2002) in resting rat microglia might be due to species differences in regulating adrenergic receptor expression.

Despite the ~10-fold down-regulation, there is detectable mRNA signal for the β_2 receptor in activated microglia (Fig. 6.1A). However, treatment of activated microglia with the β agonist isoproterenol did not affect cell ramification in isolated primary cells (Fig. 6.6A, C). It is

known that β_2 receptor expression is controlled at multiple levels, including mRNA translation and protein trafficking (Kandasamy et al., 2005; Tholanikunnel et al., 2010). Thus, one possible explanation for the lack of functional effects of β_2 agonists in activated microglia is the existence of post-translational mechanisms of expression regulation. The control of β_2 receptor expression might occur in both resting and activated microglia, or be specific to activated microglia. If the same mechanisms are in play in resting microglia, the large amounts of β_2 receptor mRNA (Fig. 6.1) might allow enough functional receptors to reach the plasma membrane to respond to agonist.

6.4.b. Differential modulation of microglial process dynamics by NE and ATP

Imaging of microglia with high resolution, time-lapse confocal microscopy showed that NE is capable of causing process retraction in both resting and LPS-activated primary microglia. The finding that the G_s-coupled β_2- and the G_i-coupled α_{2A}-adrenergic receptors modulate microglial motility represents the second pair of G_s/G_i receptors for neurotransmitters (the other being $P2Y_{12}$/ A_{2A} receptors (Gyoneva et al., 2009; Orr et al., 2009) that control microglial process dynamics.

There are both similarities and differences in the manner by which ATP and NE affect microglial motility in resting and activated microglia. Whereas both neurotransmitters activate G protein-coupled receptors and influence cAMP signaling, microglial activation produces a switch from the G_i-coupled $P2Y_{12}$ receptor to the G_s-coupled adenosine A_{2A} receptor for which the ATP breakdown product adenosine is an agonist (Orr et al., 2009). In contrast, adrenergic receptors switch during microglial activation from the G_s-coupled β_2 receptors to the G_i-coupled α_{2A} receptors, both of which are activated by the same neurotransmitter norepinephrine (Fig. 6.10). Furthermore, ATP/adenosine signaling through purinergic receptors in resting and activated microglia produces opposing effects on process dynamics and motility (Orr et al., 2009), whereas NE produces the same effect (Fig. 6.5). PTx pre-treatment reduced NE-induced process retraction

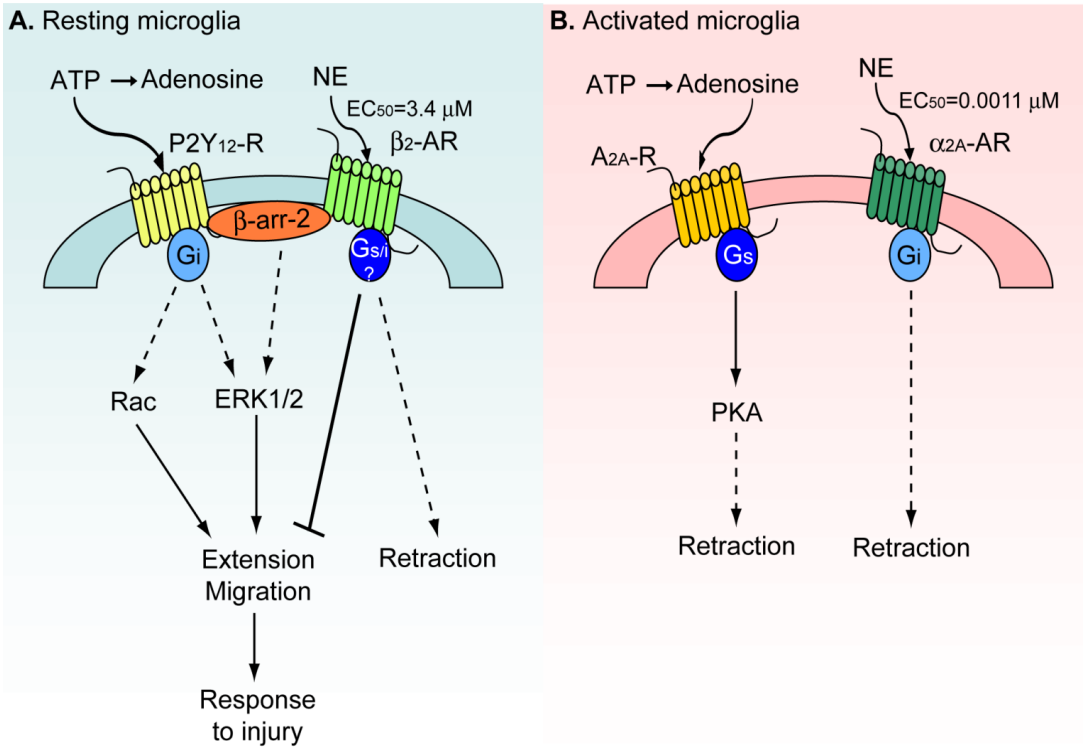

Figure 6.10. A summary of the regulation of microglial motility by adrenergic and purinergic receptors. A. Resting microglia express the purinergic $P2Y_{12}$ and the adrenergic β_2 receptors. Activation of the G_i-coupled $P2Y_{12}$ receptors by ATP results in process extension and migration to ATP through Rac, or β-arrestin-2-mediated activation of ERK1/2. In contrast, β_2 receptor activation by NE leads to process retraction and block of ATP-induced process extension and migration. Either G_i or G_s, or both types of G proteins might be involved in β_2 receptor signaling. **B.** LPS-activated microglia express the purinergic A_{2A} and the adrenergic α_{2A} receptors. Adenosine, a break-down product of ATP, activates A_{2A} receptors to induce process retraction in a PKA-dependent manner. NE activation of α_{2A} receptors also leads to process retraction. NE has substantially different potency at β_2 and α_{2A} receptors. [Figure reproduced with permission from Gyoneva and Traynelis (2013)].

in both resting and LPS-activated microglia (Fig. 6.7), suggesting that both β_2 and α_{2A} receptors use G_i proteins to exert their effects on microglial process dynamics, and could explain the similar effects of NE in resting and activated microglia.

Beta-2 receptors are thought to couple to G_s proteins, and α_{2A} receptors are thought to couple to G_i proteins. It is now clear that the signaling pathways initiated by these two adrenergic receptors are substantially more complex. Beta-2 receptors can switch their coupling from G_s to G_i in a protein kinase A (PKA)-dependent manner (Daaka et al., 1997) or might exist in a G_i-coupled state in the brain (Schutsky et al., 2011). Similarly, α_{2A} receptors can activate or inhibit cAMP synthesis depending on agonist concentration and the adenylate cyclase isoform expressed in the particular cell type (Eason et al., 1992; Federman et al., 1992). Activation of one of these non-canonical pathways in microglia might be responsible for the same downstream effect on process dynamics by β_2 and α_{2A} receptors. Indeed, the ability of the G_i inhibitor PTx to affect NE-induced process retraction (Fig. 6.7) indicates that both resting and activated microglia might employ G_i proteins to mediate the effects of NE.

Although the overall effect of adrenergic receptor activation in microglia appears the same (process retraction), NE is several orders of magnitude more potent at α_{2A} receptors than at β_2 receptors (Zhang et al., 2004), suggesting that activated microglia will be more sensitive to any NE present in the extracellular milieu. On the contrary, β_2 receptors on resting microglia might be activated only in pathological conditions (e.g. prolonged stress) that lead to release of large amounts of NE.

It is also worth noting that the three phenotypes that result from process retraction following adenosine A_{2A} or α_{2A}-adrenergic receptor activation in LPS-treated microglia and β_2-adrenergic receptor activation in resting microglia are all reminiscent of amoeboid microglia. However, it is likely that the three morphological phenotypes are three different functional states, which is consistent with the idea of microglial morphological and functional diversity (Scheffel et al., 2012). Thus, microglial exposure to various neurotransmitters (ATP and NE) might

predispose them to a given functional phenotype that will determine the ultimate response that can be achieved following additional stimuli.

Considering the divergent effects of ATP and NE on microglia, it is likely that ATP- and NE-induced changes in microglial motility serve different functions. For example, increased extracellular ATP levels are thought to be a sign of cell damage and potentially a signal for assistance to microglia (Hanisch and Kettenman, 2007); microglia extend their processes to the site of tissue damage or local ATP release without any obvious cell body movement (Davalos et al., 2005). Similarly, normal NE levels might suppress microglial reactivity (in terms of cytokine secretion) and motility; loss of NE as it occurs during neurodegeneration (Mann et al., 1980) will disinhibit microglia, allowing them to further extend their processes and monitor the cells around them.

6.4.c. Mechanism underlying the interaction between ATP and NE signaling in microglia

The ability of NE to interfere with ATP signaling in resting microglia (Figs. 6.8 and 6.9) might represent an example of heterologous desensitization, a phenomenon in which activation of one receptor prevents or attenuates the signaling through another receptor (Lohse, 1993; Pierce et al., 2002; Vazquez-Prado et al., 2003). Cross-talk between adrenergic receptors and $P2Y_{12}$ receptors has not been reported before, and the mechanisms by which it might occur remain unclear. In general, heterologous desensitization typically occurs after activation of protein kinases by one receptor that then phosphorylate and change the function of other receptors (Lohse, 1993; Pierce et al., 2002; Vazquez-Prado et al., 2003). The kinases most often implicated in this process are PKA, PKC, and to a lesser extent G protein receptor kinases (Bohm et al., 1997; Lohse, 1993; Pierce et al., 2002; Vazquez-Prado et al., 2003). In addition, both β_2-adrenergic receptor and $P2Y_{12}$ receptor can interact with β-arrestins (Goodman Jr et al., 1996; Li et al., 2011), and β-arrestin-2 is known to be involved in microglial chemotaxis to ATP through activation of ERK1/2 (Lee et al., 2012). This suggests that the interaction between adrenergic and

purinergic signaling might occur at the level of adaptor proteins and possibly affect the cellular localization of the receptors (Fig. 6.10). The ability of β receptor antagonists to prolong ATP responses in tissues might be a manifestation of their ability to block changes in $P2Y_{12}$ receptor trafficking (e.g., internalization). Lastly, although the responses of activated microglia to ATP alone or NE + ATP were not different under the present conditions (Fig. 6.8B), it is possible that NE alters the subsequent response to ATP, but that these effects cannot be detected by the analyses used here.

An alternative possibility is that there is no real heterologous desensitization happening between $P2Y_{12}$ and β_2 receptors. Rather, both receptors are activated and function independently. However, their downstream pathways might intersect at some point, antagonize each other, and result in a different motility pattern compared to if each pathway was activated alone. Thus, the mechanisms of heterologous desensitization between adrenergic and purinergic receptors, especially in the context of tissue damage and ATP release, warrant further investigation.

CHAPTER 7: Discussion and conclusions

7.1. Summary

The objective of my dissertation was to examine how inflammation influences microglial motility, and specifically, whether inflammation will alter the ability of microglia to respond to cell death in tissues. Accelerated neuronal death in specific brain regions is a feature of neurodegenerative diseases, including AD and PD (German et al., 1992; McGeer et al., 1988b; Pakkenberg et al., 1991). While it is possible to capture the disappearance of individual neurons *in vivo* in certain animal models of AD (Bittner et al., 2010; Fuhrmann et al., 2010), microglial response to cell death in real time can be studied by experimentally inducing tissue injury with a high-powered laser pulse or mechanically damaging the tissue (Davalos et al., 2005; Haynes et al., 2006; Hines et al., 2009; Krabbe et al., 2013; Nimmerjahn et al., 2005). I utilized both types of tissue damage to explore how microglia in tissues will respond under pro-inflammatory conditions. I focused on adrenergic and purinergic receptors because they are known to be involved in microglial responses to damage.

Before initiating experiments in tissues, I used pharmacological tools to analyze the contribution of different purinergic receptors to the regulation of microglial process dynamics *in vitro*. Using isolated primary microglia, I showed that $P2Y_{12}$ receptors mediate the process dynamics only in resting microglia. In contrast, adenosine A_{2A} receptors (but not A_1 or A_3 receptors) mediate the process dynamics only in LPS-activated microglia. These observations are consistent with $P2Y_{12}$ and A_{2A} receptors being expressed in resting and activated microglia, respectively (Chapter 3). This change in receptor expression and the differential effects of ATP on activated microglia compared to resting microglia resulted in reduced microglial response to mechanical damage in acute brain slices from LPS-injected animals (Chapter 4). The reduced response is also seen for microglia activated by the ongoing dopaminergic neuron degeneration in the MPTP-model of PD in slices from MPTP-treated mice (Chapter 4). To rule out the possibility

that slice preparation changes microglial properties, I examined the motility of microglia to laser-induced tissue damage *in vivo* with two-photon microscopy. In accordance with microglia in slices, microglia activated by systemic inflammation induced by a peripheral LPS injection displayed reduced response to the laser ablation (Chapter 5). The adenosine A_{2A} receptor antagonist preladenant prevented adenosine-induced process retraction *in vitro* (Chapter 3) and accelerated the response to damage in slices from MPTP-treated mice (Chapter 4) and *in vivo* in the brains of LPS-injected animals (Chapter 5), showing that it can modulate microglial motility *in vitro* and in tissues. Finally, I examined the regulation of microglial motility by adrenergic receptors because of previous evidence that NE can affect microglial migration (Chapter 6). I determined that resting microglia primarily express the G_s-coupled β_2 adrenergic receptors and activated microglia primarily express the G_i-coupled α_{2A} receptors. Despite the differential G protein coupling, NE induced process retraction in both resting and activated primary microglia *in vitro*. Importantly, NE can prevent ATP-induced process extension in resting microglia *in vitro* and in acute brain slices, suggesting that NE might interfere with the ability of microglia to respond to tissue damage *in vivo*. These findings could have implications for the clearance functions of microglia throughout a person's life.

7.2. Mechanisms of microglial activation

Despite the lack of a lymphatic system in the CNS and its perceived immune privilege, the CNS contains an innate immune system that can mount an immune response to various stimuli present in the brain (Lampron et al., 2013). As in the periphery, these include pathogens and tissue damage. Interestingly, systemic infections can indirectly activate microglia. I will briefly discuss how microglia get activated by mechanisms specific to the brain parenchyma in the next section. Then, because of the prevalence of systemic infections throughout a person's life, I will focus on how peripheral inflammation can contribute to the progression of neurodegenerative disease like AD and PD. In this work, I modeled microglial activation initiated

in the brain with the MPTP model of PD and systemic infection with a peripheral injection of LPS in order to examine how these types of activating stimuli will affect microglial motility.

7.2.a. Mechanisms initiated in the brain

Microglial activation can result from two general mechanisms: appearance of a new signal or removal of a "calming" signal [Fig. 7.1; Lucin and Wyss-Coray (2009); Perry et al. (2010)]. The new signals could be pathogens, pathogen-associated molecules, or host molecules that are not normally seen in the extracellular space (ATP, DNA, aggregated Aβ and others). Certain neurotropic pathogens can enter the brain parenchyma through paracellular (*Trypanosoma* and *Treponema* species) and transcellular (*Listeria monocytogenes*, *Mycobacterium tuberculosis*, *Haemophilius influenzae*, *Candida albicans*) mechanisms (Bencurova et al., 2011). Pathogens contain PAMPs that can be recognized by the immune system of the host, while endogenous molecules represent DAMPs. Both PAMPs and DAMPs activate TLRs, NOD-like receptors and RIG-like receptors, which are expressed mostly on microglia, but also on neurons, astrocytes, and oligodendrocytes (Hanke and Kielian, 2011). The downstream signaling pathways from these receptors in microglia generally lead to NF-κB activation and cytokine secretion to result in an inflammatory milieu (Hanamsagar et al., 2012).

The second main mechanism that leads to microglial activation is the removal of calming signals such as CX_3CL1 and CD200. These ligands activate microglial receptors (CX_3CR1 and CD200R, respectively) to inhibit microglial reactivity. The effects of CX_3CL1-CX_3CR1 and CD200-CD200R on microglia, especially how they relate to maintaining a resting microglial phenotype, were discussed in Section 1.2.c. Microglia could become activated by this mechanism in conditions that lead to neuronal death, for example in neurodegenerative diseases.

One of the main questions regarding the role of inflammation in neurodegeneration research is whether the inflammation causes the neurodegeneration or if it is a consequence of the cell death and degeneration. Efforts to answer this question have been attempted in animal

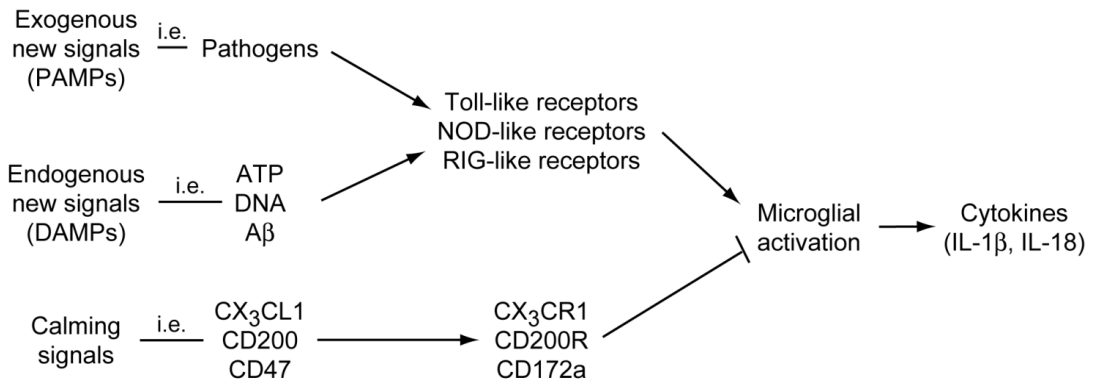

Figure 7.1. Mechanisms of microglial activation. The appearance of new signals, which can be either exogenous or endogenous, activate several receptor families that lead to microglial activation. The exogenous signals can be pathogens that display pathogen-associated molecular patterns (PAMPs). The endogenous signals are molecular entities released by damaged cells (ATP, DNA) or abnormal proteins (aggregated Aβ), which represent danger-associated molecular patterns (DAMPs). Microglial activation can also be achieved through the removal of calming signals from other cell types. For example, neuronal CX_3CL1, CD200 and CD47 bind to their corresponding receptors on microglia to inhibit their reactivity. The first steps of microglial activation consist of upregulation of cytokine genes, and processing and secretion of IL-1β and IL-18 by inflammasome complexes.

models of PD. In the acute MPTP mouse model of PD (4 injections of 10 mg/kg spaced 1 hr apart), microglial activation can be detected in the SN and striatum starting on day 1 after treatment, peaking on days 2-3, and subsiding by day 21 (Czlonkowska et al., 1996; Kohutnicka et al., 1998; Kurkowska-Jastrzebska et al., 1999). Loss of TH-positive neurons in the SN also starts on day 1 and progresses until at least day 21 (Kohutnicka et al., 1998). In this model, it appears that microglial activation and loss of dopaminergic neurons are initially observed at approximately the same time. Henry et al. (2009) set out to determine which event occurs first after inducing dopaminergic neuron degeneration by injection of 6-OHDA in the rat medial forebrain bundle or ventral tegmental area. In both cases, apoptotic cells positive for Fluoro-Jade were detected in the SN before the appearance of OX-42-positive activated microglia or a decrease in the number of dopaminergic neurons in the SN (Henry et al., 2009). Thus, the authors suggest that the impaired neuronal health is the first event in the neurodegenerative process, and microglial activation occurs in response to the dying neurons. In support of their hypothesis, they show that activated microglia were seen only in regions with ongoing degeneration, and not in regions with healthy neurons, indicating that microglia do not induce the degeneration (Henry et al., 2009). However, these results are to be expected from a model that uses a toxin that directly damages dopaminergic neurons, and does not preclude that central or peripheral inflammation induced with an inflammogen will compromise neuronal health. Furthermore, the animal models of PD capture only some of the features of the disease, and different mechanisms could drive the progression of the disease in humans.

7.2.b. Systemic inflammation and neurodegeneration

The neuroinflammation that is seen in neurodegenerative diseases can be initiated in the periphery as well, following systemic infections (Perry et al., 2007; Perry et al., 2003). The three main mechanisms through which peripheral inflammation, including LPS-induced inflammation,

can be transferred to the brain are reviewed by (Perry et al., 2007). First, vagus nerve afferents can sense inflammatory events in the abdominal cavity and communicate them in the brain. Second, peripheral cytokines can directly interact with macrophages in regions of the brain that lack a BBB, such as the circumventricular organs. Last, cytokines and pro-inflammatory mediators can interact with endothelial cells to communicate to perivascular macrophages on the brain parenchyma side of the BBB. The circumventricular and perivascular macrophages can then execute a response that leads to release of pro-inflammatory mediators in the brain parenchyma. The implications of this peripherally induced neuroinflammation are that it might affect the progression of neurological and neurodegenerative diseases.

Several groups have investigated the interaction between systemic infections, peripheral inflammation and the functional decline that is part of the progression of AD and PD. In a case-control study, having two or more infective episodes in the five years prior to examination was associated with increased risk of dementia (Dunn et al., 2005). Similarly, in a case-cohort study, subjects with increased levels of the pro-inflammatory proteins α_1-chymotrypsin or IL-6 had a higher risk for developing AD during a one-year follow-up period (Engelhart et al., 2004). Two studies have examined the effect of an inflammatory event after the onset of AD on the progression of the disease as measured by the rate of cognitive decline. Holmes et al. (2003) report that an acute episode of infection in the two months before the initiation of their study, or detectable IL-1β levels at baseline, are associated with an increased rate of cognitive decline. In another study from the same group, they determined that high baseline TNF-α levels or the presence of a systemic inflammatory event during a six-month observation period are associated with faster cognitive decline (Holmes et al., 2009). For PD, peripheral IL-6 and TNF-α are associated with subtle motor disturbances and poorer performance on certain motor tests (Dobbs et al., 1999; Scalzo et al., 2010). Furthermore, several case-control studies report increased risk for developing PD in elderly patients who experienced viral infections, including influenza (Fang et al., 2012; Harris et al., 2012; Vlajinac et al., 2013). Results like these suggest that systemic

inflammation can both increase the risk for developing a neurodegenerative disease or affect the progression of the disease. It should be noted, though, the cytokines detected in the periphery could be in response to the degeneration in the brain, and do not necessarily reflect events with peripheral origin.

In summary, both systemic and brain-specific inflammatory events can contribute to microglial activation. Inflammation is also known to affect the progression of AD and PD. Microglial motility is one of the functions affected by neuroinflammation with both central and systemic origin. Thus, I will next argue that the altered microglial activation might contribute to neurodegeneration.

7.3. Microglial motility and neurodegeneration

7.3.a. Receptor switching in microglia

At the molecular level, the purinergic $P2Y_{12}$ receptor is the primary receptor that regulates the motility of resting microglia in the healthy brain (Haynes et al., 2006). The receptor is downregulated in activated microglia, and replaced by the purinergic A_{2A} receptor (Orr et al., 2009). Both $P2Y_{12}$ and A_{2A} receptors can be activated by ATP and its breakdown products ADP and adenosine, respectively (Fig. 1.2). Thus, there is a switch in the receptor subtype that responds to a particular compound, changing the microglial response to that compound in the presence of inflammation. Specifically, the response to ATP in converted from process extension to retraction in isolated microglia *in vitro* [Fig. 3.4, 3.5; Table 7.1; Honda et al. (2001); Orr et al. (2009)]. The differential response might be mediated by differential coupling to G proteins: $P2Y_{12}$ receptors activate G_i proteins, while A_{2A} receptors activate G_s proteins. Indeed, blocking G_i signaling with PTx or G_s signaling with adenylate cyclase or protein kinase A inhibitors prevent ATP-induced process extension and retraction in resting and LPS-activated microglia, respectively (Honda et al., 2001; Orr et al., 2009). In this way, changing the type of receptor expressed on a specific cell type will be one approach to alter cellular function without changing

Table 7.1. Receptor switching in microglia

		Resting microglia	Activated microglia
Purinergic[1]	Receptor	$P2Y_{12}$	A_{2A}
	G protein coupling	G_i	G_s
	Effect on motility	Process extension, migration to ATP source	Process retraction, migration away from ATP source
Adenosine[2]	Receptor	A_1, A_3	A_{2A}
	G protein coupling	G_i	G_s
	Effect on motility	Potentiate ATP-induced migration and process extension	Process retraction, migration away from its source on its own
Adrenergic[3]	Receptor	β_2	α_{2A}
	G protein coupling	G_s, can be G_i	G_i
	Effect on motility	Process retraction	Process retraction

References: [1]Fig. 3.1, 3.2, 3.4, 3.5, 3.8; Haynes et al. (2006); Honda et al. (2001); Orr et al. (2009). [2]Fig. 3.3, 3.9; Ohsawa et al. (2012). [3]Fig. 6.1, 6.6.

other aspects of tissue physiology.

There are two more examples of receptor switching that were identified in this study, namely, switches in specific adenosine and NE receptors. Resting microglia primarily express the G_i-coupled A_1 and/or A_3 adenosine receptors (Färber et al., 2008; Ohsawa et al., 2012; van der Putten et al., 2009), but are replaced by the G_s-coupled A_{2A} receptors in activated microglia (Fig. 3.3, Table 7.1). Adenosine, acting through A_1 or A_3 receptors depending on the cell preparation, has no effect on the motility of resting microglia when administered alone [Fig. 3.5; Färber et al. (2008); Ohsawa et al. (2012)], but potentiates ATP-induced process extension and migration (Ohsawa et al., 2012). In contrast, adenosine by itself is sufficient to induce process retraction and migration away from its source in activated microglia [Fig. 3.4, 3.8; Orr et al. (2009)]. In this case, receptor switching might serve the purpose of rendering the cells responsive to a particular signal.

For NE-responsive receptors, the G_s-coupled β_2 adrenergic receptors in resting microglia are replaced by the G_i-coupled α_{2A} receptors in activated microglia (Fig. 6.1; Table 7.1). However, the functional consequences of this switch are not immediately obvious as both β_2 and α_{2A} receptor activation results in process retraction (Fig. 6.5, 6.6). One possibility is that receptor switching increases the sensitivity of microglia to NE as NE is several orders of magnitude more potent at α_{2A} receptors compared to β_2 receptors [in cAMP assays in heterologous expression system, EC_{50} = 0.0011 μM at α_{2A} receptors, EC_{50} = 3.4 μM at β_2 receptors, ~3000x difference; Zhang et al. (2004)]. PTx pre-treatment partially blocks NE-induced process retraction in both resting and activated microglia (Fig. 6.7), suggesting that G_i proteins mediate the effects of NE on microglial motility regardless of cell activation status. As mentioned in Section 6.4, there is precedence for β_2 receptors switching their coupling from G_s to G_i or existing in a G_i-coupled state in the brain (Daaka et al., 1997). The common intracellular signaling pathways by β_2 and α_{2A} receptors could explain the lack of differential effect of NE on microglial motility depending on activation status. Yet, it is possible that NE might affect other microglial functions, such as

phagocytosis or cytokine secretion, in different ways based on cell activation.

To my knowledge, there are no other reports of receptor switching at this point. However, not many receptor systems have been examined comprehensively in both resting and activated microglia. For example, the expression of serotonin and dopamine receptors has been characterized in resting microglia, but there was no data presented about their expression in activated microglia (Färber et al., 2005; Krabbe et al., 2012). Considering that many receptor families consist of multiple subtypes responsive to the same ligand, receptor switching in microglia might be a general phenomenon that is currently underappreciated.

7.3.b. Implications of impaired microglial motility under pro-inflammatory conditions

Neuronal death is part of normal aging, but the rate at which it occurs appears to be accelerated in neurodegenerative disorders. For example, (McGeer et al., 1988b) report that normal cell loss in the SN of elderly individuals is approximately 3,300 cells/year (9 cells/day), but might rise to as high as 12,000-43,000 cells/year (33-118 cells/day) after the initiation of PD progression. The rate of neuronal death in AD is likely to be higher than the 9 cell/day in healthy individuals, as well. In order to determine the effect of microglial activation on response to tissue damage, I used mechanical damage with diameter of ~100 μm (Section 4.3.a; Fig. 4.1C, D), and laser ablation with diameter of ~20 μm (Fig. 5.3). Even after considering the different cell counts between human and mouse SN and that neuronal death is distributed through the whole area of the SN, the modest injury that I used here is comparable to the daily rate of cell loss reported in PD (McGeer et al., 1988b) and possibly also in AD. Thus, I believe that the responses I observed can be used to extrapolate how microglia will respond to cell death in humans.

The results presented in the previous chapters show that microglia under pro-inflammatory conditions display a delayed response to tissue damage both in the tissues of acute brain slices and *in vivo*. The downregulation of the chemotactic $P2Y_{12}$ receptor and the concurrent upregulation of the A_{2A} receptor likely both contribute to this effect. This raises the possibility

that microglia under pro-inflammatory conditions might be less efficient in sensing and responding to tissue damage than microglia in the healthy brain in two different ways. Initially, before the onset of a neurodegenerative process, any systemic inflammation that a person experiences throughout life might also lead to neuroinflammation (Perry et al., 2007; Perry et al., 2003). The resulting microglial activation and slow resolution of small disturbances might allow debris and damage to accumulate in the brain. The damage will most certainly affect neuronal function, which over time could impair cognitive function. Later, after disease onset, activated microglia might not properly respond and clear cell debris on an acute level (within minutes) as individual cells progressively die. Again, the accumulation of damaged material in the extracellular space could affect network function and also damage nearby neurons. As a result, the reduced microglial motility and potentially reduced clearance functions might impact brain function by allowing tissue debris to spread to otherwise healthy areas (Fig. 7.2). Therefore, both motility and phagocytic functions of microglia are essential for maintaining tissue homeostasis.

Other than the removal of potentially neurotoxic constituents leaked from damaged cells, phagocytosis of cellular debris might contribute to restoring brain homeostasis indirectly through the prevention of pro-inflammatory signaling. Phagocytosis of apoptotic peripheral leukocytes or red blood cells by monocytes decreases the secretion of pro-inflammatory cytokines (IL-1, TNF-α, IL-12) and increases the secretion of anti-inflammatory cytokines (Voll et al., 1997). Similarly, phagocytosis of apoptotic T cells (unprimed or specific for myelin basic protein) by microglia decreases the expression of the pro-inflammatory cytokines TNF-α and IL-12 without affecting anti-inflammatory cytokines (Magnus et al., 2001). Ingestion of myelin itself initially increases pro-inflammatory cytokine secretion (first <6 hr), but later inhibits them (Liu et al., 2006). Consistent with the reduced microglial reactivity after phagocytosis, the recruitment of encephalogenic T cells is also reduced (Chan et al., 2006).

It is important to mention that the *TREM2* and *CD33* genes, which are mutated in many AD patients [see Section 1.4.b; Griciuc et al. (2013); Guerreiro et al. (2013); Jonsson et al.

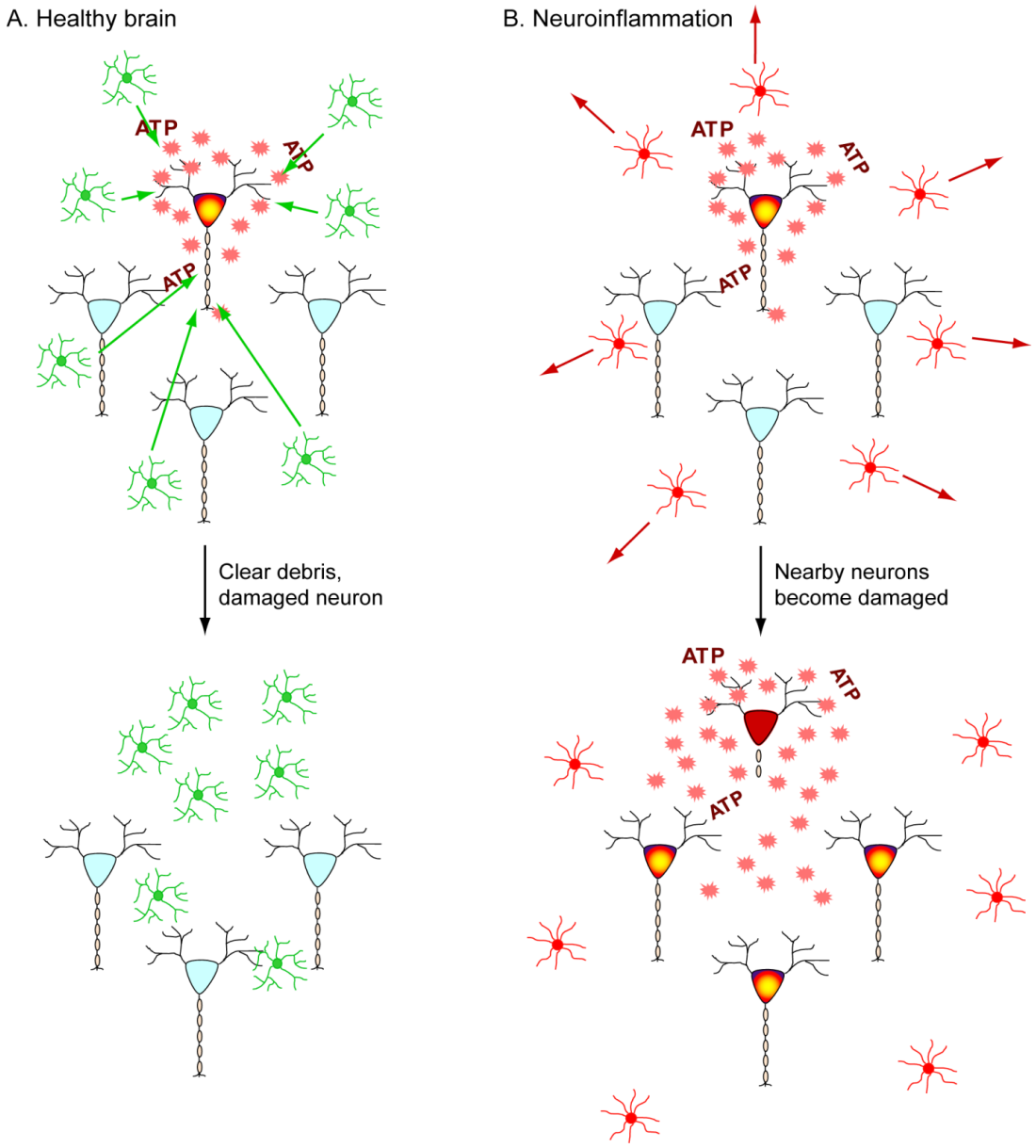

Figure 7.2. Microglial response to cell death in the healthy and inflamed brain. Neuronal death (multicolored cell body) is associated with spillout of ATP and other cellular constituents into the brain parenchyma. **A.** In the healthy brain, the ATP attracts microglia. They are able to clear the debris, remove the dead neuron, and minimize damage. **B.** In the presence of inflammation, either peripherally or centrally induced, microglia do not migrate to the damaged neuron. This allows the debris to spread to nearby neurons and compromise their health.

(2013)], mediate the phagocytic and inflammatory responses in microglia. If TREM2 expression is reduced, phagocytosis is decreased, and TNF-α and nitric oxide synthase-2 expression is increased, and vice versa when apoptotic neurons are exposed to microglia overexpressing TREM2 (Takahashi et al., 2005). In contrast, CD33 signaling reduces phagocytosis of Aβ (Bradshaw et al., 2013; Griciuc et al., 2013), but its effect on phagocytosis of apoptotic cells has not been examined. Finally, microglial phagocytosis might be detrimental in certain situations and can induce the removal of otherwise healthy neurons. Neurons exposed to Aβ or conditioned medium from LPS-treated microglia can display phosphatidylserine (PS), a phagocytic signal, on their outer cell membrane. However, blocking different steps of the PS-vitronectin receptor signaling inhibits microglial phagocytosis, leads to removal of the PS signal from neuronal membranes, and results in increased neuronal survival (Fricker et al., 2012; Neher et al., 2011; Neniskyte et al., 2011). Yet, it is not known whether these neurons are fully functional after recovery from the neurotoxic signal.

A caveat to the model proposed above is that the experimental damage used for this study and by others (Davalos et al., 2005; Haynes et al., 2006; Nimmerjahn et al., 2005) likely differs in mechanism from the apoptotic cell death that occurs during normal aging and in neurodegenerative conditions. Yet, the damaged area induced by a laser ablation increases in size if microglial process outgrowth is inhibited (Hines et al., 2009). It is worthwhile to investigate whether modulation of microglial phagocytic activity will affect the size of the damaged area following tissue damage *in vivo*, and whether changes in phagocytic activity and approach to the damaged site will have an additive effect.

If the delayed response to tissue damage is detrimental, then why would it occur? Why would microglia upregulate a receptor such as the A_{2A} receptor under pro-inflammatory conditions when its activation delays response to damage when it might be most needed? There are three possible explanations for this, all of which are highly hypothetical and speculative. First, the A_{2A} receptor-mediated process retraction might have arisen as a mechanism of negative

feedback once microglia have responded to a disturbance in the brain parenchyma. After microglia have cleared the debris from the damaged cells, it seems plausible that there will be a mechanism to instruct the responding processes to return to their original locations. A_{2A} receptor activation might serve just such a function, and the reduced response to damage under inflammatory conditions would be only an unfortunate consequence. Second, in addition to modulation of microglial motility and cytokine secretion by activated microglia (Section 3.4.c), A_{2A} receptors might be involved in yet-unidentified "beneficial" functions. The positive regulation of those functions might be sufficient to override the perceived negative effects on motility. Third, it is possible that the A_{2A} receptor-mediated repulsion might serve a protective mechanism for microglia. Some of the cellular debris that is released by damaged cells might be detrimental to microglia. Thus, process retraction from this debris could serve a protective function for microglia at the expense of possible beneficial effects to the damaged cell. In any case, it is important to continue studying A_{2A} receptors in microglia in order to understand their involvement in the healthy brain and under pathological conditions.

It should be noted that microglial activation is likely best represented by a spectrum of many possible phenotypes rather than the extremes of resting and LPS-activated microglia (Colton and Wilcock, 2010; Perry et al., 2010). The concept of alternatively activated microglia has been proposed to mirror alternatively activated, wound-healing macrophages in the periphery. Macrophages assume this phenotype following activation with IL-4 or IL-13, and upregulate mannose receptors, arginase-1 and found in inflammatory zone-1 (FIZZ1) to help with tissue repair (Gordon, 2003). Microglia with this phenotype have been identified in animal models of AD following deletion of components of the NLRP3 inflammasome or caspase-1, and are thought to mediate some of the protective effects of NLRP3 inactivation (Heneka et al., 2013). The dynamics of alternatively activated microglia, and the expression of the receptors involved in the control of motility, are likely different from those in either resting or LPS-activated microglia. Thus, both receptor expression and downstream motility should be examined under conditions

promoting alternative microglial activation.

7.3.c. Neuroprotection by A_{2A} antagonists

Adenosine A_{2A} receptors have gathered considerable attention as a possible therapeutic target (for example, see Section 3.4.a), and particularly in PD. Epidemiological studies show an inverse association between the consumption of caffeine, a non-selective adenosine receptor antagonist, and the risk for developing PD (Ascherio et al., 2001; Hancock et al., 2007; Ross et al., 2000). Caffeine, the selective A_{2A} receptor antagonists KW-6002 and SCH-58261, and genetic deletion of A_{2A} receptors are protective in the MPTP and 6-OHDA models of PD: they reduce the toxin-induced loss of dopaminergic neurons and microglial activation (Carta et al., 2009; Chen et al., 2001; Ikeda et al., 2002; Xu et al., 2002; Yu et al., 2008). Because the effects of caffeine are mimicked by A_{2A} receptor deletion or antagonists, but not A_1 receptor deletion or agonists, it appears that the effects of caffeine are mediated through the A_{2A} receptor (Chen et al., 2001). Consistent with the neuropathological findings and the localization of A_{2A} receptors to D_2 receptor-expressing neurons in the striatum, A_{2A} receptor activation can modify locomotor behavior. Activation of A_{2A} receptors with APEC reduces locomotor activity of MPTP-treated marmosets, while A_{2A} receptor antagonism with KW-6002 increases locomotion (Kanda et al., 1998a; Kanda et al., 1998b). Inhibition of A_{2A} receptor signaling also potentiates the effects of standard PD therapies such as L-Dopa and dopamine receptor agonists (Kanda et al., 2000; Pinna et al., 2001; Xiao et al., 2006). A valuable feature of A_{2A} receptor antagonists is their resistance to the development of tolerance or dyskinesias (Kanda et al., 1998a; Kanda et al., 2000; Pinna et al., 2001; Xiao et al., 2006). The recently developed highly-selective and brain-permeable A_{2A} receptor antagonist preladenant shows the same properties as well (Hodgson et al., 2009; Neustadt et al., 2007). As a result, several selective A_{2A} receptor antagonists have entered clinical trials for PD, including preladenant which was used here (Barkhoudarian and Schwarzschild, 2011; Hauser et al., 2011; Kalda et al., 2006; Schwarzschild et al., 2006; Xu et al., 2005).

Adenosine A_{2A} receptors are expressed on nigrostriatal dopaminergic neurons where they appear to oppose the effects of dopamine D_2 receptor activation (Ferre et al., 1993). Thus, the majority of the modulatory properties of A_{2A} receptor antagonists in PD models have been attributed to actions on neuronal receptors (Carta et al., 2009; Xiao et al., 2006). Neuronal A_{2A} receptors are most likely responsible for the motor effects of A_{2A} antagonists. In support of this, both global and forebrain neuron (fbn)-specific A_{2A} receptor deletion prevent the locomotory changes associated with A_{2A} receptor antagonists (Xiao et al., 2006; Yu et al., 2008).

A_{2A} receptors are also highly expressed on glial cells in the substantia nigra of healthy monkeys, and to a lower extent in the SN of healthy rats (Bogenpohl et al., 2012). Moreover, A_{2A} receptors were upregulated in the substantia nigra and striatum following treatment with 20 mg/kg/day MPTP for 5 days (Fig. 4.7), and in mice treated with 20 mg/kg MPTP once daily for 2-4 weeks (Singh et al., 2009). Thus, A_{2A} receptor antagonists will affect both neuronal and glial receptors. However, there are divergent results regarding the relative involvement of forebrain and glial A_{2A} receptors in neuroprotection through the modulation dopaminergic neuron loss and glial activation. Xu et al. (2002) were the first to suggest that the locomotor stimulant and neuroprotective properties of caffeine might occur through different mechanisms. Consistent with this, Yu et al. (2008) observed that knock out of fbnA_{2A} receptors abolish the motor stimulant effects of KW-6002, but do not affect the loss of dopaminergic neurons and gliosis induced by MPTP (3 injections of 20 mg/kg given at 2 hr intervals). Administration of KW-6002 to these mice was still able to reduce chronic MPTP toxicity (30 mg/kg once daily injections for 5 days). In contrast, Carta et al. (2009) report that deletion of fbnA_{2A} receptors completely prevents the dopaminergic neuron toxicity and gliosis in the SN of mice treated with 20 mg/kg MPTP once daily for 4 days.

Throughout this dissertation, I showed that A_{2A} receptors are expressed by activated microglia and can modulate microglial process dynamics. Inhibition of A_{2A} receptors with preladenant prevented the adenosine-induced process retraction *in vitro* (Fig. 3.7), the delayed

response of microglia to mechanical damage in slices from MPTP-treated mice (Fig. 4.6), and the LPS-induced delay in response to tissue damage *in vivo* (Fig. 5.7, 5,8). These findings suggest A_{2A} antagonists in humans will likely affect microglial motility. As a consequence, at least some of the neuroprotective properties of these antagonists might be due to effects on microglia, either through the improved ability of microglia to detect and contain cell death described here, or other mechanisms.

7.3.d. Involvement of other GPCRs in modulating microglial motility

In addition to the receptor systems described so far, there is evidence for the modulation of microglial motility by several other GPCRs, including dopamine, serotonin and morphine receptors, and some of the receptors that interact with Aβ. Despite their disease relevance, surprisingly little is known about how the neurotransmitters dopamine, serotonin and morphine affect microglial motility. Resting primary rat microglia express mRNA for the G_s-coupled D_1 and D_5 dopamine receptors, and for the G_i-coupled D_2 and D_4 receptors; D_3 receptors were not detected at the mRNA level (Färber et al., 2005). Dopamine and selective D_1-subfamily or D_2-subfamily agonists all increase microglial migration in chemotaxis chambers (Färber et al., 2005) despite the differential G protein coupling. However, the authors do not provide any information about the expression of dopamine receptors or their effect on motility in activated microglia. The same group also characterized the effects of serotonin receptors on microglia. Resting mouse cortical microglia have detectable mRNA for 5-HT_{1F}, 5-HT_{2A}, 5-HT_{2B}, 5-HT_{3B}, 5-HT_{5A} and 5-HT_7 (Krabbe et al., 2012). Serotonin treatment potentiates microglial response to tissue damage in acute brain slices, and increases microglial motility on its own and promotes ATP-induced migration in chemotaxis chambers (Krabbe et al., 2012). Yet, there was no data provided about which serotonin subtypes mediate these motile responses or how they might change following microglial activation during inflammation. Finally, stimulation of microglia with morphine induces Rac activation and enhances cell migration in a Boyden chamber assay in a PTx-sensitive

manner (Takayama and Ueda, 2005). Overall, the findings about dopamine, serotonin, and morphine increase the number of neurotransmitters that can affect microglial motility, further supporting the idea that microglia might sense and respond to synaptic activity (see Section 1.3.b). Moreover, the potentiation of ATP-induced microglial motility by serotonin represents another example of neurotransmitter modulation of motion and interaction with ATP signaling (the other one being NE), and suggests that there may be many opportunities to alter microglial motility if needed.

Finally, Aβ can interact with a large number of receptors and cell surface complexes, many of which are involved in phagocytosis, scavenging, and debris removal (see Section 1.4.b). However, it also interacts with FPR2 and FPR-like-1 receptor to induce microglial chemotaxis, both of which signal through G_i-coupled, PTx-sensitive pathways (Le et al., 2001). Both receptors are expressed on microglia associated with amyloid plaques in the brains of mice and AD patients (Tiffany et al., 2001). Activation of FPR2 also promotes Aβ uptake, indicating that a dual mechanism of action may underlie the clearance of Aβ. Moreover, treatment with TNF-α or activation of TRL2 with peptidoglycan increase FPR2 expression in microglia (Chen et al., 2006), resulting in enhanced migration to and phagocytosis of Aβ (Chen et al., 2006; Iribarren et al., 2007). Similarly, NE, which has known beneficial effects in AD (see Section 6.2), upregulates FPR2 expression to increase migration to and uptake of Aβ (Kong et al., 2010). Hence, factors known to help resolve Aβ pathology, including inflammation and NE, might act by modifying FPR2 expression to exert some of their beneficial effects. These findings provide support for the targeting of Aβ clearance as a therapeutic strategy, and also highlight the importance of microglial migration to the Aβ plaques.

An intriguing common feature of most receptors that enhance microglial migration is their coupling to G_i proteins and activation of the small GTPase Rac (Honda et al., 2001; Takayama and Ueda, 2005; Tiffany et al., 2001). The signaling mechanisms that transduce receptor activation to changes in the actin cytoskeleton and ultimately to migration are beyond the

scope of this work. Therefore, I will discuss them only briefly. While Rac activation downstream of GPCR signaling is well documented, the exact mechanism by which it occurs is not clear. Studies in mouse neutrophils and *Dictyostelium* slime mold show that the βγ subunit of an activated G protein can interact with guanine nucleotide exchange factors (GEFs), which then catalyzes the exchange of GDP for GTP to activate Rac. Some of the identified GEFs include P-Rex1 and ElmoE (Dong et al., 2005; Yan et al., 2012). Results from several cell types, for example neurons, neutrophils, and immortalized cell lines, show that GTP-bound Rac acts on several effectors to change the actin cytoskeleton. These include inhibition of capping proteins to promote actin filament elongation, phosphorylation of LIM kinase to prevent disassembly of actin filaments by cofilin, and indirect activation of Arp2/3 to promote growth of new filaments (Chernoff, 1999; Dong et al., 2005; Edwards et al., 1999; Weiner et al., 2006; Yan et al., 2012). Yet, it is not known whether the same mechanisms regulate actin dynamics in response to G_i-coupled GPCR stimulation in microglia, and whether all of the receptors that modulate microglial motility via G_i proteins use the same pathway.

Even less is known about the regulation of the cytoskeleton by G_s-coupled receptors such as the A_{2A} receptors to lead to process retraction. In neurons, Rho GTPases commonly result in growth cone retraction (Hall, 1998; Luo, 2000). However, Rho signaling is not involved in the ATP-induced process retraction in activated microglia as inhibition of Rho or its effector Rho kinase do not alter microglial process dynamics (Orr et al., 2009). Instead, inhibition of G_s itself, adenylate cyclase or protein kinase A all prevent the ATP-induced process retraction (Orr et al., 2009). However, how G_s signaling links to actin dynamics is not known. It represents a worthwhile avenue of investigation as it could lead to the identification of specific targets that will allow the modulation of microglial motility in the context of response to cell death and tissue damage.

7.4. Functional implications for the interaction between ATP and other neurotransmitters

in microglia

In Chapter 6, I examined the regulation of microglial process dynamics by adrenergic receptors. In addition to inducing process retraction in both resting and LPS-activated microglia on its own, NE unexpectedly prevented ATP-induced process extension and migration. The interaction between NE and ATP suggests that the presence of NE might prevent microglia from efficiently responding to tissue damage and cell death. This could have implications in situations of stress that involve elevated NE levels (Kvetnansky et al., 2009; Stanford, 1995). In such situations, any normal disturbance of tissue integrity in the healthy brain might result in exacerbated tissue damage. Over time, prolonged exposure to stress could lead to accumulation of unresolved or poorly resolved damaging events that could later impair brain function (see Section 7.3.b). In contrast, serotonin enhances microglial response to tissue damage (Krabbe et al., 2012), suggesting that serotonin receptor activation can be beneficial in the context of responding to damaged neurons.

Process motility and response of microglia to tissue damage are only two of many functions that microglia perform in the CNS. Microglia are also well known phagocytes and sources of cytokines and other proinflammatory mediators (Hanisch, 2002; Hanisch and Kettenman, 2007; Kim and de Vellis, 2005; Napoli and Neumann, 2009; Smith et al., 2012). ATP, NE and serotonin have been reported to separately modulate these functions (Heneka et al., 2002; Heneka et al., 2010; Kong et al., 2010; Krabbe et al., 2012; Pocock and Kettenmann, 2007; Sperlagh and Illes, 2007). Interestingly, NE pretreatment prevents the ATP-induced p38 phosphorylation and tumor necrosis factor-α (TNF-α) release by mouse spinal cord microglia (Morioka et al., 2009), suggesting that adrenergic signaling and purinergic signaling might interact at multiple levels. Serotonin and ATP signaling have opposing effects on phagocytosis, with ATP enhancing and serotonin reducing phagocytosis of *E. coli*-coated microbeads *in vitro* (Krabbe et al., 2012; Orr et al., 2009). Yet, it is still unknown whether there will be an interaction

between these two systems in mediating phagocytosis, and whether the ability of serotonin to reduce phagocytosis will have functional consequences *in vivo*.

In the brain, microglia are exposed to a variety of signals at the same time and express various neurotransmitter receptors (Pocock and Kettenmann, 2007). Thus, it is important to understand how these cells will respond to this complex milieu by examining the interactions among NE, ATP, and other signaling systems.

7.5. Conclusion

The historical view of microglia as immune cells of the brain has dramatically expanded over the last ten years after the recognition that microglia are involved in brain development and the maintenance of normal function in the healthy brain [see Section 1.3; Kettenmann et al. (2013)]. Microglia constantly survey the brain and respond to cell death and blood vessel damage (Davalos et al., 2005; Nimmerjahn et al., 2005). Even the role of microglia in neurodegenerative diseases has undergone a paradigm shift. Rather than simply being reactive bystanders in diseases such as AD and PD, inflammation and microglia might also affect disease progression. In addition to their involvement in the release of pro-inflammatory or neurotoxic factors, the clearance functions of microglia might also be important for the pathogenesis of AD and PD (Napoli and Neumann, 2009). The response to cell death and tissue damage consists of extension of microglial processes to the affected area, encircling the area, and removal of cellular debris. Here I show that microglial process extension is impaired under pro-inflammatory conditions both in systemically-induced inflammation (Chapter 4) and in degeneration-induced inflammation (Chapter 5). As discussed in Section 7.3.b, the delayed response might allow debris to accumulate in the brain parenchyma to ultimately affect the progression of diseases like AD and PD that are characterized with high rates of cell death (Fig. 7.2). The modulation of microglial motility, for example by adenosine A_{2A} receptor antagonists, in order to prevent the delayed response to damage could have a therapeutic potential.

Finally, microglia in the brain are exposed to a large variety of factors at the same time and express various neurotransmitter receptors (Pocock and Kettenmann, 2007). Interactions between the many receptors are not only possible, but likely. This is the case with adrenergic, purinergic, and serotonin receptors. Yet, the function of only a few neurotransmitters has been characterized in microglia (Sections 1.5, 7.4; Chapter 6). Many of these neurotransmitter GPCRs are already targets for drug development. Thus, studying how microglia integrate these diverse signals to regulate both helpful and harmful effects needs further attention. The findings will help us not only to understand normal microglial biology, but also how they will respond in various pathological states and how they might be modified by available therapeutics. Alternatively, nodes of interaction between neurotransmitter GPCRs in microglia might allow the development of agents to selectively modulate microglial function. Considering the importance of neuroinflammation in the etiology of many neurological diseases, agents that avoid effects on other cell types could be of great therapeutic value.

CHAPTER 8: References

Aarum J, Sandberg K, Haeberlein SLB and Persson MA (2003) Migration and differentiation of neural precursor cells can be directed by microglia. *Proceedings of the National Academy of Sciences of the United States of America* **100**(26): 15983-15988.

Ahmed I, Tamouza R, Delord M, Krishnamoorthy R, Tzourlo C, Mulot C, Nacfer M, Lambert J-C, Beaune P, Laurent-Puig P, Loriot M-A, Charron D and Elbaz A (2012) Association between Parkinson's Disease and the *HLA-DRB1* Locus. *Movement Disorders* **27**(9): 1104-1110.

Ajami B, Bennett JL, Krieger C, Tetzlaff W and Rossi FM (2007) Local self-renewal can sustain CNS microglia maintenance and function throughout adult life. *Nature Neuroscience* **10**(12): 1538-1543.

Akiyama H, Barger S, Barnum S, Bradt B, Bauer J, Cole GM, Cooper NR, Piet E, Emmerling M, Fiebich BL, Finch CE, Frautschy S, Griffin WST, Hampel H, Hull M, Landreth G, Lue L-F, Mrak R, Mackenzie IR, McGeer PL, O'Banion MK, Pachter J, Pasinetti G, Plata-Salaman C, Rogers J, Rydel R, Shen Y, Streit W, Strohmeyer R, Tooyoma I, Van Muiswinkel FL, Veerhuis R, Walker D, Webster S, Wegrzyniak B, Wenk G and Wyss-Coray T (2000) Inflammation and Alzheimer's disease. *Neurobiology of Aging* **21**: 383-421.

Akiyama H, Ikeda K, Katoh M, McGeer EG and McGeer PL (1994) Expression of MRP14, 27E10, interferon-α and leukocyte common antigen by reactive microglia in postmortem human brain tissue. *Journal of Neuroimmunology* **50**: 195-201.

Akiyama H and McGeer PL (1989) Microglial response to 6-hydroxydopamine-induced substantia nigra lesions. *Brain Research* **489**: 247-253.

Alliot F, Godin I and Pessac B (1999) Microglia derive from progenitors, originating from the yolk sac, and which proliferate in the brain. *Developmental Brain Research* **117**: 145-152.

Ard M, Cole GM, Wei J, Mehrle A and Fratkin J (1996) Scavenging of Alzheimer's Amyloid β-Protein by Microglia in Culture. *Journal of Neuroscience Research* **43**: 190-202.

Ascherio A, Zhang SM, Hernan MA, Kawachi I, Golditz GA, Speizer FE and Willett WC (2001) Prospective Study of Caffeine Consumption and Risk of Parkinson's Disease in Men and Women. *Annals of Neurology* **50**: 56-63.

Ashwell K (1991) The distribution of microglia and cell death in the fetal rat forebrain. *Developmental Brain Research* **58**: 1-12.

Askew D and Walker WS (1996) Alloantigen Presentation to Naive $CD8^+$ T Cells by Mouse Microglia: Evidence for a Distinct Phenotype Based on Expression of Surface-Associated and Soluble Costimulatory Molecules. *Glia* **18**: 118-128.

Atkinson BN and Minneman KP (1991) Multiple Adrenergic Receptor Suntypes Controlling Cyclic AMP Formation: Comparison of Brain Slices and Primary Neuronal and Glial Cultures. *J Neurochem* **56**: 587-595.

Avignone E, Ulmann L, Levacasseur F, Rassendren F and Audinat E (2008) Status Epilepticus Induces a Particular Microglial Activation State Characterized by Enhanced Purinergic Signaling. *Journal of Neuroscience* **28**(37): 9133-9144.

Banati RB, Gehrmann J, Schubert P and Kreutzberg GW (1993) Cytotoxicity of Microglia. *Glia* **7**: 111-118.

Barcia C, Bahillo AS, Fernandez-Villalba E, Bautista V, Hirsch EC and Herrero MT (2004) Evidence of Active Microglia in Substantia Nigra Pars Compacta of Parkinsonian Monkeys 1 Year After MPTP Exposure. *Glia* **46**: 402-409.

Barkhoudarian MT and Schwarzschild MA (2011) Preclinical jockeying in the translational track of adenosine A_{2A} receptors. *Experimental Neurology* **228**: 160-164.

Bazan JF, Bacon KB, Hardiman G, Wang W, Soo K, Rossi D, Greaves DR, Zlotnik A and Schall TJ (1997) A new class of membane-bound chemokine with a CX_3C motif. *Nature* **385**: 640-644.

Bencurova E, Mlynarcik P and Bhide M (2011) An insight into the ligand-receptor interactions involved in the translocation of pathogens across blood-brain barrier. *FEMS Immunol Med Microbiol* **63**: 297-318.

Bernheimer H, Birkmayer W, Hornykiewicz O, Jellinger K and Seitelberger F (1973) Brain Dopamine and the Syndromes of Parkinson and Huntington: Clinical, Morphological and Neurochemical Correlations. *Journal of the Neurological Sciences* **20**: 415-455.

Berridge CW and Waterhouse BD (2003) The locus xoeruleus-noradrenergic system: modulation of behavioral state and state-dependent cognitive processes. *Brain Res Rev* **42**: 33-84.

Bhaskar K, NKonerth M, Kokiko-Cochran ON, Cardona AE, Ransohoff RM and Lamb BT (2010) Regulation of Tau Pathology by the Microglial Fractalkine Receptor. *Neuron* **68**: 19-31.

Bianco F, Fumagalli M, Pravettoni E, D'Ambrosi N, Volonte C, Matteoli M, Abbracchio MP and Verderio C (2005) Pathophysiological roles of extracellular nucleotides in glial cells: differential expression of purinergic receptors in resting and activated microglia. *Brain Research Reviews* **48**: 144-156.

Biber K, Dijkstra I, Trebst C, De Groot C, Ransohoff RM and Boddeke HWGM (2002) Functional expression of CXCR3 in cultured mouse and human astrocytes and microglia. *Neuroscience* **112**(3).

Bittner T, Fuhrmann M, Burgold S, Ochs SM, Hoffmann N, Mitteregger G, Kretzschmar H, LaFerla FM and Herms J (2010) Multiple Events Lead to Dendritic Spine Loss in Triple Transgenic Alzheimer's Disease Mice. *PloS One* **5**(11): e15477.

Blank T and Prinz M (2013) Microglia as Modulators of Cognition and Neuropsychiatric Disorders. *Glia* **61**: 62-70.

Block ML and Hong J-S (2005) Microglia and inflammation-mediated neurodegeneration: Multiple triggers with a common mechanism. *Progress in Neurobiology* **76**: 77-98.

Block ML, Zecca L and Hong J-S (2007) Microglia-mediated neurotoxicity: uncovering the molecular mechanisms. *Nature Reviews Neuroscience* **8**: 57-69.

Blum D, Hourez R, Galas M-C, Popoli P and Schiffmann S (2003) Adenosine receptors and Huntington's disease: implications for pathogenesis and therapeutics. *The Lancet Neurology* **2**: 366-374.

Bogenpohl JW, Ritter SL, Hall RA and Smith Y (2012) Adenosine A_{2A} Receptor in the Monkey Basal Ganglia: Ultrastructural Localization and Colocalization With the Metabotropic Glutamate Receptor 5 in the Striatum. *Journal of Comparative Neurology* **520**: 570-589.

Bohm SK, Grady EF and Bunnett NW (1997) Regulatory mechanisms that modulate signalling by G-protein-coupled receptors. *Biochem J* **322**: 1-18.

Bolmont T, Haiss F, Eicke D, Radde R, Mathis CA, Klunk WE, Kohsaka S, Jucker M and Calhoun ME (2008) Dynamics of the Microglia/Amyloid Interaction Indicate a Role in Plaque Maintenance. *Journal of Neuroscience* **28**(16): 4283-4292.

Bradshaw EM, Chibnik LB, Keenan BT, Ottoboni L, Raj T, Tang A, Rosenkrantz LL, Imboywa S, Lee M, Von Korff A, The Alzheimer's Disease Neuroimaging Initiative, Morris MC, Evans DA, Johnson K, Sperling RA, Schneider JA, Bennett DA and De Jager PL (2013) *CD33* Alzheimer's disease locus: altered monocyte function and amyloid bioloy. *Nature Neuroscience* **16**(7): 848-850.

Breitner JC, Baker LD, Montine TJ, Meinert CL, Lyketsos CG, Ashe KH, Brandt J, Craft S, Evans DE, Green RC, Ismail MS, Martin BK, Mullan MJ, Sabbagh M, Tariot PN and Group AR (2011) Extended results of the Alzheimer's disease anti-inflammatory prevention trial. *Alzheimer's & Dementia* **7**: 402-411.

Brockhaus J, Moller T and Kettenmann H (1996) Phagocytozing Ameboid Microglial Cells Studies in a Mouse Corpus Callosum Slice Preparation. *Glia* **16**: 81-90.

Bronstein DM, Perez-Otano I, Sun V, Mullis Sawin SB, Chan J, Wu G-C, Hudson PM, Kong L-Y, Hong J-S and McMillian MK (1995) Glia-dependent neurotoxocity and neuroprotection in mesencephalic cultures. *Brain Research* **704**: 112-116.

Buttini M, Limonta S and Boddeke HWGM (1996) Peripheral administration of lipopolysaccharide induces activation of microglial cells in rat brain. *Neurochemistry International* **29**(1): 25-35.

Cagnin A, Brooks DJ, Kennedy AM, Gunn RN, Myers R, Turkheimer F, Jones T and Banati RB (2001) In-vivo measurement of activated microglia in dementia. *Lancet* **358**: 461-467.

Calvo C-F, Dobbertin A, Gelman M, Glowinski J and Mallat M (1998) Identification of CSF-1 as a Brain Macrophage Migratory Activity Produced by Astrocytes. *Glia* **24**: 180-186.

Capotondo A, Milazzo R, Politi LS, Quattrini A, Palini A, Plati T, Merella S, Nonis A, di Serio C, Montini E, Naldini L and Biffi A (2012) Brain conditioning is instrumental for successful microglia reconstitution following hematopoietic stem cell transplantation. *Proceedings of the National Academy of Sciences of the United States of America* **109**(37): 15018-15023.

Carta AR, Kachroo A, Schintu N, Xu K, Schwarzschild MA, Wardas J and Morelli M (2009) Inactivation of neuronal forebrain A2A receptors protects dopaminergic neurons in a mouse model of Parkinson's disease. *Journal of Neurochemistry* **111**: 1478-1489.

Cash E and Rott O (1994) Microglial cells qualify as the stimulators of unprimed $CD4^+$ and $CD8^+$ T lymphocytes in the central nervous system. *Clinical and Experimental Immunology* **98**: 313-318.

Cash E, Zhang Y and Rott O (1993) Microglia Present Myelin Antigens to T Cells after Phagocytosis of Oligodentrocytes. *Cellular Immunology* **147**: 129-138.

Chan-Palay V and Asan E (1989) Alterations in Catecholamine Neurons of the Locus Coeruleus in Senile Dementia of the Alzheimer Type and in Parkinson's Disease With and Without Dementia and Depression. *J Comp Neurol* **287**: 373-392.

Chan A, Hummel V, Weilbach FX, Kieseier BC and Gold R (2006) Phagocytosis of Apoptotic Inflammatory Cells Downregulates Microglial Chemoattractive Function and Migration of Encephalitogenic T Cells. *Journal of Neuroscience Research* **84**: 1217-1224.

Chao CC, Hu S, Molitor TW, Shaskan EG and Peterson PK (1992) Activated microglia mediate neuronal cell injury via a nitric oxide mechanism. *Journal of Immunology* **149**(8): 2736-2741.

Chen H, Jacobs E, Schwarzschild MA, McCullough ML, Calle EE, Thun MJ and Ascherio A (2005) Nonsteroidal Antiinflammatory Drug Use and the Risk for Parkinson's Disease. *Annals of Neurology* **58**: 963-967.

Chen H, Zhang SM, Hernan MA, Schwarzschild MA, Willett WC, Colditz GA, Speizer FE and Ascherio A (2003) Nonsteroidal Anti-inflammatory Drugs and the Risk of Parkinson Disease. *Archives of Neurology* **60**: 1059-1064.

Chen J-F, Xu K, Petzer JP, Staal R, Xu Y-H, Beilstein M, Sonsalla PK, Castagnoli K, Castagnoli N and Schwarzschild MA (2001) Neuroprotection by Caffeine and A_{2A} Adenosine Receptor Inactivation in a Model of Parkinson's Disease. *The Journal of Neuroscience* **21**(10): RC143.

Chen K, Iribarren P, Hu J, Chen J, Gong W, Cho EH, Lockett S, Dunlop NM and Wang JM (2006) Activation of Toll-like Receptor 2 on Microglia Promotes Cell Uptake of Alzheimer Disease-associated Amyloid β Peptide. *Journal of Biological Chemistry* **281**(6): 3651-3659.

Chen S-K, Tvrdik P, Peden E, Cho S, Wu S, Spangrude G and Capecchi MR (2010) Hematopoietic Origin of pathological Grooming in *Hoxb8* Mutant Mice. *Cell* **141**: 775-785.

Chernoff J (1999) Close encounters of the LIM-kinase. *Nature Cell Biology* **1**: E115-E117.

Chiang H-L, Lee-Chen G-J, Chen CM, Chen Y-C, Lee C-M, Liao M-H and Wu Y-R (2012) Genetic analysis of HLA-DRA region variation in Taiwanese Parkinson's disease. *Parkinsonism and Related Disorders* **18**: 391-393.

Cho S-H, Sun B, Zhou Y, Kauppinen TM, Halabisky B, Wes P, Ransohoff RM and Gan L (2011) CX3CR1 Protein Signaling Modulates Microglial Activation and Protects against Plaque-independent Cognitive Deficits in a Mouse Model of Alzheimer's Disease. *Journal of Biological Chemistry* **286**(37): 32713-32722.

Clausen BH, Lambertsen KL, Babcock AA, Holm TH, Dagnaes-Hansen F and Finsen B (2008) Interleukin-1 beta and tumor necrosis factor-alpha are expressed bydifferent subsets of microglia and macrophages after ischemic stroke in mice. *Journal of Neuroinflammation* **5**: 46.

Colton CA and Chernyshev ON (1996) Inhibition of microglial superoxide anion production by isoproterenol and dexamethasone. *Neuroschem Int* **29**(1): 43-53.

Colton CA and Gilbert DL (1987) Production of superoxide anions by a CNS macrophage, the microglia. *FEBS Letters* **223**(2): 284-288.

Colton CA and Wilcock DM (2010) Assessing Activation States in Microglia. *CNS Neurol Disord-DR* **9**(2): 174-191.

Colton CA, Yao J, Keri J and Gilbert DL (1992) Regulation of microglial function by interferons. *Journal of Neuroimmunology* **30**: 89-98.

Costes SV, Daelemans D, Cho EH, Dobbin Z, Pavlakis G and Lockett S (2004) Automatic and Quantitative Measurement of Protein-Protein Colocalization in Live Cells. *Biophysical Journal* **86**: 3993-4003.

Cotman CW, Tenner AJ and Cummings BJ (1996) β-Amyloid Converts an Acute Phase Injury Response to Chronic Injury Response. *Neurobiology of Aging* **17**(5): 723-731.

Cross AK and Woodroofe MN (1999) Chemokines Induce Migration and Changes in Actin Polymerization in Adult Rat Brain Microglia and a Human Fetal Microglial Cell Line *In Vitro*. *Journal of Neuroscience Research* **55**: 17-23.

Cunningham C (2013) Microglia and Neurodegeneration: The Role of Systemic Inflammation. *Glia* **61**: 71-90.

Cunningham CL, Martinez-Cerdeno V and Noctor SC (2013) Microglia Regulate the Number of neural Precursos Cells in the Developing Cortex. *Journal of Neuroscience* **33**(10): 4216-4233.

Czlonkowska A, Kohutnicka M, Kurkowska-Jastrzebska I and Czlonkowski A (1996) Microglial Reaction in MPTP (1-methyl-4-phenyl-1,2,3,6-tetrahydropyridine) Induced Parkinson's Disease Mice Model. *Neurodegeneration* **5**: 137-143.

Daaka Y, Luttrell LM and Lefkowitz RJ (1997) Switching of the coupling of the β_2-adrenergic receptor to different G proteins by protein kinase A. *Nature* **390**: 88-91.

Davalos D, Grutzendler J, Yang G, Kim JV, Zuo Y, Jung S, Littman DR, Dustin ML and Gan W-B (2005) ATP mediates rapid mecroglial response to local brain injury *in vivo*. *Nature Neuroscience* **8**(6): 752-758.

Davalos D, Ryu JK, Merlini M, Baeten KM, Le Moan N, Petersen MA, Deerinck TJ, Smirnoff DS, Bedard C, Hakozaki H, Murray SG, Ling JB, Lassmann H, Degen JL, Ellisman MH and Akassoglou K (2012) Fibrinogen-induced perivascular microglial clustering is required for the development of axonal damage in neuroinflammation. *Nature Communications* **3**: 1227-1242.

de Haas AH, Boddeke HWGM and Biber K (2008) Region-Specific Expression of Immunoregulatory Proteins on Microglia in the Healthy CNS. *Glia* **56**: 888-894.

De Simone R, Giampaolo A, Giometto B, Gallo P, Levi G, Peschle C and Aloisi F (1995) The costimulatory Molecule B7 Is Expressed on Human Microglia in Culture and in Multiple

Sclerosis Acute Lesions. *Journal of Neuropathology and Experimental Neurology* **54**(2): 175-187.

del Rio-Hortega P (1939) The microglia. *Lancet* **1**: 1023-1026.

Della Bianca V, Dusi S, Bianchini E, Dal Pra I and Rossi F (1999) β-Amyloid Activates the $O_2^{\cdot -}$ Forming NADPH Oxidase in Microglia, Monocytes, and Neutrophils. *Journal of Biological Chemistry* **274**(22): 15493-15499.

Denes A, Ferenczi S, Halasz J, Környei Z and Kovacs KJ (2008) Role of CX3CR1 (fractalkine receptor) in brain damage and inflammation induced by focal cerebral ischemia in mouse. *Journal of Cerebral Blood Flow & Metabolism* **28**: 1707-1721.

Derecki NC, Cronk JC, Lu Z, Xu E, Abbott SB, Guyenet PG and Kipnis J (2012) Wild-type microglia arrest pathology in a mouse model of Rett syndrome. *Nature* **484**: 105-109.

Dickman MS (2001) von Economo Encephalitis. *Archives of Neurology* **58**: 1696-1698.

Dickson DW, Farlo J, Davis P, Crystal H, Fuld P and Yen S-HC (1988) Alzheimer's Disease: A Double-Labeleing Immunohistochemical Study of Senile Plaques. *American Journal of Pathology* **132**(1): 86-101.

Dobbs R, Charlett A, Purkiss A, Dobbs S, Weller C and Peterson D (1999) Association of circulating TNF-α and IL-6 with ageing and parkinsonism. *Acta Neurol Scand* **100**: 34-41.

Dong X, Mo Z, Bokoch GM, Guo C, Li Z and Wu D (2005) P-Rex1 Is a Primary Rac2 Guanine Nucleotide Exchange Factor in Mouse Neutrophils. *Current Biology* **15**: 1874-1879.

Dunn N, Mullee M, Perry VH and Holmes C (2005) Association between Dementia and Infections Disease: Evidence from a Case-Control Study. *Alzheimer's Disease and Associated Disorders* **19**: 91-94.

Eason MG, Kurose H, Holt BD, Raymond JR and Liggett SB (1992) Simultaneous Coupling of a_2-Adrenergic Receptors to Two G-roteins with Opposing Effects. *J Biol Chem* **267**(22): 15795-15801.

Edison P, Archer HA, Gerhard A, Hinz R, Pavese N, Turkheimer FE, Hammers A, Tai YF, Fox N, Kennedy A, Rossor M and Brooks DJ (2008) Microglia, amyloid, and cognition in Alzheimer's disease: An [11C](R)PK11195-PET and [11C]PIB-PET study. *Neurobiology of Disease* **32**: 412-419.

Edwards DC, Sanders LC, Bokoch GM and Gill GN (1999) Activation of LIM-kinase by Pak1 couples Rac/Cdc42 GTPase signaling to actin cytoskeleton dynamics. *Nature Cell Biology* **1**: 253-259.

Ehrlich LC, Hu S, Sheng WS, Sutton RL, Rockswold GL, Peterson PK and Chao CC (1998) Cytokine Regulation of Human Microglial Cell IL-8 Production. *Journal of Immunology* **160**: 1944-1948.

El Khoury J, Hickman SE, Thomas CA, Cao L, Silverstein SC and Loike JD (1996) Scavenger receptor-mediated adhesion of microglia to β-amyloid fibrils. *Nature* **382**: 716-719.

El Khoury J, Toft M, Hickman SE, Means TK, Terada K, Geula C and Luster AD (2007) *Ccr2* deficiency impairs microglial accumulation and accelerates progression of Alzheimer-like disease. *Nature Medicine* **13**(4): 432-438.

Elkades S, DiCicco-Bloom EM and Black IB (1996) Brain Microglia/Macrophages Express Neurotrophins that Selectively Regulate Microglial Proliferation and Function. *Journal of Neuroscience* **16**(8): 2508-2521.

Engelhart MJ, Geerlings MI, Meijer J, Kiliaan A, Ruitenberg A, van Swieten JC, Stijnen T, Hofman A, Witteman JC and Breteler MM (2004) Inflammatory Proteins in Plasma and the Risk of Dementia: The Rotterdam Study. *Archives of Neurology* **61**: 668-672.

Etminan M, Gill S and Samii A (2003) Effect of non-steroidal anti-inflammatory drugs on risk of Alzheimer's disease: systematic review and meta-analysis of observational studies. *British Medical Journal* **327**(128-132): 128.

Fang F, Wirdefeldt K, Jacks A, Kamel F, Ye W and Chen H (2012) CNS infections, sepsis and risk of Parkinson's disease. *International Journal of Epidemiology* **41**: 1042-1049.

Färber K, Markworth S, Pannasch U, Nolte C, Prinz V, Kronenberg G, Gertz K, Endres M, Bechmann I, Enjyoji K, Robson SC and Kettenman H (2008) The Endonucleotidase *cd39*/ENTPDase1 Modulates Purinergic-Mediated Microglial Migration. *Glia* **56**: 331-341.

Färber K, Pannasch U and Kettenmann H (2005) Dopamine and noradrenaline control distinct functions in rodent microglial cells. *Mol Cell Neurosci* **29**: 128-138.

Federman AD, Conklin BR, Schrader KA, Reed RR and Bourne HR (1992) Hormonal stimulation of adenylyl cyclase through G_i-protein $\beta\gamma$ subunits. *Nature* **356**: 159-161.

Ferre S, O'Connor WT, Fuxe K and Ungerstadt U (1993) The Striatopallidal Neuron: A Main Locus for Adenosine-Dopamine Interactions in the Brain. *Journal of Neuroscience* **13**: 5402-5406.

Ferre S, von Euler G, Johansson B, Fredholm BB and Fuxe K (1991) Stimulation of high-affinity adenosine A_2 receptors decreases the affinity of dopamine D_2 receptors in rat striatal membranes. *Proceedings of the National Academy of Sciences of the United States of America* **88**: 7238-7241.

Fiebich BL, Biber K, Lieb K, van Calker D, Berger M, Bauer J and Gebicke-Haerter PJ (1996) Cyclooxygenase-2 Expression in Rat Microglia Is Induced by Adenosine A_{2a}-Receptors. *Glia*(18): 152-160.

Fink JS, Weaver DR, Rivkees SA, Peterfreund RA, Pollack AE, Adler EM and Reppert SM (1992) Molecular cloning of the rat A_2 adenosine receptor: selective co-expession with D_2 dopamine receptors in rat striatum. *Molecular Brain Research* **14**: 186-195.

Floden A and Combs C (2007) Microglia repetitively isolated fro, in vitro mixed glial cultures retain their initial phenotype. *Journal of Neuroscience Methods* **164**: 218-224.

Flynn G, Maru S, Loughlin J, Romero IA and Male D (2003) Regulation of chemokine receptor expression in human microglia and strocytes. *Journal of Neuroimmunology* **136**: 84-93.

Fornai F, Alessandri MG, Torracca MT, Bassi L and Corsini GU (1997) Effects of Noradrenergic Lesions on MPTP/MPP+ Kinetics and MPTP-Induced Nigrostriatal Dopamine Depletions. *J Pharmacol Exp Ther* **283**: 100-107.

Frackowiak J, Wisniewski H, Wegiel J, Merz G, Iqbal K and Wang K (1992) Ultrastructure of the microglia that phagocytose amyloid and the microglia that produce β-amyloid fibrils. *Acta Neuropathologica* **84**: 225-233.

Franchetti P, Cappellacci L, Marchettu S, Trincavelli L, Martini C, Mazzoni MR, Lucacchini A and Grifantini M (1998) 2'-*C*-Methyl Analogues of Selective Adenosine Receptor Agonists: Synthesis and Binding Studies. *Journal of Medicinal Chemistry* **41**: 1708-1715.

Frautschy S, Cole GM and Baird A (1992) Phagocytosis and Deposition of Vascular β-amyloid in Rat Brains Injected with Azlheimer β-amyloid. *American Journal of Pathology* **140**(6): 1389-1399.

Fredholm BB, Battig K, Holmen J, Nehlig A and Zvartau EE (1999) Actions of Caffeine in the Brain with Special Reference to Factors That Contribute to Its Widespread Use. *Pharmacological Reviews* **51**(1): 83-133.

Fredholm BB, Irenius E, Kull B and Schulte G (2001) Comparison of the potency of adenosine as an agonist at human adenosine receptors expressed in Chinese hamster ovary cells. *Biochemical Pharmacology* **61**: 443-448.

Fricker M, Neher JJ, Zhao J-W, Thery C, Tolkovsky AM and Brown GC (2012) MFG-E8 Mediates Primary Phagocytosis of Viable Neurons during Neuroinflammation. *Journal of Neuroscience* **32**(8): 2657-2666.

Fuhrmann M, Bittner T, Jung CKE, Burgold S, Page RM, Mitteregger G, Haass C, LaFerla FM, Kretzschmar H and Herms J (2010) Microglial *Cx3cr1* knockout prevents neuron loss in a mouse model of Alzheimer's disease. *Nature Neuroscience* **13**(4): 411-413.

Fujita H, Tanaka J, Maeda N and Sakanaka M (1998) Adrenergic agonists suppress the proliferation of microglia through b2-agrenergic receptor. *Neurosci Lett* **242**: 37-40.

Gagne JJ and Power MC (2010) Anti-inflammatory drugs and risk of Parkinson disease: A meta-analysis. *Neurology* **74**: 995-1002.

Gallo-Rodriguez C, Ji X-d, Melman N, Siegman BD, Sanders LH, Orlina J, Fischer B, Pu Q, Olah ME, van Galen PJM, Stiles GL and Jacobson KA (1994) Structure-Activity Relationships of N^6-Benzyladenosine-5'-uronamides as A_3-Selective Adenosine Agonists. *Journal of Medicinal Chemistry* **37**: 636-646.

Gamboa ET, Wold A, Yahr MD, Harter DH, Duffy PE, Barden H and Hsu KC (1974) Influenza Virus Antigen in Postencephalitic Parkinsonism Brain: Detection by Immunofluorescence. *Archives of Neurology* **31**: 228-232.

Gao H-M, Hong J-S, Zhang W and Liu B (2002) Distinct Role for Microglia in Rotenone-Induced Degeneration of Dopaminergic Neurons. *Journal of Neuroscience* **22**(3): 782-790.

Gao H-M, Hong J-S, Zhang W and Liu B (2003a) Synergistic Dopaminergic Neurotoxicity of the Pesticide Rotenone and Inflammogen Lipopolysaccharide: Relevance to the Etiology of Parkinson's Disease. *Journal of Neuroscience* **23**(4): 1228-1236.

Gao H-M, Liu B and Hong J-S (2003b) Critical Role for Microglial NADPH Oxidase in Rotenone-Induced Degeneration of Dopaminergic Neurons. *Journal of Neuroscience* **23**(15): 6181-6187.

Gao H-M, Liu B, Zhang W and Hong J-S (2003c) Critical role of microglial NADPH oxidase-derived free radicals in the in vitro MPTP model of Parkinson's disease. *FASEB Journal* **17**(13): 1954-1956.

Gao H-M, Liu B, Zhang W and Hong J-S (2003d) Synergisitc dopaminergic neurotoxicity of MPTP and inflammogen lipopolysaccharide: relevance to the etiology of Parkinson's disease. *FASEB Journal* **17**: 1957-1959.

Gao H-M, Zhou H, Zhang F, Wilson BC, Kam W and Hong J-S (2011a) HMGB1 Acts on Microglia Mac1 to Mediate Chronic Neuroinflammation That Drives Progressive Neurodegeneration. *Journal of Neuroscience* **31**(3): 1081-1092.

Gao X, Chen H, Schwarzschild MA and Ascherio A (2011b) Use of ibuprofen and risk of Parkinson disease. *Neurology* **76**: 863-869.

Garton KJ, Gough PJ, Blobel CP, Murphy G, Greaves DR, Dempsey PJ and Raines EW (2001) Tumor Necrosis Factor-α-converting Enzyme (ADAM17) Mediates the Cleavage and Shedding of Fractalkine (CX3CL1). *Journal of Biological Chemistry* **276**(41): 37993-38001.

Gebicke-Haerter PJ, Christoffel F, Timmer J, Northoff H, Berger M and van Calker D (1996) Both adenosine A1- and A2-receptors are required to stimulate microglial proliferation. *Neurochem Int* **29**(1): 37-42.

Gehrmann J, Banati RB and Kreutzberg GW (1993) Microglia in the immune surveillance of the brain: Human microglia constitutuvely expres HLA-DR molecules. *Journal of Neuroimmunology* **48**: 189-198.

Gerhard A, Pavese N, Hotton G, Turkheimer F, Es M, Hammers A, Eggert K, Oertel W, Banati RB and Brooks DJ (2006) In vivo imaging of microglial activation with [^{11}C](*R*)-PK11195 PET in idiopathic Parkinson's disease. *Neurobiology of Disease* **21**: 404-412.

German DC, Manaye KF, White III CL, Woodward DJ, McIntire DD, Smith WK, Kalaria RN and Mann DMA (1992) Disease-specific Patterns of Locus Coeruleus Cell Loss. *Ann Neurol* **32**: 667-676.

Ginhoux F, Greter M, Leboeuf M, Nandi S, See P, Gokhan S, Mehler MF, Conway SJ, Ng LG, Stanley ER, Samokhvalov IM and Merad M (2010) Fate Mapping Analysis Reveals That Adult Microglia Derive from Primitive Macrophages. *Science* **330**: 841-845.

Ginhoux F, Lim S, Hoeffel G, Low D and Huber T (2013) Origin and differentiation of microglia. *Frontiers in Cellular Neuroscience* **7**: Article 45: 41-14.

Giulian D and Baker TJ (1986) Characterization of Ameboid Microglia Isolated from Developing Mammalian Brain. *Journal of Neuroscience* **6**(8): 2163-2178.

Giulian D, Baker TJ, Shih L-CN and Lachman LB (1986) Interleukin 1 of the central nervous system is produced by amoeboid microglia. *Journal of Experimental Medicine* **164**: 594-604.

Giulian D, Johnson B, Krebs JF, George JK and Tapscott M (1991) Microglial Mitogens Are Produced in the Developing and Injured Mammalian Brain. *Journal of Cell Biology* **112**(2): 323-333.

Giulian D, Vaca K and Corpuz M (1993) Brain Glia Release Factors with Opposing Actions upon Neuronal Survival. *Journal of Neuroscience* **13**(1): 29-37.

Goddard AW, Ball SG, Martinez J, Robinson MJ, Yang CR, Russell JM and Shekhar A (2010) Current perspectives of the roles of the central norepinephrine system in anxiety and depression. *Depression and Anxiety* **27**: 339-350.

Godoy MCP, Tarelli R, Ferrari CC, Sarchi MI and Pitossi FJ (2008) Central and systemic IL-1 exacerbates neurodegeneration and motor symptoms in a model of Parkinson's disease. *Brain* **131**: 1880-1894.

Gomes CA, Simoes PF, Canas PM, Quiroz C, Sebastiao AM, Ferre S, Cunha RA and Ribeiro JA (2009) GDNF control of the glutamatergic cortico-striatal pathway requires tonic activation of adenosine A_{2A} receptors. *Journal of Neurochemistry* **108**: 1208-1219.

Gomes CA, Vaz SH, Ribeiro JA and Sebastiao AM (2006) Glial cell line-derived neurotrophic factor (GDNF) enhances dopamine release from striatal nerve endings in an adenosine A_{2A} receptor-dependent manner. *Brain Research* **1113**: 129-136.

Goodman Jr OB, Krupnick JG, Santini F, Gurevich VV, Penn RB, Gagnon AW, Keen JH and Benovic JL (1996) β-Arrestin acts as a clathrin adaptor in endocytosis of the β_2-adrenergic receptor. *Nature* **383**: 447-450.

Gordon S (2003) Alternative activation of macrophages. *Nature Reviews Immunology* **3**: 23-35.

Gottschall P, Yu X and Bing B (1995) Increased Production of Gelatinase B (Matrix Metalloproteinase-9) and Interleukin-6 by Activated Rat Microglia in Culture. *Journal of Neuroscience Research* **42**: 335-342.

Grathwohl SA, Kälin RE, Bolmont T, Prokop S, Winkelmann G, Kaeser SA, Odenthal J, Radde R, Eldh T, Gandy S, Aguzzi A, Staufenbiel M, Mathews PM, Wolburg H, Heppner FL and Jucker M (2009) Formation and maintenance of Alzheimer's disease β-amyloid plaques in the absence of microglia. *Nature Neuroscience* **12**(11): 1361-1363.

Greter M and Merad M (2013) Regulation of Microglia Development and Homeostasis. *Glia* **61**: 121-127.

Griciuc A, Serrano-Pozo A, Parrado AR, Lesinski AN, Asselin CN, Mullin K, Hooli B, Choi SH, Hyman BT and Tanzi RE (2013) Alzheimer's Disease Risk Gene *CD33* Inhibits Microglial Uptake of Amyloid Beta. *Neuron* **78**: 631-643.

Group AR (2006) Cardiovascular and Cerebrovascular Events in the Randomized, Controlled Alzheimer's Disease Anti-Inflammatory Prevention Trial (ADAPT). *PLoS Clinical Trials* **1**(7): e33.

Group AR, Lyketsos C, Breitner JC, Green RC, Martin BK, Meinert C, Piantadosi S and Sabbagh M (2007) Naproxen and celecoxib do not prevent AD in early results from a randomized controlled trial. *Neurology* **68**: 1800-1808.

Guerreiro R, Wojtas A, Bras J, Carrasquillo M, Rogaeva E, Majounie E, cruchaga C, Sassi C, Kauwe JSK, Younkin S, Hazrati L, Collinge J, Pocock J, Lashley T, Williams J, Lambert J-C, Amouyel P, Powell J, St. George-Hyslop P, Singleton A and Hardy J (2013) *TREM2* Variants in Alzheimer's Disease. *New England Journal of Medicine* **368**: 117-127.

Gyoneva S, Orr AG and Traynelis SF (2009) Differential regulation of microglial motility by ATP/ADP and adenosine. *Parkinsonism and Related Disorders* **15S3**: S195-S199.

Gyoneva S and Traynelis SF (2013) Norepinephrine Modulates the Motility of Resting and Activated Microglia via Different Adrenergic Receptors. *Journal of Biological Chemistry* **288**(21): 15291-15302.

Haga S, Akai K and Ishii T (1989) Demostration of microglial cells in and around senile (neuritic) plaques in the Alzheimer brain. *Acta Neuropathologica* **77**: 569-575.

Hall A (1998) Rho GTPases and the Actin Cytoskeleton. *Science* **279**: 509-514.

Hamza TH, Zabetian CP, Tenesa A, Laederach A, Montimurro J, Yearout D, Kay DM, Doheny KF, Paschall J, Pugh E, Kusel VI, Collura R, Roberts J, Griffith A, Samii A, Scott WK, Nutt J, Factor SA and Payami H (2010) Common genetic variation in the *HLA* region is associated with late-onset sporadic Parkinson's disease. *Nature Genetics* **42**(9): 781-785.

Hanamsagar R, Hanke ML and Kielian T (2012) Toll-like receptor (TLR) and inflammasome actions in the central nervous system. *Trends in Immunology* **33**(7): 333-342.

Hancock DB, Martin EB, Stajich JM, Jewett R, Stacy MA, Scott BL, Vance JM and Scott WK (2007) Smoking, Caffeine, and Nonsteroidal Anti-inflammatory Drugs in Families With Parkinson Disease. *Archives of Neurology* **64**: 576-580.

Hanisch U-K (2002) Microglia as a Source and Target of Cytokines. *Glia* **40**: 140-155.

Hanisch U-K and Kettenman H (2007) Microglia: active sensors and versatile effector cells in the normal and pathologic brain. *Nature Neuroscience* **10**(11): 1387-1394.

Hanke ML and Kielian T (2011) Toll-like receptors in health and disease in the brain: mechanisms and therapeutic potential. *Clinical Science* **121**: 367-387.

Hansson E and Ronnback L (2004) Astrocytic receptors and second messenger systems. *Advances in Molecular and Cell Biology* **31**: 475-501.

Hardy J and Allsop D (1991) Amyloid deposition as the central event in the aeriology of Alzheimer's disease. *Trends Pharmacol Sci* **12**: 383-388.

Hardy J and Selkoe DJ (2002) The Amyloid Hypothesis of Alzheimer's Disease: progress and Problems on the Road to Therapeutics. *Science* **297**: 353-356.

Harms AS, Barnum CJ, Ruhn KA, Varghese S, Trevino I, Blesch A and Tansey MG (2011) Delayed Dominant-Negative TNF Gene Therapy Halts Progressive Loss of Nigral Dopaminergic Neurons in a Rat Model of Parkinson's Disease. *Molecular Therapy* **19**: 46-52.

Harms AS, Lee J-K, Nguyen TA, Chang J, Ruhn KM, Trevino I and Tansey MG (2012) Regulation of Microglial Effector Functions by Tumor Necrosis Factor Signaling. *Glia* **60**: 189-202.

Harris MA, Tsui JK, Marion SA, Shen H and Teschke K (2012) Association of parkinson's Disease With Infections and Occupational Exposure to Possible Vectors. *Movement Disorders* **27**(9): 1111-1117.

Harrison JK, Jiang Y, Chen S, Xia Y, Maciejewski D, McNamara RK, Streit WJ, Salafranca MN, Adhikari S, Thompson DA, Botti P, Bacon KB and Feng L (1998) Role for neuronally derived fractalkine in mediating interactions between neurons and CX3CR1-expressing microglia. *Proceedings of the National Academy of Sciences of the United States of America* **95**: 10896-10901.

Haskell CA, Cleary MD and Charo IF (1998) Molecular Uncoupling of Fractalkine-mediated Cell Adhesion and Signal Transduction: Rapid Flow Arrest of CX_3CR1-expressing Cells is Independent of G-protein Activation. *Journal of Biological Chemistry* **274**(15): 10053-10058.

Hasko G, Pacher P, Vizi ES and Illes P (2005) Adenosine receptor signaling in the brain immune system. *Trends in Pharmacological Sciences* **26**(10): 511-516.

Hatori K, Nagai A, Heisel R, Ryu JK and Kim SU (2002) Fractalkine and Fractalkine Receptors in Human Neurons and Glial Cells. *Journal of Neuroscience Research* **69**: 418-426.

Hauser RA, Cantillon M, Pourcher E, Micheli F, Mok V, Onofrj M, KHuyck S and Wolski K (2011) Preladenant in patients with Parkinson's disease and motor fluctuations: a phase 2, double blind, randomised trial. *Lancet Neurology* **10**(3): 221-229.

Hayashi M, Luo Y, Laning J, Strieter RM and Dorf ME (1995) Production and function of monocyte chemoattractant protein-1 and other β-chemokines in murine glial cells. *Journal of Neuroimmunology* **60**: 143-150.

Haynes S, Hollopeter G, Yang G, Kurpius D, Dailey ME, Gan W-B and Julius D (2006) The $P2Y_{12}$ receptor regulates microglial activation by extracellular nucleotides. *Nature Neuroscience* **9**(12): 1512-1519.

He Y, Appel S and Le W (2001) Minocycline inhibits microglial activation and protects nigral cells after 6-hydroxydopamine injection into mouse striatum. *Brain Research* **909**: 187-193.

Heese K, Fiebich BL, Bauer J and Otten U (1997) Nerve growth factor (NGF) expression in rat microglia is induced by adenosine A_{2a}-receptors. *Neuroscience Letters* **231**: 83-86.

Heneka MT, Galea E, Gavrilyuk V, Dumitrescu-Ozimek L, Daeschner J, O'Banion MK, Weinberg G, Klockgether T and Feinstein DL (2002) Noradrenergic Depletion Potentiates b-Amyloid-Induced Cortical Inflammation: Implications for Alzheimer's Disease. *J Neurosci* **22**(7): 2434-2442.

Heneka MT, Kummer MP, Stutz A, Delekate A, Schwartz S, Vieira-Saecker A, Griep A, Axt D, Remus A, Tzeng T-C, Gelpi E, Halle A, Korte M, Latz E and Golenbock DT (2013) NLRP3 is activated in Alzheimer's disease and contributes to pathology in APP/PS1 mice. *Nature* **493**: 674-678.

Heneka MT, Nadrigny F, Regen T, Martinez-Hernandez A, Dumitrescu-Ozimek L, Terwel D, Jardanhazi-Kurutz D, Walter J, Kirchhoff F, Hanisch U-K and Kummer MP (2010) Locus ceruleus controls Alzheimer's disease pathology by modulating microglial functions through norepinephrine. *Proc Nat Acad Sci USA* **107**(13): 6058-6063.

Henry V, Paille V, Lelan F, Brachet P and Damier P (2009) Kinetics of Microglial Activation and Degeneration of Dopamine-Containing Neurons in a Rat Model of Parkinson Disease

Induced by 6-Hydroxydopamine. *Journal of Neuropathology and Experimental Neurology* **68**(10): 1092-1102.

Herbomel P, Thisse B and Thisse C (2001) Zebrafish Early Macrophages Colonize Cephalic Mesenchyme and Developing Brain, Retina, and Epidermis through a M-CSF Receptor-Dependent Invasive Process. *Developmental Biology* **238**: 274-288.

Hernan MA, Logroscino G and Rodriguez LAG (2006) Nonsteroidal anti-inflammatory drugs and the incidence of Parkinson disease. *Neurology* **66**: 1097-1099.

Herrera AJ, Castano A, Venero JL, Cano J and Machado A (2000) The Single Intranigral Injection of LPS as a New Model for Studying the Selective Effects of Inflammatory Reactions on Dopaminergic System. *Neurobiology of Disease* **7**: 429-447.

Hickman SE, Allison EK and El Khoury J (2008) Microglial Dysfunction and Defective β-Amyloid Clearance Pathways in Aging Alzheimer's Disease Mice. *Journal of Neuroscience* **28**(33): 8354-8360.

Higley MJ and Sabatini BL (2010) Competitive regulation of synaptic Ca^{2+} influx by D2 dopamine and A2A adenosine receptors. *Nature Neuroscience* **13**(8): 958-966.

Hines DJ, Hines RM, Mulligan SJ and Macvicar BA (2009) Microglia Processes Block the Spread of Damage in the Brain and Require Functional Chloride Channels. *Glia* **57**: 1610-1618.

Hodgson RA, Bertorelli R, Varty GB, Lachowicz JE, Forlani A, Fredduzzi S, Cohen-Williams ME, Higgins GA, Impagnatiello F, Nicolussi E, Parra LE, Foster C, Zhai Y, Neustadt BR, Stamford AW, Parker EM, AReggiani A and Hunter J (2009) Characterization of the Potent and Highly Selective A_{2A} Receptor Antagonists Preladenant and SCH 412348 [7-[2-[4-2,4-Difluorophenyl]-1-piperazinyl]-2-(2-furanyl)-7*H*-pyrazolo[4,3-*e*][1,2,4]triazolo[1,5-*c*]pyrimidin-5-amine] in Rodent Models of Movement Disorders and Depression. *Journal of Pharmacology and Experimental Therapeutics* **330**(1): 294-303.

Hoek RM, Ruuls SR, Murphy CA, Wright GJ, Goddard R, Zurawski SM, Blom B, Homola ME, Streit WJ, Brown MH, Barclay AN and Sedgwick JD (2000) Down-Regulation of the Macrophage Lineage Through Interaction with OX2 (CD200). *Science* **290**: 1768-1771.

Holmes C, Cunningham C, Zotova E, Woolford J, Dean C, Kerr S, Culliford D and Perry VH (2009) Systemic inflammation and disease progression in Alzheimer disease. *Neurology* **73**: 768-774.

Holmes C, El-Okl M, Williams A, Cunningham C, Wilcockson D and Perry VH (2003) Systemic infection, interleukin-1β, and cognitive decline in Alzheimer's disease. *J Neurol Neurosurg Psychiatry* **74**: 788-789.

Honda S, Sasaki Y, Ohsawa K, Imai Y, Nakamura Y, Inoue K and Kohsaka S (2001) Extracellular ATP or ADP Induce Chemotaxis of Cultured Microglia through $G_{i/o}$-Coupled P2Y Receptors. *Journal of Neuroscience* **21**(6): 1975-1982.

Hoskin DW, Butler JJ, Drapeau D, Haeryfar SM and Blay J (2002) Adenosine acts through an A_3 receptor to prevent the induction of murine anti-CD3-activated killer T cells. *Int J Cancer* **99**: 386-395.

Huell M, Strauss S, Volk B, Berger M and Bauer J (1995) Interleukin-6 is present in early stages of plaque formation and is restricted to the brains of Alzheimer's disease patients. *Acta Neuropathologica* **89**: 544-551.

Hughes PM, Botham MS, Frentzel S, Mir A and Perry VH (2002) Expression of Fractalkine (CX3CL1) and Its Receptor, CX3CR1, During Acute and Chronic Inflammation in Rodent CNS. *Glia* **37**: 314-327.

Hutchinson AJ, Webb RL, Oei HH, Ghai GR, Zimmerman MB and Williams M (1989) CGS 21680C, an A2 Selective Adenosine Receptor Agonist with Preferential Hypotensive Activity. *Journal of Pharmacology and Experimental Therapeutics* **251**(1): 47-55.

Ikeda K, Kurokawa M, Aoyama S and Kuwana Y (2002) Neuroprotection by adenosine A_{2A} receptor blockade in experimental models of Parkinson's disease. *Journal of Neurochemistry* **80**: 262-270.

Imai Y, Hieshima K, Haskell C, Baba M, Nagira M, Nishimura M, Kakizaki M, Takagi S, Nomiyama H, Schall TJ and Yoshie O (1997) Identification and Molecular Characterization of Fractalkine Receptor CX_3CR1, which Mediates Both Leukocyte Migration and Adhesion. *Cell* **91**: 521-530.

in't Veld BA, Ruitenberg A, Hofman A, Launer LJ, van Duijn CM, Stijnen T, Breiteler MM and Stricker BH (2001) Nonsteroidal antiinflammatory drugs and the risk of Alzheimer's disease. *New England Journal of Medicine* **345**: 1515-1521.

Iribarren P, Chen K, Gong W, Cho EH, Lockett S, Uranchimeg B and Wang JM (2007) Interleukin 10 and TNFα synergistically enhance the expression of the G protein-coupled formylpeptide receptor 2 in microglia. *Neurobiology of Disease* **27**: 90-98.

Itagaki S, Akiyama H, Saito H and McGeer PL (1994) Ultrastructural localization of complement membrane attack complex (MAC)-like immunoreactivity in brains of patients with Alzheimer's disease. *Brain Research* **645**: 78-84.

Iversen LL, Rossor MN, Reynolds GP, Hills R, Roth M, Mountjoy CQ, Foote SL, Morrison JH and Bloom FE (1983) Loss of pigmented dopamine-b-hydroxylase positive cells from locus coeruleus in senile dementia of Alzheimer's type. *Neurosci Lett* **39**: 95-100.

Jackson-Lewis V and Przedborski S (2007) Protocol for the MPTP mouse model of Parkinson's disease. *Nature Protocols* **2**: 141-151.

Jang H, Boltz D, McClaren J, Pani AK, Smeyne M, Korff A, Webster R and Smeyne RJ (2012) Inflammatory Effects of Highly Pathogenic H5N1 Influenza in the CNS of Mice. *Journal of Neuroscience* **32**(5): 1545-1559.

Jang H, Boltz D, Sturm-Ramirez K, Shepherd KR, Jiao Y, Webster R and Smeyne RJ (2009a) Highly pathogenic H5N1 influenza virus can enter the central nervous system and induce

neuroinflammation and neurodegeneration. *Proceedings of the National Academy of Sciences of the United States of America* **106**(33): 14063-14068.

Jang H, Boltz DA, Webster RG and Smeyne RJ (2009b) Viral parkinsonism. *Biochimica et Biophysica Acta* **1792**: 714-721.

Jardanhazi-Kurutz D, Kummer MP, Terwel D, Vogel K, Thiele A and Heneka MT (2011) Distinct adrenergic system changes and neuroinflammation in response to induced locus ceruleus degeneration in APP/PS1 transgenic mice. *Neuroscience* **176**: 396-407.

Jarvis MF, Schulz R, Hutchinson AJ, Do UH, Sills MA and Williams M (1989) [^{3}H]CGS 21680, A Selective A_2 Adenosine Receptor Agonist Directly Labels A_2 Receptors in Rat Brain. *Journal of Pharmacology and Experimental Therapeutics* **251**(3): 888-893.

Jarvis MF and Williams M (1989) Direct autoradiographic localization of adenosine A_2 receptors in the rat brain using the A_2-selective agonist, [^{3}H]CGS 21680. *European Journal of Pharmacology* **168**: 243-246.

Jonsson T, Stefansson H, Steinberg S, Jonsdottir I, Jonsson PV, Snaedal J, Bjornsson S, Huttenlocker J, Levey AI, Lah JJ, Rujescu D, Hampel H, giegling I, Andreassen OA, Engedal K, Ulstein I, Srjdan D, Ibrahim-Verbaas C, Hofman A, Ikram MA, van Duijn CM, Thorsteinsdottir U, Kong A and Stefansson K (2013) Variant of *TREM2* Associated with the Risk of Alzheimer's Disease. *New England Journal of Medicine* **368**(2): 107-116.

Jucker M and Heppner FL (2008) Cerebral and Peripheral Amyloid Phagocytes - an Old Liason with a New Twist. *Neuron* **59**: 8-10.

Jung S, Aliberti J, Graemmel P, Sunshine MJ, Kreutzberg GW, Sher A and Littman DR (2000) Analysis of Fractalkine Receptor CX_3CR1 Function by Targeted Deletion and Green Fluorescent Protein Reporter Gene Insertion. *Molecular and Cellular Biology* **20**(11): 4106-4114.

Jurgens HA, Amancherla K and Johnson RW (2012) Influenza Infection Induces Neuroinflammation, Alters Hippocampal Neuron Morphology, and Impairs Cognition in Adult Mice. *Journal of Neuroscience* **32**(12): 3958-3968.

Kalaria RN and Harik SI (1989) Increased α_2- and β_2-adrenergic receptors in cerebral microvessels in Alzheimer disease. *Neuroscience Letters* **106**: 233-238.

Kalaria RN and Hedera P (1995) Differential degeneration of the cerebral microvasculature in Alzheimer's disease. *NeuroReport* **6**: 477-480.

Kalda A, Yu L, Oztas E and Chen J-F (2006) Novel neuroprotection by caffeine and adenosine A2A receptor antagonists in animal models of Parkinson's disease. *Journal of Neurological Sciences* **248**: 9-15.

Kanaan NM, Kordower JH and Collier TJ (2008) Age and Region-Specific Responses of Microglia, but not Astrocytes, Suggest a Role in Selective Vulnerability of Dopamine Neurons After 1-Methyl-4-phenyl-1,2,3,6-tetrahydropyridine Exposure in Monkeys. *Glia* **56**: 1199-1214.

Kanda T, Jackson MJ, Smith LA, Pearce RKB, Nakamura J, Kase H, Kuwana Y and Jenner P (1998a) Adenosine A_{2A} Antagonist: A Novel Antiparkinsonian Agent that Does Not Provoke Dyskinesia in Parkinsonian Monkeys. *Annals of Neurology* **43**: 507-513.

Kanda T, Jackson MJ, Smith LA, Pearce RKB, Nakamura J, Kase H, Kuwana Y and Jenner P (2000) Combined Use of the Adenosine A_{2A} Antagonist KW-6002 with $_L$-DOPA or withSelective D1 or D2 Dopamine Agonists Increases Antiparkinsonian Activity but Not Dyskinesia in MPTP-Treated Monkeys. *Experimental Neurology* **162**: 321-327.

Kanda T, Tashiro T, Kuwana Y and Jenner P (1998b) Adenosine A_{2A} receptors modify motor function in MPTP-treated common marmosets. *NeuroReport* **9**: 2857-2860.

Kandasamy K, Joseph K, Subramaniam K, Raymond JR and Tholanikunnel BG (2005) Translational Control of β_2-Adrenergic Receptor mRNA by T-cell-restricted Intracellular Antigen-related Protein. *Journal of Biological Chemistry* **280**(3): 1931-1943.

Katayama T, Kobayashi H, Okamura T, Yamasaki-Katayama Y, Kibayashi T, Kimura H, Ohsawa K, Kohsaka S and Minami M (2012) Accumulating Microglia Phagocytose Injured Neurons in Hippocampas Slice Cultures: Involvement of p38 MAP Kinase. *PloS One* **7**(7): e40813.

Kettenmann H, Kirchhoff F and Verkhratsky A (2013) Microglia: New Roles for the Synaptic Stripper. *Neuron* **77**: 10-18.

Kiefer R, Lindholm D and Kreutzberg GW (1993) Interleukin-6 and Transforming Growth Factor-β1 mRNAs are Induced in Rat Facial Nucleus Following Motoneuron Axotomy. *European Journal of Neuroscience* **5**: 775-781.

Kim K-W, Vallon-Eberhard A, Zigmond E, Farache J, Shezen E, Shakhar G, Ludwig A, Lira SA and Jung S (2011) In vivo structure/function and expression analysis of the CX_3C chemokine fractalkine. *Blood* **118**(22): e156-e167.

Kim SU and de Vellis J (2005) Microglia in Health and Disease. *J Neurosci Res* **81**: 302-313.

Kim W-G, Mohney RP, Wilson B, Jeohn G-H, Liu B and Hong J-S (2000) Regional Difference in Susceptibility to Lipopolysaccharide-Induced Neurotoxicity in the Rat Brain: Role of Microglia. *Journal of Neuroscience* **20**(16): 6309-6319.

Kish SJ, Shannak K and Hornykiewicz O (1988) Uneven pattern of dopamine loss in the striatum of patients with idiopathic Parkinson's disease. *New England Journal of Medicine* **318**: 876-880.

Kitazawa M, Oddo S, Yamasaki TR, Green KN and LaFerla FM (2005) Lipopolysaccharide-Induced Inflammation Exacerbates Tau Pathology by a Cyclin-Dependent Kinase 5-Mediated Pathway in a Transgenic Model of Alzheimer's Disease. *Journal of Neuroscience* **25**(39): 8843-8853.

Kiyota T, Yamamoto M, Xiong H, Lambert MP, Klein WL, Gendelman HE, Ransohoff RM and Ikezu T (2009) CCL2 Accelerates Microglia-Mediated Aβ Oligomer Formation and Progression of Neurocognitive Dysfunction. *PLoS One* **4**(7): e6197.

Klotz K-N (2000) Adenosine receptors and their ligands. *Naunyn-Schmiedeberg's Archives of Pharmacology* **362**: 382-391.

Klotz K-N, Hessling J, Hegler J, Owmn C, Kull B, Fredholm BB and Lohse MJ (1998) Comparative pharmacology of human adenosine receptor subtypes - characterization of stably transfected receptors in CHO cells. *Naunyn-Schmiedeberg's Archives of Pharmacology* **357**: 1-9.

Kohutnicka M, Lewandowska E, Kurkowska-Jastrzebska I, Czlonkowska A and Czlonkowski A (1998) Microglial and astrocytic involvement in a murine model of Parkinson's disease induced by 1-methyl-4-phenyl-1,2,3,6-tetrahydropyridine (MPTP). *Immunopharmacology* **39**: 167-180.

Kong Y, Ruan L, Qian L, Liu X and Le Y (2010) Norepinephrine Promotes Microglia to Uptake and Degrade Amyloid b Peptide through Upregulation of Mouse Formyl Peptide Receptor 2 and Induction of Insulin-Degrading Enzyme. *J Neurosci* **30**(35): 11848-11857.

Koning N, Swaab DF, Hoek RM and Huitinga I (2009) Distribution of the Immune Inhibitory Molecules CD200 and CD200R in the Normal Central Nervous System and Multiple Sclerosis Lesions Suggests Neuron-Glia and Glia-Glia Interactions. *Journal of Neuropathology and Experimental Neurology* **68**(2): 159-167.

Kook S-Y, Hong HS, Moon M, Ha CM, Chang S and Mook-Jung I (2012) $A\beta_{1-42}$-RAGE Interaction Disrupts Tight Junctions of the Blood-Brain Barrier Via Ca^{2+}-Calcineurin Signaling. *Journal of Neuroscience* **32**(26): 8845-8854.

Krabbe G, Halle A, Matyash V, Rinnenthal JL, Eom GD, Berngardt U, Miller KR, Prokop S, Kettenman H and Heppner FL (2013) Functional Impairment of Microglia Coincides with Beta-Amyloid Deposition in Mice with Alzheimer-Like Pathology. *PloS One* **8**(4): e60921.

Krabbe G, Matyash V, Pannasch U, Mamer L, Boddeke HWGM and Kettenmann H (2012) Activation of serotonin receptors promotes microglial injury-induced motility but attenuates phagocytic activity. *Brain Behav Immun* **26**: 419-428.

Kreutzberg GW (1996) Microglia: a sensor for pathological events in the CNS. *Trends in Neurosciences* **19**: 312-318.

Kurkowska-Jastrzebska I, Wronska A, Kohutnicka M, Czlonkowski A and Czlonkowska A (1999) The Inflammatory Reaction Following 1-Methyl-4-phenyl-1,2,3,6-tetrahydropyridine Intoxication in Mouse. *Experimental Neurology* **156**: 50-61.

Kurpius D, Nolley EP and Dailey ME (2007) Purines Induce Directed Migration and Rapid Homing of Microglia to Injured Pyramidal Neurons in Developing Hippocampus. *Glia* **55**: 873-884.

Küst BM, Biber K, Van Calker D and Gebicke-Haerter PJ (1999) Regulation of K^+ Channel mRNA Expression by Stimulation of Adenosine A_{2a}-Receptors in Cultured Rat Microglia. *Glia* **25**: 120-130.

Kvetnansky R, Sabban EL and Palkovits M (2009) Catecholaminergic Systems in Stress: Structural and Molecular Genetic Approaches. *Physiol Rev* **89**: 535-606.

Lambert C, Ase AR, Seguela P and Antel JP (2010) Distinct migratory and cytokine responses of human microglia and macrophages to ATP. *Brain, Behavior, and Immunity* **24**: 1241-1248.

Lambert J-C, Heath S, Even G, Campion D, Sleegers K, Hiltunen M, Combarros O, Zelenika D, Bullido M, Tavernier B, Letenneur L, Bettens K, Berr C, Pasquier F, Fievet M, Barberger-Gatau P, Engelborghs S, De Deyn P, Mateo I, Franck A, Helisalmi S, Porcellini E, Hanon O, Investigators EAsDI, de Pancorbo MM, Lendon C, Dufouil C, Jaillard C, Leveillard T, Alvarez V, Bosco P, Mancuso M, Panza F, Nacmias B, Bossu P, Piccardi P, Annoni G, Seripa D, Galimberti D, Hannequin D, Licastro F, Soininen H, Ritchie K, Blanche H, Dartigues J-F, Tzourio C, Gut I, Van Broeckhoven C, Alperovitch

A, Lathrop M and Amouyel P (2009) Genome-wide association study identifies variants at *CLU* and *CR1* associated with Alzheimer's disease. *Nature Genetics* **41**(10): 1094-1099.

Lampron A, ElAli A and Rivest S (2013) Innate Immunity in the CNS: Redefining the Relationship between the CNS and Its Environment. *Neuron* **78**: 214-232.

Langston J, Forno L, Tetrud J, Reeves A, Kaplan J and Karluk D (1999) Evidence of Active Nerve Cell Degeneration in the Substantia Nigra of Humans Years after 1-Methyl-4-Phenyl-1,2,3,6-Tetrahydropyridine Exposure. *Annals of Neurology* **46**: 598-605.

Lawson L, Perry V, Dri P and Gordon S (1990) Heterogeneity in the distribution and morphology of microglia in the normal adult mouse brain. *Neuroscience* **39**: 151-170.

Lawson L, Perry VH and Gordon S (1992) Turnover of resident microglia in the normal adult mouse brain. *Neuroscience* **48**(2): 405-415.

Le Y, Gong W, Tiffany HL, Tumarov A, Nedospasov S, Shen W, Dunlop NM, Gao J-L, Murphy PM, Oppenheim JJ and Wang JM (2001) Amyoid β_{42} Activates a G-Protein-Coupled Chemoattractant Receptor, FPR-Like-1. *The Journal of Neuroscience* **21**(RC123): 1-5.

Lee CJ, Mannaioni G, Yuan H, Woo DH, Gingrich MB and Traynelis SF (2007) Astrocytic control of synaptic NMDA receptors. *J Physiol* **581**: 1057-1081.

Lee S-H, Hollingsworth R, Kwon H-Y, Lee N and Chung CY (2012) β-Arrestin 2-Dependent Activation of ERK1/2 is Required for ADP-Induced Paxillin Phosphorylation at Ser^{83} and Microglia Chemotaxis. *Glia* **60**: 1366-1377.

Lee S, Varvel NH, Konerth ME, Xu G, Cardona AE, Ransohoff RM and Lamb BT (2010) CX3CR1 Defficiency Alters Microglial Activation and Reduces Beta-Amyloid Deposition in Two Alzheimer's Disease Mouse Models. *American Journal of Pathology* **177**(5): 2549-2562.

Lee SC, Liu W, Dickson DW, Brosnan CF and Berman JW (1993) Cytokine Production by Human Fetal Microglia and Astrocytes: Differential Induction by Lopipolysaccharide and IL-1β. *Journal of Immunology* **150**(7): 2659-2667.

Leverenz JB, Miller MA, Dobie DJ, Peskind ER and Raskind MA (2001) Increased alpha 2-adrenergic receptor binding in locus coeruleus projection areas in dementia with Lewy bodies. *Neurobiol Aging* **22**: 555-561.

Li D, D'Angelo L, Chavez M and Woulfe DS (2011) Arrestin-2 Differentially Regulates PAR4 and ADP Receptor Signaling in Platelets. *J Biol Chem* **286**(5): 3805-3814.

Li Y, Du X-f, Liu C-s, Wen Z-l and Du J-l (2012) Reciprocal Regulation between Resting Microglial Dynamics and neuronal Activity In Vivo. *Developmental Cell* **23**: 1189-1202.

Liu B, Du L and Hong J-S (2000) Naloxone Protects Rat Dopaminergic Neurons against Inflammatory Damage through Inhibition of Microglia Activation and Superoxide Generation. *Journal of Pharmacology and Experimental Therapeutics* **293**(2): 607-617.

Liu Y, Hao W, Letiembre M, Walter S, Kulanga M, Neumann H and Fassbender K (2006) Suppression of Microglial Inflammatory Activity by Myelin Phagocytosis: Role of p47-PHOX-Mediated Generation of Reactive Oxygen Species. *Journal of Neuroscience* **26**(50): 12904-12913.

Livak KJ and Schmittgen TD (2001) Analysis of Relative Gene Expression Data Using Real-Time Quantitative PCR and the $2^{-\Delta\Delta CT}$ Method. *Methods* **25**: 402-408.

Loane DJ and Byrnes KR (2010) Role of Microglia in Neurotrauma. *Neurotherapeutics* **7**: 366-377.

Lohse MJ (1993) Molecular mechanisms of membrane receptor desensitization. *Biochim Biophys Acta* **1179**: 171-188.

Long-Smith CM, Sullivan AM and Nolan YM (2009) The influence of microglia on the pathogenesis of Parkinson's disease. *Progress in Neurobiology* **89**: 277-287.

Lucin KM and Wyss-Coray T (2009) Immune Activation in Brain Aging and Neurodegeneration: Too Much or Too Little? *Neuron* **64**: 110-120.

Luo L (2000) Rho GTPases in neuronal morphogenesis. *Nature Reviews Neuroscience* **1**: 173-180.

Maciejewski-Lenoir D, Chen S, Feng L, Maki R and Bacon KB (1999) Characterization of Fractalkine in Rat Brain Cells: Migratory and Activation Signals for CX_3CR-1-Expressing Microglia. *Journal of Immunology* **163**: 1628-1635.

Mackenzie IR, Hao C and Munoz DG (1995) Role of Microglia in Senile Plaque Formation. *Neurobiology of Aging* **16**(5): 797-804.

Magnus T, Chan A, Grauer O, Toyka KV and Gold R (2001) Microglial Phagocytosis of Apoptotic Inflammatory T Cells Leads to Down-Regulation of Microglial Immune Activation. *Journal of Immunology* **167**: 5004-5010.

Malm TM, Koistinaho MK, Parepalo M, Vatanen T, Ooka A, Karlsson S and Koistinaho J (2005) Bone-marrow-derived cells contribute to the recruitment of microglial cells in resposne to β-amyloid deposition in APP/PS1 double transgenic Alzheimer mice. *Neurobiology of Disease* **18**: 134-142.

Mandrekar-Colucci S, Karlo JC and Landreth GE (2012) Mechanisms Underlying the Rapid Peroxisome Proliferator-Activated Receptor-γ-Mediated Amyloid Clearance and Reversal of Cognitive Deficits in a Murine Model of Alzheimer's Disease. *Journal of Neuroscience* **32**(30): 10117-10128.

Mann DMA, Lincoln J, Yates PO, Stamp JE and Toper S (1980) Changes in the Monoamine Containing Neurones of the Human CNS in Senile Dementia. *Brit J Psychiat* **136**: 533-541.

Marik C, Felts PA, Bauer J, Lassmann H and Smith KJ (2007) Lesion genesis in a subset of patients with multiple sclerosis: a role for innate immunity? *Brain* **130**: 2800-2815.

Marin-Teva JL, Dusart I, Colin C, Gervais A, van Rooijen N and Mallat M (2004) Microglia Promote the Death of Developing Purkinje Cells. *Neuron* **41**: 535-547.

Martinez-Mir M, Probst A and Palacios J (1991) Adenosine A2 receptors: Selective localization in the human basal ganglia and alterations with disease. *Neuroscience* **42**(3): 697-706.

Mata IF, Yarout D, Alvarez V, Coto E, de Mena L, Ribacoba R, Lorenzo-Betancor O, Samaranch L, Pastor P, Cervantes S, Infante J, Garcia-Gorostiaga I, Sierra M, Combarros O, Snapinn KW, Edwards KL and Zabetian CP (2011) Replication of *MAPT* and *SNCA*, but not *PARK16-18*, as Susceptibility Genes for Parkinson's Disease. *Movement Disorders* **26**(5): 819-823.

McCall S, Henry JM, Reid AH and Taubenberger JK (2001) Influenza RNA not Detected in Archival Brain Tissues from Acute Encephalitis Lathargica Cases or in Postencephalitic Parkinson Cases. *Journal of Neuropathology and Experimental Neurology* **60**(7): 696-704.

McCall S, Vilensky JA, Gilman S and Taubenberger JK (2008) The relationship between encephalitis lethargica and influenza: A critical analysis. *Journal of NeuroVirology* **14**: 177-185.

McCoy MK, Martinez TN, Ruhn KA, Szymkowski DE, Smith CG, Botterman BR, Tansey KE and Tansey MG (2006) Blocking Soluble Tumor Necrosis Factor Signaling with Dominant-Negative Tumor Necrosis Factor Inhibitor Attenuates Loss of Dopaminergic Neurons in Models of Parkinson's Disease. *Journal of Neuroscience* **26**: 9365-9375.

McCoy MK, Ruhn KA, Martinez TN, McAlpine FE, Blesch A and Tansey MG (2008) Intranigral Lentiviral Delivery of Dominant-negative TNF Attenuates Neurodegeneration and Behavioral Deficits in Hemiparkinsonian rats. *Molecular Therapy* **16**: 1572-1579.

McGeer P, Otagaki S, Boyes B and McGeer E (1988a) Reactive microglia are positive for HLA-DR in the substantia nigra of Parkinson's and Alzheimer's disease brains. *Neurology* **38**: 1285-1291.

McGeer PL, Akiyama H, Itagaki S and McGeer EG (1989) Activation of the classical complement pathway in brain tisse of Alzheimer patients. *Neuroscience Letters* **107**: 341-346.

McGeer PL, Itagaki S, Akiyama H and McGeer EG (1988b) Rate of Cell Death in Parkinsonims Indicates Active Neuropathological Process. *Annals of Neurology* **24**: 574-576.

McGeer PL, Itagaki S, Hisao T and McGeer EG (1987) Reactive microglia in patients with senile dementia of the Alzheimer type are positive for the histocompatibility glycoprotein HLA-DR. *Neuroscience Letters* **79**: 195-200.

McGeer PL, Schulzer M and McGeer EG (1996) Arthritis and anti-inflammatory agents as possible protective factors for Alzheimer's disease: A review of 17 epidemiological studies. *Neurology* **47**: 425-432.

McGeer PL, Schwab C, Parent A and Doudet D (2003) Presence of Reactive Microglia in Monkey Substantia Nigra Years after 1-Methyl-4-Phenyl-1,2,3,6-Tetrahydropyridine Administration. *Annals of Neurology* **54**: 599-604.

Meuth SG, Simon OJ, Grimm A, Melzer N, Herrmann AM, Spitzer P, Landgraf P and Wiendl H (2008) CNS inflammation and neuronal degeneration is aggravated by impaired CD200-CD200R-mediated macrophage silencing. *Journal of Neuroimmunology* **194**: 62-69.

Mildner A, Schlevogt B, Kierdorf K, Böttcher C, Erny D, Kummar MP, Quinn M, Brück W, Beckmann I, Heneka MT, Priller J and Prinz M (2011) Distinct and Non-Redundant Roles of Microglia and Myeloid Subsets in Mouse Models of Alzheimer's Disease. *Journal of Neuroscience* **31**(31): 11159-11171.

Mildner A, Schmidt H, Nitsche M, Merkler D, Hanisch U-K, Mack M, Heikenwalder M, Brück W, Priller J and Prinz M (2007) Microglia in the adult brain arise from Ly-6C^{hi}CCR2^{+} monocytes only under defined host conditions. *Nature Neuroscience* **10**(12): 1544-1553.

Mogi M, Harada M, Kondo T, Riederer P, Inagaki H, Minami M and Nagatsu T (1994) Interleukin-1β, interleukin-6, epidermal growth factor and transforming growth factor-α are elevated in the brain from parkinsonian patients. *Neuroscience Letters* **180**: 147-150.

Möller T, Kann O, Verkhratsky A and Kettenman H (2000) Activation of mouse microglial cells affects P2 receptor signaling. *Brain Research* **853**: 49-59.

Moore S and Thanos S (1996) The concept of microglia in relation to central nervous system disease and regeneration. *Progress in Neurobiology* **48**: 441-460.

Morelli M, Carta AR, Kachroo A and Schwarzschild MA (2010) Pathophysiological roles for purines: adenosine, caffeine and urate. *Progress in Brain Research* **183**: 183-208.

Morgan SC, Taylor DL and Pocock JM (2004) Microglia release activators of neuronal proliferation mediated by activation of mitogen-activated protein kinase, phosphatidylinositol-3-kinase/Akt and delta-Notch signalling cascades. *Journal of Neurochemistry* **90**: 89-101.

Mori I, Imai Y, Kohsaka S and Kimura Y (2000) Upregulated Expression of iba1 Molecules in the Central Nervous System of Mice in Response to Neurovirulent Influenza A Virus Infection. *Microbiol Immunol* **44**(8): 729-735.

Mori K, Ozaki E, Zhang B, Yang L, Yokoyama A, Takeda I, Maeda N, Sakanaka M and Tanaka J (2002) Effects of norepinephrine on rat cultured microglial cells that express α1, α2, β1 and β2 adrenergic receptors. *Neuropharmacology* **43**: 1026-1034.

Morioka N, Tanabe H, Inoue A, Dohi T and Nakata Y (2009) Noradrenaline reduces the ATP-stimulated phosphorylation of p38 MAP kinase via β-adrenergic receptors-cAMP-protein kinase A-dependent mechanisms in cultured rat spinal microglia. *Neurochem Int* **55**: 226-234.

Murphree LJ, Sullivan GW, Marshall MA and Linden J (2005) Lipopolysaccharide rapidly modifies adenosine receptor transcripts in murine and human macrophages: role of NF-κB in A_{2A} adenosine receptor induction. *Biochemical Journal* **391**(575-580): 575.

Murta V and Ferrari CC (2013) Influence of Peripheral inflammation on the progression of multiple sclerosis: Evidence from the clinic and experimental animal models. *Molecular and Cellular Neuroscience* **53**: 6-13.

Nalls MA, Plagnol V, Hernandez DG, Sharma M, Sheerin U-M, Saad M, Simon-Sanchez J, Schulte C, Lesage S, Sweindjörnsdottir S, Stefansson K, Martinez M, Hardy J, Heutink P, Brice A, Gasser T, Singleton AB and Wood NW (2011) Imputation of sequence variants for identification of genetic risks for Parkinson's disease: a meta-analysis of genome-wide association studies. *Lancet* **377**: 641-649.

Napoli I and Neumann H (2009) Microglial clearance functions in health and disease. *Neuroscience* **158**: 1030-1038.

Neher JJ, Neniskyte U, Zhao J-W, Bal-Price A, Tolkovsky AM and Brown GC (2011) Inhibition of Microglial Phagocytosis Is Sufficient To Prevent Inflammatory Neuronal Death. *Journal of Immunology* **186**: 4973-4983.

Neniskyte U, Neher JJ and Brown GC (2011) Neuronal Death Induced by Nanomolar Amyloid β Is mediated by Primary Phagocytosis of Neurons by Microglia. *Journal of Biological Chemistry* **286**(46): 39904-39913.

Neustadt BR, Hao J, Lindo N, Greenlee WJ, Stamford AW, Tulshian D, Ongini E, Hunter J, Monopoli A, Bertorelli R, Foster C, Arik L, Lachowicz J, Ng K and Feng K-I (2007) Potent, selective, and orally active adenosine A_{2A} receptor antagonists: Arylpiperazine derivatives of pyrazolo[4,3-*e*]-1,2,4-triazolo[1,5-*c*]pyrimidines. *Bioorganic & Medicinal Chemistry Letters* **17**(5): 1376-1380.

Nimmerjahn A, Kirchhoff F and Helmchen F (2005) Resting Microglial Cells Are Highly Dynamic Surveillants of Brain Parenchyma in Vivo. *Science* **308**: 1314-1318.

Nolte C, Kirchhoff F and Kettenman H (1997) Epidermal Growth Factor is a Motility Factor for Microglial Cells In Vitro: Evidence for EGF Receptor Expression. *European Journal of Neuroscience* **9**: 1690-1698.

Nolte C, Moller T, Walter T and Kettenman H (1996) Complement 5a controls motility of murine microglial cells *in vitro* via activation of an inhibitory G-protein and the rearrangement of the actin cytoskeleton. *Neuroscience* **73**(4): 1091-1107.

Ogden KK and Traynelis SF (2013) Contribution of the M1 Transmembrane Helix and Pre-M1 Region to Positive Allosteric Modulation and Gating of *N*-Methyl-D-Aspartate Receptors. *Molecular Pharmacology* **83**: 1045-1056.

Ohgami T, Kitamoto T, Shin R-W, Kaneko Y, Ogomori K and Tateishi J (1991) Increased senile plaques without microglia in Alzheimer's disease. *Acta Neuropathologica* **81**: 242-247.

Ohsawa K, Sanagi T, Nakamura Y, Suzuki E, Inoue K and Kohsaka S (2012) Adenosine A3 receptor is involved in ADP-induced microglial process extension and migration. *Journal of Neurochemistry* **121**: 217-227.

Ongini E, Dionisotti S, Gessi S, Irenius E and Fredholm BB (1999) Comparison of CGS 15943, ZM 241385 and SCH 58261 as antagonists at human adenosine receptors. *Naunyn-Schmiedeberg's Archives of Pharmacology* **359**: 7-10.

Orr AG, Orr AL, Li X-J, Gross RE and Traynelis SF (2009) Adenosine A_{2A} receptor mediates microglial process retraction. *Nature Neuroscience* **12**: 872-878.

Pakkenberg B, Møller A, Gundersen H, Mouritzen Dam A and Pakkenberg H (1991) The absolute number of nerve cells in substantia nigra in normal subjects and in patients with Parkinson's disease estimated with an unbiased stereological method. *Journal of Neurology, Neurosurgery and Psychiatry* **54**: 30-33.

Paolicelli RC, Bolasco G, Pagani F, Maggi L, Scianni M, Panzanelli P, Giustetto M, Ferreira TA, Guiducci E, Dumas L, Ragozzino D and Gross CT (2011) Synaptic Pruning by Microglia Is Necessary for Normal Brain Development. *Science* **333**: 1456-1458.

Parkinson FE and Fredholm BB (1990) Autoradiographic evidence for G-protein coupled A_2-receptors in rat neostriatum using [^{3}H]-CGS 21680 as a ligand. *Naunyn-Schmiedeberg's Archives of Pharmacology* **342**: 85-89.

Paspalas CD and Papadopolous DC (1998) Ultrastructural Evidence for Combined Action of Noradrenaline and Vasoactive Intestinal Polypeptide Upon Neurons, Astrocytes, and Blood Vessels of the Rat Cerebral Cortex. *Brain Res Bull* **45**(3): 247-259.

Pedata F, Corsi C, Melani A, Bordoni F and Latini S (2001) Adenosine Extracellular Brain Concentrations and Role of A_{2A} Receptor in Ischemia. *Annals New York Academy of Sciences* **939**: 74-84.

Perea G, Navarrete M and Araque A (2009) Tripartite synapses: astrocytes process and control synaptic information. *Trends in Neurosciences* **32**(8): 421-431.

Perlmutter L, Scott S, Barron E and Chui H (1992) HMC Class II-Positive Microglia in Human Brains: Association with Alzheimer Lesions. *Journal of Neuroscience Research* **33**: 549-558.

Perry VH, Cunningham C and Holmes C (2007) Systemic infections and inflamamtion affect chronic neurodegeneration. *Nature Reviews Immunology* **7**: 161-167.

Perry VH and Gordon S (1988) Macrophages and microglia in the nervous system. *Trends in Neurosciences* **11**(6): 273-277.

Perry VH, Hume D and Gordon S (1985) Immunohistochemical localization of macrophages and microglia in the adult and developing mouse brain. *Neuroscience* **15**(2): 313-326.

Perry VH, Newman TA and Cunningham C (2003) The impact of systemic infection on the progression of neurodegenerative disease. *Nature Reviews Neuroscience* **4**: 103-112.

Perry VH, Nicoll JA and Holmes C (2010) Microglia in neurodegenerative disease. *Nature Reviews Neurology* **6**: 193-201.

Peterfreund RA, MacCollins M, Gusella JF and Fink S (1996) Characterization and Expression of the Human A2a Adenosine Receptor Gene. *Journal of Neurochemistry* **66**: 362-368.

Petersen MA and Dailey ME (2004) Diverse Microglial Motility Behaviors During Clearance of Dead Cells in Hippocampal Slices. *Glia* **46**: 195-206.

Phillis JW (1995) The effects of selective A_1 and A_{2a} adenosine receptor antagonists on cerebral ischemic injury in the gerbil. *Brain Research* **705**: 79-84.

Pierce KL, Premont RT and Lefkowitz RJ (2002) Seven-transmembrane receptors. *Nat Rev Mol Cell Biol* **3**: 639-650.

Pihlstrom L, Axelsson G, Bjornara KA, Dizdar N, Fardell C, Forsgren L, Holmberg B, Larsen JP, Linder J, Nissbrandt H, Tysnes O-B, Ohman E, Dietrichs E and Toft M (2013) Supportive evidence for 11 loci from genome-wide association studies in Parkinson's disease. *Neurobiology of Aging* **34**: 1708.e1707-1708.e1713.

Pinna A, Fenu S and Morelli M (2001) Motor Stimulant Effects of the Adenosine A_{2A} Receptor Antagonist SCH 58261 Do Not Develop Tolerance After Repeated Treatments in 6-Hydroxydopamine-Lesioned Rats. *Synapse* **39**: 233-238.

Pocock JM and Kettenmann H (2007) Neurotransmitter receptors on microglia. *Trends Neurosci* **30**(10): 527-535.

Polazzi E, Altamira LEP, Eleuteri S, Barbaro R, Casadio C, Contestabile A and Monti B (2009) Neuroprotection of microglial conditioned medium on 6-hydroxydopamine-induced neuronal death: role of transforming growth factor beta-2. *Journal of Neurochemistry* **110**: 545-556.

Pollack AE, Harrison MB, Wooten GF and Fink JS (1993) Differential localization of A2a adenosine receptor mRNA with D1 and D2 dopamine receptor mRNA in striatal output pathways following a selective lesion of striatonigral neurons. *Brain Research* **631**: 161-166.

Popoli P, Blum D, Martire A, Ledent C, Ceruti S and Abbracchio MP (2007) Functions, dysfunctions and possible therapeutic relevance of adenosine A_{2A} receptors in Huntigton's disease. *Progress in Neurobiology* **81**: 331-348.

Powers KM, Kay DM, Factor SA, Zabetian CP, Higgins DS, Samii A, Nutt JG, Griffith A, Leis B, Roberts JW, Martinez ED, Montimurro JS, Checkoway H and Payami H (2008) Combined Effects of Smoking, Coffee, and NSAIDs on Parkinson's Disease Risk. *Movement Disorders* **23**(1): 88-95.

Priller J, Flügel A, Wehner T, Boentert M, Haas CA, Prinz M, Fernandez-Klett F, Prass K, Bechmann I, de Boer BA, Frotscher M, Kreutzberg GW, Persons DA and Dirnagl U (2001) Targeting gene-modified hematopoietic cells to the central nervous system: Use of green fluorescent protein uncovers microglial engraftment. *Nature Medicine* **7**(12): 1356-1361.

Prinz M and Hanisch U-K (1999) Murine Microglial Cells Produce and Respond to Interleukin-18. *Journal of Neurochemistry* **72**: 2215-2218.

Puschmann A, Verbeeck C, Heckman MC, Soto-Ortolaza AI, Lynch T, Jasinska-Myga B, Opala C, Krygowska-Wajs A, Barcikowska M, Uitti RJ, Wszolek ZK and Ross OA (2011) Human leukocyte antigen variation and Parkinson's disease. *Parkinsonism and Related Disorders* **17**: 376-378.

Qin L, Liu Y, Wang T, Wei S-J, Block ML, Wilson B, Liu B and Hong J-S (2004) NADPH Oxidase Mediates Lipopolysaccharide-induced Neurotoxicity and Proinflammatory Gene Expression in Activated Microglia. *Journal of Biological Chemistry* **279**: 1415-1421.

Qin L, Wu X, CBlock ML, Liu Y, Breese GR, Hong J-S, Knapp DJ and Crews FT (2007) Systemic LPS Causes Chronic Neuroinflammation and Progressive Neurodegenration. *Glia* **55**: 453-462.

Ransohoff RM (2009) Chemokines and Chemokine Receptors: Standing at the Crossroads of Immunology and Neurobiology. *Immunity* **31**: 711-721.

Ransohoff RM and Perry VH (2009) Microglial Physiology: Unique Stimuli, Specialized Responses. *Annual Reviews of Immunology* **27**: 119-145.

Ravenholt R and Foege WH (1982) 1918 influenza, encephalitis lethargica, parkinsonism. *Lancet*: 860-864.

Reed-Geaghan EG, Savage JC, Hise AG and Landreth GE (2009) CD14 and Toll-Like Receptors 2 and 4 Are Required for Fibrillar Aβ-Stimulated Microglial Activation. *Journal of Neuroscience* **29**(38): 11982-11992.

Reid AH, McCall S, Henry JM and Taubenberger JK (2001) Experimenting on the Past: The Enigma of von Economo's Encephalitis Lethargica. *Journal of Neuropathology and Experimental Neurology* **60**(7): 663-670.

Rinne J (1991) Nigral degeneration in Parkinson's disease in relation to clinical features. *Acta Neurol Scand* **84**(S136): 87-90.

Robinson SR, Bishop GM, Lee H-g and Münch G (2004) Lessons from the AN 1792 Alzheimer vaccine: lest we forget. *Neurobiology of Aging* **25**: 609-615.

Rogers J, Luber-Narod J, Styren SD and Civin WH (1988) Expression of Immune System-Associated Antigens by Cells of the Human Central Nervous System: Relationship to the Pathology of Alzheimer's Disease. *Neurobiology of Aging* **9**: 339-349.

Rogers JT, Morganti JM, Bachstetter AD, Hudson CE, Peters MM, Grimmig BA, Weeber EJ, Bickford PC and Gemma C (2011) CX3CR1 Deficiency Leads to Impairment of Hippocampal Cognitive Function and Synaptic Plasticity. *Journal of Neuroscience* **31**(45): 16241-16250.

Rohn TT and Catlin LW (2011) Immunolocalization of Influenza A Virus and markers of Inflamamtion in the Human Parkinson's Disease Brain. *PloS One* **6**(5): e20495.

Rommelfanger KS, Edwards GL, Freeman KG, Liles LC, Miller GW and Weinshenker D (2007) Norepinephrine loss produces more profound motor deficits than MPTP treatment in mice. *Proc Nat Acad Sci USA* **104**(34): 13804-13809.

Rommelfanger KS and Weinshenker D (2007) Norepinephrine: The redheaded stepchild of Parkinson's disease. *Biochem Pharmacol* **74**: 177-190.

Rommelfanger KS, Weinshenker D and Miller GW (2004) Reduced MPTP toxicity in noradrenergic transporter knockout mice. *J Neurochem* **91**: 1116-1124.

Rosin DL, Robeva A, Woodward RL, Guyenet PG and Linden J (1998) Immunohistochemical Localization of Adenosine A_{2A} Receptors in the Rat Central Nervous System. *Journal of Comparative Neurology* **401**: 163-186.

Ross GW, Abbott RD, Petrovich H, Morens DM, Grandinetti A, Tung K-H, Tanner CM, Masaki KH, Blanchette PL, Curb JD, Popper JS and White LR (2000) Association of Coffee and Caffeine Intake with the Risk of Parkinson Disease. *JAMA* **283**(20): 2674-2679.

Saiki M, Baker A, Williams-Gray CH, Foltynie T, Goodman RS, Taylor CJ, Compston DAS, Barker RA, Sawcer SJ and Goris A (2010) Association of the human leukocyte antigen region with susceptibility to Parkinson's disease. *J Neurol Neurosurg Psychiatry* **81**: 890-891.

Samii A, Etminan M, Wiens MO and Jafari S (2009) NSAID Use and the Risk of Parkinson's Disease. *Drugs Aging* **26**(9): 769-779.

Sara SJ and Bouret S (2012) Orienting and Reorienting: The Locus Coeruleus Mediates Cognition through Arousal. *Neuron* **76**: 130-141.

Sasaki A, Yamagushi H, Ogawa A, Sugihara S and Nakazato Y (1997) Microglial activation in early stages of amyloid β protein deposition. *Acta Neuropathologica* **94**: 316-322.

Saura J, Angulo E, Ejarque A, Casado V, Tusell JM, Moratalla R, Chen J-F, Schwarzschild MA, Liuis C, Fransco R and Serratosa J (2005) Adenosine A_{2A} receptor stimulation potentiates nitric oxide release by activated microglia. *Journal of Neurochemistry* **95**: 919-929.

Savi P, Labouret C, Delesque N, Guette F, Lupker J and Herbert J (2001) $P2Y_{12}$, a New Platelet ADP Receptor, Target of Clopidogrel. *Biochemical and Biophysical Research Communications* **283**: 379-383.

Sawada M, Kondo H, Suzumura A and Marunouchi T (1989) Production of tumor nectosis factor-alpha by microglia and astrocytes in culture. *Brain Research* **491**: 394-397.

Scalzo P, Kümmer A, Cardoso F and Teixeira AL (2010) Serum levels of interleukin-6 are elevated in patients with Parkinson's disease and correlate with physical performance. *Neuroscience Letters* **468**: 56-58.

Schafer DP, Lehrman EK, Kautzman AG, Koyama R, Mardinly AR, Yamasaki R, Ransohoff RM, Greenberg ME, Barres BA and Stevens B (2012) Microglia Sculpt Postnatal Neural Circuits in an Activity and Complement-Dependent Manner. *Neuron* **74**: 691-705.

Schafer DP, Lehrman EK and Stevens B (2013) The "Quad-Partite" Synapse: Microglia-Synapse Interactions in the Developing and Mature CNS. *Glia* **61**: 24-36.

Scheffel J, Regen T, van Rossum D, Seifert S, Ribes S, Nau R, Parsa R, Harris RA, Boddeke HWGM, Chuang H-N, Pukrop T, Wessels JT, Jürgens T, Merkler D, Brück W, Schnaars M, Simons M, Kettenmann H and Hanisch U-K (2012) Toll-Like Receptor Activation Reveals Developmental Reorganization and Unmasks Responder Subsets of Microglia. *Glia* **60**: 1930-1943.

Schenk D, Barbour R, Dunn W, Gordon G, Grajeda H, Guido T, Hu K, Huang J, Johnson-Wood K, Khan K, Kholodenko D, Lee M, Liao Z, Lieberburg I, Motter R, Mutter L, Soriano F, Shopp G, Vasquez N, Vandevert C, Walker S, Wogulis M, Yednock T, Games D and Seubert P (1999) Immunization with amyloid-β attenuates Alzheimer-disease-like pathology in the PDAPP mouse. *Nature* **400**: 173-177.

Schiefer J, Kampe K, Dodt H, Zieglgänsberger W and Kreutzberg GW (1999) Microglial motility in the rat facial nucleus following peripheral axotomy. *Journal of Neurocytology* **28**: 439-453.

Schiffmann SN, Jacobs O and Vanderhaeghen J-J (1991a) Striatal Restricted Adenosine A_2 Receptor (RDC8) Is Expressed by Enkephalin but Not by Substance P Neurons: An In Situ Hybridization Histochemistry Study. *Journal of Neurochemistry* **57**: 1062-1067.

Schiffmann SN, Libert F, Vassart G and Vanderhaeghen J-J (1991b) Distribution of adenosine A_2 receptor mRNA in the human brain. *Neuroscience Letters* **130**: 177-181.

Schutsky K, Ouyang M, Castelino CB, Zhang L and Thomas SA (2011) Stress and Clucocorticoids Impair Memory Retrival via β_2-Agrenergic, $G_{i/o}$-Coupled Suppression of cAMP Signaling. *J Neurosci* **31**(40): 14172-14181.

Schwarzschild MA, Agnati L, Fuxe K, Chen J-F and Morelli M (2006) Targeting adenosine A_{2A} receptors in Parkinson's disease. *Trends in Neurosciences* **29**(11): 647-654.

Sebastiao AM and Ribeiro JA (1996) Adenosine A_2 receptor-mediated excitatory actions on the nervous system. *Progress in Neurobiology* **48**: 167-189.

Seniuk N, Tatton W and Greenwood C (1990) Dose-dependent destruction of the coeruleus-cortical and nigral-striatal projections by MPTP. *Brain Research* **527**: 7-20.

Shaffer LM, Dority MD, Gupta-Bansal R, Frederickson RC, Younkin SG and Brunden KR (1995) Alyloid β Protein (Aβ) Removal by Neuroglial Cells in Culture. *Neurobiology of Aging* **16**(5): 737-745.

Simard AR and Rivest S (2004) Bone marrow stem cells have the ability to populate the entire central nervous system into fully differentiated parenchymal microglia. *FASEB Journal* **18**: 998-1000.

Simard AR, Soulet D, Gowing G, Julien J-P and Rivest S (2006) Bone Marrow-Derived Microglia Play a Critical Role in Restricting Senile Plaque Formation in Alzheimer's Disease. *Neuron* **49**: 48-502.

Simon-Sanchez J, van Hilten JJ, van de Warrenburg B, Post B, Berendse HW, Arepalli S, Hernandez DG, de Bie RM, Velseboer D, Scheffer H, Bloem B, van Dijk KD, Rivadeneira F, Hofman A, Uitterlinder AG, Rizzu P, Bochdanovits Z, Singleton AB and Heutink P (2011) Genome-wide association study confirms extant PD risk loci among the Dutch. *European Journal of Human Genetics* **19**: 655-661.

Singh S, Singh K, Gupta SP, Patel DK, Singh VK, Singh RK and Singh MP (2009) Effect of caffeine on the expression of cytochrome P450 1A2, adenosine A_{2A} receptor and

dopamine transporter in control and 1-methyl 4-phenyl 1, 2, 3, 6-tetrahydropyridine treated mouse striatum. *Brain Research* **1283**: 115-126.

Smith JA, Das A, Ray SK and Banik NL (2012) Role of pro-inflammatory cytokines released from microglia in neurodegenerative diseases. *Brain Research Bulletin* **87**: 10-20.

Sperlagh B and Illes P (2007) Purinergic modulation of microglial cell activation. *Purinerg Signal* **3**: 117-127.

Sriram K, Matheson JM, Benkovic SA, Miller DB, Luster MI and O'Callaghan JP (2006a) Defficiency of TNF receptors suppresses microglial activation and alters the susceptibility of brain regions to MPTP-induced neurotoxicity: role of TNF-α. *FASEB Journal* **20**: 670-682.

Sriram K, Miller DB and O'Callaghan JP (2006b) Minocycline attenuates microglial activation but fails to mitigate striatal dopaminergic neurotoxicity: role of tumor necrosis factor-α. *Journal of Neurochemistry* **96**: 706-718.

Stalder AK, Ermini F, Bondolfi L, Krenger W, Burbach GJ, Deller T, Coomaraswamy J, Staufenbiel M, Landmann R and Jucker M (2005) Invasion of Hematopoietic Cells into the Brain of Amyloid Precursor Protein Transgenic Mice. *Journal of Neuroscience* **25**(48): 11125-11132.

Stanford SC (1995) Central noradrenergic neurones and stress. *Pharmacol Ther* **68**(2): 297-342.

Stence N, Waite M and Dailey ME (2001) Dynamics of Microglial Activation: A Confocal Time-Lapse Analysis in Hippocampal Slices. *Glia* **33**: 256-266.

Stevens B, Allen NJ, Vazquez LE, Howell GR, Christipherson KS, Nouri N, Micheva KD, Mehalow AK, Huberman AD, Stafford B, Sher A, Litke AM, Lambris JD, Smith SJ, John SW and Barres BA (2007) The Classical Complement Cascade Mediates CNS Synapse Elimination. *Cell* **131**: 1164-1178.

Stewart WF, Kawas C, Corrada M and Metter J (1997) Risk of Alzheimer's disease and duration of NSAID use. *Neurology* **48**: 626-632.

Storch A, Ludolph A and Schwarz J (2004) Dopamine transporter: involvement in selective dopaminergic neurotoxicity and degeneration. *Journal of Neural Transmission* **111**: 1267-1286.

Streit W, Graeber MB and Kreutzberg GW (1989) Peripheral nerve lesion produces increased levels of major histocompatibility complex antigens in the central nervous system. *Journal of Neuroimmunology* **21**: 117-123.

Styren SD, Civin WH and Rogers J (1990) Molecular, Cellular, and pathologic Characterization of HLA-DR Immunoreactivity in Normal Elderly and Alzheimer's Disease Brain. *Experimental Neurology* **110**: 93-104.

Sudduth TL, Greenstein A and Wilcock DM (2013) Intracranial Injection of Gammagard, a Human IVIg, Modulates the Inflamamtory Response of the Brain and Lowers Aβ in APP/PS1 Mice Along a Different Time Course than Anti-Aβ Antibodies. *Journal of Neuroscience* **33**(23): 9684-9692.

Sun C, Wei L, Luo F, Li Y, Li J, Zhu F, Kang P, Xu R, Xiao L, Liu Z and Xu P (2012) HLA-DRB1 Alleles Are Associated with the Susceptibility to Sporadic Parkinson's Disease in Chinese Han Population. *PLoS One* **7**(11): e48594.

Takahashi K, Rochford CD and Neumann H (2005) Clearance of apoptotic neurons without inflammation by microglial triggering receptor on myeloid cells-2. *Journal of Experimental Medicine* **201**(4): 647-657.

Takahashi RN, Pamplona FA and Prediger RDS (2008) Adenosine receptor antagonists for cognitive dysfunction: a review of animal studies. *Frontiers in Bioscience* **13**: 2614-2632.

Takasaki J, Kasazumi K, Saito T, Matsumoto M, Matsumoto S-I, Ohishi T, Soga T, Matsushime H and Furuichi K (2001) Molecular Cloning of the Platelet $P2T_{AC}$ ADP Receptor: Pharmacological Comparison with Another ADP Receptor, the $P2Y_1$ Receptor. *Molecular Pharmacology* **60**(3): 432-439.

Takayama N and Ueda H (2005) Morphine-Induced Chemotaxis and Brain-Derived Neurotrophic Factor Expression in Microglia. *Journal of Neuroscience* **25**(2): 430-435.

Takeuchi H, Jin S, Wang J, Zhang G, Kawanokuchi J, Kuno R, Sonobe Y, Mizuno T and Suzumura A (2006) Tumor Necrosis Factor-α Induces Neurotoxicity via Glutamate Release from Hemichannels of Activated Microglia in an Autocrine Manner. *Journal of Biological Chemistry* **281**(30): 21362-21368.

Tansey MG and Goldberg MS (2010) Neuroinflammation in Parkinson's disease: Its role in neuronal death and implications for therapeutic intervention *Neurobiology of Disease* **37**: 510-518.

Tatton N and Kish S (1997) *In situ* detection of apoptotic nuclei in the substantia nigra compacta of 1-methyl-4-phenyl-1,2,3,6-tetrahydropyridine-treated mice using terminal deoxynucleotidyl transferase labelling and acridine orange staining. *Neuroscience* **77**: 1037-1048.

Tha KK, Okuma Y, Miyazaki H, Murayama T, Uehara T, Hatakeyama R, Hayashi Y and Nomura Y (2000) Changes in expressions of proinflammatory cytokines IL-1β, TNF-α and IL-6 in the brain of senescence accelerated mouse (SAM) P8. *Brain Research* **885**: 25-31.

Tholanikunnel BG, Joseph K, Kandasamy K, Baldys A, Raymond JR, Luttrell LM, McDermott PJ and Fernandes DJ (2010) Novel Mechanisms in the Regulation of G Protein-coupled Receptor Trafficking to the Plasma Membrane. *Journal of Biological Chemistry* **285**(44): 33816-33825.

Tiffany HL, Lavigne MC, Cui Y-H, Wang J-M, Leto TL, Gao J-L and Murphy PM (2001) Amyloid-β Indues Chemotaxis and Oxidant Stress by Acting at Formylpeptide Receptor 2, a G Protein-coupled Receptor Expressed in Phagocytes and Brain. *Journal of Biological Chemistry* **276**: 23645-23652.

Tomas-Camardiel M, Rite I, Herrera AJ, de Pablos RM, Cano J, Machado A and Venero JL (2004) Minocycline reduces the lipopolysaccharide-induced inflammatory reaction,

peroxynitrite-mediated nitration of proteins, disruption of the blood-brain barrier, and damage in the nigral dopaminergic system. *Neurobiology of Disease* **16**: 190-201.

Ton TG, Heckbert SR, Longstreth W, Rossing MA, Kukull WA, Franklin GM, Swanson PD, Smith-Weller T, COHN-S and Checkoway H (2006) Nonsteroidal Anti-Inflamamtory Drugs and Risk of parkinson's Disease. *Movement Disorders* **21**(7): 964-969.

Tooyama I, Kimura H, Akiyama H and McGeer PL (1990) Reactive microglia express class I and class II major histocompatibility complex antigens in Alzheimer's disease. *Brain Research* **523**: 273-280.

Tran TA, McCoy MK, Sporn MB and Tansey MG (2008) The synthetic triterpenoid CDDO-methyl ester modulates microglial activities, inhibits TNF production, and provides dopaminergic neuroprotection. *Journal of Neuroinflammation* **5**: 14.

Tremblay M-E, Lowery RL and Majewska AK (2010) Microglial Interactions with Synapses Are Modulated by Visual Experience. *PLos Biology* **8**(11): e1000527.

Ueno M, Fujita Y, Tanaka T, Nakamura Y, Kikuta J, Ishii M and Yamashita T (2013) Layer V cortical neurons require microglial support for survival during postnatal development. *Nature Neuroscience* **16**(5): 543-551.

Ulvestad E, Williams Jr K, Bo L, Trapp B, Antel J and Mork S (1994a) HLA class II molecules (HLA-DR, -DP, -DQ) on cells in the human CNS studies *in situ* and *in vitro*. *Immunology* **82**: 535-541.

Ulvestad E, Williams K, Bjerkvig R, Tiekitter K, Antel J and Matre R (1994b) Human microglial cells have phenotypic and functional characteristics in common with both macrophages and dendritic antigen-presenting cells. *Journal of Leukocyte Biology* **46**: 732-740.

Ulvestad E, Williams K, Mork S, Antel J and Nyland H (1994c) Phenotypic Differences between Human Monocytes/Macrophages and Microglial Cells Studied *In Situ* and *In Vitro*. *Journal of Neuropathology and Experimental Neurology* **53**(5): 492-501.

Vaca K and Wendt E (1992) Divergent Effects of Astroglial and Microglial Secretions on Neuron Groeth and Survival. *Experimental Neurology* **118**: 62-72.

van der Putten C, Zuiderwijk-Sick EA, van Straalen L, de Geus ED, Boven LA, Kondova I, IJzerman AP and Bajramovic JJ (2009) Differential Expression of Adenosine A_3 Receptors Controls Adenosine A_{2A} Receptor-Mediated Inhibition of TLR Responses in Microglia. *Journal of Immunology* **182**: 7603-7612.

Varvel NH, Grathwohl SA, Baumann F, Liebig C, Bosch A, Brawek B, Thal DR, Charo IF, Heppner FL, Aguzzi A, Garaschuk O, Ransohoff RM and Jucker M (2012) Microglial repopulation model reveals a robust homeostatic process for replacing CNS myeloid cells. *Proceedings of the National Academy of Sciences of the United States of America* **109**(44): 18150-18155.

Vazquez-Prado J, Casas-Gonzalez P and Garcia-Sainz JA (2003) G protein-coupled receptor cross-talk: pivotal roles of protein phosphorylation and protein-protein interactions. *Cell Signal* **15**: 549-557.

Vedeler C, Ulvestad E, Grundt I, Conti G, Nyland H, Matre R and Pleasure D (1994) Fc receptor for IgG (FcR) on rat microglia. *Journal of Neuroimmunology* **49**: 19-24.

Vela JM, Dalmau I, Gonzalesz B and Castellano B (1995) Morphology and Distribution of Microglial Cells in the Young and Adult Mouse Cerebellum. *Journal of Comparative Neurology* **361**: 602-616.

Venneti S, Lopresti BJ and Wiley CA (2013) Molecular Imaging of Microglia/Macrophages in the Brain. *Glia* **61**: 10-23.

Vlad SC, Miller DR, Kowall NW and Felson DT (2008) Protective effects of NSAIDs on the development of Alzheimer disease. *Neurology* **70**: 1672-1677.

Vlajinac H, Dzoljic E, Maksimovic J, Marinkovic J, Sipetic S and Kostic V (2013) Infections as a risk factor for Parkinson's disease: a case-control study. *International Journal of Neuroscience* **123**(5): 329-332.

Voll RE, Herrmann M, Roth EA, Stach C and Kalden JR (1997) Immunosuppresive effects of apoptotic cells. *Nature* **390**: 350-351.

von Kugelgen I and Wetter A (2000) Molecular pharmacology of P2Y-receptors. *Naunyn-Schmiedeberg's Archives of Pharmacology* **362**: 310-323.

Wake H, Moorhouse AJ, Jinno S, Kohsaka S and Nabekura J (2009) Resting Microglia Directly Monitor the Functional State of Synapses *In Vivo* and Determine the Fate of Ischemic Terminals. *J Neurosci* **29**(13): 3974-3980.

Walker DG, Dalsing-Hernandez JE, Campbell NA and Lue L-F (2009) Decreased expression of CD200 and CD200 receptor in Alzheimer's disease: A potential mechanism leading to chronic inflammation. *Experimental Neurology* **215**: 5-19.

Walton NM, Sutter BM, Laywell ED, Levkoff LH, Kearns SM, Marshall II GP, Scheffler B and Steindler DA (2006) Microglia Instruct Subventricular Zone Neurogenesis. *Glia* **54**: 815-825.

Walz W, Ilschner S, Ohlemeyer C, Banati RB and Kettenman H (1993) Extracellular ATP activates a Cation Conductance and a K^+ Conductance in Cultures Microglial Cells from Mouse Brain. *Journal of Neuroscience* **13**(10): 4403-4411.

Wang X-J, Zhang S, Yan Z-Q, Zhao Y-X, Zhou H-Y, Wang Y, Lu G-Q and Zhang J-D (2011) Impaired CD200-CD200R-mediated microglia silencing enhances midbrain dopaminergic neurodegeneration: Roles of aging, superoxide, NADPH oxidase, and p38 MAPK. *Free Radical Biology & Medicine* **50**: 1094-1105.

Wegiel J and Wisniewski H (1990) The complex of microglial cells and amyloid star in three-dimensional reconstruction. *Acta Neuropathologica* **81**: 116-124.

Weiner OD, Rentel MC, Ott A, Brown GE, Jedrychowski M, Yaffe MB, Gygi SP, Cantley LC, Bourne HR and Kirschner MW (2006) Hem-1 Complexes Are Essential for Rac Activation, Actin Polyperization, and Myosin Regulation during Neutrophil Chemotaxis. *PLoS Biology* **4**(2): e38.

Williams Jr K, Ulvestad E, Cragg L, Blain M and Antel J (1993) Induction of Primary T Cell Responses by Human Glial Cells. *Journal of Neuroscience Research* **36**: 382-390.

Williams K, Bar-Or A, Ulvestad E, Oliver A, Antel J and Yong VW (1992) Biology of Adult Human Microglia in Culture: Comparisons with Peripheral Blood Monocytes and Astrocytes. *Journal of Neuropathology and Experimental Neurology* **51**(5): 538-549.

Winkler DT, Bondolfi L, Herzig mC, Jann L, Calhoun ME, Wiederhold K-H, Tolnay M, Staufenbiel M and Jucker M (2001) Spontaneous Hemorrhagic Stroke in a Mouse Model of Cerebral Amyloid Angiopathy. *Journal of Neuroscience* **21**(5): 1619-1627.

Wisniewski H, Vorbrodt A, Wegiel J, Morys J and Lossinsky A (1990) Ultrastructure of the Cells Forming Amyloid Fibers in Alzheimer Disease and Scrapie. *American Journal of Medical Genetics* **S7**: 287-297.

Wollmer MA, Lucius R, Wilms H, Held-Feindt J, Sievers J and Mentlein R (2001) ATP and adenosine induce ramification of microglia in vitro. *Journal of Neuroimmunology* **115**: 19-27.

Woodroofe MN, Hayes G and Cuzner M (1989) Fc receptor density, MHC antigen expression and superoxide production are increased in intergeron-gamma-treated microglia isolated from adult rat brain. *Immunology* **68**: 421-426.

Wright GJ, Jones M, Puklavec MJ, Brown MH and Barclay AN (2001) The unusual distribution of the neuronal/lymphoid cell surface CD200 (OX2) glycoprotein is conserved in humans. *Immunology* **102**: 173-179.

Wright GJ, Puklavec MJ, Willis AC, Hoek RM, Sedgwick JD, Brown MH and Barclay AN (2000) Lymphoid/Neuronal Cell Surface OX2 Glycoprotein Recognizes a Novel Receptor on Macrophages Implicated in the Control of Their Function. *Immunity* **13**: 233-242.

Wu DC, Jackson-Lewis V, Vila M, Tieu K, Teismann P, Vadseth C, Choi D-K, Ischiropoulos H and Przedborski S (2002) Blockade of Microglial Activation is Neuroprotective in the 1-

Methyl-4-Phenyl-1,2,3,6-Tetrahydropyridine Mouse Model of Parkinson Disease. *Journal of Neuroscience* **22**(5): 1763-1771.

Wyss-Coray T and Mucke L (2002) Inflammation in Neurodegenerative Disease - A Double-Edged Sword. *Neuron* **35**: 419-432.

Xiao D, Bastia E, Xu Y-H, Benn CL, Cha J-HJ, Peterson TS, Chen J-F and Schwarzschild MA (2006) Forebrain Adenosine A_{2A} Receptors Contribute to $_{L}$-3,4-Dihyrdoxyphenylalanine-Induced Dyskinesia in Hemiparkinsonian Mice. *Journal of Neuroscience* **26**(52): 13548-13555.

Xu K, Bastia E and Schwarzschild MA (2005) Therapeutic potential of adenosine A_{2A} receptor antagonists in Parkinson's disease. *Pharmacology & Therapeutics* **105**: 267-310.

Xu K, Xu Y-H, Chen J-F and Schwarzschild MA (2002) Caffeine's neuroprotection against 1-methyl-4-phenyl-1,2,3,6-dihydropyridine toxicity shows no tolerance to chronic caffeine administration in mice. *Neuroscience Letters* **322**: 13-16.

Yamamoto M, Horida M, Buescher JL, Walsh SM, Gendelman HE and Ikezu T (2007) Interferon-γ and Tumor Necrosis Factor-α Regulate Amyloid-β Plaque Deposition and β-Secretase Expression in Swedish Mutant APP Transgenic Mice. *American Journal of Pathology* **170**(2): 680-692.

Yan J, Mihaylov V, Xu X, Brzostowski JA, Li H, Liu L, Veenstra TD, Parent CA and Jin T (2012) A Gβγ Effector, ElmoE, Transduces GPCR Signaling to the Actin Network during Chemotaxis. *Developmental Cell* **22**: 92-103.

Yan SD, Chen X, Fu J, Chen M, Zhu H, Roher A, Slattery T, Zhao L, Nagashima M, Morser J, Migheli A, Nawroth P, Stern D and Schmidt AM (1996) RAGE and amyloid-β peptide neurotoxicity in Alzheimer's disease. *Nature* **382**(685-691).

Yao J, Harvath L, Gilbert DL and Colton CA (1990) Chemotaxis by a CNS Macrophage, the Microglia. *Journal of Neuroscience Research* **27**: 36-42.

Yenari MA, Kauppinen TM and Swanson RA (2010) Microglial Activation in Stroke: Therapeuric Targets. *Neurotherapeutics* **7**: 378-391.

Yip AG, Green RC, Huyck M, Cupples LA and Farrer LA (2005) Nonsteroidal anti-inflammatory drug use andAlzheimer's disease risk: the MIRAGE Study. *BMC Geriatrics* **5**(2).

Yu L, Shen H-Y, Coelho JE, Araujo IM, Huang Q-Y, Day Y-J, Rebola N, Canas PM, Rapp EK, Ferrara J, Taylor D, Muller CE, Linden J, Cunha RA and Chen J-F (2008) Adenosine A_{2A} Receptor Antagonists Exert Motor and Neuroprotective Effects by Distinct Cellular Mechanisms. *Annals of Neurology* **63**: 338-346.

Zandi PP, Anthony JC, Hayden KM, Mehta K, Mayer L and Breitner JC (2000) Reduced incidence of AD with NSAID but not H2 receptor antagonists. *Neurology* **59**(6): 880-886.

Zhang FL, Luo L, Gustafson E, Lachowicz J, Smith M, Qiao X, Liu Y-H, Chen G, Pramanik B, Laz TM, Palmer K, Bayne M and Monsma J, Frederick J (2001) ADP Is the Cognate Ligand for the Orphan G Protein-coupled Receptor SP1999. *Journal of Biological Chemistry* **276**(11): 8608-8615.

Zhang W-P, Ouyang M and Thomas SA (2004) Potency of catecholamines and other L-tyrosine derivatives at the cloned mouse adrenergic receptors. *Neuropharmacology* **47**: 438-449.

Zhang W, Wang T, Pei Z, Miller DS, Wu X, Block ML, Wilson B, Zhang W, Zhou Y, Hong J-S and Zhang J (2005) Aggregated α-synuclein activates microglia: a process leading to disease progression in Parkinson's disease. *FASEB Journal* **19**: 533-542.

Zietlow R, Dunnett S and Fawsett J (1999) The effect of microglia on embryonic dopaminergic neuronal survival *in vitro*: diffusible signals from neurons and glia change microglia from neurotoxic to neuroprotective. *European Journal of Neuroscience* **11**: 1657-1667.

Zimmermann H (1994) Signalling via ATP in the nervous system. *TINS* **17**(10): 420-426.

Zimmermann H (2000) Extracellular metabolism of ATP and other nucleotides. *Naunyn-Schmiedeberg's Archives of Pharmacology* **362**: 299-309.

Zujovic V, Benavides J, Vige X, Carter C and Taupin V (2000) Fractalkine Modulates TNF-α Secretion and Neurotoxicity Induced by Microglial Activation. *Glia* **29**: 305-315.

Zujovic V, Schussler N, Jourdain D, Duverger D and Taupin V (2001) In vivo neutralization of endogenous brain fractalkine increases hippocampal TNFα and 8-isoprostane production induced by intracerebroventricular injection of LPS. *Journal of Neuroimmunology* **115**: 135-143.